

Synthesis and Characterization of Novel Silicones with Antimicrobial Properties

Dissertation

zur

Erlangung des akademischen Grades

doctor rerum naturalium (Dr. rer. nat.)

der Mathematisch-Naturwissenschaftlichen Fakultät

der Universität Rostock

vorgelegt von **Annika Dietrich** (geb. Kottmann)

geb. am 18.01.1991 in Recklinghausen

Rostock, den 23.04.2019

Erklärung

Ich versichere hiermit an Eides statt, dass ich die vorliegende Arbeit selbstständig angefertigt und ohne Hilfe verfasst habe, keine außer den von mir angegebenen Hilfsmitteln und Quellen dazu verwendet habe und die den benutzten Werken inhaltlich und wörtlich entnommenen Stellen als solche kenntlich gemacht habe.

Annika Dietrich

Rostock, den 23.04.2019

Die vorliegende Arbeit wurde von Oktober 2016 bis April 2019 am Lehrstuhl für Technische Chemie der Universität Rostock unter der Betreuung von Prof. Dr. Udo Kragl angefertigt.

1. Gutachter: Prof. Dr. Udo Kragl

2. Gutachter: Prof. Dr. Gerrit A. Luinstra

Tag der mündlichen Prüfung: 09.07.2019

Danksagung

Die vorliegende Arbeit wurde in der Zeit von Oktober 2016 bis April 2019 am Leibnitz-Institut für Katalyse e. V. an der Universität Rostock (LIKAT Rostock) in der Arbeitsgruppe von Prof. Dr. Udo Kragl angefertigt.

Mein besonderer Dank gilt Herrn Prof. Dr. Udo Kragl, der mich in seiner Arbeitsgruppe aufgenommen hat und mich über fünf Jahre von meinem Masterstudium bis zu meinem Doktor begleitet und unterstützt hat. Er hat mir nicht nur die Erstellung dieser Doktorarbeit ermöglicht, sondern auch meine persönliche Entwicklung gefördert.

Ich danke auch der Henkel AG & Co. KGaA für die Möglichkeit, meine Doktorarbeit in einer Industriekooperation anzufertigen und so einen sehr guten Einblick in die industrielle Denkweise zu erhalten. Mein Dank gilt dabei besonders den Mitgliedern unserer Kooperationsabteilung Dr. Andrea Gutacker, Dr. Johann Klein und Kerstin Unger, die mir das Thema der Doktorarbeit ermöglicht haben und für sehr konstruktive und schöne Diskussionen gesorgt haben. Dr. Andrea Gutacker stand mir stets bei Fragen und Problemen zur Seite und ich bin ihr sehr verbunden, dass sie auch stets meine persönliche Entwicklung gefördert hat. Da zu Beginn meiner Doktorandenzeit die Betreuung von Dr. Thérèse Hémerly übernommen wurde, bin ich auch ihr zu Dank verpflichtet für die gute Aufnahme in das Thema. Weiter danke ich auch Dr. Christian Kastner und seinen Labormitarbeitern aus der mikrobiologischen Abteilung von Henkel. Sie haben die Tests auf antimikrobielle Aktivität meiner Proben durchgeführt und standen mir als Ansprechpartner jederzeit zur Seite. Patric Sielaff aus der analytischen Abteilung von Henkel danke ich für seine Unterstützung bei den Langzeit-NMR-Messungen.

Ein sehr großes Dankeschön gilt Dr. Esteban Mejía. Er hat mich unterstützt, meine praktische Arbeit zu koordinieren und hatte immer ein offenes Ohr für mich, um für aufkommende Probleme schnell eine Lösung zu finden oder bei vorkommenden Durststrecken die Motivation aufrecht zu erhalten. Darüber hinaus haben mir die tiefgreifenden, fachlichen Diskussionen ermöglicht, meine Arbeit immer wieder aus neuen Blickwinkeln zu betrachten. Serendipity bedeutet auch mal einen Schritt nach rechts und links zu wagen und unerwarteten Ergebnissen einen neuen Blickwinkel zu verleihen.

Auch möchte ich der gesamten Arbeitsgruppe und besonders Nayereh Mohebbati danken. Sie hat mich im Rahmen ihrer Masterarbeit und ihrer Tätigkeit als wissenschaftliche Hilfskraft tatkräftig unterstützt. Ihre zielstrebige und offene Art hat die Zusammenarbeit mit ihr sehr angenehm gestaltet. Auch danke ich Marc Gongoll, der notwendige Messungen meiner Proben zeitnah und zuverlässig durchgeführt hat. Auf beide konnte mich voll und ganz verlassen. Meine Arbeitskolleginnen und -kollegen Abel, Ahmad, Lea, Theresia, Marion, Felix, Paul und Niklas haben nicht nur für gute Laune am Arbeitsplatz gesorgt, sondern auch für unvergessliche Ausflüge. So konnte ich meine Arbeit jeden Tag mit viel Freude und Elan beginnen.

Weiter möchte ich dem Team der Analytik im LIKAT danken. Es hat meine Proben immer sehr zeitnah gemessen und ausgewertet, wodurch die gezielte und schnelle Durchführung der praktischen Arbeit erst möglich war. Zudem stand es mir immer bei jeder Frage zur Analytik zur Seite und hat geholfen neue Analysenmethoden zu testen, um aussagekräftige Ergebnisse zu erhalten. Auch gilt mein Dank

Prof. Dr. Hermann Seitz am Lehrstuhl für Mikrofluidik und besonders Robert Mau. Sie haben mir das Kontaktwinkelmessgerät zur Verfügung gestellt, um Messungen im Rahmen meiner Forschungsarbeit anzufertigen.

Als letztes bedanke ich mich bei meiner Familie. Mein Mann Daniel Dietrich ist mit mir während der zeitweise sehr stressigen Doktorandenzeit den Bund der Ehe eingegangen. Seine ruhige und ausgleichende Art ist als Unterstützung unbezahlbar! Meine Eltern Paul und Barbara Kottmann und meine Geschwister Sabrina und Matthias und deren Familien waren immer für mich da, auch wenn mir der Stress zu viel wurde. Sie haben und werden mir immer Halt geben.

„Der Zufall begünstigt nur den vorbereiteten Geist.“

Louis Pasteur (1822 – 1885)

Abstract

The progress of society's technological advancement and the high medical standards make it increasingly important, to introduce novel functionalities into given polymeric materials for specialty applications. Siloxanes are helpful starting compounds for the production of materials with antimicrobial compounds. Their inherent properties, such as self-healing, biocompatibility and biodurability, as well as their easy functionalization, make them very interesting for further developments. The increasing number of publications in the last decades containing antimicrobial compounds clearly reflects this interest.

This research is focused on the functionalization of siloxanes to introduce antimicrobial properties. On the one hand, a synthetic route is developed to form polysiloxane polypropyleneglycol brush copolymers containing anti-adhesion properties. This two-step process includes side-group hydrosilylation and consecutive propoxylation. The synthetic pathway is described and discussed and the products are characterized. Kinetic studies are performed and the synthesis is optimized to obtain products with controlled conversion. These products lead to the control of surface energy, which has an effect on the microbial adhesion.

The second part of this research presents the introduction of bactericidal and fungicidal properties into the silicone. The two-step synthesis includes the side-group halosilation and consecutive quaternization (Menshutkin reaction) to obtain halogenalkyl and QAS-functionalized siloxanes (quaternary ammonium salts). The synthetic pathways are discussed and compared to the literature. Mechanistic and kinetic studies are performed. The obtained products are characterized and bactericidal and fungicidal properties are determined by different antimicrobial test methods.

To gain a bi-functionalized siloxane containing both anti-adhesion and bactericidal/fungicidal properties, further investigations are focused on the successive introduction of the already mentioned functional groups into the same polymer backbone. Based on the described hydrosilylated products with controlled conversion, consecutive halosilation reactions are achieved. The obtained products are characterized and the synthetic pathway is optimized. These novel materials offer the opportunity to produce bi-functional silicones containing both anti-adhesion and bactericidal/fungicidal properties, which raises a big industrial interest.

Table of Contents

List of Abbreviations	XI
Index of Schemes	XIII
Index of Figures	XV
Index of Tables	XXI
1 Introduction	1
1.1 Microorganisms	3
1.1.1 Structural Features of Bacteria	5
1.1.1.1 Adhesion Properties of Bacteria	6
1.1.2 Structural Features of Molds	7
1.2 Polymers containing Antimicrobial Properties	8
1.2.1 Possible Weak Points for Antifungal active Compounds.....	11
1.2.2 Testing Methods for Antimicrobial Agents	12
2 Objectives and Motivation.....	13
3 Part I: Introduction of Anti-Adhesion Properties into Silicones.....	14
3.1 Background.....	14
3.1.1 Hydrosilylation	15
3.1.2 Alkoxylation.....	18
3.2 Results and Discussion	22
3.2.1 Synthesis of fully-converted Polysiloxane Polypropyleneglycol Brush Copolymers	22
3.2.2 Characterization of fully-converted Polysiloxane Polypropyleneglycol Brush Copolymers.....	28
3.2.3 Optimization Process to synthesize Polysiloxane Propyleneglycol Brush Copolymers with controlled partial Conversion.....	32
3.2.3.1 Kinetic Studies	32
3.2.3.2 Optimized Synthetic Pathway for the Partial Hydrosilylation of PDMS-PHMS Copolymers.....	33
3.2.3.3 Synthesis of Half-converted Polysiloxane Polypropyleneglycol Brush Copolymers	35
3.3 Determination of Antimicrobial Properties	37
3.3.1 Anti-Adhesion Assay.....	37
3.4 Conclusion and Outlook	40
4 Part II: Introduction of Bactericidal and Fungicidal Properties into Silicones	41
4.1 Background.....	41

4.1.1	Halosilation	41
4.1.2	Menshutkin Reaction	42
4.2	Results and Discussion	45
4.2.1	Part IIa: Halosilation.....	45
4.2.1.1	Synthesis of Halogenalkyl functionalized Siloxanes.....	45
4.2.1.2	Kinetic Studies (Comparison of Pt- and Pd-catalyzed Halosilation).....	49
4.2.1.3	Proposed Reaction Mechanism of Pt-catalyzed Halosilation	51
4.2.1.4	Replacement of Halogen Source and Heterocyclic Compounds	53
4.2.1.5	Characterization.....	56
4.2.2	Part IIb: Menshutkin Reaction	58
4.2.2.1	Synthesis	58
4.2.2.2	Kinetic Studies of Menshutkin Reaction	64
4.2.2.3	Characterization.....	65
4.3	Determination of Antimicrobial Properties	68
4.3.1	Kirby-Bauer Test.....	68
4.3.2	Minimum Inhibitory Concentration (MIC)	71
4.3.3	ISO 22196:2011	74
4.4	Conclusion and Outlook	76
5	Part III: Successive Introduction of Hydrosilylated and Halosilated Side-Groups into Silicones	77
5.1	Background.....	77
5.2	Results and Discussion	79
5.2.1	Synthesis	79
5.2.2	Characterization.....	83
5.3	Conclusion and Outlook	86
6	Outlook.....	87
7	Summary	89
8	References	91
	Appendix	98
A1.	Equipment and Testing methods.....	98
A2.	Materials	102
A3.	Appendix to Part I	105

A4.	Appendix to Part IIa	137
A5.	Appendix to Part IIb	153
A6.	Appendix to Part III	186
A7.	Scientific Contributions	193
A8.	Curriculum Vitae	194

List of Abbreviations

Å	Angstrom unit	IR	Infrared spectroscopy
CA	Contact angle	IUPAC	International union of pure and applied chemistry
CDCl₃	Deuterated chloroform	LIKAT	Leibniz institute for catalysis Rostock
δ	Chemical shift [ppm]	M	Molecular mass
D₃D^H	1,1',3,3',5,5',7-Heptamethyl-cyclotetrasiloxane	MALDI	Matrix-assisted laser desorption/ionization
DDAC	Didecyl dimethyl ammonium chloride	MBC	Minimum bactericidal concentration
D^H₄	1,3,5,7-Tetramethyl-cyclotetrasiloxane	MIC	Minimum inhibitory concentration
DMC	Double metal-cyanide complex	MRSA	Methicillin-resistant <i>Staphylococcus aureus</i>
DMF	Dimethylformamide	MU	Monomer unit
DMSO	Dimethylsulfoxide	n/d	Not detectable
DMSO-d₆	Deuterated dimethylsulfoxide	n/s	Not specified
DOTL	Diocetyl tin dilaurate	NMR	Nuclear magnetic resonance
DSC	Differential scanning calorimetry	Oxepane	Hexamethylene oxide
EO	Ethylene oxide	PD	Polydispersity
EPS	Extracellular polymeric substances	PdCl₂	Palladium(II+)chloride
EtOH	Ethanol	PDI	Polydispersity
g	Gram	PDMS	Polydimethylsiloxane
GF40	3-/isocyanatopropyl trimethoxysilane	PEG	Polyethylene glycol
h	Hours	PHMS	Polyhydridomethylsiloxane
Ha	Halosilation cycle	PIL	Polymerized ionic liquid
H	Hazen factor	PO	Propylene oxide
Hy	Hydrosilylation cycle	PPG	Polypropylene glycol
IL	Ionic liquids	PTC	Phase transfer catalysts

Pt@C	Platinum, 10% supported on charcoal	TDI	Toluene-2,4-diisocyanate
QAS	Quaternary ammonium salts	THF	Tetrahydrofuran
ROP	Ring-opening polymerization	THP	Tetrahydropyran
RT	Room temperature	T_g	Glass transition temperature
t	Time	TOF	time-of-flight mass spectrometer
T	Temperature	Yi	Yellowness index

Index of Schemes

Scheme 3-1: Side-group hydrosilylation reaction of PDMS-PHMS copolymer with 1-(allyloxy)propan-2-ol in the presence of a platinum catalyst and consecutive propoxylation reaction with propylene oxide in the presence of DMC catalyst.	14
Scheme 3-2: Chalk-Harrod mechanism for hydrosilylation of olefins catalysed by late transition metal complexes (adapted from ^[9a]).	15
Scheme 3-3: Forming of α - and β -isomers during the hydrosilylation reaction of pseudohalogen containing allylic compounds (adapted from ^[76d]).	17
Scheme 3-4: Overview of possible side-reactions next to hydrosilylation; O-silylation can only take place when R ² is an hydroxy group (adapted from ^[60]).	17
Scheme 3-5: Left: general alkoxylation reaction; right: the most famous representative PEG and PPG.	18
Scheme 3-6: Proposed mechanism of ring-opening polymerization of PO by heterogeneous DMC catalyst ^[89c] . The entire catalyst structure is not shown for simplification.	20
Scheme 3-7: Propoxylation reaction with two different options of the formed product.	20
Scheme 3-8: Side-group hydrosilylation reaction of PDMS-PHMS copolymer with 1-(allyloxy)propan-2-ol in the presence of a platinum catalyst and consecutive propoxylation reaction with propylene oxide in the presence of DMC catalyst; the red highlighted part represents the first monomer unit of propylene oxide.	22
Scheme 3-9: Curing of Polysiloxane Polyalkyleneglycol Brush Copolymers via polyurethane synthesis.	30
Scheme 4-1: Specific example of Pd-catalyzed halosilated silanes; this are one of the first reactants reported in literature. ^[110]	42
Scheme 4-2: General Menshutkin reaction with X = Br, Cl, I.	43
Scheme 4-3: left: polydimethylsiloxane backbone with hydroxyl functionalized carbamate and trimethylammonium iodide end-groups within the main chain; right: curable composition of PDMS containing imidazolium chloride side-groups linked by ether bridge, mercapto-functionalized and phosphonium containing compounds.	44
Scheme 4-4: Method for quaternization of siloxanes; Route (I) represents first halogenation and then substitution reaction with amines, route (II) shows the amination and consecutive quaternization by adding halogen-containing compounds; in general hydrosilylation is the preferred reaction.	44
Scheme 4-5: Halosilation of PHMS with THF and allyl bromide as halogen source.	45
Scheme 4-6: Proposed reaction mechanism of halosilation cycle (Ha) and possible hydrosilylation cycle (Hy) as competitive reaction.	52
Scheme 4-7: General quaternization reaction (Menshutkin reaction) with halosilated siloxanes and amines in the absence of any catalyst	58
Scheme 4-8: General structure of the synthesized Menshutkin products; Product class A is based on pyridine and includes pyridinium bromide groups, product class B on 1-methyl-1H-imidazole (1-methylimidazolium bromide groups) and product class C on 1-butyl-1H-imidazole (1-butylimidazolium bromide groups).	58

Scheme 4-9: Proposed hydrolysis process of the quaternized samples and further curing of the siloxane backbone; the blue letters mark the groups of Figure 4-12 and Figure 4-13	63
Scheme 5-1: Structure A illustrates the bi-functionalized product after hydrosilylation and halosilation; Structure B illustrates the general structure after consecutive propoxylation and quaternization.	77
Scheme 5-2: left: polydimethylsiloxane backbone with hydroxyl functionalized carbamate and trimethylammonium iodide end-groups within the main chain; right: PDMS containing imidazolium chloride side-groups linked by ether bridge.....	78
Scheme 5-3: Consecutive halosilation of hydrosilylated PHMS with THF and allyl bromide.	79
Scheme 5-4: Possible chemical structures that can be formed during bi-functionalization; A is the desired product, B illustrates a condensation of the formed functional groups and C shows the function of allylic groups as protection groups.	82
Scheme A-1: Curing of Polysiloxane Polyalkyleneglycol Brush Copolymers via polyurethane synthesis.....	103
Scheme A-2: Curing of Polysiloxane Polyalkyleneglycol Brush Copolymers via polyurethane synthesis (A) and consecutive polycondenzation (B) embedded in standard PDMS formulation.	104

Index of Figures

Figure 1-1: Shorthand notation for siloxane polymer units; R could be e.g. H, alkyl, aryl or halogens, but no oxygen.	1
Figure 1-2: Development of publications containing “silicone” during the last two decades (Scifinder, January 2019).	2
Figure 1-3: Overview of bacterial infections in the human body (adapted from ^[11]).	4
Figure 1-4: Sketch for the gram-negative and gram-positive bacteria wall.	6
Figure 1-5: Reproductive cycle of molds with growth phase and proliferative phase.	8
Figure 1-6: Development of publications containing “antimicrobial” and “antimicrobial + silicone” during the last two decades (Scifinder, January 2019).	9
Figure 1-7: Schematic representation of antifungal activity; avoiding adhesion of spores, growing and/or sporulation.	11
Figure 2-1: Charting of the schematic structure of this thesis; PPG = polypropylene glycol; X = Br, Cl; QAS = quaternary ammonium salts.	13
Figure 3-1: Structure of Karstedt catalyst (Platinum-divinyltetramethyldisiloxane complex).	16
Figure 3-2: Chemical structure of a general double metal-cyanide complex (DMC) with an undefined ligand (L) (adapted from ^[89c]).	19
Figure 3-3: ¹ H-NMR of 3.4 in deuterated chloroform (400 MHz, 24 °C), the separated signals from the first monomer unit are shown.	25
Figure 3-4: Degree of polymerization shows linearity (PPG wt-% vs. monomer units) in a logarithmic plotted diagram; the plotting is necessary due to already existing PPG wt-% in the hydrosilylated starting materials 3.1a to 3.3a ; blue curve belongs to products 3.4 to 3.7 , red curve belongs to 3.8 to 3.11 and green curve belongs to 3.12 to 3.32 ; dark green data points illustrate the calculated degree of polymerization for 3.12 to 3.32 ; the standard deviations were calculated from two to three repetitions.	26
Figure 3-5: Comparison of calculated molecular weights and measured ones of 3.12 to 3.32 made from 3.3a in a logarithmic plotted diagram; the plotting is necessary due to already existing PPG wt-% in the hydrosilylated starting materials 3.3a ; the green curve illustrates the calculated degree of polymerization for 3.12 to 3.32 ; the standard deviations were calculated from two to three repetitions.	27
Figure 3-6: Viscosity results of hydrosilylated products 3.1a to 3.3b in homogeneous (Karstedt) and heterogeneous catalytical systems (Pt@C); the standard deviations were calculated from two to three repetitions.	28
Figure 3-7: Viscosity results of propoxylated products 3.4 to 3.32 ; 3.1a to 3.3a ; blue curve belongs to products 3.4 to 3.7 , red curve belongs to 3.8 to 3.11 and green data points belong to 3.12 to 3.32 ; the green curve is a trend line to illustrate the trend; the standard deviations were calculated from two to three repetitions.	29
Figure 3-8: Time-resolved contact angles of chosen products made from SM-15 and reference materials (standard PDMS formulation and PPG reference material); the black curves belong to the references, the blue curve belongs to the hydrosilylated product; the red curves are part of the	

propoxylated samples which show the spreading effect and the green curves belong to the propoxylated samples without any decreasing effect.....	31
Figure 3-9: Logarithmic-plotted diagram of time-resolved kinetic studies of hydrosilylation product 3.1a at different temperatures. The activation energy is about 206.7 ± 7.9 [kJ/(mol)].	33
Figure 3-10: Anti-Adhesion Test results of chosen products from 3.1a to 3.31 ; the results are ordered by the starting material; the standard deviations were calculated from three repetitions.	38
Figure 3-11: Anti-Adhesion Test Results of PDMS formulations containing the product 3.20 ; the wt-% of the product 3.20 is varied; the standard deviations were calculated from three repetitions.	39
Figure 4-1: Ratio between halosilation and hydrosilylation as side-reaction of 4.1a to 4.10 ; yields of products were calculated by integration of the integrals of the signals in ^1H -NMR; the standard deviations were calculated from two to three repetitions.	46
Figure 4-2: ^1H - ^{13}C -HSQC-NMR of 4.1a in deuterated chloroform (400 MHz, 25 °C); the overlapping of the signals of the halosilated and hydrosilylated products is shown.	47
Figure 4-3: Molecular weights of halosilated products; comparison of calculated and measured molecular weights of 4.1a to 4.10 ; the molecular masses were measured by GPC in THF; the standard deviations were calculated from two to three repetitions.	49
Figure 4-4: Kinetic studies of the synthesis of 4.1a at different temperatures; the reaction follows zero order depending on the siloxane. The activation energy is about 47.4 ± 2.2 kJ/(mol).	50
Figure 4-5: Kinetic studies of sample 4.1b at different temperatures; the reaction follows first order depending on the siloxane; the diagram is logarithmic plotted. The activation energy is about 80.4 ± 3.1 kJ/(mol).	51
Figure 4-6: Intended sequences of the experiments 4.12 to 4.18	56
Figure 4-7: Viscosity results of halosilated products 4.1a to 4.10 ; the data of the siloxane starting materials were added as well; the standard deviations were calculated from two to three repetitions.	57
Figure 4-8: ^1H - ^{13}C -HSQC-NMR of 4.19 in deuterated chloroform (400 MHz, 25 °C); for reasons of simplification the methyl groups on the silicon have been grouped together as a	59
Figure 4-9: Solvent-screening of samples 4.19 , 4.20 and 4.21 ; the solvents are arranged by their polarity (according to the elution strength).	60
Figure 4-10: Solubility tests of SM-100 and SM-100 based samples; the green fields show solubility, the red fields show insolubility, and the yellow fields represents the change from solubility to precipitation over time or increasing in concentration; n/s = not specified.	61
Figure 4-11: Solubility tests of SM-15 and SM-15 based samples; the green fields show solubility, the red fields show insolubility, and the yellow fields represents the change from solubility to precipitation over time or increasing in concentration.	62
Figure 4-12: Time-resolved ^1H -NMR of 4.19 in deuterated DMSO (400 MHz, 26 °C); it is an example for the hydrolysis of the pyridinium-functionalized side-group.	63
Figure 4-13: Time-resolved ^1H -NMR of 4.20 in deuterated DMSO (400 MHz, 26 °C); it is an example for the hydrolysis of the imidazolium-functionalized side-group.	64
Figure 4-14: Kinetic studies of sample 4.19 at different temperatures; the overall reaction follows second order; the y-axis contains the squared data.	65

Figure 4-15: DSC measurements of the quaternized products; blue: product class A (including pyridinium bromide groups), red: product class B (including 1-methylimidazolium bromide groups), green: product class C (including 1-butylimidazolium bromide groups); the black bars are the starting materials and the grey bars are the corresponding halosilated intermediates; measured values in the lower part of the diagram are outside the measuring range (below -75 °C); the standard deviations were calculated from two to three repetitions.	66
Figure 4-16: DSC measurements of the quaternized products based on SM-100; blue: product class A (4.19, 4.24, 4.27), red: product class B (4.20, 4.25, 4.28), green: product class C (4.21, 4.26, 4.29); the black bar is the starting material SM-100 and the grey bars are the corresponding halosilated intermediates 4.1a, 4.12 and 4.13, measured values in the lower part of the diagram are outside the measuring range (below -75 °C); the standard deviations were calculated from two to three repetitions.	67
Figure 4-17: Kirby-Bauer Test of brominated (4.1a to 4.4) quaternized products (4.19 to 4.38); the red bars symbolize the zone of inhibition in which the maximum number can be 45 mm due to the diameter of the petri dishes; the slightly red highlighted substrates are references; Bardac® is a disinfectant containing Didecyl dimethyl ammonium chloride (DDAC).	70
Figure 4-18: Minimum Inhibition Concentration of SM-50 based samples 4.30, 4.31 and 4.32; DMSO is tested as blank; the green fields are clear solutions, so here the test substance is antimicrobially active; The yellow fields illustrate the beginning of growth and the red fields indicate growth of the molds and thus inactivity of the test substance.	72
Figure 4-19: Minimum Inhibition Concentration of SM-15 based samples 4.36, 4.37 and 4.38; the green fields are clear solutions, so the test substance is antimicrobially active; The yellow fields illustrate the beginning of growth and the red fields indicate growth of the molds and thus inactivity of the antimicrobial substance.	73
Figure 4-20: ISO 22196:2011 test for the measurement of antibacterial activity on plastics and other nonporous surfaces; the test is evaluated after 24 hours (light blue bars) and 48 hours (dark blue bars); the samples are sorted by amines and descending number of side-groups; the reference is a standard PDMS formulations; the standard deviations were calculated from three repetitions.	75
Figure 5-1: ¹ H- ¹³ C-HSQC-NMR of 5.3 in deuterated chloroform (400 MHz, 25 °C); the overlapping of the signals of the halosilated and hydrosilylated products are shown; the methyl groups at silicon have been grouped together as a; signals b to h belong to the hydrosilylated group and signals i to m belong to the halosilated one.	80
Figure 5-2: Pictures of sample 5.7 during storage; the product gets darker and precipitation is formed; the product is cured on day five.	81
Figure 5-3: Molecular weights of bi-functionalized products; comparison of calculated and measured molecular weights Mn of 5.3 to 5.7; the PDI is given as well.	83
Figure 5-4: Rheological behavior of Newtonian and non-Newtonian fluids.	84
Figure 5-5: Viscosity results of sample 5.3 and 5.5; both samples have a non-Newtonian behavior; the trend line is calculated by a power function.	85

Figure A-1: Standard six-well plate with test material for the Anti-Adhesion Assay; the picture is adapted from Henkel Corporation Dusseldorf (microbiological department).	100
Figure A-2: Illustration of the Kirby-Bauer Test and its evaluation; the picture is adapted from Henkel Corporation Dusseldorf (microbiological department).	100
Figure A-3: Test equipment with test substrate (left) and reference (right) for the MIC; clear vials represent concentrations, in which the test substrate is antimicrobial active; the picture is adapted from Henkel Corporation Dusseldorf (microbiological department).	101
Figure A-4: ^1H -NMR of 3.4 in deuterated chloroform (400 MHz, 24 °C); the separated signals from the first monomer unit are shown.	110
Figure A-5: GPC result of 3.4 in THF (shown GPC results are an average of two measurements).	110
Figure A-6: Logarithmic-plotted diagram of time-resolved kinetic studies of hydrosilylation. The activation energy is about 206.7 ± 7.9 [kJ/(mol)].	127
Figure A-7: ^1H - ^{13}C -HSQC-NMR of 4.1a in deuterated chloroform (400 MHz, 24 °C); the overlapping of the signals of the halosilated and hydrosilylated products are shown.	138
Figure A-8: GPC result of 4.1a in THF (shown GPC results are an average of two measurements).	138
Figure A-9: Kinetic studies of sample 4.1a at different temperatures; the reaction follows zero order depending on the siloxane. The activation energy is about 47.4 ± 2.2 kJ/(mol).	143
Figure A-10: Kinetic studies of sample 4.1b at different temperatures; the reaction follows first order depending on the siloxane; the diagram is logarithmic plotted. The activation energy is about 80.4 ± 3.1 kJ/(mol).	144
Figure A-11: Static contact angles of platinum-catalyzed halosilation products 4.1a to 4.6 and reference material (standard PDMS formulation).	146
Figure A-12: ^1H - ^{13}C -HSQC-NMR of 4.19 in deuterated chloroform (300 MHz, 24 °C); the shifting of the signals promotes a separation of the signals; for reasons of simplification the methyl groups on the silicon have been grouped together as a .	155
Figure A-13: Time-resolved ^1H -NMR of 4.19 in deuterated DMSO (400 MHz, 26 °C); it is an example for the hydrolysis of the pyridinium-functionalized side-group.	156
Figure A-14: Time-resolved ^1H -NMR of 4.20 in deuterated DMSO (400 MHz, 26 °C); it is an example for the hydrolysis of the imidazolium-functionalized side-group.	157
Figure A-15: Solubility tests of SM-100 and SM-100 based samples 4.1a , 4.12 , 4.14 , 4.19 to 4.21 and 4.24 to 4.29 ; the green fields show solubility, the red fields show insolubility, and the yellow fields represents the change from solubility to precipitation over time or increasing in concentration.	171
Figure A-16: Solubility tests of SM-50 and SM-50 based samples 4.2 and 4.30 to 4.32 ; the green fields show solubility, the red fields show insolubility, and the yellow fields represents the change from solubility to precipitation over time or increasing in concentration.	171
Figure A-17: Solubility tests of SM-25 and SM-25 based samples 4.3 and 4.33 to 4.35 ; the green fields show solubility, the red fields show insolubility, and the yellow fields represents the change from solubility to precipitation over time or increasing in concentration.	172
Figure A-18: Solubility tests of SM-15 and SM-15 based samples 4.4 and 4.36 to 4.38 ; the green fields show solubility, the red fields show insolubility, and the yellow fields represents the change from solubility to precipitation over time or increasing in concentration.	172

Figure A-19: Solubility tests of D_3D^H and D_3D^H based samples 4.5a and 4.39 to 4.41 ; the green fields show solubility, the red fields show insolubility, and the yellow fields represents the change from solubility to precipitation over time or increasing in concentration.	173
Figure A-20: Solubility tests of D^H_4 and D^H_4 based samples 4.6 and 4.42 to 4.44 ; the green fields show solubility, the red fields show insolubility, and the yellow fields represents the change from solubility to precipitation over time or increasing in concentration.	173
Figure A-21: Kinetic studies of sample 4.19 at different temperatures; the overall reaction follows second order; the y-axis contains the squared data.	174
Figure A-22: Static contact angles of quaternized products 4.19 to 4.21 , 4.30 to 4.44 and reference material (standard PDMS formulation); the standard deviations were calculated from two to three repetitions.	177
Figure A-23: Kirby-Bauer Test of brominated samples (4.1a to 4.13); the red bars symbolize the zone of inhibition in which the maximum number can be 45 mm due to the diameter of the petri dishes; the slightly red highlighted substrates are references; Bardac is a disinfectant containing Didecyl dimethyl ammonium chloride (DDAC).....	179
Figure A-24: Kirby-Bauer Test of quaternized products (4.19 to 4.38); the red bars symbolize the zone of inhibition in which the maximum number can be 45 mm due to the diameter of the petri dishes...	180
Figure A-25: Minimum Inhibition Concentration of SM-100 based samples 4.19 , 4.20 , 4.21 , 4.26 and 4.29 ; the green fields are clear solutions, so here the test substance is antimicrobially active, the yellow fields illustrate the beginning of growth and the red fields indicate growth of the molds and thus inactivity of the antimicrobial substance.	181
Figure A-26: Minimum Inhibition Concentration of SM-50 based samples 4.30 , 4.31 and 4.32 ; the green fields are clear solutions, so here the test substance is antimicrobially active, the yellow fields illustrate the beginning of growth and the red fields indicate growth of the molds and thus inactivity of the antimicrobial substance.	182
Figure A-27: Minimum Inhibition Concentration of SM-25 based 4.33 , 4.34 and 4.35 ; the green fields are clear solutions, so here the test substance is antimicrobially active, the yellow fields illustrate the beginning of growth and the red fields indicate growth of the molds and thus inactivity of the antimicrobial substance.	182
Figure A- 28: Minimum Inhibition Concentration of SM-15 based samples 4.36 , 4.37 and 4.38 ; the green fields are clear solutions, so here the test substance is antimicrobially active, the yellow fields illustrate the beginning of growth and the red fields indicate growth of the molds and thus inactivity of the antimicrobial substance.	183
Figure A-29: Minimum Inhibition Concentration of cyclosiloxane based samples 4.41 , 4.42 , 4.43 and 4.44 ; DMSO is tested as blank; the green fields are clear solutions, so here the test substance is antimicrobially active, the yellow fields illustrate the beginning of growth and the red fields indicate growth of the molds and thus inactivity of the antimicrobial substance.....	183
Figure A-30: ISO 22196:2011 test for the measurement of antibacterial activity on plastics and other nonporous surfaces; the test is evaluated after 24 hours (light blue bars) and 48 hours (dark blue bars); the samples are sorted by amines and descending number of side-groups; the reference and	

the blank are a standard PDMS formulations; the standard deviations were calculated from three repetitions.	184
Figure A-31: ^1H - ^{13}C -HSQC-NMR of 5.3 in deuterated chloroform (400 MHz, 25 °C); the overlapping of the signals of the halosilated and hydrosilylated products are shown; for reasons of simplification the methyl groups on the silicon have been grouped together as a ; signals b to h belong to the hydrosilylated group and signals i to m belong to the halosilated one.....	188
Figure A-32: GPC result of 5.3 in THF.	188
Figure A-33: Viscosity results of sample 5.3 and 5.5 ; both samples have a non-Newtonian behavior at 25 °C; the trend line is calculated by a power function; the first data point at 1.0 is not shown in the graph.....	191

Index of Tables

Table 1-1: Microorganisms commonly described in the literature; the microbes in bold are utilized in this study.....	5
Table 1-2: Test methods for antimicrobial properties and short description (adapted from ^[11a]).....	12
Table 3-1: Summary of the products 3.1a to 3.3b ; unless otherwise indicated, the desired conversion is 100% and the general reaction time is 24 hours; the yields are; the yields are calculated from the average of several experiments.	23
Table 3-2: Summary of the products 3.4 to 3.32 ; starting material, PPG wt-%, theoretically and experimental monomer unit, isolated yield and the Viscosity are listed; the yields are calculated from the average of several experiments.	24
Table 3-3: Summary of the parameter settings for the optimized synthetic pathway of half-converted polysiloxane propyleneglycol brush copolymers; Unless otherwise indicated, the desired conversion is 50 % and the general reaction time is 24 hours.	34
Table 3-4: Summary of the products 3.36 to 3.39 made from 3.34 (SM-25), PPG wt-%, theoretically and experimental monomer unit, isolated yield and the Viscosity are listed; the results will be compared to products 3.8 to 3.11	36
Table 4-1: Hazen Factor and Yellowness Index of sample 4.1a to 4.4 and 4.1b	47
Table 4-2: Summary of the products 4.7 to 4.11 in which the halogen source is varied; unless otherwise indicated, siloxane starting material is SM-100, the cyclic ether is THF and the general reaction conditions were used.....	54
Table 4-3: Summary of the products 4.12 to 4.18 in which the heterocyclic compounds are varied; unless otherwise indicated, siloxane starting material is SM-100, the halogen source is allyl bromide and the general reaction conditions were used.....	55
Table 5-1: Summary of the products 5.1 to 5.7 ; unless otherwise indicated, the ratio SiCH ₂ :SiOR is 1:1; the conversions and formed amounts were calculated by integration of ¹ H-NMR.....	79
Table 5-2: Viscosity results of the samples 5.1 to 5.7 ; the sample 5.6 and 5.7 follow the behavior of Newtonian liquids; n/d = not detectable.....	84
 Table A-1: Summary of the PHMS starting materials; the molecular masses, viscosities and ratio of hydridomethyl siloxane units and dimethyl siloxane units in different polysiloxane is given; the numbers are calculated by the molecular mass and arithmetically averaged.....	103
Table A-2: Summary of the products 3.1a to 3.3a ; unless otherwise indicated, the desired conversion is 100% and the general reaction time is 24 hours; the yields are calculated from the average of several experiments.	105
Table A-3: Summary of the products 3.4 to 3.32 ; starting material, PPG wt-%, theoretically and experimental monomer unit, isolated yield and the Viscosity are listed; the yields are calculated from the average of several experiments.	108
Table A-4: Summary of the contact angles of the products 3.1a to 3.32 ; standard PDMS and PPG are added for comparison reasons; samples were cured into a standard PDMS formulation with an amount of 10% (s. Scheme A-2); the standard deviations were calculated from two to three repetitions.	125

Table A-5: Summary of the contact angles of the products 3.1a to 3.32 ; samples were cured in a homogeneous pure film (s. Scheme A-1); the standard deviations were calculated from two to three repetitions.	126
Table A-6: Data of the kinetic studies of 3.1a were calculated via integration of the $^1\text{H-NMR}$ analytics; unfilled rows were not measured due to the individual monitoring at each temperature, the equations are based on the slope of the trend line of the logarithmic plotted diagram (s. Figure 3-9).....	128
Table A-7: Data of the Anti-Adhesion Assay of sample 3.20 which was cured into a PDMS standard formulation with different amounts ranges from 0.5 to 80%.	129
Table A-8: Data of the Anti-Adhesion Assay of samples which were cured into a PDMS standard formulation with an amount of 10 %; n/s = not specified; the standard deviations were calculated from three repetitions.	130
Table A-9: Summary of the parameter settings for the optimized synthetic pathway of half-converted polysiloxane propyleneglycol brush copolymers; unless otherwise indicated, the desired conversion is 50 % and the general reaction time is 24 hours.	133
Table A-10: Summary of the products 3.36 to 3.39 made from 3.34 (SM-25), PPG wt-%, theoretically and experimental monomer unit, isolated yield and the Viscosity are listed; the results will be compared to products 3.8 to 3.11 ; the standard deviations were calculated from two to three repetitions.	134
Table A-11: Summary of the products 4.1a to 4.6 ; unless otherwise indicated, the desired conversion of SiH groups is 100 % and the general reaction time is 24 hours; the yields are calculated from the average of several experiments.	137
Table A-12: Data of the kinetic studies of 4.1a calculated by integration of the $^1\text{H-NMR}$ analytics; the equations are based on the slope of the trend line (s. Figure A-9).	144
Table A-13: Data of the kinetic studies of 4.1b calculated by integration of the $^1\text{H-NMR}$ analytics; the equations are based on the slope of the trend line of the logarithmic plotted diagram (Figure A-10).	145
Table A-14: Summary of the contact angles of the products 4.1a to 4.6 ; standard PDMS is added for comparison reasons; samples were cured into a standard PDMS formulation with an amount of 10 % (Scheme A-2).....	146
Table A-15: Summary of the products 4.7 to 4.11 in which the halogen source is varied; unless otherwise indicated, siloxane starting material is SM-100, the cyclic ether is THF and the general reaction conditions were used.	147
Table A-16: Summary of the products 4.12 to 4.18 in which the heterocyclic compounds are varied; unless otherwise indicated, siloxane starting material is SM-100, the halogen source is allyl bromide and the general reaction conditions were used.	150
Table A-17: Summary of the products 4.19 to 4.44 ; unless otherwise indicated, the starting materials were made with THF and the general reaction time is 24 hours; 1-methyl-1H-imidazole and 1-butyl-1H-imidazole are shortened to Me-Imi and Bu-Imi; the yields were calculated from several repetitions.	153
Table A-18: Solvent-Screening of Samples 4.19 , 4.20 and 4.21 ; conversions and comments are added.	170

Table A-19: Data of the kinetic studies based on integrals of the ^1H -NMR analytics; the equations are based on the slope of the trend line (s. Figure A-21); the standard deviations were calculated from two to three repetitions.	175
Table A-20: DSC measurements of quaternized products and starting materials and halosilated intermediates for comparison reasons; results which T_g is outside of the measuring range are marked with “below -75 °C”; the standard deviations were calculated from two to three repetitions.	176
Table A-21: Summary of the contact angles of the products 4.19 to 4.21 and 4.30 to 4.44 ; standard PDMS is added for comparison reasons; samples were cured into a standard PDMS formulation with an amount of 10% (s. Appendix A2).	178
Table A-22: Data of the ISO 22196:2011 test for the measurement of antibacterial activity on plastics and other nonporous surfaces; the samples are sorted by amines and descending number of side-groups; the reference and the blank are a standard PDMS formulations; the standard deviations were calculated from three repetitions.	185
Table A-23: Summary of the products 5.1 to 5.7 ; unless otherwise indicated, the ratio $\text{SiCH}_2\text{:SiOR}$ is 1:1; the conversions and formed amounts were calculated by integration of ^1H -NMR.	186
Table A-24: Viscosity results of the samples 5.1 to 5.7 ; the sample 5.6 and 5.7 follow the behavior of Newtonian liquids.	191
Table A-25: Rheological data of the samples 5.3 and 5.5 at 25 °C; both samples have a non-Newtonian behavior.	192

1 Introduction

Silicones have great importance in the chemical society, but also in popular science and our everybody products. Silicone chemistry has a long history and is part of organic chemistry. It deals with the chemistry of certain organic derivatives of the element silicon (Si, atomic number 14). Silicon in pure form was first discovered by Berzelius^[1] and Friedel and Craft synthesized the first silicon organic compound tetraethylsilane in 1863.^[2] Its great importance is due to the English chemist Frederick Stanley Kipping. Between 1899 and 1944 he coined the term 'silicone' as he thought that his siloxanes were the silicon analogues of ketones. He also researched and described the characteristics of silicones in 'The Bakerian Lecture. Organic Derivatives of Silicon' and opened the way for silicone chemistry.^[3]

In 1940s, Eugene G. Rochow and Richard Müller reported independently the up to now most common technology for preparing chloromethylsilanes on an industrial scale, which are very important starting materials for silicones.^[4] It is called direct process or Müller-Rochow process. In general, chloromethane reacts with powdery silicon in presence of 5-10% Copper (in form of CuO) to form a mixture of chloromethylsilanes. They can be separated by distillation or the formation of main product can be promoted by addition of 0.1-1% of electropositive metals (e.g. Ca, Mg, Zn, Al). Silanols can be formed by consecutive hydrolysis. These silanols can further condensate to silicones. The driving force of hydrolysis is the high Si-O binding energy ((Si-C) = 381 kJ/mol, (Si-O) = 452 kJ/mol).^[4-5] Up to now, there are different theories about the exact mechanism.^[6]

Today the more precise label poly(organo)siloxanes is used in literature because of the wide range of silicone classes. The general formula of linear poly(organo)siloxanes is $R_3Si-[O-SiR_2]_n-O-SiR_3$ (R = e.g. H, alkyl, aryl, halogens). As it is shown in Figure 1-1, the siloxane unit $[O-SiR_2]$ of linear polymers is called D-unit, because it contains two connections to oxygen. Branched poly(organo)siloxanes or three dimensional oligomeric or polymeric networks contain mostly T- und Q-units. This is a difference to silanes, in which the silicon atoms are connected directly to each other or to other atoms,^[7] such as carbon or further heteroatoms. Unlike carbon, silicon has a very low electronegativity, so Si-O bonds have a strong single-sided electron distribution. In addition, siloxanes have a high torsional flexibility due to the differences between the Si-O-Si (145°) and O-Si-O (110°) bond angles.^[8] The M-unit is also known as end-group of a poly(organo)siloxane, because there is no possibility of further siloxane chain growing.^[9]

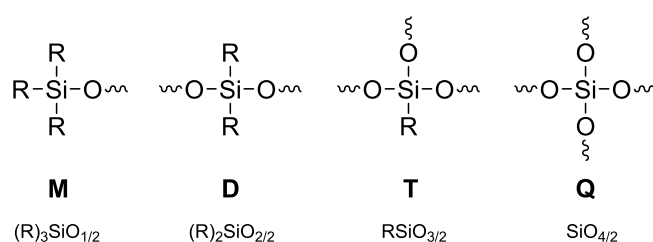


Figure 1-1: Shorthand notation for siloxane polymer units; R could be e.g. H, alkyl, aryl or halogens, but no oxygen.

In the last decades, silicone chemistry raised and gained more and more importance. So the number of publications increased as well, as seen in Figure 1-2 (limited to the last 20 years). Nowadays, silicones are used in nearly every application field. Their outstanding properties can differ for the individual product groups. The most important representative for silicones is polydimethylsiloxane (PDMS). Silicones contain special properties like electrical insulation or conduction. They are inert against high and/or low temperatures, weather and UV exposure, as well as oil and hot-air contact. Furthermore, they resist dynamic stress and show good flame resistance, arcing resistance and gas permeability. Silicones can be used for contact with foods and living tissue, adhesive surfaces or transparent articles of high optical quality. They also benefit from low cost, high durability and flexibility, ease of fabrication and self-healing properties, as well as oxygen permeability, biocompatibility and biodurability.^[9f, 9g]

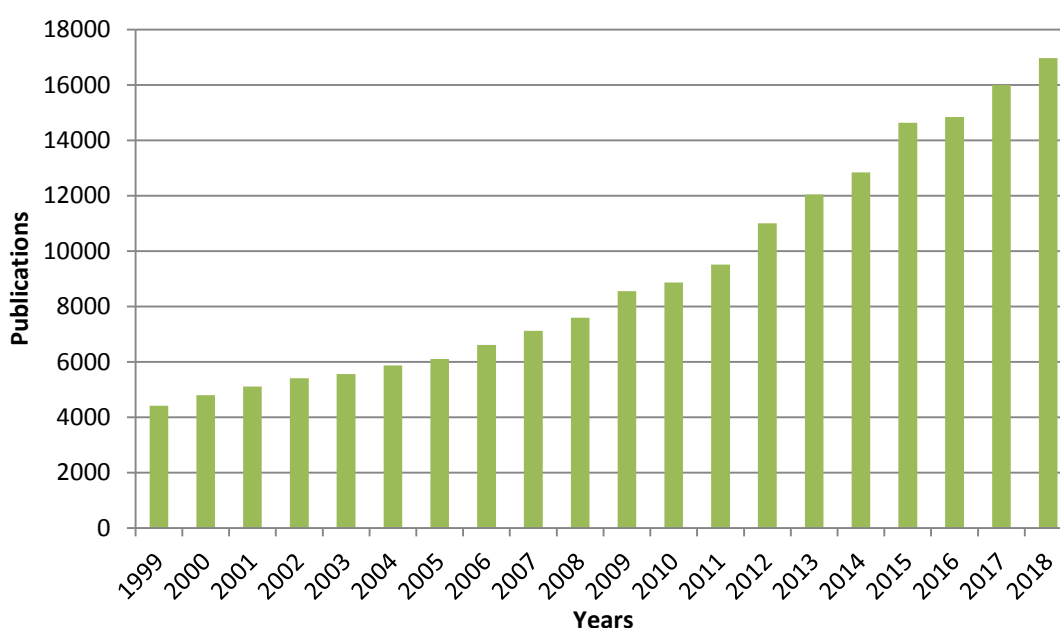


Figure 1-2: Development of publications containing “silicone” during the last two decades (Scifinder, January 2019).

In general, silicones are important materials for industrial application, such as water repellents, manufacturing textiles, leather goods, paper, antifoams or softeners. They are also utilized in products for personal care and households, for example conditioners (hair-care products), softeners (skin-care products), additives in polish formulations, water proofers, as well as products for automotive industry.^[9f, 9g]

Silicones in medical applications get more and more important. Due to the mentioned properties, such as self-healing properties, biocompatibility and biodurability, as well as the easy introduction of new properties, silicones are a helpful starting material. They are utilized as implants in beauty treatments or plastic surgery, in dental application fields and in internal medicines.^[10] Hygienics in clinical environments are very important to avoid diseases, epidemic plaques or pandemics. These problems are provoked by bacteria, viruses or other microorganisms like fungi or worms. But also in our daily life, bacterial or mildew infestations are problematic, such as in household (bathrooms, showers,

corners in windows), air conditioning systems (filters, aeroplanes), water taps, as well as waste water systems, textile industry, nonfouling paintings or food packaging.^[11]

Therefore, silicones establish a basis for antimicrobial active compounds due to their inherent properties, as well as the possibility of introducing new ones. The development of such silicones has to deal with new antimicrobial properties, which lower the growing of microorganisms, but do not affect the silicone properties.

1.1 Microorganisms

Microorganisms, in short microbes, are microscopic organisms (cells), which live single-celled or they form colonies. The existence of microbes was supposed long time ago, but first observations under the microscope were reported by Antonie van Leeuwenhoek in the 1670s.^[12] In the 1850s, Louis Pasteur discovered that food spoilage is caused by microorganisms, which shows their great importance in our daily live. Together with Ferdinand Cohn and Robert Koch, Pasteur is known as the "father of microbiology".^[13]

Microorganisms can be split into prokaryotes and eukaryotic organisms. Prokaryotes are unicellular organism, such as archaea and bacteria, which do not contain a membrane-bound nucleus, mitochondria, or any other membrane-bound organelles. In contrast, species with nuclei and organelles are eukaryotes. Eukaryotes include fungi, protozoa, eukaryotic algae, as well as plants and animals.^[14]

There are uncountable numbers of small cells. It is estimated, that there are at least 10^{14} bacteria in the human body, which are essential for survival. Most are located in the gastro-intestinal system and support the alimentary system. There are a lot of beneficial microorganisms, for example in geochemical application fields (nitrogen cycle, N_2 -fixation, waste water treatment), in food industry (brewing, cheese factory), as well as in biotechnology to produce pharmaceuticals (antibiotics, such as penicillin, or insulin) or in pest control.^[15] But there are also many pathogenic microorganisms, which can infest humans (for example see Figure 1-3). They can be found in medical equipment (healthcare and medical devices for internal or partially internal use; e.g. from artificial hearts, breast implants, catheters, to orthopedics and prosthetics or pharmaceutical applications) or on hospital surfaces. Biofouling on medical devices generally causes adverse complications, such as thrombosis, infection, and pathogenic calcification. Microbes also cause biofouling on food (human and pet food, drinks, agrochemistry, manufacturing and supply), so demanding regulations like FDA (Food and Drug Administration) approvals exist.^[16] Special diligence should also be necessary in sanitary areas or in wet environments (bathroom, air conditioning, clean rooms or plumbing fixtures and swimming pools), with "hygiene requiring devices" (such as vacuum cleaners, kitchen equipment or products, refrigerators, air filters) and construction materials (door hardware, grout, tile, surface coatings etc.), or consumer materials (elevator buttons, sinks, transportations, office and school products, computer keyboard, shoes, textiles etc.).^[17]

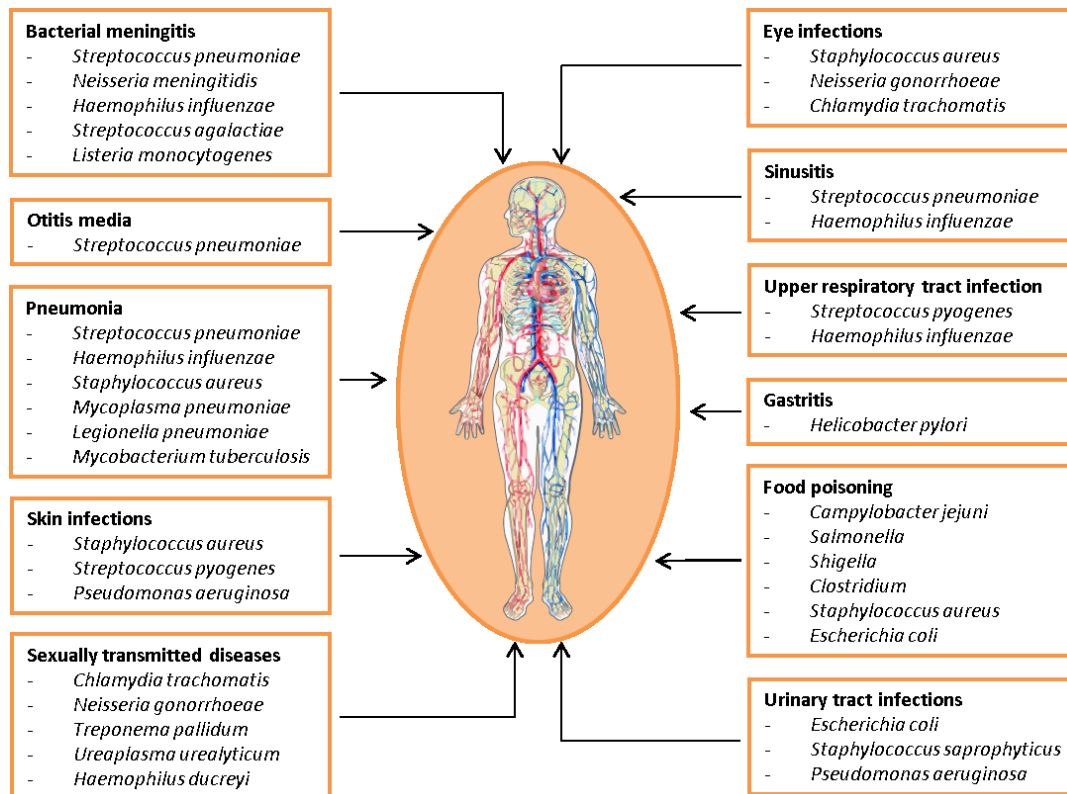


Figure 1-3: Overview of bacterial infections in the human body (adapted from ^[11]).

Besides the great variety of cells, there are some structural characteristics, which have all cells in common. All cells contain a thin membrane (cell wall and cytoplasmic membrane), which holds the cell together and separates it from its environment. This cytoplasmic membrane is selective permeable to create a mass exchange into or out of the cell. In general, this cytoplasmic membrane contains a lipid bilayer with some proteins. Furthermore, the cell contains the cytoplasm, in which most of the enzyme catalyzed reactions of the cell metabolism take place. Ribosomes are located in the cytoplasm, which are responsible for the protein synthesis. At least every cell contains besides a cell wall either a nucleus, or a core zone, in which the genetic material can be replicated (DNA, short for deoxyribonucleic acid).^[14b]

Bacteria and molds, which are often used in literature for antimicrobial tests, are shown in Table 1-1. The microbes written in bold are utilized in this report. Among others, methicillin-resistant *Staphylococcus aureus* (MRSA) and *Pseudomonas aeruginosa* are both known as hospital bugs.

Table 1-1: Microorganisms commonly described in the literature; the microbes in bold are utilized in this study.

Gram-negative bacteria	Gram-positive bacteria	Fungi
<i>Acinetobacter baumannii</i>	<i>Bacillus subtilis</i>	<i>Aspergillus brasiliensis</i>
<i>Aeromonas hydrophila</i>	<i>Enterococcus faecalis</i>	<i>Botrytis cinerea</i>
<i>Enterobacter aerogenes</i>	<i>Enterococcus hirae</i>	<i>Candida albicans</i>
<i>Escherichia coli</i>	<i>Lactococcus lactis</i>	<i>Candida glabrata</i>
<i>Halomonas pacifica</i>	<i>Rothia dentocariosa</i>	<i>Candida krusei</i>
<i>Klebsiella pneumoniae</i>	<i>Staphylococcus aureus</i>	<i>Candida parapsilosis</i>
<i>Porphyromonas endodontalis</i>	<i>Staphylococcus capitis</i>	<i>Candida tropicalis</i>
<i>Prevotella nigrescens</i>	<i>Staphylococcus epidermidis</i>	<i>Exophiala dermatitidis</i>
<i>Proteus mirabilis</i>	<i>Streptococcus salivarius</i>	<i>Fusarium oxysporum</i>
<i>Proteus vulgaris</i>	<i>Streptococcus sanguis</i>	<i>Penicillium spec.</i>
<i>Pseudomonas aeruginosa</i>	<i>Streptococcus thermophiles</i>	<i>Rhizoctonia solani</i>
<i>Pseudomonas mirabilis</i>	<i>Streptomyces spec.</i>	

1.1.1 Structural Features of Bacteria

The name bacteria originate from the Greek βακτήριον (bakterion) and means rods. This is caused by the shape of bacteria (mostly rods, coccuses or filaments). Today there are round about 5×10^{30} bacteria on Earth,^[18] which belong to the domain of prokaryotic microorganisms. In 1976 C.R. Woese described two different kingdoms; archaeobacteria and eubacteria.^[19]

Bacteria are composed of one cell, so proliferation is an asexual reproduction via cell division. They contain a cell wall, which surrounds the cytoplasmic membrane, and a nucleus without a nuclear membrane. The cell wall protects the bacteria against bursting due to osmotic pressure and stabilizes their structural shape. Different than mostly expected, the cell wall is not the same than the cytoplasmic membrane. Both are essential for the survival of bacteria due to the selective permeability, which allows a controlled mass exchange into or out of the cell. Antimicrobial active compounds get in contact with the cell wall or cytoplasmic membrane first, so the following gives a closer look to their structural compositions.^[14a]

In general the cytoplasmic membrane consists of a lipid bilayer with some proteins (s. Figure 1-4). The lipid bilayer is a polar membrane made of two layers of lipid molecules, which is only a few nanometers thick.^[20] Lipids are amphiphilic compounds, which possess both, a hydrophilic (polar) head and a lipophilic (nonpolar) tail (mostly hydrocarbon chains). Due to the lipid bilayer's impermeability to most water-soluble, hydrophilic molecules and its particularly impermeability to ions, the cell is able to regulate osmotic pressure, salt concentrations and pH, acid-base-balance and adhesion and excretion of substances by transporting ions across their membranes using proteins (ion pumps). The cell wall of bacteria is 150-350 Å thick. The construction of the cell wall can differ, so bacteria are split into Gram-negative and Gram-positive ones. Both contain an inner membrane, called murein (lat. murus = wall), which is in contact with the cytoplasmic membrane. The murein layer

consists of peptidoglycans (polysaccharide-peptide complexes), made of polysaccharide chains made from alternating *N*-acetylglucosamine and *N*-acetylmuramic acid. *N*-acetylglucosamine is connected to a pentapeptide, which can form networks with other polysaccharide chains. The murein layer of Gram-positive bacteria is a large-meshed layer and constitutes 10 to 50% of the cell wall. Gram-negative bacteria have a much smaller murein layer (10% of the cell wall). Furthermore, there is an outer membrane. This second lipid bilayer has embedded lipoproteins, lipopolysaccharides and polysaccharides. Lipopolysaccharides act as permeability barrier, stabilize the cell and protect the cell against toxins, antibiotics or infections. In addition there are porins, which are vesicular proteins, which regulate the mass transport as well. ^[14a, 20-21]

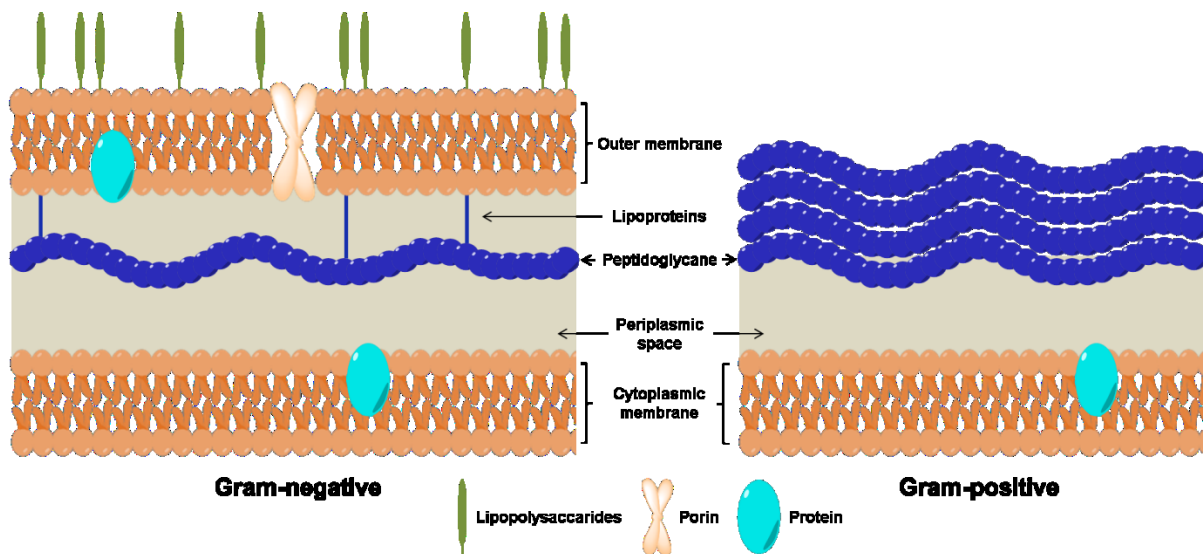


Figure 1-4: Sketch for the gram-negative and gram-positive bacteria wall.

Most bacteria cell walls contain among others phosphatidylethanolamine. This compound belongs to the group of lipids. It ranges up to 70% of the lipid bilayer and provides a negatively charged membrane. ^[22]

1.1.1.1 Adhesion Properties of Bacteria

The adhesion mechanism on different surfaces is a complex process. In fluent environments, bacteria were able to adhere at a certain place, to gain different essential nutrients maintaining their own metabolism. There is a big correlation between bacteria adherence and wettability of surfaces, so bacteria effectively adhere onto polymer surfaces with water contact angles of 40 – 70 °. ^[23]

First of all it is an electrostatic and hydrophobic effect. The bacteria are able to adhere with their electrically charged cell wall due to the phosphatidylethanolamine, as well as hydroxyl groups. This interaction depends on the electrostatic properties and composition of the different surfaces. ^[23-24] Some gram-negative bacteria produce extracellular polymeric substances (EPS), which are secretions made from exopolysaccharides and peptides of high molecular masses as well as specialized cell-wall proteins. These fimbriae (adhesins) are able to adhere on one another, animal cells or some inanimate objectives. A fimbria is an appendage (3-10 nanometers in diameter and up to several micrometers long) and contains proteins. ^[24a, 25]

1.1.2 Structural Features of Molds

Molds (or mildews) are counted among the eukaryotic organisms, which possess a membrane-bound nucleus and mitochondria.^[26] They belong to the thallophytes, which are multicellular fungi. As opposed to plant cell cultures, molds are not able to gain energy through photosynthesis. Molds exist in diverse habitats, depending on their physical and biological properties.^[15]

In comparison to bacteria, the fungal cell wall is structurally unique and also differs from the cellulose-based plant cell wall. It is made of chitin, glucans, and glycoproteins in the main, which are covalently cross-linked together (similar to insects). This cross-linking is a dynamic process that occurs extracellularly. The cell wall must protect the mold against osmotic pressure, while it has to retain its plasticity for cell growth, cell division and the formation of a great number of cell types during the fungus' life cycle. It is also a signaling center to activate signal transduction pathways within the cell, as well as interaction with its surroundings.^[27]

Glucan is the major structural polysaccharide of the fungal cell wall (50-60%). It mainly consists of beta-1,3-glucan, which gives the backbone to which other components can covalently bind. Chitin occurs with a range of 1-2% or 10-20% in the fungal cell wall, according to whether the mold is a filamentous fungus. It is a long linear homopolymer of beta-1,4-linked *N*-acetylglucosamine, which forms a crystalline polymer due to hydrogen bonding and is able to provide the structural integrity of the cell wall due to its great tensile strength. Fungal cell walls further consist of glycoproteins (such as mannose, which are mostly modified with N-linked and O-linked oligosaccharides. Their amount ranges between 15-50%, relative to the fungi. Besides unexpected proteins, whose function is not known yet, traditional cell wall proteins' functions include among others the maintaining and protection of the cell shape, mediation adhesion of migration or fusion steps, transmitting intracellular signals and the synthesis of cell wall components.

Unlike bacteria, molds reproduce sexually via growth phase and proliferative phase (shown in Figure 1-5), although an asexual reproduction is possible as well. Flying spores adhere to a suitable surface and start to grow. This germination is the start of the growing phase. The spores grow up to hyphae (hyphal growth). These hyphae are elongated filaments, which can be divided (septated) or non-divided. Hyphae grow on the forefront, although branching through growing on the lateral walls is also possible. Anastomosis is the confluence of two separated hyphae (merging). These merging and branching form a reticular network, which is called mycelium. Molds form their multicellular filaments on the surface of substrates (surface mycelium) or inside of the substrates (substrate mycelium). These filaments can be observed as some colored points in the substrate over time and it can start to smell moldy. Only in good living conditions (mostly in warm and humid environments) and with a sufficient food availability (organic components, such as carbohydrates, fats, proteins) the mold changes to the proliferative phase. Here the spores are formed, which are determined as fluffy surface. The sporulation is the properly generative step. During sporulation spores (2 - 20 µm) are spread into the environment to form new colonies.^[15, 27-28]

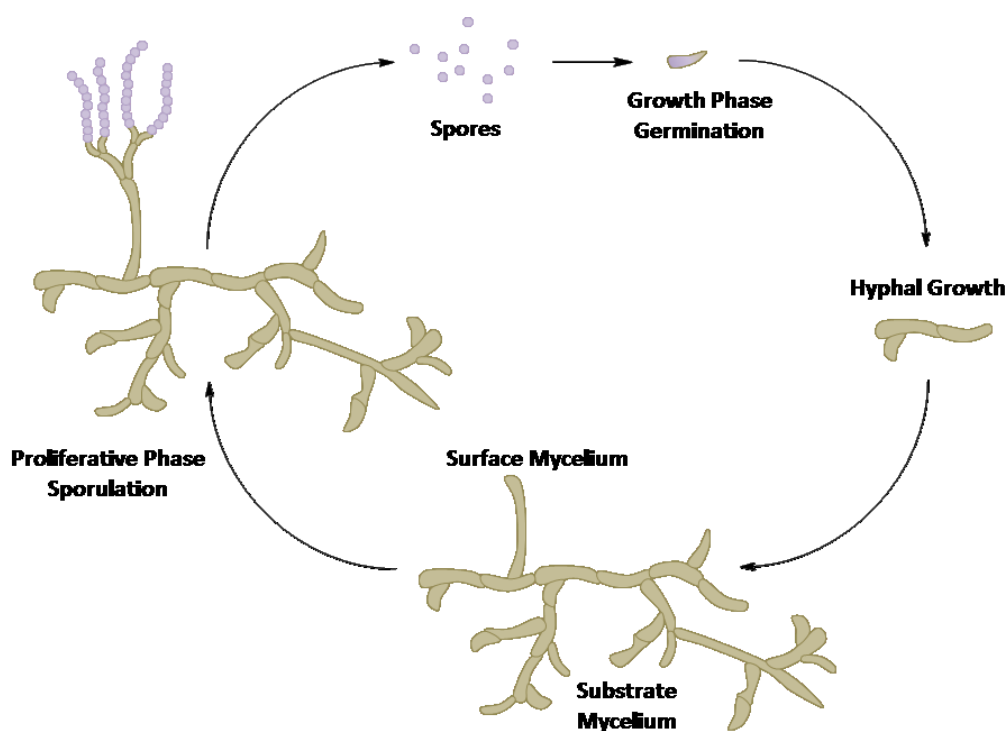


Figure 1-5: Reproductive cycle of molds with growth phase and proliferative phase.

1.2 Polymers containing Antimicrobial Properties

The development of antimicrobial active compounds was increasing a lot in the last two decades. As it is shown in Figure 1-6, the number of publications containing “antimicrobial” increased from around 5000 to more than 30000 in 2018. Compared to that, the number of publications containing “antimicrobial + silicone” increased as well, but in a much smaller scale, up to 130 publications in 2018.

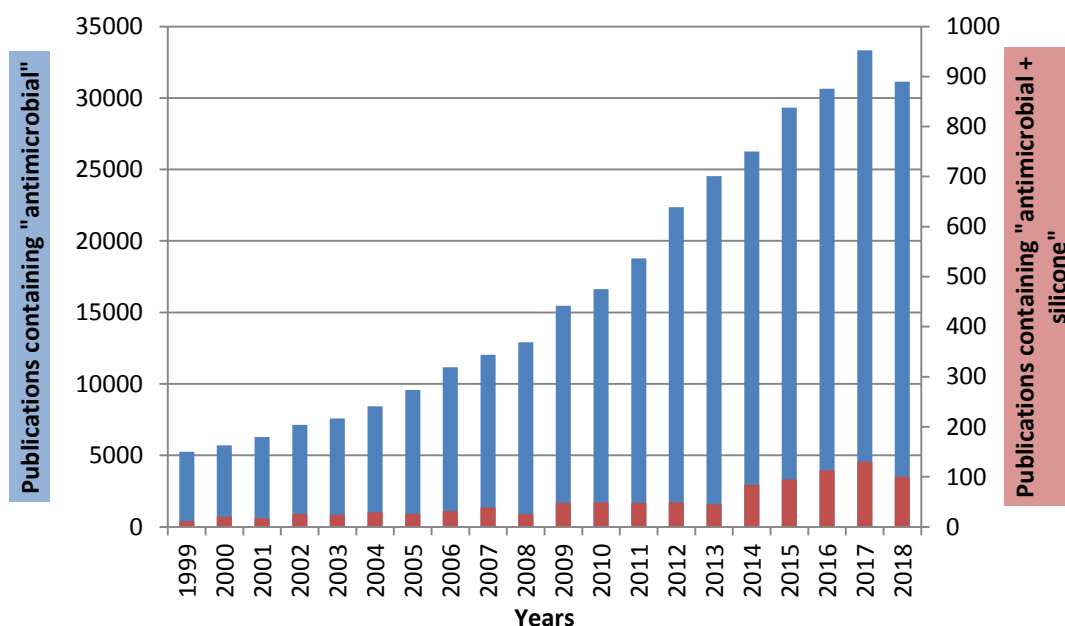


Figure 1-6: Development of publications containing “antimicrobial” and “antimicrobial + silicone” during the last two decades (Scifinder, January 2019).

During the last decades, comprehensive reviews dealing with antimicrobial polymeric and non-polymeric materials have appeared in the specialized literature.^[10a, 10d, 22, 29] These accounts are sorted either by the type of antifungal agents, the active functional groups or by the polymeric matrix.

At the beginning of this work, a review was written, which deals exclusively with antimicrobial silicones.^[11a] Silicones are some of the most common polymeric materials in several application fields and the review gives an ample overview about silicones with antimicrobial activity according to its preparation method, including physical treatments (layer-by-layer, incorporation, swell-encapsulation), chemical treatments (hydrosilylation, ring-opening polymerization, condensation, plasma) and copolymerizations (grafting onto, grafting from). The development of these materials requires the introduction of biocide activity, which either hampers the growing of microorganisms or kills them, while showing long-term stabilities and not affecting their elastomeric properties.

In general there are four different ways to introduce antimicrobial activity to polymers, especially silicones; 1) polymers with covalently bonded functional groups, such as quaternary ammonium salt groups (QAS),^[30] 2) polymers containing metallic nanoparticles or oxides,^[31] 3) antimicrobial polymers which affect the surface energy^[32] and 4) polymers with some other additives, mostly inhibitors.^[33]

Up to now, the structural reasons for antimicrobial activity are not discovered and understood completely. There are several reports about the structure-activity relationship, but the prediction of newly developed compounds is not possible yet. For example, the replacement of a group, which seems to be not involved into the effect mechanism, can already change the antimicrobial activity. In addition, due to the different structures of bacteria and molds, the antibacterial activity can differ from the antifungal activity. Most reports are about antibacterial agents, so there is little known about antifungals.

Quaternary ammonium salts (QAS) are the biggest group of antimicrobial compounds. They are able to kill a wide range of microorganisms including Gram-positive and Gram-negative bacteria, yeast and molds. The highly positive charged density of the QAS can exert a strong electrostatic interaction with the negatively charged cell membrane of the bacteria. They can adhere and diffuse through the cell wall. Due to exchange of protons with Ca^{2+} and Mg^{2+} of the cell wall, as well as the releasing of potassium and other constituents out of the cell wall, the cell dies.^[22, 34] Although QAS containing polymers are the most developed antimicrobial compounds, they contain the drawback of uncontrolled leaching of antimicrobial compounds. Furthermore, antibacterial resistances can arise. Further information about QAS and their synthetic pathways are given in chapter 4.

Polymeric-based materials with antimicrobial inorganic systems can contain silver,^[35] copper^[36] or gold nanoparticles^[37], as well as oxides such as titanium dioxide,^[38] chloride dioxide, zinc oxide,^[39] or nitric oxide.^[40] There are some studies that the metal ions from the nanoparticles can interact with the mold surfaces and causes cell death due to the destabilization of the charge balance or they generate pits in the outer membrane which results in necrosis.^[38a] Other nanoparticles, such as silver, are able to bind to proteins and cause structural changes in the cell wall and also in the nuclear membranes. The ability to form complexes with the bases of RNA and DNA inhibits the microorganism replication.^[22, 30e, 35, 37, 41] The highly active metal ions can be formed due to humidity, as well as by the action of light.

There is also another category of Light-Activated Antimicrobial Agents (LAAAs), such as Crystal Violet, Methylene blue or Toluidine blue. They form Reactive Oxygen Species (ROS), upon a transition from their low energy ground state (singlet) to higher triplet state. There are two different mechanisms. In type I reaction, the ROS reacts with biomolecules to generate free radicals. This results in membrane damage due to the formation of lipid hydroperoxides and hydroxyl radicals that may react or combine with biomolecules to generate cytotoxic hydrogen peroxides in situ. In type II reaction, (which is known as main pathway) the molecular oxygen generates highly reactive singlet oxygen and this may oxidize many biological structures including proteins, nucleic acids and lipids.^[22]

In general polymers containing nanoparticles or oxides show quite often problems with health policies due to the high toxicity of these compounds.

Inhibitors or other additives, which are just mixed into the polymer, can attack the microbes due to their special structure. So they do targeted killing by attacking a special protein, enzyme or DNA/RNA. Polydopamin attacks the anionic cell wall,^[42] while phenols are able to liquidate the cell wall.^[22] Amphotericin B increases the permeability of the cell by demethylation of lanosterol and disruption of fatty acid oxidation and chitin synthesis.^[43] These compounds are very important for building a new cell membrane. Neuraminic acid is known as inhibitor of neuraminidase,^[22] while Cilofungin and Nikkomycin can inhibit the beta3-Glucan synthase and Chitin-synthase.^[43b] Azoles, such as imidazole, miconazole, ketoconazole, triazole, fluconazole or itraconazole can interact with the cytochrome p-450. This disturbs the liver enzymes, which causes increasing of intracellularly cytotoxic compounds.^[15] Furanoses does not attack the cell itself, but they are able to interfere with the cell-to-cell communication pathways and block the Quorum sensing (cell communication of bacteria via signal molecules). The cells are not able to form colonies anymore, so bioformation is not possible.^[29a]

Polymers which affect the surface energy show no antimicrobial activity *per se*. They are not able to attack or to kill microbes. But they are able to change the surface energy to form superhydrophobic, as well as superhydrophilic surfaces.^[44] In both cases, the microbes cannot adhere to the surface and biofilm formation is reduced. Bacteria effectively adhere onto polymer surfaces with water contact angles of 40–70°.^[23] Superhydrophobic surfaces imitate the lotus leaves (so-called lotus-effect) and have a contact angle (CA) more than 150°. The lotus-effect is known from the leaves of the Nelumbo or “lotus flower”. The leaves contain self-cleaning properties due to the roughness of the leaves’ surface.^[45] Superhydrophilic surfaces, however have a water CA less than 30°. Further information about their synthetic pathways and testing methods are given in chapter 3.

1.2.1 Possible Weak Points for Antifungal active Compounds

As it is already mentioned, the exact mechanism of antimicrobial activity is often not discovered and understood completely. Not only the structure-activity relationship has to be developed further, but also antifungal activity is not as developed as the antibacterial one. There are three weak points of molds known, which are shown in Figure 1-7. Due to the rate of reproductive cycle, molds gain currency by spores. First weak point would be the avoidance of adhesion. The germination of molds just starts after adhesion on suitable surfaces. Second weak point would be the hindrance of growing itself. Here, mainly antifungal components are utilized, which inhibit the synthesis of fungal cell wall components, for example inhibition of chitin synthase or glucan synthase.^[43b] Last weak point would be to stop the proliferative phase (sporulation) due to the creation of an uncomfortable environment. Molds just start sporulation only in good living conditions (mostly in warm and humid environments) and with a sufficient food availability.^[28]

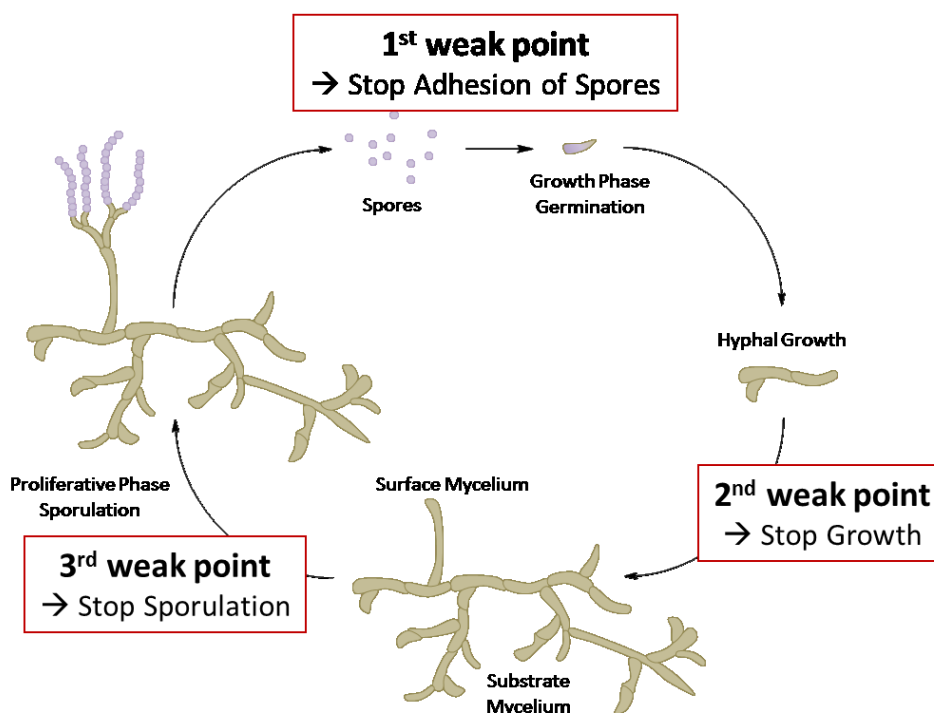


Figure 1-7: Schematic representation of antifungal activity; avoiding adhesion of spores, growing and/or sporulation.

1.2.2 Testing Methods for Antimicrobial Agents

There are several antimicrobial testing methods known in the literature with a wide range of assay conditions and the great number of microbes which were used as test strains. So it is hardly possible to name the most important testing methods in literature.

Table 1-2 gives an overview about the most common ones.^[46] Although there are standardized testing methods, research groups report a great number of different methods.

Table 1-2: Test methods for antimicrobial properties and short description (adapted from ^[11a]).

Test Method	Description
<i>Kirby–Bauer technique</i>	Agar diffusion test of the antibiotic sensitivity of bacteria, in which the extent to which bacteria are affected by antibiotics are tested on antibiotic-impregnated wafers.
<i>Minimum Bactericidal Concentration (MBC)</i>	Detection of the lowest concentration at which an antimicrobial agent will kill a particular microorganism.
<i>Minimum Inhibitory Concentration (MIC)</i> ^[47]	Detection of the lowest concentration of an antimicrobial agent that prevents visible growth of bacteria.
<i>Contact angle (CA) measurement</i> ^[a]	Characterization of the wettability of surfaces (superhydrophobic (>150°) and superhydrophilic surfaces (<30°)); calculation standards by Wenzel and Cassie-Baxter.
<i>Cell attachment method</i>	Can be split into two tests; (I) attachment assay, which employs a colorimetric detection of bound cells, and (II) spreading assay, which employs phase contrast microscopy to measure the flattening of adherent cells.
<i>Crystal violet assay (life-dead staining)</i>	Quick and reliable screening method cell inhibition and death; crystal violet binds to proteins and DNS only of living cells.
<i>ISO 22196:2011</i> ^[48]	Measurement of antibacterial activity on plastics and other non-porous surfaces.
<i>EN ISO 846:1997</i> ^[49]	Evaluation of the action of microorganisms on plastics; (I;II) detection of plastics' resistance against fungi and fungicidal activity; (III) detection of plastics' resistance against bacteria; (VI) detection of plastics' resistance against ground containing microorganisms.
<i>ASTM E2149</i>	"Shake Flask" test for antimicrobial objects and textiles; detection the antimicrobial activity of antimicrobial agents under dynamic contact conditions.

^[a] Although it is no antimicrobial test method *per se*, CA is an important parameter on anti-biofilm preparations

2 Objectives and Motivation

The progress of the society's technological advancement and the high medical standard make it more and more important, to implement novel functionalities into given applications. Siloxanes are helpful starting materials for antimicrobial compounds. Their inherent properties, such as self-healing properties, biocompatibility and biodurability, as well as the easy functionalization, make them very interesting for further developments.

Hence, this research is focused on the functionalization of siloxanes to form antimicrobial silicones for industrial applications and patents. In the best case, these antimicrobial active siloxanes should show a long-term stability of antimicrobial activity, as well as the antimicrobial activity should be resistant against curing systems (for example in bathroom applications). Furthermore, the combination of two systems to form a bi-functional siloxane leads to a better versatility, as well as uniqueness. Figure 2-1 shows the schematic structure and the interdependence of the individual parts of this research.

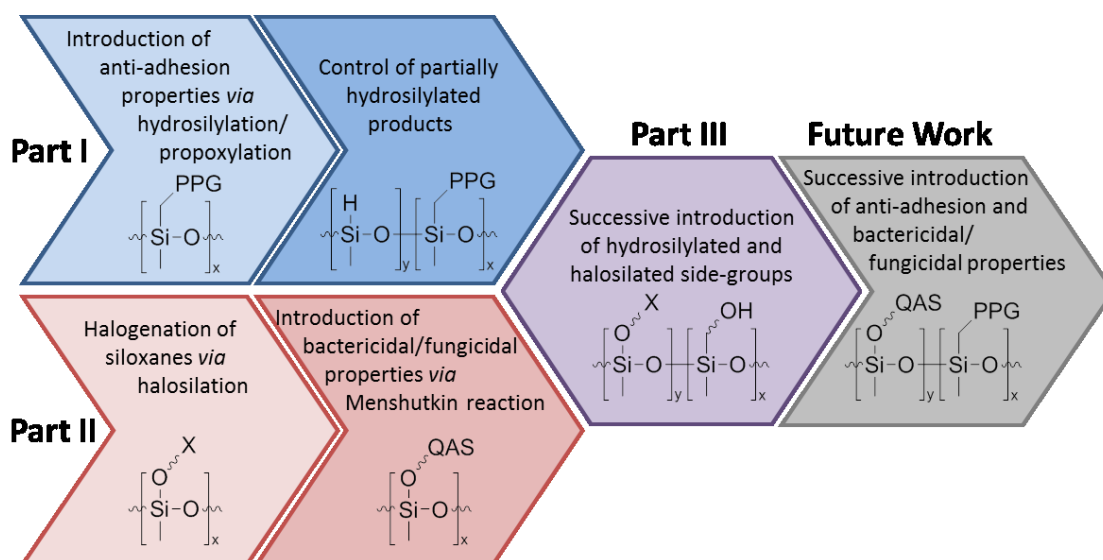


Figure 2-1: Charting of the schematic structure of this thesis; PPG = polypropylene glycol; X = Br, Cl; QAS = quaternary ammonium salts.

In Part I (blue boxes in Figure 2-1), the integration of anti-adhesion properties due to polypropylene glycol (PPG) side-chains is in focus. The integration of hydrophilic side-groups leads to the control of surface energy, which can have an effect on the microbes' adhesion (chapter 3).

Part II (red boxes in Figure 2-1) deals with the integration of bactericidal and fungicidal properties into siloxane compounds. The desired products show antimicrobial activity due to quaternary ammonium salt groups (QAS) and so this is a direct way to reduce microbes (chapter 4).

This report also covers the preparative work of the bi-functionalized siloxane containing both hydrosilylated and halosilated side-groups (Part III, purple box in Figure 2-1, chapter 5). Since this work was done as part of an industrial cooperation, the research will be continued even after submitting the thesis (Future work, grey box in Figure 2-1). The goal is to synthesize a bi-functional PDMS-based siloxane with both the anti-adhesion properties of Part I and the bactericidal and fungicidal properties of Part II.

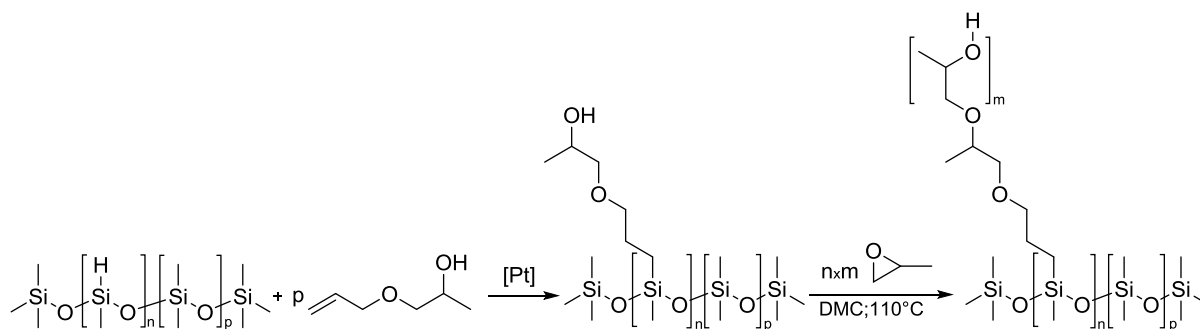
3 Part I: Introduction of Anti-Adhesion Properties into Silicones

This part includes experiments of the research project and master thesis of Nayereh Mohebbati. The research was done from October 2017 to October 2018 in the working group of Prof Dr. Udo Kragl and it was part of this dissertation.

Furthermore, the following part deals with the topic of the patent applications EP 18210646.8 (Preparation of polysiloxane polyalkyleneglycol brush copolymers) and EP 18210647.6 (Curable composition comprising polysiloxane polyalkyleneglycol brush copolymers), which were both submitted to the European patent office on the 6th of December 2018.

3.1 Background

The integration of anti-adhesion properties to silicones can be split into a two-step reaction, in which a hydrophilic polyalkylene side-group is bonded to a hydrophobic siloxane backbone. The first synthesis is a hydrosilylation reaction, in which a functional side-group – particularly a (propoxy)propan-2-ol group – is linked to the siloxane backbone. This group already contains a secondary OH-group. This OH- group can be polymerized with propylene oxide via propoxylation reaction (s. Scheme 3-1). Here, the propoxylation reaction is a “grafting from” polymerization and takes place in an autoclave system. Alkyleneglycol groups are known to affect the surface energy.^[50]



Scheme 3-1: Side-group hydrosilylation reaction of PDMS-PHMS copolymer with 1-(allyloxy)propan-2-ol in the presence of a platinum catalyst and consecutive propoxylation reaction with propylene oxide in the presence of DMC catalyst.

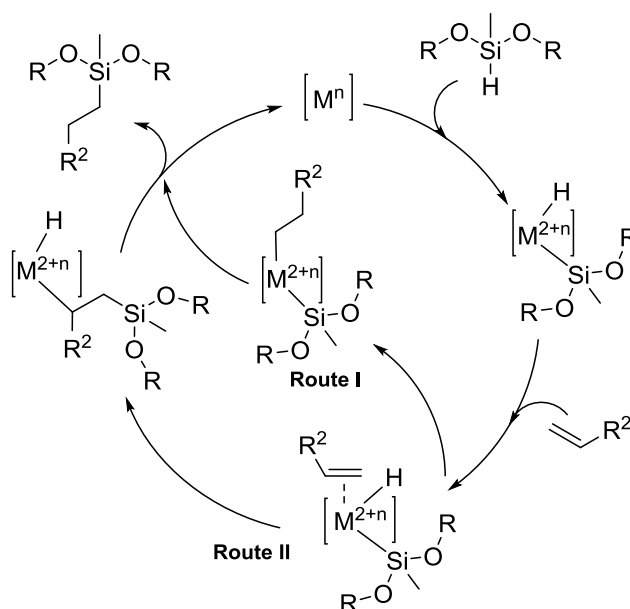
In the beginning the side-group hydrosilylation using homogeneous and heterogeneous platinum catalysts and DMC catalyzed propoxylation are described and several polymeric compounds are synthesized and characterized (inclusive contact angle measurements). In addition, the propoxylation rate is developed up to 95 wt-% of PPG and changes of physical and chemical properties are evaluated.

In the second part, the reaction conditions of side-group hydrosilylation are optimized to obtain controlled partially converted hydrosilylation products. Therefore, different reaction parameters (such as concentration, reaction temperature, solvent) were varied. The optimization was performed on the basis of kinetic studies.

In the end, the anti-adhesion properties of all compounds in this chapter are determined and discussed. Therefore, the compounds were tested embedded in a defined silicone formulation as well.

3.1.1 Hydrosilylation

Hydrosilylation is a well-known synthetic pathway which refers to the addition of organic and inorganic silicon hydrides across multiple bonds. The first example of hydrosilylation was done by Leo Sommer in 1947.^[51] Later John L. Speier discovered hexachloroplatinic acid as a very efficient precursor of the Pt-catalyst in 1957, so it is also known as Speier process.^[52] The most important mechanism of hydrosilylation was reported by Chalk and Harrod in 1965 (Scheme 3-2).^[53] This mechanism concerns the hydrosilylation reaction by late transition metal complexes. The first step is an oxidative addition of a trisubstituted silane to a metal which changes its formal oxidation state to M^{2+n} . To this complex an alkene ligand is coordinated. The general Chalk-Harrod mechanism (Route I) describes the migratory insertion via insertion of an alkene into the M-H bond. The intermediate metal(silyl)(alkyl) complex is formed. This undergoes a reductive elimination with Si-C bond formation. The metal(0) species is regenerated. Route II is the modified Chark-Harrod mechanism, in which it is possible that a metal(silyl)(alkyl) complex is formed first and the unsaturated bond gets inserted between the silicon and the metal.^[9a, 52-53]



Scheme 3-2: Chalk-Harrod mechanism for hydrosilylation of olefins catalysed by late transition metal complexes (adapted from^[9a]).

Early transition metal complexes, such as organolanthanide, organoyttrium and actinide complexes have gained interest in past few years for hydrosilylation. They are utilized as active precursors for olefins and acetylene hydrosilylation. The hydrosilylation mechanism with early transition metal complexes differs from the well-known Chark-Harrod mechanism involving a rapid actelyene insertion into the M-H bond and a consecutive silicon-carbon bond formation via σ -bond metathesis.^[54] Common catalysts also include titanium, zirconium, and rhodium.^[55]

The more common catalysts for hydrosilylation reaction are late transition metal complexes, such as platinum, palladium^[56] and nickel complexes,^[57] as well as complexes of the cobalt^[58] or iron triads.^[59] Nevertheless, platinum complexes are the most commonly used catalyst for hydrosilylation reaction.

Besides the good selectivity, they are also, highly stable towards heat, oxygen, and moisture.^[60] As already mentioned, hexachloroplatinic acid was used for hydrosilylation (Speier's catalyst). It is the most widely used platinum catalyst.^[52, 56b, 61] Certain organic compounds provide the opportunity for activation of platinum to catalytically active species of Pt(0), such as, cyclodextrin complexes,^[62] unsaturated secondary and tertiary alcohols,^[63] vinyl-norborne^[64], peroxides^[65] or quinones^[56b, 66], but the necessity of platinum activation and the often necessary presence of a co-catalyst is a drawback for catalytic systems.

In 1973, the Karstedt's catalyst was discovered through the treatment of hexachloroplatinic acid with divinyl containing disiloxanes (Figure 3-1), but the breakthrough of Karstedt catalyzed hydrosilylation reactions came in the late 1980s.^[67] In comparison to Speier's catalyst, the Karstedt catalyst contains Pt(0). It shows higher catalytic activity and selectivity, as well as a better solubility in polysiloxanes.^[53a, 68]

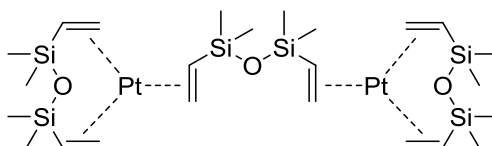
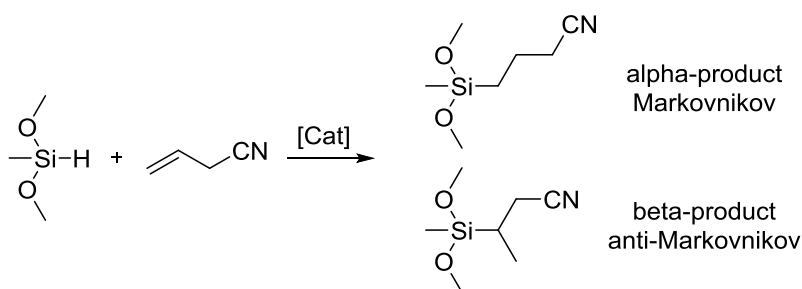


Figure 3-1: Structure of Karstedt catalyst (Platinum-divinyltetramethyldisiloxane complex).

During the last decades, several Pt(0) Karstedt derivatives were developed, which contain different ligands, such as phosphines,^[69] quinones,^[66] N-heterocyclic carbenes,^[70] η^2 -norbornenes,^[71] imines and diimines^[72], as well as chelating carbene ligands.^[73] The different ligand environments show advantages or disadvantages in selectivity, activity or catalyst poisoning compared to Karstedt.^[55c]

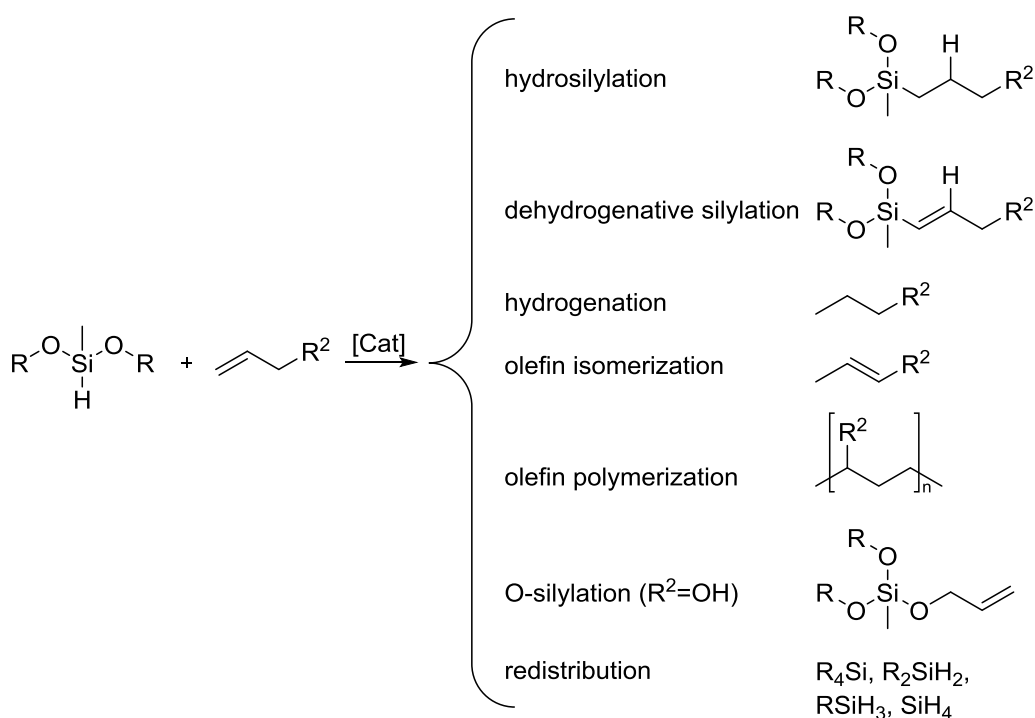
Besides the type of catalyst, the type of reactant is important for the hydrosilylation reaction as well. The addition of unsaturated alcohols to SiH groups is one way to functionalize polydimethylsiloxane. Kircheldorf reported the use of allyl alcohols in 1996.^[74] The hydrosilylation reaction with allylic compounds can form α - and β -isomers, according to whether the Markovnikov or anti-Markovnikov product is favored. The selectivity depends on the catalysts, as well as on the rest of the allylic compound.^[75] For example, allyl cyanide or halogen-containing allylic compounds form α - and β -products with Karstedt catalyst. In general the α -product (Markovnikov product) is favored.^[76] It has to be mentioned, that there can be a misunderstanding of Markovnikov rule, due to the fact, that the partial charge of a SiH bond is different to HBr bonds. Here, hydrogen the more electronegative atom (EN 2.2 according to Pauling) and silicon acts as the electropositive part (EN 1.9).^[77]



Scheme 3-3: Forming of α - and β -isomers during the hydrosilylation reaction of pseudohalogen containing allylic compounds (adapted from ^[76d]).

Platinum catalyzed hydrosilylation reactions compete with some side-reactions, such as dehydrogenative silylation, hydrogenation of olefins, and isomerization of olefins, olefin oligomerization/polymerization and redistribution of hydrosilanes (Scheme 3-4).^[60] O-silylation is a further competitive reaction, but it can only take place, when the allylic compound contains a hydroxyl group. In general, O-silylation happens with alkoxysilanes, but the SiH-group of the siloxane can also react with the hydroxyl group forming a silyl- oxy bond with an unsaturated end-group. This end-group can form networks with left SiH groups and the compounds starts to cure.^[78]

Side-reactions lead to lower yields of the main-products, as well as difficult purification steps due to inseparable side-products. The avoidance of side-reactions or at least their reduction can be controlled by a well-defined catalyst-design with higher selectivity and activity to hydrosilylation reactions, as well as the structure of the allylic compounds. Furthermore, the reaction conditions, such as reaction temperatures or catalyst loadings, can favour the main-reaction.^[60]

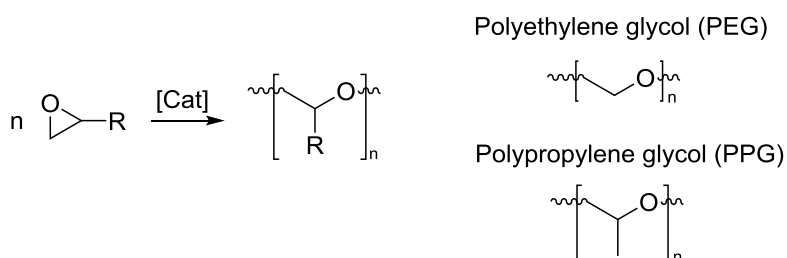


Scheme 3-4: Overview of possible side-reactions next to hydrosilylation; O-silylation can only take place when R^2 is an hydroxy group (adapted from ^[60]).

In the following work, the focus is set on hydrosilylation reactions with polymeric hydridomethyl siloxanes and hydroxyl functionalized allylic compounds. The reactions are catalyzed by platinum catalysts, for example Karstedt.

3.1.2 Alkoxylation

Alkoxylation is a chemical reaction, in which an alkylene oxide is ring-opened by a suitable catalyst and attached to another compound via polyaddition (s. Scheme 3-5).^[79] In 1863 the first polymerization of ethylene oxide (EO) was reported by Wurtz.^[80] Nowadays, ethoxylation and propoxylation are the most important alkoxylation reactions. Important application fields for alkoxylation are mass productions of poly(ethyleneglycol), poly(propyleneglycol), and ethylene oxide/ propylene oxide copolymers. They are used for chemical intermediates, lubricants, industrial surfactants and cosmetics and personal care products.^[81]



Scheme 3-5: Left: general alkoxylation reaction; right: the most famous representative PEG and PPG.

Ethoxylation and propoxylation refer to the ring-opening of EO and propylene oxide (PO), so it belongs to ring-opening polymerizations (ROP). The ROP is a specific form of polymerization. Here the monomer is a cyclic molecule. The cyclic monomers are forced to open in a chain growth polymerization. The terminal end of a polymer chain acts as a reactive center where further cyclic monomers can react by opening its ring system and form a longer polymer chain.^[81-82] IUPAC defines ROP like: "A polymerization in which a cyclic monomer yields a monomeric unit which is acyclic or contains fewer cycles than the monomer." Today typical monomers of ROPs are alkanes and alkenes or compounds with heteroatoms like oxygen (ethers, acetals, esters, lactones), sulfur (polysulfur, sulfides, polysulfides), nitrogen (amines, amides, imides), phosphorus (phosphates, phosphonates, phosphites, phosphines, phosphazenes) and silicon (siloxanes, silathers, carbosilanes, silanes).^[81-83]

Ethoxylation is the most important alkoxylation reaction. It was firstly mentioned in 1930.^[84] Ethylene oxide is a very reactive monomer, which reacts with a wide range of chemicals, such as alcohols, phenols, acids, fatty alcohols and fatty acids, ammonia, amines or mercaptans, to produce polyethylene glycol (PEG). The ethoxylation reaction takes place in semi-batch reactors at temperatures between 40°C and 200°C under pressures ranging from atmospheric to 100 bar, and shows an exothermic behavior. The danger of EO is its thermal instability in the liquid phase, as well as the gas phase and its high reactivity with other chemicals including water. Therefore, the ethoxylation reaction contains several hazards, such as a gas phase explosion hazard related to the flammability of EO in the presence of air or oxygen or EO's instability, which appears in decomposition flames with pressure effects in vessels, even in the absence of oxygen. In addition, EO is highly toxic

and may cause cancer. Even in solution, EO may cause severe burns. Also the thermal stability of liquid EO is influenced by the temperature, which can cause in uncontrolled decomposition reactions due to exothermic effects in ethoxylation reaction.^[85]

Propoxylation is the analogous reaction using propylene oxide as monomer. This cyclic ether has a melting point of 34°C, so it can be utilized as a liquid in propoxylation reactions. This advantage and the better thermal stability, as well as lowered reactivity, makes it to a good alternative to ethoxylation reactions. First reports date back to the 1960th.^[79b, 86]

The propoxylation of hydroxyl-functionalized compounds using double metal-cyanide complex (DMC) as catalyst is a common method. DMC catalysts were developed in the 1963,^[87] but they gained more importance in the 1980th.^[88] The catalyst contains metal complexes of zinc and cobalt, which are precipitated from metal halogenides and hexacyanometallates solutions in the presence of coordinated organoligand systems (Figure 3-2). The ligands in the structure can be some hydroxyl containing compounds, such as *tert*-butanol. DMC is able to homo- and co-polymerize propylene oxide to linear oligomers and polymers. Compared to conventional catalysts, such as (alkali earth) metal alkoxides or (alkali earth) metal hydroxides (e.g. KOH), DMC yields to polyethers with lower levels of unsaturation, narrow molecular weight distributions (low polydispersity) and low Viscosity. Furthermore, using alkali methyl hydroxides can have the drawback of proton abstraction during polymerization, also known as chain transfer reaction.^[89]

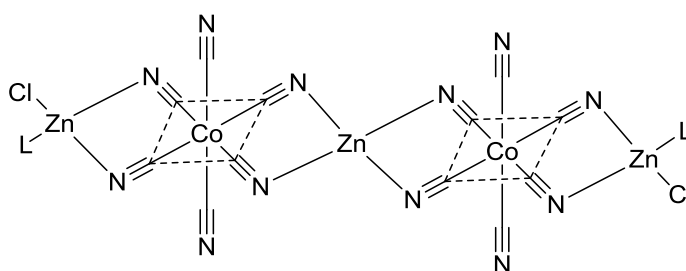
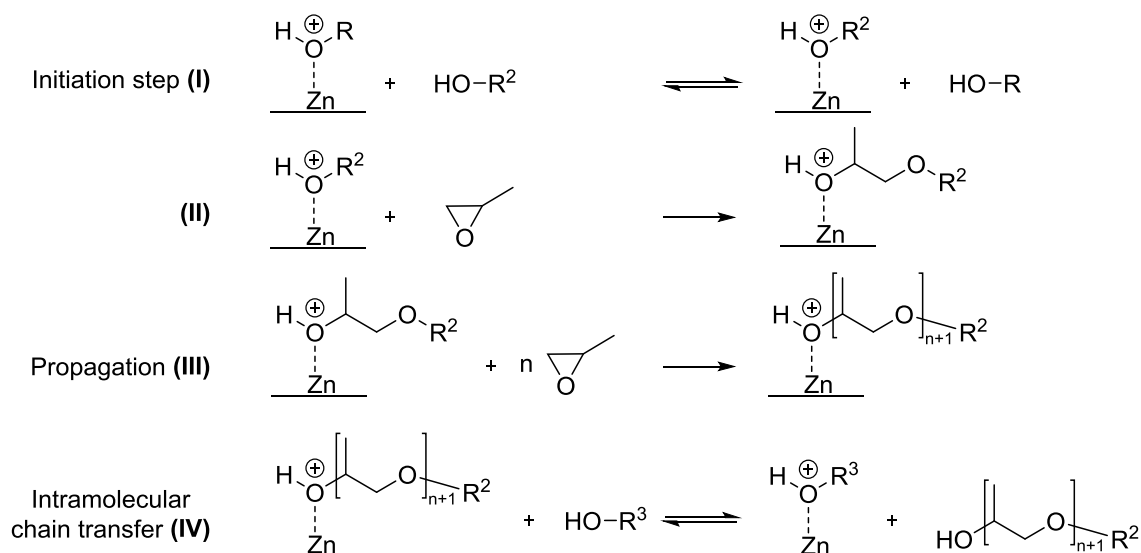


Figure 3-2: Chemical structure of a general double metal-cyanide complex (DMC) with an undefined ligand (L) (adapted from ^[89c]).

DMC is able to ring-open propylene oxide and polymerize it in a heterogeneous catalytic polymerization reaction. Therefore, DMC needs an initiator containing hydroxyl groups. Due to the fact, that the initiator can also contain other functional groups or it can be an oligomeric or polymeric starter, copolymers are possible too.^[90]

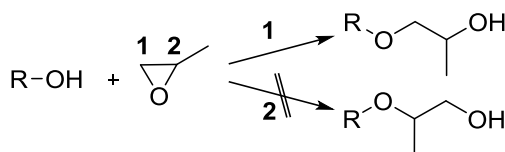
Kim *et al.* proposed a suitable reaction mechanism for ring-opening polymerization of PO by heterogeneous DMC catalyst (s. Scheme 3-6).^[89c, 89e] The entire catalyst structure is not shown for simplification of the mechanism, although group “R” represents the rest of the catalyst as shown in Figure 3-2. The zinc ion is the center ion in DMC, while cobalt improves the activity of the center ion.^[89d] The initiation step includes two reactions, first the formation of the active site in the catalyst surface through the initiator (I), followed by the formation of a polymerization center (II). The Polymerization center contains already one monomer unit of a ring-opened PO. In the propagation step (III) the insertion of PO monomers takes place to form linear high molecular weight polymers.

Propoxylation is an exothermic reaction due to the ring-opening of PO. The degree of polymerization in this step depends on the amount of PO. In addition, intermolecular chain transfer reactions (IV) can stop the growing of the chain due to substitution with hydroxyl containing compounds. This results in lower molecular weight polymers, but it can be also seen as deactivation and regeneration of the catalyst respectively. The induction period of this reaction depends on the speed of initiation step (I).^[89c-e, 91]



Scheme 3-6: Proposed mechanism of ring-opening polymerization of PO by heterogeneous DMC catalyst^[89c]. The entire catalyst structure is not shown for simplification.

As it is shown in Scheme 3-7, upon ring opening of propylene oxide two possible products can be formed, depending if the CH₂ group (1) is linked to the hydroxyl group of the initiator (secondary alcohol), or the CH group (2) (primary alcohol). Santacesaria *et al.* reported that even if the initiator is a secondary or primary alcohol, propylene oxide forms always a secondary alcohol. So the propoxylation reaction is a selective reaction.^[92]



Scheme 3-7: Propoxylation reaction with two different options of the formed product.

Copolymers of polysiloxane and polypropyleneglycol, which can be compared to the copolymers synthesized in this work, are known in literature. Common application fields are surfactants, adhesives or sealants. The preparation of polysiloxane polypropyleneglycol copolymers can be done with various methods. Block copolymers can be formed by reaction of difunctionally terminated siloxane oligomers with mono- or difunctionally terminated alkylene glycol monomers or oligomers.^[93] DMC catalyzed propoxylation reactions of polysiloxane polyalkyleneglycol block copolymers are already known.^[94] The starting materials are silanol-terminated polydialkylsiloxanes to form linear block copolymers.

The preparation of polysiloxane polyalkyleneglycol brush copolymers requires functional groups in the polysiloxane side-groups. There are several preparation methods, which use the *grafting onto* method. *Grafting onto* consists of tethering of preformed polymer chains with reactive ends or side-groups that are linked to reactive groups of the substrate.^[29a, 95] A common synthetic pathway is the already mentioned hydrosilylation reaction of a polysiloxane oligomer containing SiH groups and a vinyl group of an alkyleneglycol oligomer.^[94, 96] The polymers are linked to each other by carbon-carbon bond. Another option would be polymerization via thioether linkage.^[97] Polymers, which were synthesized by *grafting onto* method have molecular masses which are limited to the molecular mass of the starting materials.

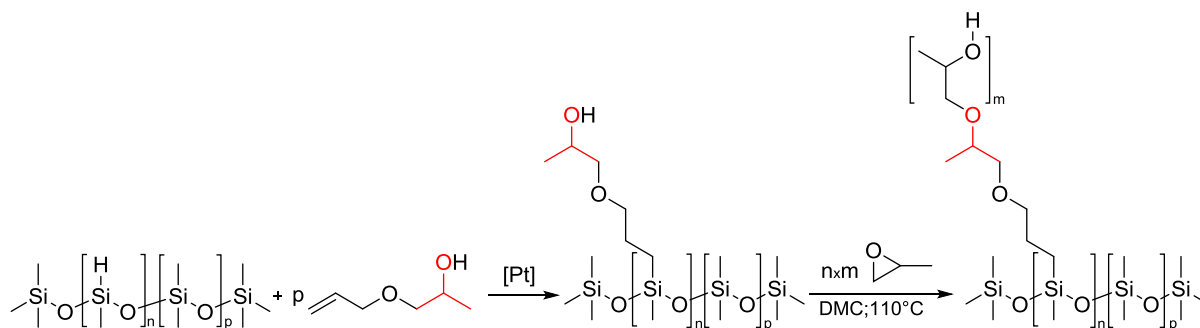
The favorite polymerization method to form the following polysiloxane polyalkyleneglycol brush copolymers is the *grafting from* method. *Grafting from* deals with the polymerization of secondary monomers initiated by reactive groups of the substrate.^[29a, 95] In general, the *grafting from* copolymerization technique is used more often than its counterpart, mainly due to the higher efficiency and selectivity of the reaction between smaller, less sterically hindered monomers.

3.2 Results and Discussion

In the following chapter, side-group hydrosilylation and consecutive propoxylation reaction is made from three different polyhydridomethylsiloxane (PHMS) starting materials. Their difference is given in the ratio between hydridomethylsiloxane units and dimethylsiloxane units; SM-50, SM-25 and SM-15. Further characterizations are shown in Appendix A2.

3.2.1 Synthesis of fully-converted Polysiloxane Polypropyleneglycol Brush Copolymers

In the beginning the focus was set on the side-group hydrosilylation of PDMS-PHMS copolymers with 1-(allyloxy)propan-2-ol followed by the *grafting from* propoxylation with propylene oxide (PO) as it is shown in Scheme 3-8. Utilized polyhydridosiloxane starting materials are linear SM-50, SM-25 and SM-15, whereas the number belongs to the percentage of SiH groups (further details in Appendix A2).



Scheme 3-8: Side-group hydrosilylation reaction of PDMS-PHMS copolymer with 1-(allyloxy)propan-2-ol in the presence of a platinum catalyst and consecutive propoxylation reaction with propylene oxide in the presence of DMC catalyst; the red highlighted part represents the first monomer unit of propylene oxide.

The used allylic compound is only known in literature as a suitable reactant for end-group hydrosilylation.^[93b] Consequently the here presented side-group hydrosilylation with that compound represents a new successful hydrosilylation reaction. The end-group hydrosilylation with 1-(allyloxy)propan-2-ol is selective and only Markovnikov-product is formed (s. chapter 3.1.1.)^[77] This great selectivity is also seen in the side-group hydrosilylation of products **3.1a** to **3.3b** (Table 3-1). The anti-Markovnikov product was not detectable, neither other side-products (s. Scheme 3-4).

Table 3-1: Summary of the products **3.1a** to **3.3b**; unless otherwise indicated, the desired conversion is 100% and the general reaction time is 24 hours; the yields are; the yields are calculated from the average of several experiments.

Sample	Starting Material	Catalyst	PPG [wt-%]	Conversion [%]	Isolated Yield [%]
3.1a	SM-50	Karstedt	44.5	>99	55 - 80
3.1b		Pt@C		81	32
3.2a	SM-25	Karstedt	35.7	>99	80 - 90
3.2b		Pt@C		84	46
3.3a	SM-15	Karstedt	21.1	>99	80 - 99
3.3b		Pt@C		85	55

The selective side-group hydrosilylation is possible in homogeneous catalytic systems (Karstedt catalyst) in various scales, as well as in heterogeneous ones (Pt supported on charcoal). Higher isolated yields were obtained with homogeneous systems. Both systems show an increasing isolated yield as the number of reactive side-groups in the substrate decreases. The content of SiH group left in the polysiloxane backbone is less than 0.5×10^{-6} wt% (calculated by the total moles of silicon atoms in the obtained polysiloxane) when Karstedt is utilized (calculated by $^1\text{H-NMR}$). Comparable reports in literature show an SiH content about 0.02 wt%.^[98]

Based on further investigations, it is known that the heterogeneous catalyzed hydrosilylation needs higher platinum loadings (0.5mol% Pt compared to siloxane starting material). Nevertheless, with Pt supported on charcoal (**3.1b**, **3.2b** and **3.3b**) there is no full conversion of SiH groups in side-group hydrosilylation. The conversion reached only 80 to 85 %.

As a consequence, only the Karstedt catalyzed products **3.1a**, **3.2a** and **3.3a** were utilized as starting materials for the preparation of propoxylated products **3.4** to **3.32** (s. Scheme 3-8, second reaction). Samples are listed in Table 3-2. The reactions were carried out in a 100 mL autoclave system with a semi-batch process, so a defined volume of PO was added after the mixture (containing starting material, DMC catalyst and solvent) was already heated up to 110 °C. While opening the system to the PO storage vessel, the pressure increased (evaporation of PO) and the temperature was decreased (PO was not heated up before). All experiments had an initiation time between five and 70 minutes. The outcome of the propoxylation reaction was visible through the decrease of pressure and the simultaneous increase of the temperature.

Table 3-2: Summary of the products **3.4** to **3.32**; starting material, PPG wt-%, theoretically and experimental monomer unit, isolated yield and the Viscosity are listed; the yields are calculated from the average of several experiments.

Sample	Starting Material	PPG [wt-%]	Monomer Unit (theor.)	Monomer Unit (exp.)	Isolated Yield [%]
3.4	3.1a	64.9	2.61	2.89 ± 0.071	80 - 95
3.5		74.3	5.22	5.24	95
3.6		79.8	7.82	9.83 ± 3.465	93 - 97
3.7		83.3	10.43	11.15 ± 2.383	80 - 95
3.8	3.2a	59.3	3.25	3.61 ± 0.283	90 - 95
3.9		70.3	6.50	7.43 ± 0.177	90 - 97
3.10		76.6	9.75	10.51 ± 0.403	95 - 96
3.11		80.7	13.00	13.95 ± 0.099	93 - 95
3.12	3.3a	27.2	1.78	1.80 ± 0.064	91 - 94
3.13		32.4	2.57	2.18 ± 0.088	91 - 92
3.14		36.9	3.35	2.84 ± 0.057	89
3.15		40.8	4.14	4.25 ± 0.460	87 - 92
3.16		44.3	4.92	4.19 ± 0.240	89 - 94
3.17		47.4	5.71	5.76 ± 0.028	87 - 92
3.18		50.1	6.49	6.13 ± 0.910	76 - 99
3.19		58.8	9.63	9.47 ± 0.057	90 - 91
3.20		63.5	11.98	10.97 ± 0.603	80 - 92
3.21		67.3	14.33	14.24 ± 0.141	87 - 92
3.22		71.3	17.47	19.04 ± 0.027	66 - 98
3.23		73.6	19.82	19.96 ± 0.672	83 - 88
3.24		76.3	22.96	24.30 ± 0.759	86 - 96
3.25		77.9	25.31	28.13 ± 3.804	84 - 94
3.26		80.6	30.02	34.67 ± 5.339	80 - 90
3.27		81.7	32.37	37.28 ± 2.942	83 - 92
3.28		85.6	43.35	46.16 ± 0.021	91
3.29		88.1	54.33	53.18 ± 6.307	90 - 94
3.30		89.9	65.31	67.95 ± 4.511	89 - 90
3.31		91.2	76.29	80.02 ± 7.616	90 - 92
3.32		92.2	87.28	98.94 ± 13.782	91 - 93

Although the propoxylated products contain no novel but repeated groups compared to the hydrosilylated intermediate, in order to assess the progress of the propoxylation reaction, particularities of the NMR spectra of the propoxylated product were exploited. In the aforementioned products, the first monomer unit shows signals in the ^1H -NMR spectra separated from the monomer units of the PPG side-chain. Figure 3-3 illustrates this feature through the example of sample **3.4**.

While the signals **a**, **b**, **c**, **d**, **g/g'** and **h** show no divergences, the signals of **f/f'** and **e/e'** are split into two signals each. This is caused by the presence of a chiral center that makes **e** and **g** protons diastereotopic. The first monomer group is located closer to the silicon backbone and the C3 carbon chain also shows a different chemical environment. Moreover, the first group **e** is split into **e1** and **e2**. A possible splitting of the signal **e'** cannot be proved yet due to the overlapping with signal **d**. This signal splitting represents all further propoxylated products. The splitting can be seen in the ^{13}C -NMR as well.

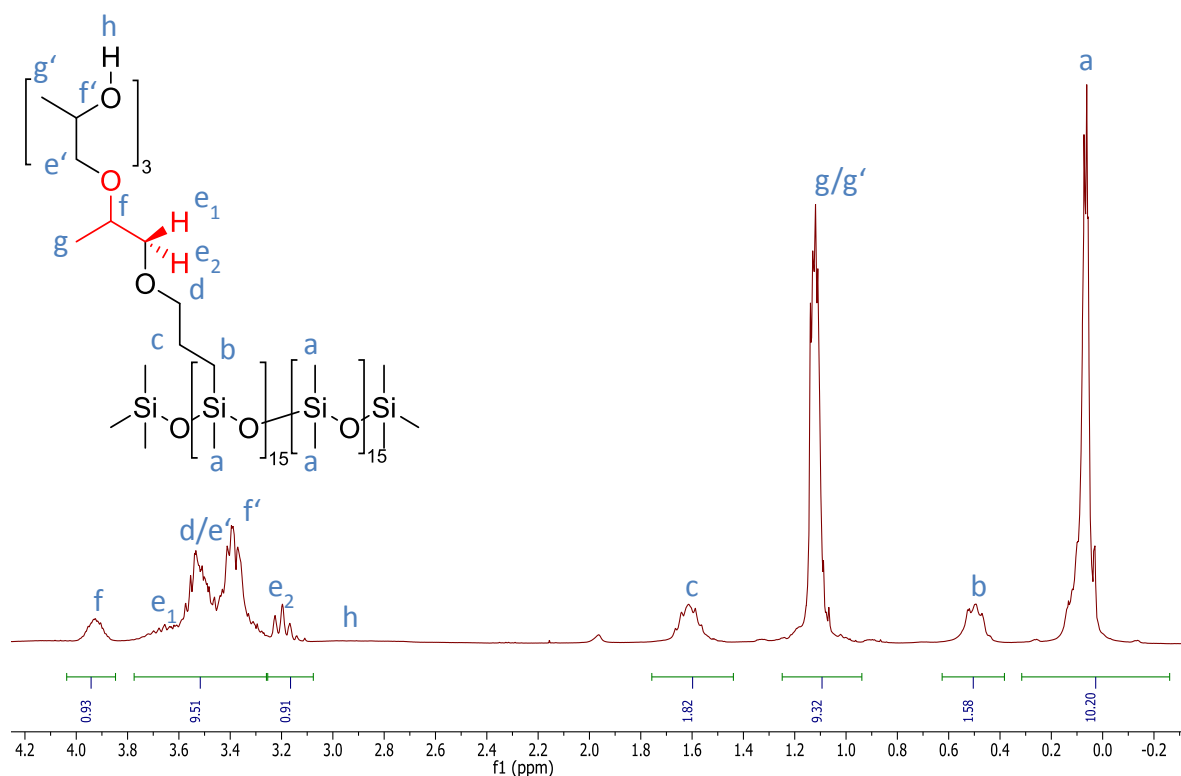


Figure 3-3: ^1H -NMR of **3.4** in deuterated chloroform (400 MHz, 24 °C), the separated signals from the first monomer unit are shown.

The number of the monomer units in the PPG side-chain indicates its length. It can be calculated by the ratio between the integrals of signal **a** and **g** in the ^1H -NMR spectrum. Signal **g** is growing by increasing chain length while **a** stays constant.

In Figure 3-4 the great proportionality between the desired chain-lengths of the propoxylated side-groups and the added volume of PO could be proven. Since the volume is an absolute value, the proportionality is shown between the PPG wt-% of the products and the degree of polymerization. The graph is logarithmic plotted to keep the linear trend, because the starting materials already contain the first monomer unit of the PPG side-chain (s. Scheme 3-8, red highlighted part). This linearity is independent from the number of side-groups in the starting material. The propoxylation reaction with starting material **3.3a** was enlarged to the shortest possible chain length (22.8 PPG wt-%, monomer unit 1) and a chain length of around 87.89 monomer units (90.3 PPG wt-%). The diagram shows a great correlation between the calculated degree of polymerization (green line) and the measured one (green triangles). In conclusion it is possible to synthesize polysiloxane polypropyleneglycol brush

copolymers with desired and controlled lengths and numbers of side-groups. Thereby no bottom or upper limit was detectable and the propoxylation can be done with direct or step-wise addition of PO.

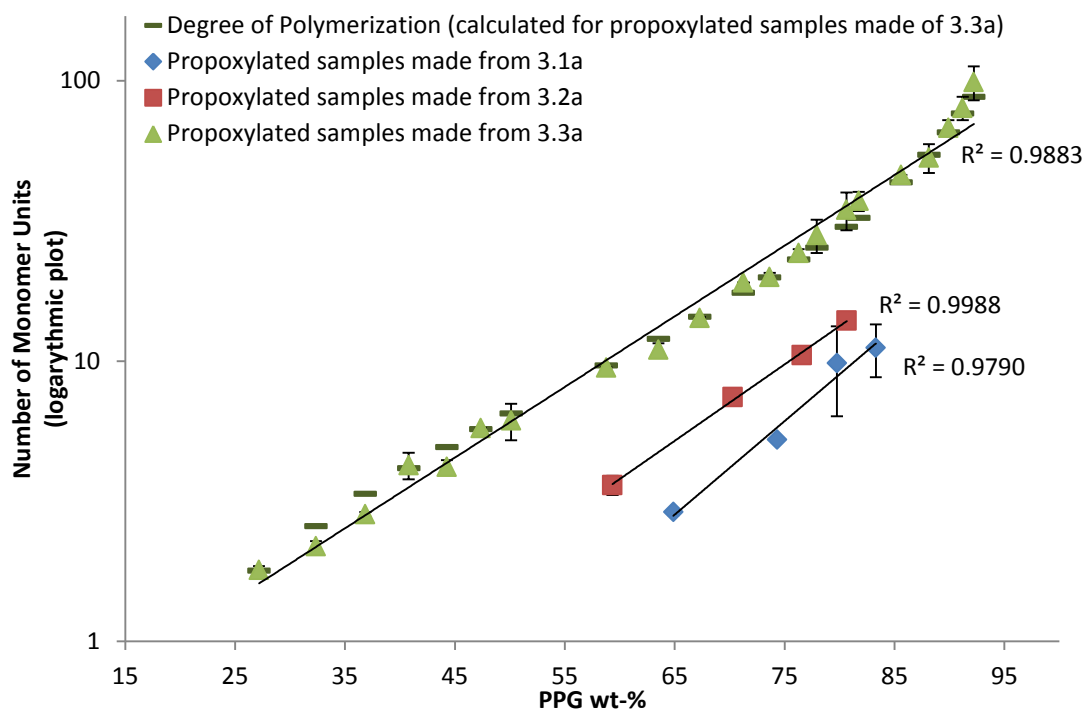


Figure 3-4: Degree of polymerization shows linearity (PPG wt-% vs. monomer units) in a logarithmic plotted diagram; the plotting is necessary due to already existing PPG wt-% in the hydrosilylated starting materials **3.1a** to **3.3a**; blue curve belongs to products **3.4** to **3.7**, red curve belongs to **3.8** to **3.11** and green curve belongs to **3.12** to **3.32**; dark green data points illustrate the calculated degree of polymerization for **3.12** to **3.32**; the standard deviations were calculated from two to three repetitions.

In addition, the progress of molecular masses was monitored as well. The results made from starting material **3.3a** are taken as an example in Figure 3-5 (logarithmic plotted graph). The calculated molecular masses (blue bars) are compared to the measured ones (red bars), whereby the degree of polymerization (green data points) is considered as well. With shorter side-chains (lower PPG wt-%) the measured molecular masses fit very well with the calculated ones. But with higher polypropylene glycol side-chains, the measured molecular weights do not grow with increasing chain-length anymore. Furthermore, the standard deviation is increasing. This phenomenon can be explained by the morphology of the polymers, because they show a brush-like shape. This shape and the possibility of entanglement cause a smaller hydrodynamic volume. The molecular masses are measured by in the gel-permeation chromatography (GPC). This method gives relative molar masses compared to a standard, so the hydrodynamic volume influences the measurement. In general small molecules have a small hydrodynamic volume and stay longer in the GPC column. Big molecules (higher hydrodynamic volume) pass the column faster. Moreover the utilized GPC column was calibrated for linear polymers, which show less entanglements and so higher hydrodynamic volumes.^[99] Thus, the difference between measured and calculated molecular weights is a problem of the method of measurement and not of the synthesis route. A possible alternative for further investigations could be a MALDI-TOF (matrix-assisted laser desorption/ionization with a time-of-flight mass spectrometer).

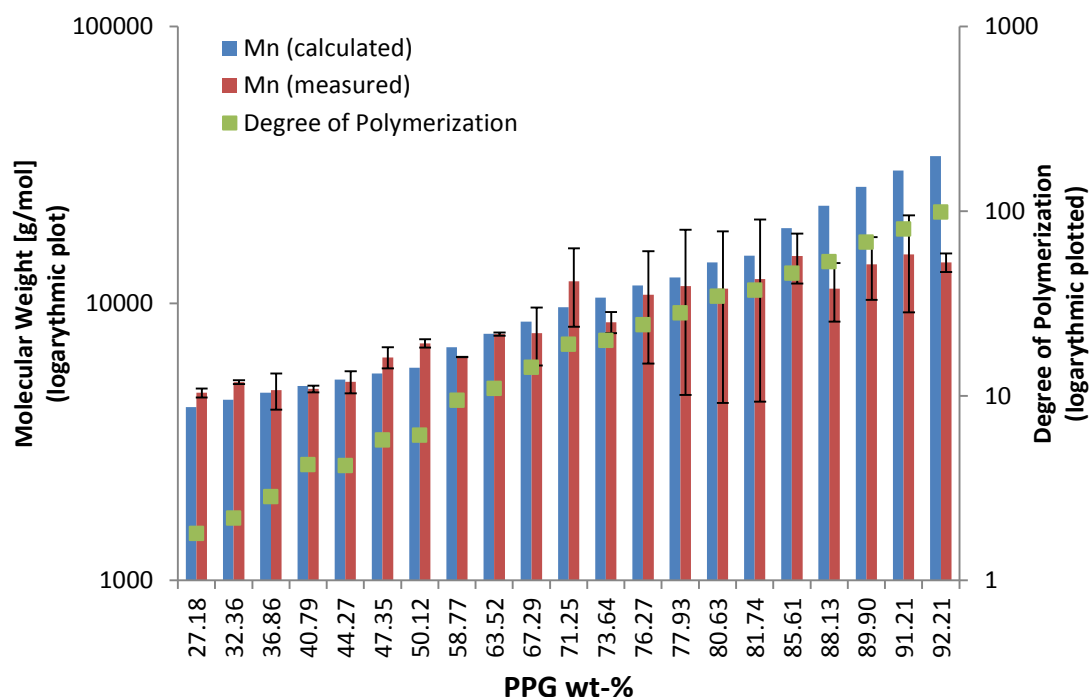


Figure 3-5: Comparison of calculated molecular weights and measured ones of **3.12** to **3.32** made from **3.3a** in a logarithmic plotted diagram; the plotting is necessary due to already existing PPG wt-% in the hydrosilylated starting materials **3.3a**; the green curve illustrates the calculated degree of polymerization for **3.12** to **3.32**; the standard deviations were calculated from two to three repetitions.

The presented results show a novel synthetic pathway to form polysiloxane polypropyleneglycol brush copolymers. The side-group hydrosilylation has a great selectivity towards the α -product and is possible in heterogeneous and homogeneous catalytical systems, whereas the last one shows conversions with less than $0.5 \cdot 10^{-6}$ wt% SiH groups in the backbone. The consecutive propoxylation reaction is controllable by the added amount of propylene oxide and shows a big variability in the number and length of the side-chains. In the tested range of the chain lengths it is possible to produce any desired number and length of the side-chains, so the presented synthetic pathway is very robust referring to number and length of side-groups.

3.2.2 Characterization of fully-converted Polysiloxane Polypropyleneglycol Brush Copolymers

Besides the development of a synthetic pathway for its preparation, also the properties of the formed products, such as Viscosity and their effect on surface properties like surface energy (contact angle), were evaluated. They can give information on the relationship between the structure of the compounds with their hydrophilic side-groups and the change of their behavior (e.g. influence of the surface tension).

For characterization of compounds **3.1a** to **3.32** Viscosity was measured for hydrosilylated (s. Figure 3-6), as well as propoxylated products (s. Figure 3-7). The Viscosity results in Figure 3-6 show a high increase compared to the starting materials. This is correlated to the increasing bulkiness due to the formed side-groups, because the starting material is a linear polymer, whereas the formed products are brush-like. The correlation to the bulkiness can be seen in comparison to the number of side-groups as well. The Viscosity decreases with decreasing number of side-groups, which corresponds with a decreasing bulkiness.

The results of heterogeneous catalyzed samples show the same effect as the homogeneous catalyzed ones, but the viscosities are lowered. Probably this is due to the lowered conversion degree, which lowers the number of side-groups as well as the degree of bulkiness.

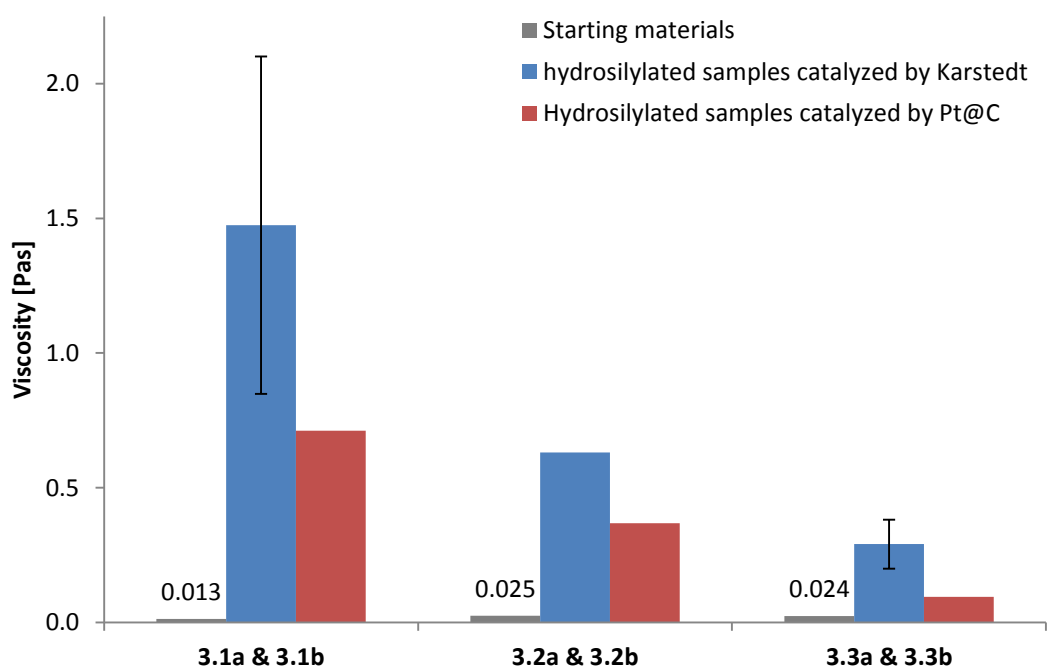


Figure 3-6: Viscosity results of hydrosilylated products **3.1a** to **3.3b** in homogeneous (Karstedt) and heterogeneous catalytical systems (Pt@C); the standard deviations were calculated from two to three repetitions.

The Viscosity results of propoxylated products **3.4** to **3.32** are shown in Figure 3-7. The same trend as mentioned before can be seen here. The Viscosity is increasing with increasing number and chain-length of side-groups, which increases the bulkiness. This effect is independent of the number of side-

groups, but proportional to the number of monomer units in the side-groups. However, the measurement of Viscosity shows high standard deviations, especially with increased PPG wt-%. Probably this has a comparable reason than the deviating molecular masses in Figure 3-5. The longer the side-chains are, the higher is the bulkiness. However, the entanglement among the chains can turn out to vary strongly, so that the polymers are tangled rather loosely or very tightly. This can be compared to a ball of wool that was either neatly wrapped (easy to untangle), or knotted. Although it is the same ball in both cases, it costs different levels of effort to unravel the ball.

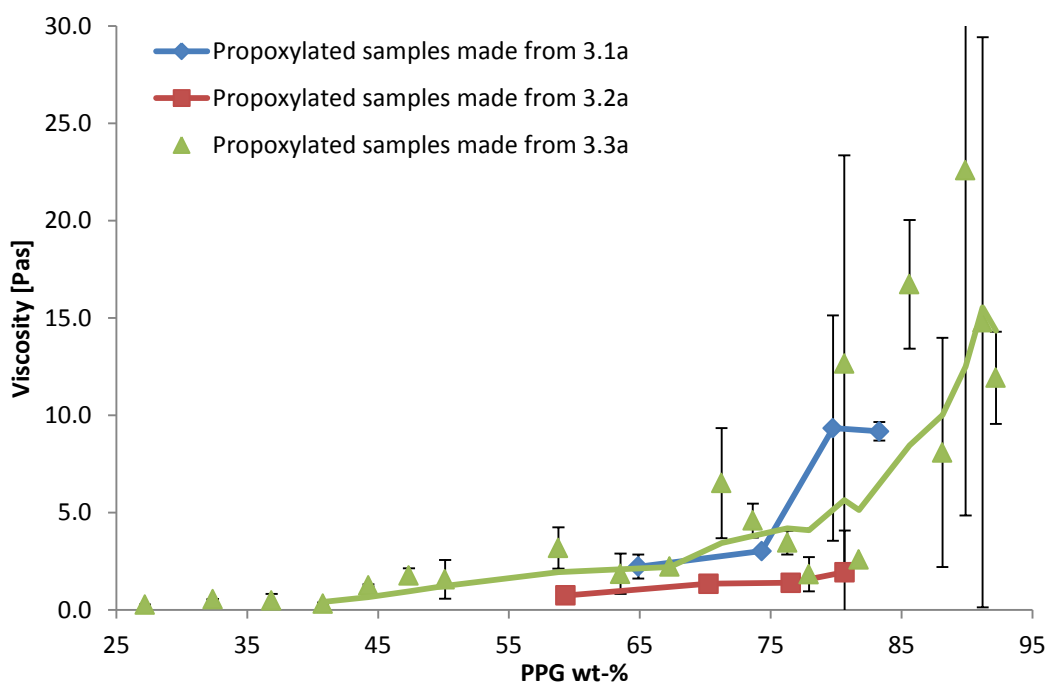
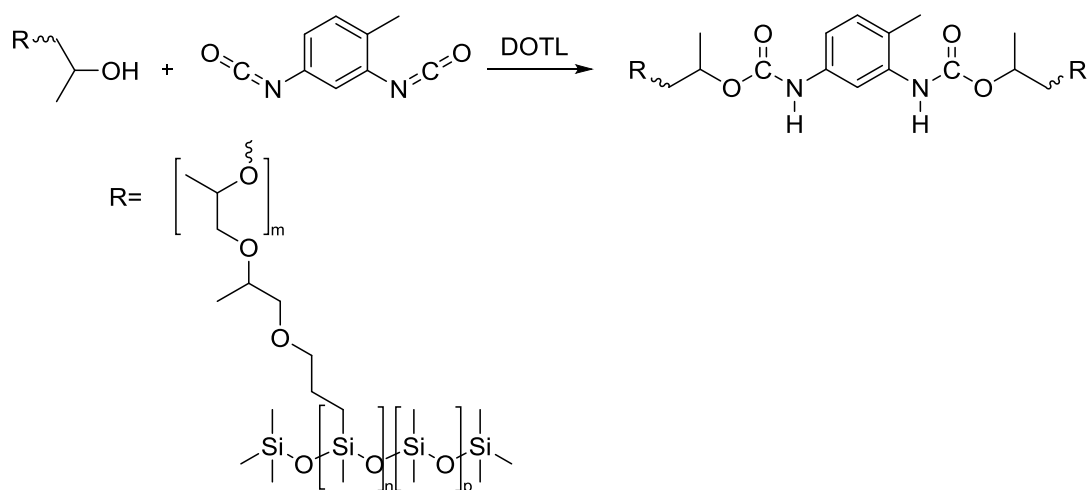


Figure 3-7: Viscosity results of propoxylated products 3.4 to 3.32; 3.1a to 3.3a; blue curve belongs to products 3.4 to 3.7, red curve belongs to 3.8 to 3.11 and green data points belong to 3.12 to 3.32; the green curve is a trend line to illustrate the trend; the standard deviations were calculated from two to three repetitions.

Furthermore, contact angles (CA) of all samples were taken. The contact angle can be used as implicit term for surface energies. Low contact angles mean high surface energies and high interfacial tensions, whereas high contact angles imply low surface energies and low interfacial tensions.^[100]

As it is shown in Appendix A1, The samples have to be solid to determine the solid-liquid-CA between the sample and a water droplet. Therefore, two different sample preparations were done in which the curing was generated via reaction of the secondary OH-groups and added isocyanate groups to form urethane groups (the general reaction is shown in Scheme 3-9). In the first sample preparation this curing was done with the pure samples and in the second one with an amount of 10 % in the medium of a PDMS standard formulation. Further details are shown in Appendix A2.



Scheme 3-9: Curing of Polysiloxane Polyalkyleneglycol Brush Copolymers via polyurethane synthesis.

For reasons of clarity only contact angle results of chosen products embedded in the PDMS standard formulation are shown in Figure 3-8. The other results are shown in Appendix A3 (Table A-4 and Table A-5), as well as their standard deviations. The products shown were chosen to represent all important observations.

The shown contact angles are compared to the pure PDMS standard formulation, as well as a PPG reference material. The PDMS standard formulation, as well as the PPG reference material show constant contact angles at $\sim 105^\circ$ and $\sim 95^\circ$ (Figure 3-8, black curves). Conversely, the hydrosilylated product **3.3a**, as well as the products **3.18**, **3.20**, **3.22** and **3.24** show a decrease of the contact angle during time (Figure 3-8, blue and red curves). The difference after 90 seconds of measuring can be up to 30° . This means, that the surface energy increases during time from a hydrophobic to a hydrophilic character. This decreasing effect is representative for the products **3.1a** to **3.27** with lengths of the PPG side-chains up to 32.59 (77.92 PPG wt-%). The detected decreasing of the contact angle can be seen until sample **3.28**. Samples **3.28** to **3.32** contain the highest lengths of side-chains and there is no decreasing of the contact angle detectable anymore. The contact angle is constant during time (Figure 3-8, green curves). It is hypothesized that the longer side-chains of the PDMS-PPG-block copolymer form layers, which avoids the decreasing effect of the CA. To the best of our knowledge there is no comparable observation of the decreasing effect reported in literature.

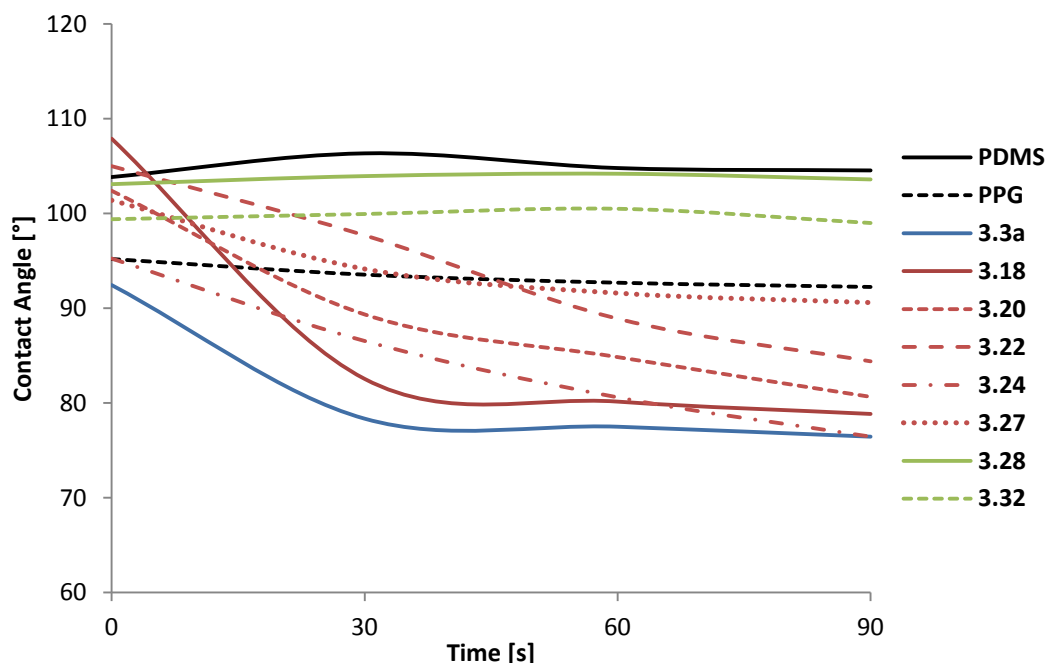


Figure 3-8: Time-resolved contact angles of chosen products made from SM-15 and reference materials (standard PDMS formulation and PPG reference material); the black curves belong to the references, the blue curve belongs to the hydrosilylated product; the red curves are part of the propoxylated samples which show the spreading effect and the green curves belong to the propoxylated samples without any decreasing effect.

Although there were no differences noticeable in the synthetic pathway of the presented polymers, there is a detectable change in the contact angle. The formed products can change their behavior on the surface energy from a special length of the PPG-side-chains. Further investigations should be done made from SM-50 and SM-25. An alternative to the classic contact angle would be the dynamic contact angle, which occurs in the course of wetting (advancing angle) or dewetting (retreating angle) of a solid surface.^[101] They could give further information about this decreasing effect and should be considered as additional investigations.

3.2.3 Optimization Process to synthesize Polysiloxane Propyleneglycol Brush Copolymers with controlled partial Conversion

The introduction of polypropyleneglycol side-chains onto a polyhydrosiloxane represents the first part of this thesis with the insertion of an anti-adhesion feature. As it was mentioned in chapter 2, a consecutive reaction is desirable to insert the bactericidal and fungicidal properties. Therefore, further investigations were done to synthesize mainly half-converted polysiloxane propyleneglycol copolymers and to have an optimized synthetic pathway to get controlled conversions. Here the hydrosilylation reaction is in focus. Further propoxylation reactions were just tested as a proof of concept.

The following optimization process deals with the settings of different reaction parameters (time, concentration SiH, solvent, ratio SiH to C-C double bond, temperature and catalyst). The main target is to achieve a better temperature control due to the exothermic behavior of the hydrosilylation reaction, which will be described in the following.

3.2.3.1 Kinetic Studies

At the beginning of this research part, kinetic studies were performed to determine the behavior of the presented hydrosilylation reaction. Concentration data for the kinetic analysis was obtained by integration of $^1\text{H-NMR}$ of samples collected from the reaction at different times. Experiments were done using SM-50 as starting material (the products are comparable to sample **3.1a**). Due to the high number of side-groups in the polymer, the size of the integrals of the Si-CH₃ group and the signal of the side-groups do not show such a big difference. This can minimize the error of the measurement. The evaluation of the reaction order and activation energy is done with a linear regression and the Arrhenius equation.^[102]

As it is shown in Figure 3-9, the hydrosilylation reaction with 1-(allyloxy)propan-2-ol follows first order depending on siloxane starting material. The clear assessment of the reaction order for the overall reaction is not possible yet. In literature, different orders for hydrosilylation reactions are known depending on the reactants and catalysts.^[103] Second order is mentioned mostly due to the formation of α - and β -isomers.^[76d, 104] As it is mentioned before the here presented hydrosilylation reaction shows a very high selectivity towards the α -product, which can explain the first reaction order. The activation energy is about 206.7 ± 7.9 [kJ/(mol)] based on the used reaction parameters (Table A-6, s. Appendix A3). Compared to other hydrosilylation systems (30 – 140 kJ/mol),^[76d, 103-104] the activation energy of this reaction is higher, so it needs more energy to initiate. However, since the reaction takes place under mild reaction conditions (including 35 °C, 0.1 wt-% catalyst loading), the increased activation energy for the further course is not a problem.

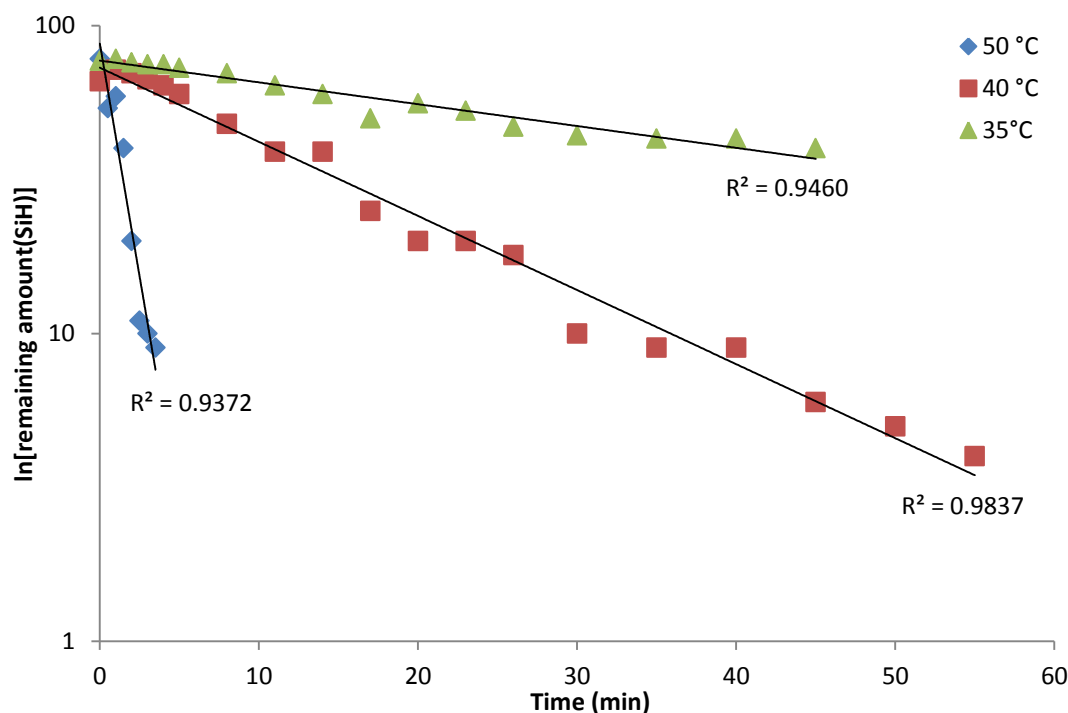


Figure 3-9: Logarithmic-plotted diagram of time-resolved kinetic studies of hydrosilylation product **3.1a** at different temperatures. The activation energy is about 206.7 ± 7.9 [kJ/(mol)].

It has to be mentioned that the hydrosilylation reaction is very fast and highly exothermic. With the reaction conditions which were utilized in chapter 3.2.1 (120 °C reaction temperature), the reaction could not be monitored, because the technical equipment is not available. Furthermore the monitoring of the temperatures showed a high local maximum in the beginning, which showed higher temperatures than the temperature set in the oil bath. This change in reaction temperature led to biased kinetic parameters. Probably this is also one reason that the overall reaction order could not be determined yet. In order to avoid the increase of temperature due to exothermic effects, the experiments took place at external temperatures between 35 and 50 °C, as well as the concentration of the reactants was decreased to get a better control of the reaction. The adjusted parameters led to controllable kinetic studies.

3.2.3.2 Optimized Synthetic Pathway for the Partial Hydrosilylation of PDMS-PHMS Copolymers

The following optimization of partially hydrosilylated polysiloxane propyleneglycol copolymers is made from SM-15 firstly (this correlated with partially converted **3.3a**). This PHMS contains the lowest amount of SiH groups and seemed to be suitable, because the lowered concentration of SiH groups in the solution gives lowered exothermic effects. First target was set to 50 % conversion. This would lead to an equimolar distribution of side-groups with anti-adhesion features and ones with bactericidal and fungicidal properties.

In a second step, following investigations were then extended to SM-25 and SM-50. The converted amount of SiH-groups, as well as the resulting amount of hydrosilylated products (indicated by the

formation of Si-CH₂ groups) was analyzed by integration of ¹H-NMR. The parameter settings and the obtained data are summarized in Table 3-3.

Table 3-3: Summary of the parameter settings for the optimized synthetic pathway of half-converted polysiloxane propyleneglycol brush copolymers; Unless otherwise indicated, the desired conversion is 50 % and the general reaction time is 24 hours.

Sample	Starting Material	c(SiH) [mol/L]	Solvent	Catalyst	Ratio SiH:C=C	Temperature [°C]	Converted	Formed
							Amount SiH [%]	Amount SiCH ₂ [%]
3.33a	SM-15	0.5641	toluene	Karstedt	2:1	100	74.0	37.6
3.33b		0.3372	toluene	Karstedt	2:1	100	77.0	33.5
3.33c		0.1836	toluene	Karstedt	2:1	100	74.0	39.0
3.33d		0.1705	toluene	Karstedt	2:1	100	68.0	39.0
3.33e		0.1142	toluene	Karstedt	2:1	100	64.0	33.5
3.33f		0.0747	toluene	Karstedt	2:1	100	39.6	32.5
3.33g		0.0565	toluene	Karstedt	2:1	100	67.0	44.5
3.33h		0.0565	toluene	Karstedt	2:1	35	50.2	36.6
3.33i		0.0565	toluene	Karstedt	2:1	50	57.0	36.3
3.33j		0.0565	toluene	Karstedt	2:1	60	71.0	35.8
3.33k		0.0565	toluene	Karstedt	2:1	80	70.1	35.5
3.33l		0.0565	heptane	Karstedt	2:1	35	13.2	n.d.
3.33m		0.0565	THF	Karstedt	2:1	35	71.4	37.7
3.33n		0.3372	THF	Karstedt	2:1	100	70.9	43.1
3.33o		0.3372	toluene	Pt@C	2:1	100	47.0	35.4
3.34	SM-25	0.9057	toluene	Pt@C	2:1	120	46.0	78.0
3.35	SM-50	0.7325	toluene	Pt@C	2:1	90	56.0	38.5

Initially it was tried to reach a controlled partial conversion by limiting the reaction time (equimolar ratio SiH:C=C). Calculations of reaction time were done referring to the kinetic results. Unfortunately, the unreacted double bonds caused a consecutive curing during working-up. Therefore, for further experiments the amount of double bonds was reduced. The analytical results in Table 3-3 show that the concentration of SiH groups has a great influence on the conversion (**3.33a** to **3.33g**). Although the amount of double bonds should only be able to convert 50 % of the SiH groups, up to 77 % were converted. It is assumed that this is caused by the exothermic behavior of the hydrosilylation reaction. The higher the concentration and respectively the reaction's enthalpy is, the higher is the conversion of SiH groups through uncontrolled reactions. But there are no side-products detectable (s. Scheme 3-4), so there has to be another reason as well. Probably this phenomenon could also be caused by problems with the measurements due to exchanges of different groups in the product or there could be some interactions (such as hydrogen bonds), which can have an effect on the integrals in the ¹H-NMR measurement. It is known that the hydrogen-bonded structure can change the integrals.^[105]

In addition to the concentration effect, the temperature can influence the control as well (**3.33h** to **3.33k**). The lower the external temperature, the lower the maximal temperature caused by the

exothermic effect and as a consequent the lower the difference between target-performance conversions. For example the conversion of SiH groups in **3.33h** is about 50% at 35 °C reaction temperature.

Further investigations dealt with the solvent. The polysiloxane starting materials have a low polarity and they are soluble in non-polar solvents preferentially, but the formed polypropyleneglycol side-chains are soluble in polar media. Therefore, further tests with different solvents were done (**3.33i** (THF) to **3.33n** (heptane)). It can be shown that heptane cannot promote the hydrosilylation, while the more polar solvent THF causes too high conversions of the SiH-groups. It is supposed that the polarity of heptane is too low to promote the hydrosilylation with the unipolar allylic reactant. This shows that toluene was already a good choice.

At last, further investigations were done with Pt supported on charcoal. This heterogeneous catalyst was already utilized in the full-converted hydrosilylation reaction (s. subchapter 3.2.1), but it could not promote quantitative conversions. Here the lowered activity of the heterogeneous catalyst gives better opportunity to control the partial conversion (**3.33o**). Therefore, no optimization of the reaction parameters is necessary. Also the transferring of this reaction conditions to SM-25 (**3.34**) and SM-50 (**3.35**) gives comparable and controllable conversions of SiH-groups. There is no explanation yet, why the yield of formed side-groups in **3.34** is higher than the conversion of SiH groups.

It has to be mentioned that in almost every experiment in this section, the formed amount of hydrosilylated product (testified by the amount of Si-CH₂ groups) does not reach 50 %. There is no clear explanation yet. If it would be caused by wrong calculations due to the polymeric substrate, also the full-converted products should show lower conversions. But that is not the case. Probably the lowered conversion is caused by the first order kinetic, in which the reaction speed depends on the concentration of the substrate. The initial concentration of the allylic reactant is already lowered and the optimized reaction parameters cause decreased concentration as well, so the initial reaction speed has to be lowered as well.

3.2.3.3 Synthesis of Half-converted Polysiloxane Polypropyleneglycol Brush Copolymers

In a first proof of concept, product **3.34** (made from SM-25) was propoxylated consecutively to compare it to the products **3.8** to **3.11**. The results are shown in Table 3-4. The propoxylation reactions and working-ups show no differences to the full-converted comparable samples. However, the numbers of monomer units are smaller than expected and the viscosities are higher. Probably the increasing of Viscosity is due to some interactions (such as van der Waals forces or hydrogen bonds) between the left SiH groups and the formed secondary OH-groups on the side-chains.

Table 3-4: Summary of the products **3.36** to **3.39** made from **3.34** (SM-25), PPG wt-%, theoretically and experimental monomer unit, isolated yield and the Viscosity are listed; the results will be compared to products **3.8** to **3.11**.

Sample	Starting Material	PPG [wt-%]	Monomer Unit (theor.)	Monomer Unit (exp.)	Isolated Yield [%]	Viscosity [Pas]
3.8	3.2a	59.34	3.25	3.61 ± 0.283	90 - 95	0.748 ± 0.1082
3.9		70.27	6.50	7.43 ± 0.177	90 - 97	1.348 ± 0.1655
3.10		76.56	9.75	10.51 ± 0.403	95 - 96	1.395 ± 0.1513
3.11		80.66	13.00	13.95 ± 0.099	93 - 95	1.938 ± 2.1397
3.36	3.34	50.50	5.34	3.17	89	2.939
3.37		63.80	10.68	5.78	95	9.590
3.38		71.47	16.01	8.72	93	11.500
3.39		76.46	21.35	11.91	95	8.289

The first results of consecutive propoxylated half-converted polysiloxane propyleneglycol brush copolymers show that further reactions are possible (sample **3.36** to **3.39**). But the results should be considered with care, because they are not reproduced yet.

3.3 Determination of Antimicrobial Properties

The introduction of polypropyleneglycol side-chains into a polysiloxane backbone does not integrate an antimicrobial activity by definition (inhibition of growing). As already mentioned (chapter 1.2), these compounds affect the surface energy but do not kill germs. They are able to change the surface energy to form more hydrophilic surfaces. The Anti-Adhesion Assay is an antimicrobial test method to measure the adhesive quality of black yeast on modified surfaces. Therefore, only the samples embedded in the PDMS formulation were used (s. Appendix A2). In short, after the sedimentation and adhesion phase of a cell suspension, the test surfaces are washed and the remaining cells are washed and counted by plating on a culture medium. The utilized strain is *Exophiala dermatitidis* (isolate) which belongs to the black yeasts. Further details are shown in Appendix A1.

As it is shown in chapter 3.2.2 the grafted PPG side-chain have an influence on the contact angle, which can be correlated to the surface energy.

3.3.1 Anti-Adhesion Assay

Anti-adhesion test results of chosen full-converted samples are shown in Figure 3-10. Because of the huge sample quantity, the anti-adhesion test could not be done for all samples, hence, examples representative of all products were chosen and subject to the test.

The reference is a PDMS standard formulation without any PPG side-chains. The reference was provided by the microbiological department and is set to 100%, so all samples were compared to the reference.

Figure 3-10 shows the test results of different samples which were cured into a PDMS standard formulation with an amount of 10 % of the propoxylated samples. It has to be mentioned that the anti-adhesion test is not robust. The results can be influenced by different parameters, such as temperature, sample preparation or the cell number and live rate of the strains. So the data of the anti-adhesion test have to be evaluated with care. They should be seen as trend-setting, but for a clear statement, further repetitions should be done.

Nevertheless, these test results show the trend that with increased number of side-groups, the adhesion of black yeast is lowered. The samples derived from SM-50 (**3.1a**, **3.4** to **3.7**) show a germination number compared to the reference of around 40% with a low standard deviation. Samples obtained from SM-25 (**3.2a**, **3.8** to **3.11**) show a low germination number as well, but the results differ from each other and the error is higher. However, the samples made from SM-15 (**3.3a**, **3.18** to **3.31**) show higher adhesion. Although the samples with lower PPG side-chains show less germination, the standard deviation is very high (18-60 %). With increased number of side-groups (**3.27** to **3.31**), the germination number increases as well and the results are in the same range of the reference. To sum up, the anti-adhesion results depend on the number of side-groups and the chain-length. The higher the number of side-groups is, the better is the reproducibility and the lower are the adhesion properties of the cells. As consequence, less, but longer side-groups worsen the anti-adhesion effect and cause better cell adhesion.

These conclusions can be correlated to the preliminary findings of the contact angle measurements (s. Figure 3-8). The time-resolved CA measurements showed a spreading effect of the water droplet during time, which stopped with high lengths of PPG side-chains. Thus, there is an apparent correlation between the contact angle of a surface and its behavior in the Anti-Adhesion Assay.

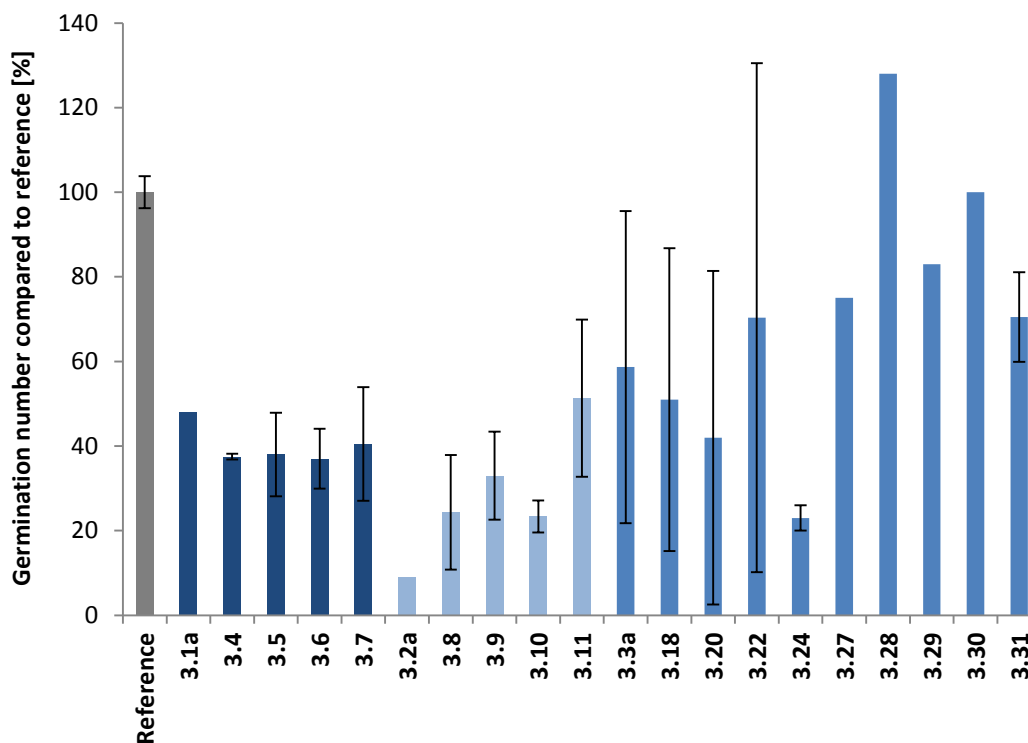


Figure 3-10: Anti-Adhesion Test results of chosen products from **3.1a** to **3.31**; the results are ordered by the starting material; the standard deviations were calculated from three repetitions.

In a second run the sample **3.20** was tested in the Anti-Adhesion Assay with different amounts of copolymer embedded in the PDMS standard formulation. The results are shown in Figure 3-11. The amount ranges from 0.5 % to 80 %. Films with higher amounts were prepared, but the high amount of polysiloxane polypropyleneglycol brush copolymer inhibited the curing of the film. Again, all results are trend-setting, but for a clear statement, further repetitions should be done.

The results show that an effect on the surface energy is already observed with an amount of 0.5% of the sample in the PDMS standard formulation (5% germination number compared to reference). Since the PPG amount in sample **3.20** averages 63.52 wt-%, the total amount of PPG in the film is only 0.32%. Altogether there is a large range, in which the sample has a positive effect on the germination number without marked differences (ca. 1-50 %). With higher amounts of copolymer, the germination number increases until the results are above the reference. Consequently, with higher amounts of the copolymer embedded in the PDMS standard formulation, the results in the Anti-Adhesion Assay are inverted: the adhesion of the cell will not be avoided anymore, but promoted. One reason can be the changed surface, since the films containing higher amounts of sample **3.20** seem to be stickier and slightly humid.

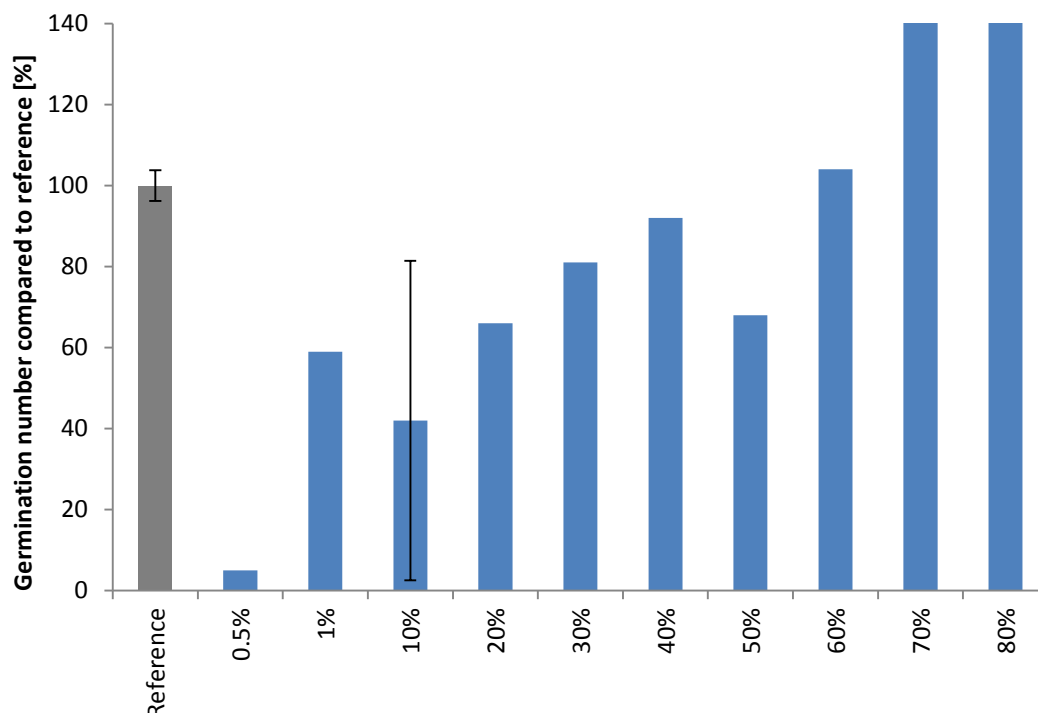


Figure 3-11: Anti-Adhesion Test Results of PDMS formulations containing the product **3.20**; the wt-% of the product **3.20** is varied; the standard deviations were calculated from three repetitions.

The given anti-adhesion test results show a good correlation between the anti-adhesion effect and the number and length of PPG side-chains. This effect also correlates with the results from the contact angle measurements. In this case, the statement of the contact angle agrees with the one of the Anti-Adhesion Assay. However, this is due to the fact that both relate to the influence of the surface energy. Based on the contact angles, presumption of the results of the Anti-Adhesion Assay can be made. But a confirmation is always necessary.

However, the presented anti-adhesion test results have to be evaluated with care. Before any statements can be made, further tests and more repetitions should be done. It would be also interesting to assess the anti-adhesion behavior of pure sample films, although this could not be tested yet because the brittleness of the films precludes their direct use in the Anti-Adhesion Assay.

3.4 Conclusion and Outlook

Part I deals with the introduction of anti-adhesion properties into silicones via side-group hydrosilylation and consecutive propoxylation to form polysiloxane propyleneglycol brush copolymers.

The successful synthesis of polysiloxane polypropyleneglycol brush copolymers could be proven. Thereby, the side-group hydrosilylation has a great selectivity towards the α -product and is possible in heterogeneous and homogeneous catalytic systems, whereas the last one shows conversions with less than $0.5 \cdot 10^{-6}$ wt% SiH groups in the backbone. The consecutive propoxylation reaction is controllable by the added amount of propylene oxide and shows a big variability in the number and length of the side-chains. In the tested range of the chain lengths it is possible to produce any desired number and length of the side-chains, so the presented synthetic pathway (semi-batch process) is very robust referring to number and length of side-groups. Further investigations should include repetitions, as well as the extension of the siloxane starting materials (including SM-50 and SM-25) and the alkylene oxide (e.g. ethylene oxide or mixtures of PO/EO) in order to extend the portfolio of product design.

The desired products show the expected results in molecular masses and rheological behavior. But the results also reveal that the GPC measurements (with a linear standard) differ with longer side-chains, because the difference between the hydrodynamic volume and the real molecular mass increases. Further investigations should be the redetermination of the molecular masses by further analytical methods (e.g. MALDI TOF measurements), to avoid the problem of deviating hydrodynamic volumes in the GPC.

The contact angle measurements show a considerable spreading effect during time, which is not detectable with the reference (PDMS standard). This proves the influence of the PPG side-chains on the surface energy. This effect depends on the length of the PPG side-chains, because the spreading effect could not be detected anymore when the chain-length exceeded 43 monomer units. Moreover the Anti-Adhesion Assay proved the worsened adhesion of microbes. The results are comparable to the CA measurements, because samples with a spreading effect of the water droplet showed a better anti-adhesion effect. This shows that the results are related to surface energy. In general, further anti-adhesion tests should be out in order to obtain a statistically reliable statement. Further measurements could be dynamic contact angles among others to get a deeper understanding between morphology of the hydrophilic copolymer and the effect on the surface energy.

In the hydrosilylation reaction with controlled conversions of SiH groups it is essential that there is control over the temperature increase due to the exothermic behavior. With the right parameter setting the preparation of polysiloxane propyleneglycol copolymers with 25, 50 and 75 % targeted conversion were possible.

4 Part II: Introduction of Bactericidal and Fungicidal Properties into Silicones

The following part II deals with the topic of the patent application EP 18209736.0 (Process for the Preparation of Functionalized Polysiloxanes, priority: 3rd of December 2018).

4.1 Background

The integration of bactericidal and fungicidal properties can be split into a two-step reaction. The first synthesis is called halosilation (Part IIa), in which a functional side-group – particularly a halogen alkyl group – is integrated into the siloxane via silyl-oxy bond. This functional group is then substituted by an amine to form the antimicrobial ammonium group via Menshutkin reaction (Part IIb).

In Part IIa the halosilation reaction based on platinum catalysis is described and several polymeric and monomeric compounds are synthesized and characterized (inclusive contact angle measurements). In addition, the platinum-catalyzed halosilation is compared to the state-of-the-art palladium-catalyzed version and benefits and drawbacks are discussed taking into account the reaction pathway, as well as product appearance and stability. In this context kinetic studies, side-reactions and the reaction mechanism are discussed as well.

In Part IIb, the already mentioned halosilated compounds are utilized as starting materials in the consecutive Menshutkin reaction, which is a quaternization reaction. The synthetic pathway of these compounds is described inclusive kinetic studies and optimization of reaction parameters. Then the compounds are characterized by chemical and physical properties.

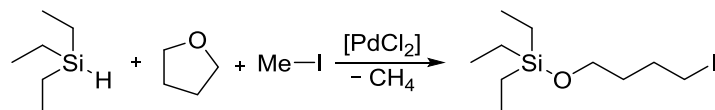
In the end, the antimicrobial properties of all compounds in this chapter are determined and discussed. Therefore, the compounds were tested in the pure form and chosen compounds were tested embedded in a defined silicone formulation as well.

4.1.1 Halosilation

The introduction of halogens into siloxanes is a very common procedure. These functionalized silicones are widely used in flame-retardant applications.^[106] Moreover, halogens are good leaving groups, so their introduction can also be used for further reactions, such as quaternization (Menshutkin reaction) to form zwitterionic polymers.^[30a, 30k, 34a, 107] Common synthetic pathways are hydrosilylation or condensation reaction to form halogenated siloxanes.^[30a, 108] Thereby, it has to be considered that the introduction of halogens into side-groups of siloxane oligomers and siloxanes poses several challenges compared to the rather straightforward end-chain functionalization. Their steric hindrances through the tail or the smaller space for the formed functional groups, as well as entanglements causes lower conversions and longer reaction times. But the side-group functionalization gives the opportunity to introduce more side-groups, because in linear polymers would be only two end-groups.^[30a, 108]

Moreover halogen functionalized siloxanes, as described above, contain a silicon-carbon bond. This bond can yield to less stable silicones, because halogens are known as initiators for radical polymerizations, so they can be radicalized by UV light.^[109] Another way to form halogen functionalized siloxanes via silyl-oxy bond, is the so-called halosilation (bromosilation or iodosisilation referred to the

halogen). This reaction was first mentioned by Ohshita et.al. in 1999 (s. Scheme 4-1).^[110] The formed silyl-oxy bond forms polymers in which the stability of the compound seems to be increased. First investigations were done with small silanes. Later on, the reaction was extended to siloxanes, as well as polysiloxanes and different starting materials were tested.^[106b, 111] The reaction is commonly catalyzed by palladium chloride. A cyclic ether (such as THF) is ring-opened by a halogen source and linked to the SiH group of the siloxane via silyl-oxy bond. Most of the preferred halogen source is methyl iodide. The halogen is then linked to the carbon that featured the ether bond and its accompanying group is released with the hydridic proton of the silane.



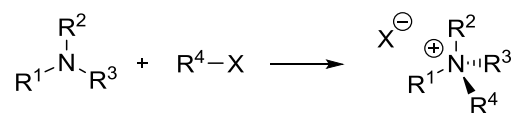
Scheme 4-1: Specific example of Pd-catalyzed halosilated silanes; this are one of the first reactants reported in literature.^[110]

In further studies, Zhou *et.al* performed kinetic analysis on the halosilation reaction, in which the conversion was detected at different temperatures and reaction times.^[111f] But their results give know information about the reaction order. Furthermore, Zhou *et.al* also proposed a reaction mechanism, as follows: “CH₃I was used as the iodine source, and the oxygen atom (O) of tetrahydrofuran (THF) was used as the nucleophilic reagent, respectively. First, the Si-H bonds of poly(hydridomethylsiloxane) (PHMS) cleavage occurred on the Pd²⁺ metal surface in the presence of PdCl₂ catalyst. Then, the nucleophilic oxygen atom (O) attached to the siloxy radical leading to the cleavage of C-O bond of THF, and the resulting ring-opened intermediate abstract the iodine from CH₃I simultaneously, to afford the corresponding poly(4-iodobutoxymethylsiloxane) (PIBMS)”.^[111f] The feasibility of this reaction mechanism has to be discussed due to the fact that a Pd⁴⁺ species should be formed then (detailed answer is given in subchapter 4.2.1.1).

Additional investigations were done by Fan et.al., who developed a rhodium catalyzed halosilation reaction (Rh(COD)Cl).^[112] The main disadvantage of this system is the relatively high price of Rh compared to other precious metals.

4.1.2 Menshutkin Reaction

The Menshutkin reaction (also spelled as Menšutkin or Menshutkin) was discovered in 1890 by Nikolai Menshutkin.^[113] It is the conversion of tertiary amines into quaternary ammonium salts (QAS) by S_N2 type reaction with alkyl halides (Scheme 4-2).^[113-114] QAS can be used as phase transfer catalysts (PTC), surfactants, as well as in battery technologies or as catalysts for the chemical fixation of CO₂.^[115] The reaction takes place non-catalyzed and requires several hours to several weeks depending on the reaction temperature.



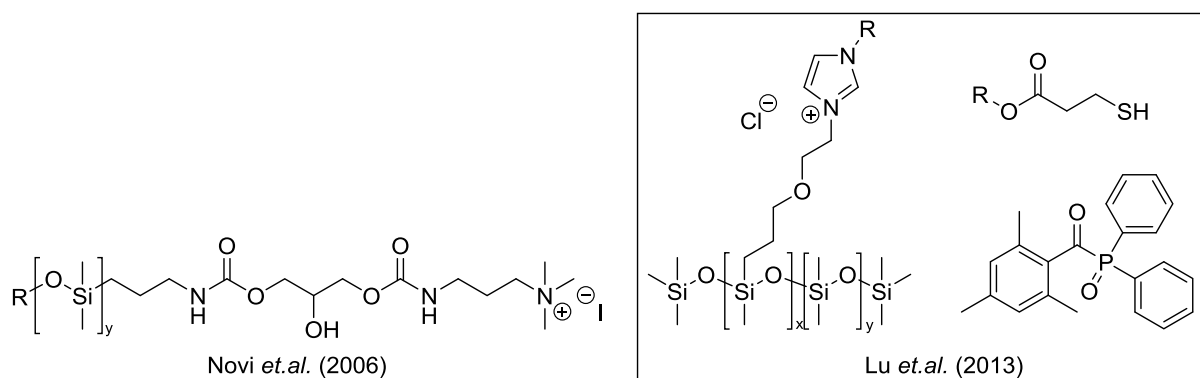
Scheme 4-2: General Menshutkin reaction with $\text{X} = \text{Br}, \text{Cl}, \text{I}$.

As mentioned before, the compounds containing quaternary ammonium groups (QAS) show a high antimicrobial activity. This activity is due to the highly positive charge density, which can get in contact with cell walls (s. chapter 1.2). There are also some other onium-functionalized zwitterionic compounds from the 15th or 16th group of the periodic table, such as phosphonium or sulfonium groups, which could have this antimicrobial activity, although there are very few clinical studies or scientific reports about it.^[116]

The integration of quaternary ammonium groups has the most advanced development. There are different ways to perform such an introduction, for instance in curing systems in which silicones and QAS-containing compounds are mixed, but not covalently connected.^[117] Unfortunately, these mixtures have drawbacks such as the formation of inhomogeneous mixtures and an uncontrollable and very fast leaching or loss of the QAS-containing compounds.

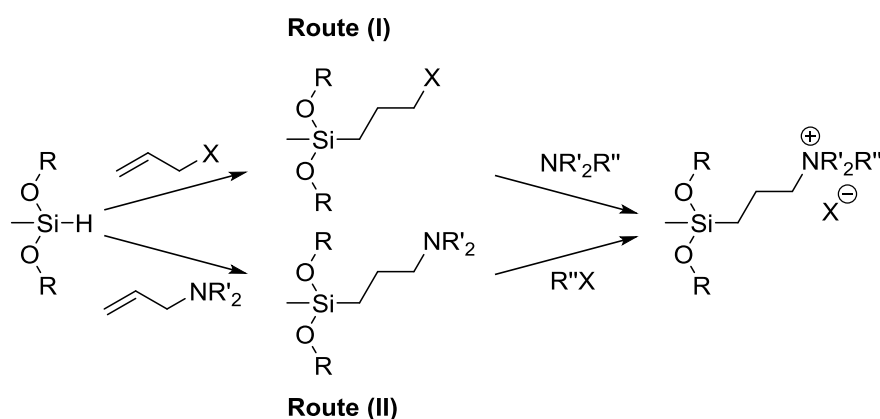
Another way is the integration of the QAS-group either into the main chain of the polymer (block-copolymers), or in the end-groups. Novi *et al.* developed a so-called carbonate coupler, which combines monodisperse or polymeric, functional building blocks within a single molecule (s. Scheme 4-3, left structure).^[30b]

The patent WO 2013096211 describes a curable composition comprising compounds with free-radical polymerizable groups, mercapto-functional organic compounds and polysiloxanes containing quaternary phosphonium and ammonium groups (exemplary structures are shown in the right part of Scheme 4-3).^[118] The polysiloxanes are synthesized via hydrosilylation of polyhydrosiloxane and 2-chloroethylvinyl ether followed by a consecutive quaternization. Here the resulting oxygen bridge is formed between two carbons in the side-group compared to the silyl-oxy bridge, which is formed in chapter 4.2.1. The resulting ether bridge shows a different hydrolysis stability, so it needs harsh conditions to be hydrolyzed.



Scheme 4-3: left: polydimethylsiloxane backbone with hydroxyl functionalized carbamate and trimethylammonium iodide end-groups within the main chain; right: curable composition of PDMS containing imidazolium chloride side-groups linked by ether bridge, mercapto-functionalized and phosphonium containing compounds.

Apart from QAS-functionalization of polysilsesquioxanes and oligosilsesquioxanes^[107a], there are several reports of QAS introduction into the side-groups of siloxanes.^[30a, 30d, 30f, 30h, 34a, 107b, 119] The side-group quaternization has the advantage that the antimicrobial active group can get in contact with the microbes' cell wall much easier than QAS groups within the main chain due to less steric hindrances. A side-group quaternization can be performed by first amination of the siloxane and consecutive Menshutkin reaction using alkyl halides (s. Scheme 4-4, route (II)).^[30d, 30f, 30h, 30j, 119b, 120] The alternative way is the halogenation of the silicone followed by quaternization by nucleophilic substitution with an amine (Route (I)).^[30a, 30k, 34a, 107] Route (I) has the advantage that no halogen containing reactant can be remained in the product, because it is already removed in the first step. In general hydrosilylation is the preferred reaction. In this work, the already halogenated siloxane is quaternized by tertiary amines (second part of Route I).



Scheme 4-4: Method for quaternization of siloxanes; Route (I) represents first halogenation and then substitution reaction with amines, route (II) shows the amination and consecutive quaternization by adding halogen-containing compounds; in general hydrosilylation is the preferred reaction.

4.2 Results and Discussion

Part II is split into two parts, synthesis of halogenalkyl-functionalized siloxanes via halosilation and preparation of ammonium-functionalized siloxanes via Menshutkin reaction. In this chapter, both synthetic pathways will be discussed separately. The research is based on four different PHMS starting materials. Their difference is given in the ratio between hydridomethylsiloxane units and dimethylsiloxane units; SM-100, SM-50, SM-25 and SM-15. These starting materials were already utilized in the previous chapter (Part I). Further characterizations are shown in Appendix A2.

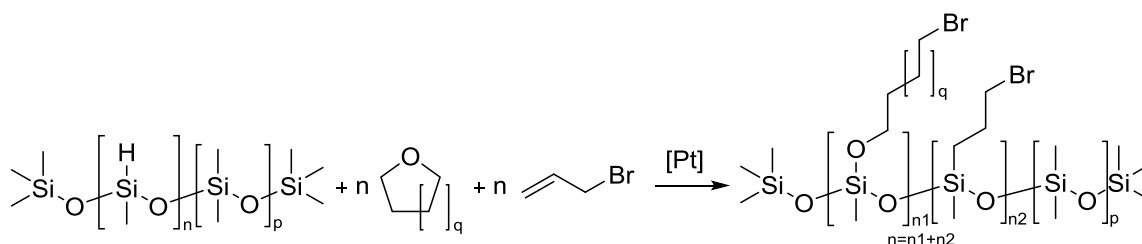
In the end, the antimicrobial properties of all compounds in Part II are determined and discussed together.

4.2.1 Part IIa: Halosilation

Halogenalkyl functionalized siloxanes were obtained via halosilation reaction with the Pt-based Karstedt catalyst. Commonly, Karstedt catalyst is used for hydrosilylation reactions.^[55c, 67] The hydrosilylation reaction takes place in different solvents. But when THF is used as solvent it gets involved into the reaction and the halosilation reaction takes place preferably. As already mentioned, the halosilation reaction is already known.^[106b, 111] In all cases, palladium chloride was the used catalyst, which forms a heterogeneous system. In these reports different halogen sources, as well as cyclic ethers and lactones, THF and iodomethane were utilized.

4.2.1.1 Synthesis of Halogenalkyl functionalized Siloxanes

In the beginning the focus was set on the platinum catalyzed synthesis of bromoalkyl functionalized siloxanes as it is shown in the general equation in Scheme 4-5. The utilized starting materials are linear SM-100, SM-50, SM-25 and SM-15, (where the number belongs to the mol-% of SiH groups), as well as 1,3,5,7-Tetramethyl-cyclotetrasiloxane (D^H_4) and 1,1',3,3',5,5',7-Heptamethyl-cyclotetrasiloxane (D_3D^H) (further details in Appendix A2). Unless otherwise indicated, THF and allyl bromide were used as reactants.



Scheme 4-5: Halosilation of PHMS with THF and allyl bromide as halogen source.

Bromoalkyl-functionalized products **4.1a** to **4.6** (Appendix A4, Table A-11) were synthesized with Karstedt catalyst, while **4.1b** and **4.5b** are produced with $PdCl_2$ as comparative examples. The yields of the formed products are shown in Figure 4-1. It has to be mentioned, that the yields were calculated by integration of 1H -NMR. Signal **a** was compared to signal **b** and **c**, (s. Figure 4-2), so higher yields than 100 % are due to integration/calculation errors. The products **4.1a** to **4.4** (polymeric starting materials) show high yields up quantitative. Products **4.5a** to **4.6** (based on cyclic starting materials)

with low molecular weights) show lower yields (~85-93 %). All products show full conversion of the SiH groups.

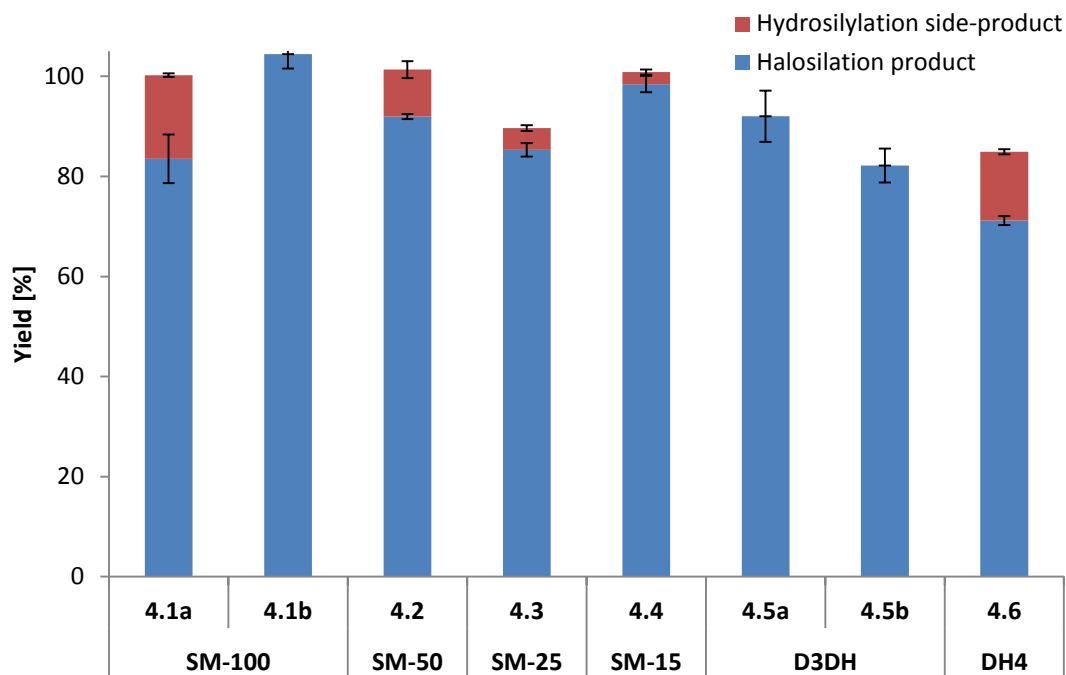





Figure 4-1: Ratio between halosilation and hydrosilylation as side-reaction of **4.1a** to **4.10**; yields of products were calculated by integration of the integrals of the signals in $^1\text{H-NMR}$; the standard deviations were calculated from two to three repetitions.

The Pt-catalyzed halosilation reaction takes place at 50°C or higher, whereas the optimum temperature ranges from 80 to 120 °C. The catalyst loading is about 0.1 mol-% based on the siloxane starting material, so the total mol-% catalyst referred to the SiH-groups is lower. Conversely, the best reaction temperature reported for Pd-catalyzed halosilation reactions is 50 °C.^[119] However, the catalyst loading is about 1.6 mol-% based on the SiH-groups. Consequently the Pd-catalyst takes place at milder reaction conditions, although more catalyst is needed.

This is reflected in the appearance and composition of the final products. The Platinum-catalyzed products are clear and colourless to slightly yellow, low viscous liquid (**4.1a** to **4.4**). The Hazen Factor is about 40 to 120 H and the yellowness index is about 10 to 30 Yi (Table 4-1, further details to the methods, s. Appendix A1). In contrast, the palladium-catalyzed products **4.1b** look yellow to brown and slightly milky. Their appearance changes to a dark brown crumbly solid during time with a brown precipitation. With freshly prepared samples the detection of the yellowing is not possible, because the discoloration is already out of the working range of the instrument. A solution with THF (ratio 1:3 compared to the PHMS starting material) shows results which are seven to ten times higher (compared to **4.1a** to **4.4**). It is assumed that the coloration is related to the amount of metal left in the product. There is 5.305 wt-% (± 1.469 wt-%) palladium left in the purified product, while in the sample with platinum it is only 0.011 wt-% (± 0.008 wt-%).

Table 4-1: Hazen Factor and Yellowness Index of sample **4.1a** to **4.4** and **4.1b**.

	4.1a	4.2	4.3	4.4	4.1b^a	4.1b^b
Hazen Factor [H]	112	42	118	72	734	n/d
Yellowness Index [Yi]	26.4	10.6	27.8	17.7	103.9	n/d

^a product is diluted in THF (1:3 compared to the PHMS starting material)

^b purified product (decolorizing by adding activated carbon and filtration through celite; s. Appendix A5)

Analytical results show no by-products in the Pd-catalyzed reactions. The SiH groups are converted to the desired bromobutoxy groups quantitatively. This looks different for the Pt-catalyzed reactions. Here, the formation of hydrosilylation by-products is possible (Figure 4-1, red bars). As an example the ^1H - ^{13}C -HSQC-NMR spectra of product **4.1a** is shown in Figure 4-2. The four signals **b**, **e**, **d** and **c** belong to the four CH_2 -groups of the desired halosilated product. The by-product is nearly invisible in the ^1H -NMR, because signal **h** and **g** are overlapped with signal **e** and **d**. In the ^1H - ^{13}C -HSQC-NMR the overlapping can be visualized. The allegedly separated signals **e** and **d** correlate with two carbon atoms each. Consequently these signals are composed of two groups in the compound.

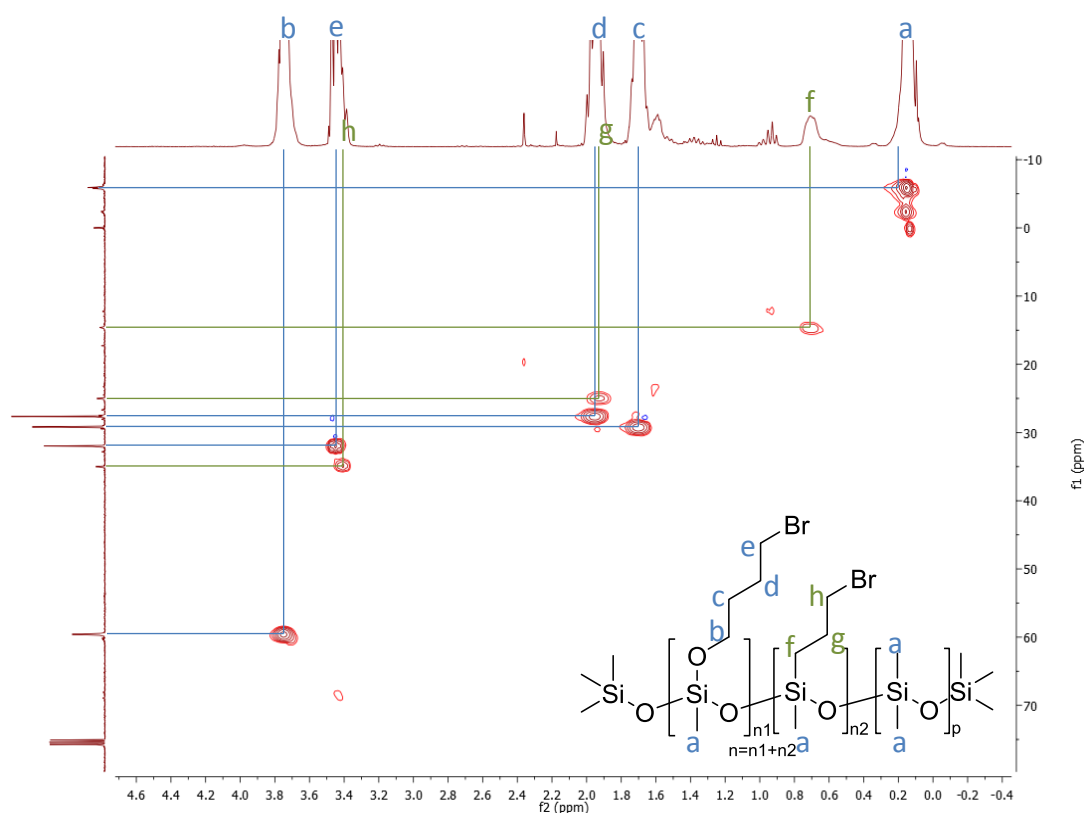


Figure 4-2: ^1H - ^{13}C -HSQC-NMR of **4.1a** in deuterated chloroform (400 MHz, 25 °C); the overlapping of the signals of the halosilated and hydrosilylated products is shown.

The Karstedt catalyst is commonly used for hydrosilylation reactions (s. chapter 3.1.1). The typical reaction conditions for halosilation and hydrosilylation reaction differ only in the presence or absence of THF, so there is a competition between both reaction pathways. The proposed reaction mechanism is discussed in chapter 4.2.1.3. The halosilation reaction is preferred, but it is hypothesized that it is affected by steric hindrances of the ring-opening of THF. The ratio halosilation:hydrosilylation (Figure 4-1) can be influenced by the amount of hydridomethylsiloxane units in the starting material. The more SiH groups in the starting material, the higher the steric hindrance by neighbored bromoalkyl functionalized side-groups and as a consequence the higher is the amount of hydrosilylation by-products. Product **4.1a** contains the most SiH-groups and as a consequence the most bromopropyl side-groups (16.7 %). However, **4.4** contains only 2.4 % by-product (using SM-15 as starting material) and in **4.5a** there is no hydrosilylated by-product detectable. **4.5a** is based on D₃D^H. Compared to the polymeric structures, this cyclic siloxane contains exact four siloxane units, which have a fixed conformation. This defined conformation causes hardly steric hindrances and the by-product is not promoted.

Figure 4-3 shows the obtained molecular masses compared to the expected ones. The results were measured by GPC with a linear styrene standard (s. chapter 3.2.1). As it was already described in chapter 3.2.1 the measured molecular masses of the polymeric starting materials differ from the calculated ones. On the one hand this is explicable by the bulkiness of the products, which causes a smaller hydrodynamic volume. On the other hand the presence of the bromine seems to disturb the measurement as well. The more bromine is in the product, the bigger are the differences. This is also supported by sample **4.5a** and **4.6** which are based on small cyclosiloxanes both. The onefold brominated product **4.5a** shows nearly no divergence, whereas the fourfold brominated sample **4.6** differs a lot. Probably a possible alternative for further investigations could be again MALDI-TOF.

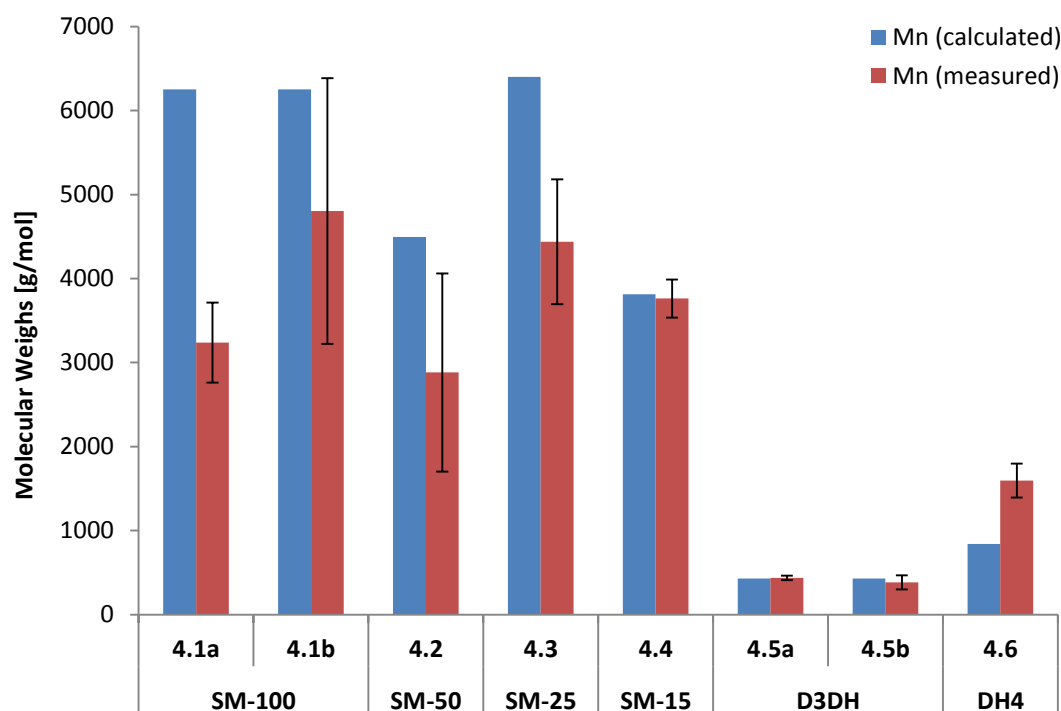


Figure 4-3: Molecular weights of halosilated products; comparison of calculated and measured molecular weights of **4.1a** to **4.10**; the molecular masses were measured by GPC in THF; the standard deviations were calculated from two to three repetitions.

The aforementioned results show that the halosilation reaction can be achieved with both palladium and platinum catalysts. The synthetic pathways differ in their reaction conditions and the purity and appearance of the products. The Pd-catalyzed samples from the literature show no by-products and quantitative conversions. But the products are discolored and the catalyst cannot be removed completely. The Pt-based halosilated products contain hydrosilylated bromopropyl groups as by-products, but the catalyst can be removed better and the appearance of the products show less discolorations. Both synthetic pathways are suitable for the halosilation reaction, but they show different advantages and drawbacks each.

4.2.1.2 Kinetic Studies (Comparison of Pt- and Pd-catalyzed Halosilation)

The concentration/conversion data for the kinetic analysis were calculated by integration of $^1\text{H-NMR}$ (further information, see Appendix A4). The evaluation of the reaction order and activation energy is done with a linear regression and the Arrhenius equation.^[102] The experiments were done with polysiloxane SM-100 to get optimized ratios of the different integrals. As it is shown in Figure 4-4, kinetic experiments of sample **4.1a** take place at 80 °C, 100 °C and 120 °C. The halosilation reaction follows zero order depending on siloxane starting material. The overall reaction is expected to follow zero order as well (the data are listed in Appendix A4, Table A-12). The calculated activation energy is about 47.4 ± 2.2 kJ/(mol). Due to the novelty of the platinum catalyzed halosilation reaction, there are no literature reports to compare it with.

Based on the standard reaction parameters (120 °C, 0.1 % mol Pt in the mixture, s. Representative procedure C, Appendix A4), the platinum-catalyzed halosilation reaction reaches quantitative

conversion after nine hours. This means that the set reaction time of 24 hours is not needed. Furthermore, it is possible to control the conversion due to the reaction order zero either by reaction time, or by decreasing the amount of allyl bromide.

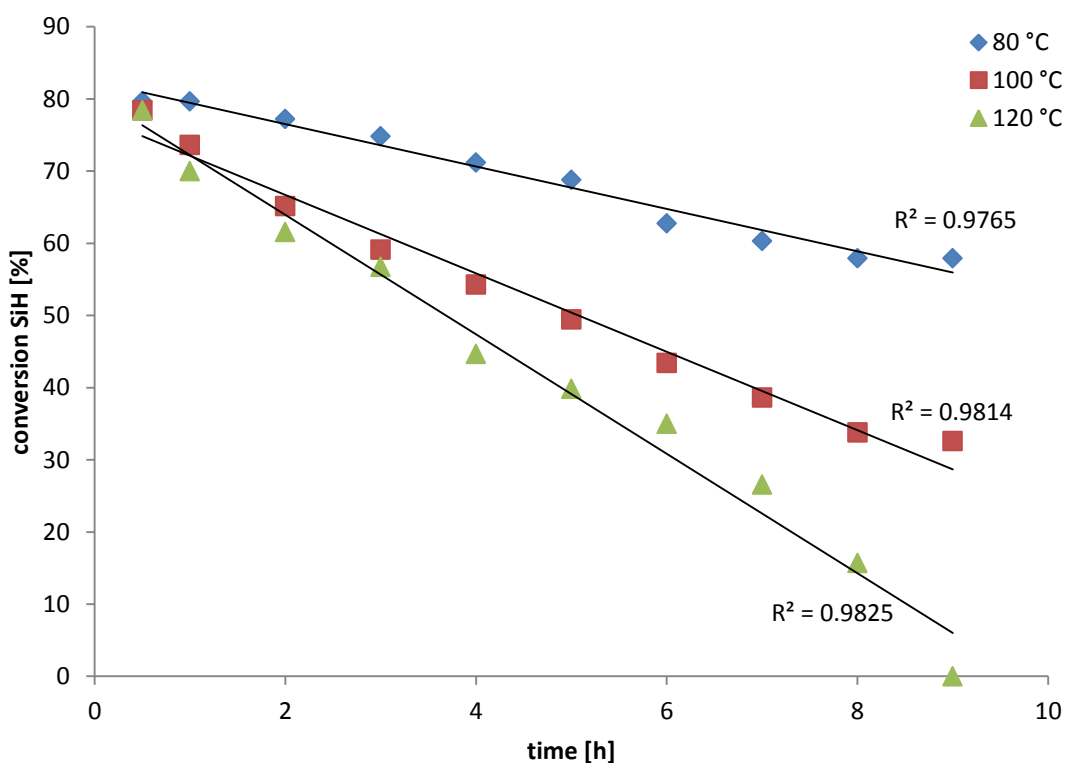


Figure 4-4: Kinetic studies of the synthesis of **4.1a** at different temperatures; the reaction follows zero order depending on the siloxane. The activation energy is about 47.4 ± 2.2 kJ/(mol).

The Pd-catalyzed halosilation reaction is known in the literature. First time-resolved measurements were already done by Dong *et al.*^[111f] The conversion was detected at different reaction times and temperatures, but the results provide no information about the reaction order. As it is shown in Figure 4-5, kinetic experiments of sample **4.1b** were done at 50 °C, 60 °C and 70 °C. The halosilation reaction follows first order depending on the siloxane starting material. The overall reaction follows second order (the data are listed in Appendix A4, Table A-13).

Consequently, the palladium catalyzed halosilation reaction has a different reaction order and hence a different mechanism to the one catalyzed by Karstedt. The given kinetic results show that a standard halosilation reaction with PdCl_2 reaches quantitative conversion after 24 hours.^[111d] This is much longer than the previously calculated nine hours with platinum. The calculated activation energy is about 80.4 ± 3.1 kJ/(mol). Although the reaction needs lower reaction temperatures, the activation energy is nearly doubled.

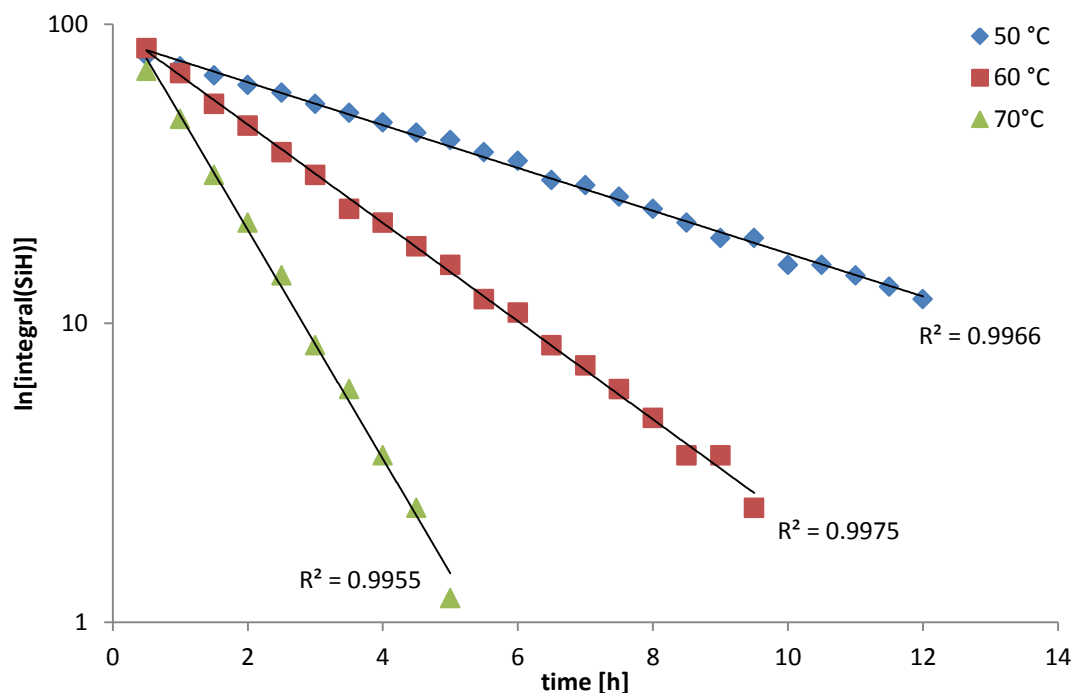


Figure 4-5: Kinetic studies of sample **4.1b** at different temperatures; the reaction follows first order depending on the siloxane; the diagram is logarithmic plotted. The activation energy is about $80.4 \pm 3.1 \text{ kJ/(mol)}$.

The investigations in the kinetics showed that the platinum and palladium catalyzed halosilation reactions follow two different reaction orders depending on the substrates, as well as the overall reactions. The Karstedt catalyzed reaction does not just follow zero order, but already achieves full conversion after nine hours. In addition, it takes place at higher reaction temperatures, although the activation energy is much lower. Considered kinetically, this reaction is favored.

4.2.1.3 Proposed Reaction Mechanism of Pt-catalyzed Halosilation

The aforementioned results show that the Pt-catalyzed synthetic pathway differs a lot from the Pd-catalyzed one. There is not just a change in the reaction order, but also the possibility of a hydrosilylated by-product. Therefore, a look at the reaction mechanism was taken.

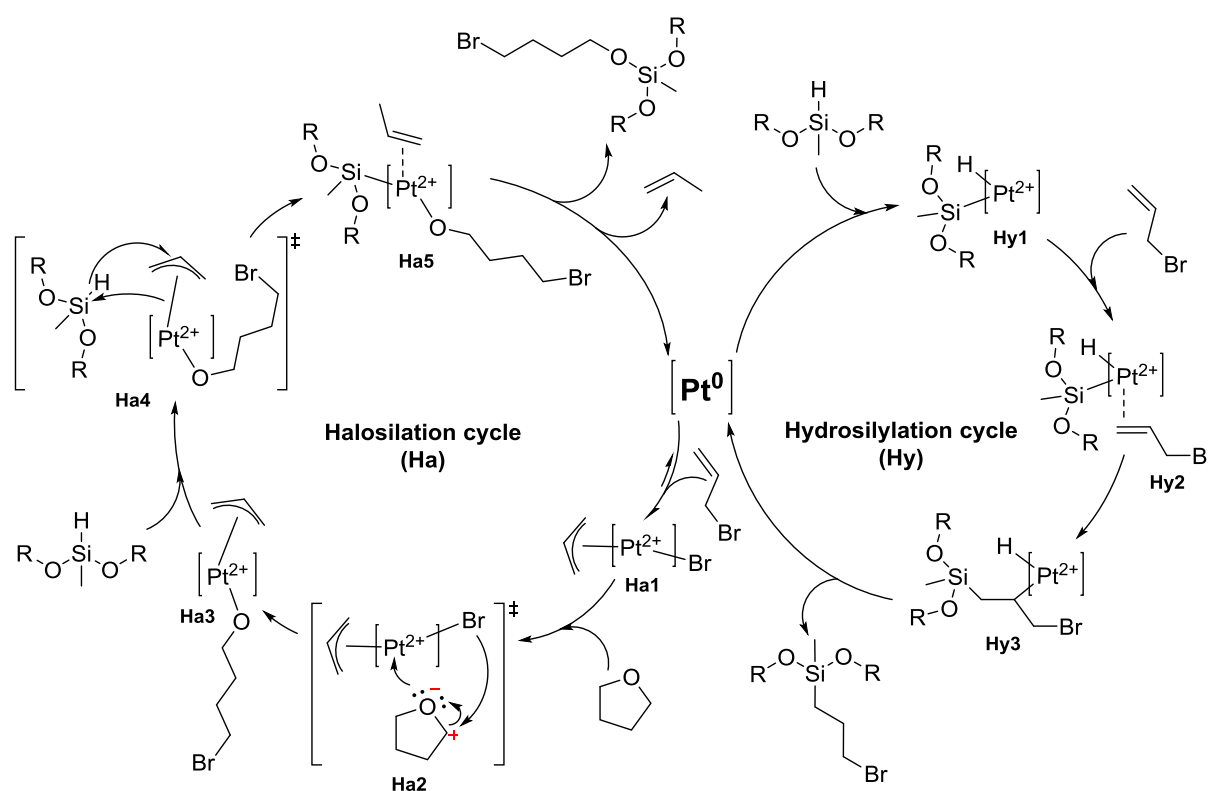
In literature, a proposed mechanism is given by Zhou *et.al.*^[111f] As it was mentioned before, he describes the palladium(II) chloride as the active catalytic species. The SiH groups of PHMS get in contact with the Pd^{2+} metal surface. The oxygen atom of THF, which is the nucleophilic reagent, can attach to the siloxy radical and leads to the cleavage of C-O bond of THF. The ring-opened intermediate of the nucleophilic reagent binds to the iodine from the iodomethane.^[111f]

This proposed mechanism would lead to a Pd^{4+} species after oxidative addition. There are reports in literature which mention the usage of Pd(II) catalysts.^[55c, 121]

For the newly developed platinum catalyzed halosilation the following reaction mechanism is proposed considering the fact that a hydrosilylation can take place as a competitive reaction (s. Scheme 4-6). The left cycle represents the halosilation cycle (**Ha**), while the right one stands for the hydrosilylation

cycle (**Hy**), which is the subordinated reaction pathway in this case. The hydrosilylation path follows a Chalk-Harrod mechanism as it is described in chapter 3.1.1.

The active catalyst is a Pt(0) species. In the beginning of the halosilation cycle, Pt⁰ gets in contact with allyl bromide and forms a Pt²⁺ complex (**Ha1**, oxidative addition). The coordination of the cyclic ether (here THF) leads to intermediate **Ha2**. The positively charged platinum gets in contact with the partial negatively charged oxygen of the ring. The electron-rich bromine interacts with the partial positive charged vicinal carbon of the ring. The intermediate **Ha2** cannot be formed when either steric hindrances avoid it, or in the absence of the cyclic ether. The migratory insertion of the ring-opened THF into the Pt-Br bond produces complex **Ha3**. THF is ring-opened between the oxygen and carbon and the platinum is connected to the oxygen while the bromine binds to the carbon. The coordination of the silane leads to intermediate **Ha4**. The following migratory insertion of the Si-H bond into the Pt-allyl bond produces **Ha5**. Due to the replacement of the hydrogen of the SiH group to the unsaturated allylic compound, the platinum forms a complex with the silicon and the oxygen of the bromobutoxy groups. In a reductive elimination the bromobutoxy functionalized siloxane is released as the main product and propylene as the leaving group. The Pt(0) catalyst is recovered.



Scheme 4-6: Proposed reaction mechanism of halosilation cycle (**Ha**) and possible hydrosilylation cycle (**Hy**) as competitive reaction.

As already mentioned before, the intermediate **Ha2** can only be formed in the presence of cyclic ethers. If there are any steric hindrances or the cyclic ether is not present, the formation of **Ha1** is reversible and the competitive hydrosilylation cycle (**Hy**) is favored (Chalk-Harrod mechanism, s. chapter 3.1.1). This can be confirmed by the fact that the two reactions differ only in the absence/presence of THF. As shown in Figure 4-1, the proportion of by-product can be controlled by

the concentration of SiH groups. The concentration of SiH groups is an indirect indication of steric hindrances.

Unfortunately, it was not possible to isolate and characterize the different intermediates **Ha1** to **Ha5**. However, it is hypothesized, that the reaction mechanism of the Pt-catalyzed halosilation differs from the Pd-catalyzed one. This hypothesis is supported by the fact that there are other intermediates mentioned in the literature, as well as the changed reaction order of Pd-catalyzed reactions (compare subchapter 4.2.1.2). On the other hand, hydrosilylated by-products are not detectable in the Pd-catalyzed experiments.

4.2.1.4 Replacement of Halogen Source and Heterocyclic Compounds

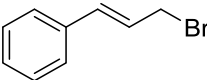
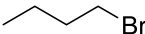
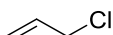
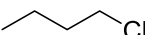
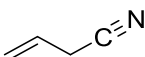
The Pt-catalyzed halosilation reaction represents a new synthetic pathway to form halogenated siloxanes with silyl-oxy bonds. The following screening was performed to show which variations of the halogen sources and the heterocycles are possible.

In the beginning the halogen sources were varied. Table 4-2 summarizes the experiments in which allyl bromide was replaced by different halogen sources. All experiments were performed with the general reaction conditions, so the desired products should contain bromobutoxymethyl siloxane *resp.* chlorobutoxymethyl siloxane units depending on whether a bromo or chloro source was used. All experiments show a strong decrease in the conversion of SiH groups if no allylic halogenide was utilized. **4.7** and **4.9** have a quantitative conversion of SiH, whereas their comparable saturated sources show only 12% (**4.8**) *resp.* 23% (**4.10**) conversion. Here, the importance of the leaving group becomes clear. Allylic groups can be stabilized by their π -electron system better in the reaction cycle than for example butyl groups (s.Scheme 4-6, **Ha1** to **Ha4**).

In addition, derivatization of the allylic compound can influence the yield of halosilation product as well (**4.7**). The standard reaction (**4.1a**) has $83.5 \pm 4.8\%$ halosilation product, but **4.7** gives only 69.5%. The purification was more difficult as well. If we compare the bromine source with the chlorine one, there is a clear decrease in activity. Iodine was not tested in this research, but based on the literature it is a very good and favored halogen source for halogenation reactions.^[111a-f] The assumed order of activity is $I > Br > Cl$.

At last, pseudohalogen functionalized allylic compounds were tested. Allyl cyanide was tested as representative (**4.11**). Unfortunately, there is no formation of halogenated groups, but the favored reaction is the hydrosilylation. There is no clear explanation yet, but it is assumed that halogens form a more polarized C-X bond than cyanide with which the platinum can interact better.

Table 4-2: Summary of the products **4.7** to **4.11** in which the halogen source is varied; unless otherwise indicated, siloxane starting material is SM-100, the cyclic ether is THF and the general reaction conditions were used.

Sample	Halogene Source	Conversion	Yield		Isolated Yield
		SiH [%]	Halosilation [%]	Hydrosilylation [%]	
4.7		>99	69.5	16.5	83
4.8		12	25.9	0.0	26
4.9^a		>99	13.0	47.8	56
4.10		23	86.2	not evaluable	64
4.11		43	0.0	43.0	36

^a Experiment was done with SM-50.

Further investigations were done in the replacement of THF as standard heterocyclic compound. Some investigations were already reported in literature. Different heterocyclic compounds were tested in the halosilation reaction of silanes in combination with iodomethane^[110] and allyl bromide.^[111a, 111b] The halosilation of polysiloxanes was implemented either with other heterocyclic compounds than the shown here^[111c] or with dimethylhydridosiloxane-terminated polysiloxanes.^[111d] Thus the following shows not only the possible applications of the Platinum catalyst, but also novel products.

The conversions and different yields of the experiments **4.12** to **4.18** are summarized in Table 4-3. The intended halosilated sequences of the samples are illustrated in Figure 4-6. Here the allylic bromide was utilized in all experiments to keep the comparability.

Table 4-3: Summary of the products **4.12** to **4.18** in which the heterocyclic compounds are varied; unless otherwise indicated, siloxane starting material is SM-100, the halogen source is allyl bromide and the general reaction conditions were used.

Sample	Heterocyclic Compounds	Conversion SiH [%]	Yield Halosilation [%]	Yield Hydrosilylation [%]	Isolated Yield [%]
4.12		99	56.9	23.0	40-44
4.13		96	60.9	22.5	59
4.14		>99	n/d	n/d	n/d
4.15		>99	0.0	27.5	37
4.16^a		89	n/d	not evaluable	30
4.17^b		>99	84.9	0.0	83
4.18^b		>99	88.8	0.0	82

^a Thiolane is a sulfur analogon to THF.

^b Experiments were done with D₃D^H.

On closer consideration, it is noticeable that the system achieves good results with cyclic ethers. Experiments **4.12** and **4.17**, as well as **4.13** and **4.18** were utilized with tetrahydropyran (THP) *resp.* Hexamethylene oxide (Oxepane). Both are cyclic ethers with a ring size of six *resp.* seven atoms. Although the isolated yield of the polymeric samples (**4.12** and **4.13**) is lower (compared to **4.1a**, 71-93%), the conversion of the SiH groups is quantitative. Moreover, the halosilated product is the main product. The samples based on the cyclosiloxane (**4.17** and **4.18**) show comparable results to the standard reactions (**4.5a**, 57-84%). Again, there is no hydrosilylated by-product detectable.

However, as soon as other heterocycles are tested, the platinum-catalyzed system reaches its limits. If the cyclic ester ϵ -caprolactone (**4.14**) or the THF sulfur analoga thiolane (**4.16**) were utilized, there was no product detectable due to curing processes during reaction. Even the evaluation was hardly possible, because a mixture of different by-products was formed. The cyclic diether 1,4-dioxane (**4.15**) shows hydrosilylated by-product, but no halosilation product as well.

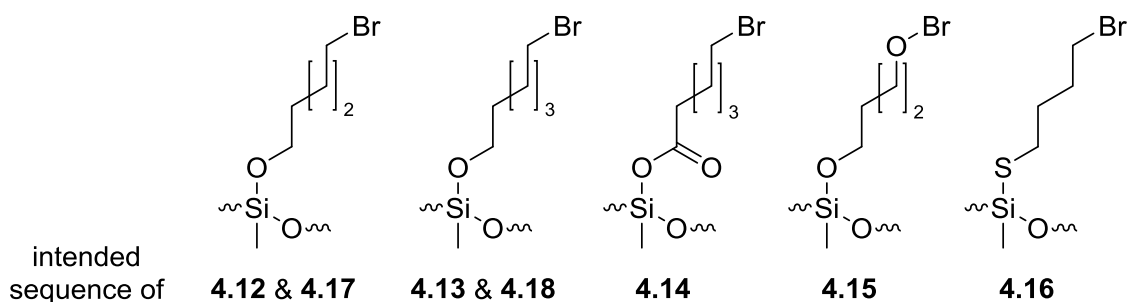


Figure 4-6: *Intended sequences of the experiments 4.12 to 4.18.*

The investigations in the replacement of the standard reactants allyl bromide and THF showed that there is a good possibility to expand the portfolio of reaction conditions and end products. It also showed the limits of the Pt-catalyzed halosilation reaction. The allylic structure is very important to form a stable intermediate, as well as the replacement of THF by esters or other heterocycles increases the amount of by-products.

4.2.1.5 Characterization

The aforementioned comparison between Pt- and Pd-catalyzed halosilation reactions showed already some differences in the synthetic pathway. Since both catalytic systems aim to produce the same product, special focus will be placed on the Pt-catalyzed products. In the following, their properties, such as Viscosity and surface energy (contact angle), were evaluated.

The Viscosity results are shown in Figure 4-7. Due to curing and decomposing processes, it was not possible to analyze the Viscosity of all samples. The given results show low viscosities (< 0.7Pas) when the standard reaction parameters were utilized. Thus, bromination does not appear to have much effect on the Viscosity of the products. For comparison, the viscosities of the hydrosilylated products of Part Ia were 0.3 to 1.5 Pas (s. Appendix A3, Table A-2).

There are big differences between the products **4.1a** (Pt-catalyzed) and **4.1b** (Pd-catalyzed). The Pd-based product has an increased Viscosity from more than 2 Pas. Probably this can be explained by the metallic contamination even after purification processes, which causes also coloring and curing during time. Furthermore, the products **4.9**, **4.12** and **4.13** show increased viscosities as well. **4.9** is the chlorobutoxy-functionalized product, but the main product is the hydrosilylated by-product. As already mentioned (s. chapter 3.2.2), hydrosilylated products generally have a higher Viscosity. The products **4.12** and **4.13**, on the other hand, contain bromopentoxy and bromohexyloxy functionalized siloxane units. The increasing in the carbon chain causes a higher bulkiness which has an influence on the Viscosity. However, the standard deviation of **4.12** is extremely large, since the two individual experiments deviate very much from each other. It is assumed, that either some networking processes took place in one experiment, or the entanglement was bigger.

All in all, the described products show viscosities which are suitable for consecutive reactions or further applications.

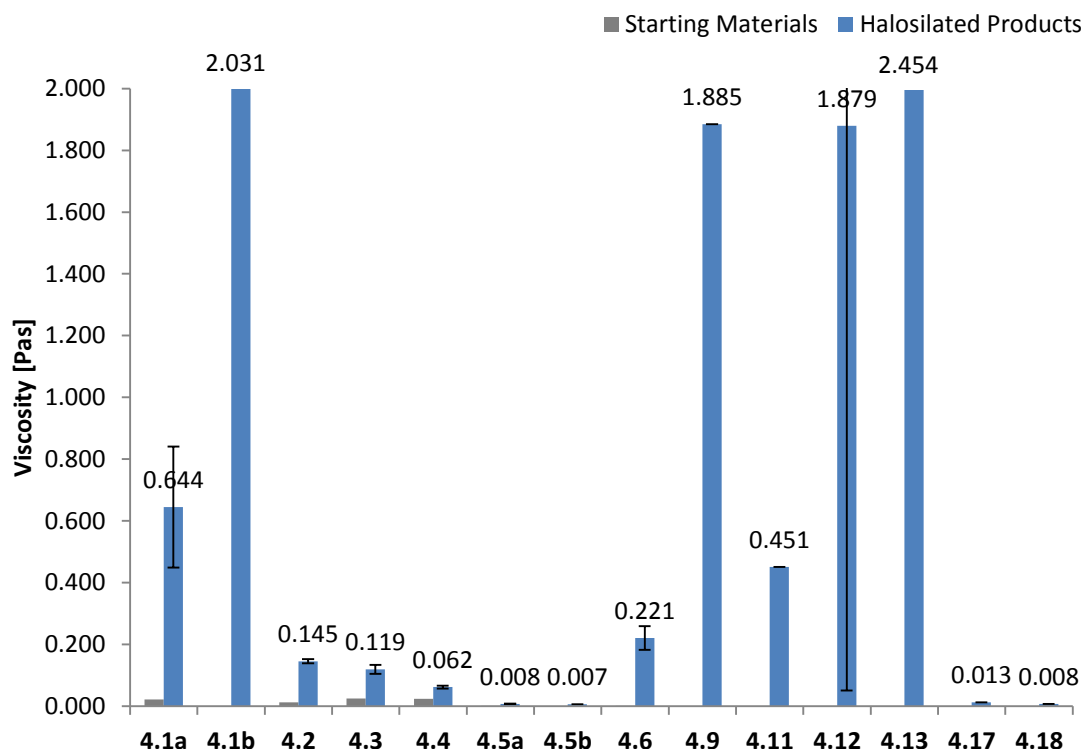


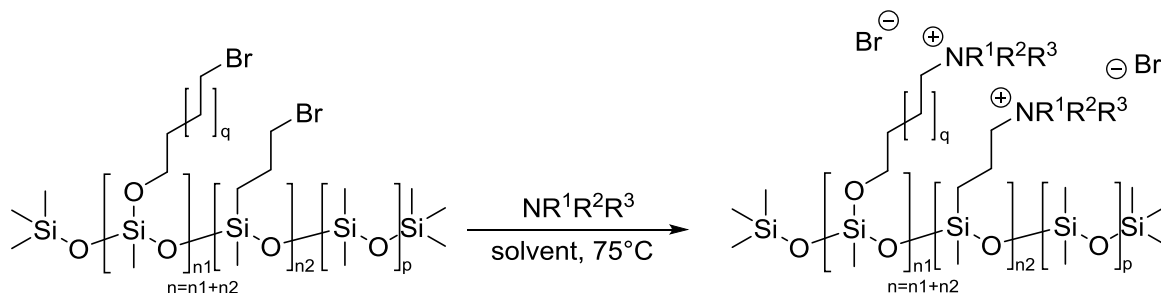
Figure 4-7: Viscosity results of halosilated products **4.1a** to **4.10**; the data of the siloxane starting materials were added as well; the standard deviations were calculated from two to three repetitions.

Furthermore, contact angles (CA) of all samples **4.1a** to **4.6** were taken. Since this part of the research should not have any direct influence on the surface energy, the measured values were only used as controls. As expected, the samples show no significant change in the contact angles. The results are listed in Table A-14 (Appendix A4).

In conclusion the investigations in the Pt-catalyzed halosilation reactions utilized a successful synthetic pathway to synthesize halogenalkyl functionalized products. Not only the reaction conditions, variation of compounds, as well as the kinetic studies make it suitable as a good alternative route to the Pd-based halosilation reaction. The evaluation of the Viscosity of the halogenalkyl functionalized products of Part IIa also showed, that their properties are suitable for consecutive reactions or further applications. As already mentioned, the halosilated products are used as intermediates for the Menshutkin reaction (it will be discussed in the following).

4.2.2 Part IIb: Menshutkin Reaction

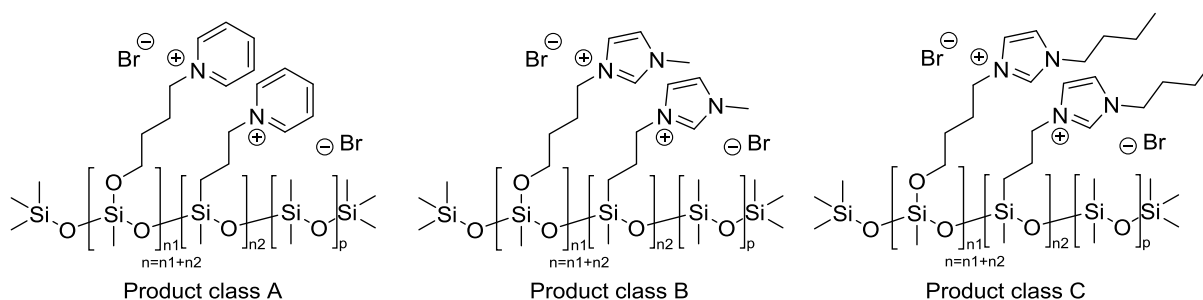
In this part the synthesized halogenated products of Part IIa will be quaternized in a consecutive step, also known as Menshutkin reaction. The general structure of the desired products is shown in Scheme 4-7. The quaternization reaction itself is already known in literature,^[107b, 122] but the novel connection between QAS-group and siloxane backbone via silyl-oxy bond is unknown, which allows the development of novel properties and applications.



Scheme 4-7: General quaternization reaction (Menshutkin reaction) with halosilated siloxanes and amines in the absence of any catalyst

4.2.2.1 Synthesis

The quaternizations were done based on the aforementioned halosilated products **4.1a** to **4.5a**, **4.6** as well as **4.12** and **4.13**. These are the Pt-catalyzed samples, except of **4.1b** for comparison reasons (further details are shown in Table A-17, Appendix A4). In the beginning, several amines were tested, although only pyridine, 1-methyl-1*H*-imidazole and 1-butyl-1*H*-imidazole were successful. The formed product classes are shown in Scheme 4-8. The product class A was made with pyridine and the synthetic pathway is based on Chen *et al.*^[30h] The product classes B and C, for which two different imidazoles are utilized, were already described by Mizerska *et al.*^[107b] However, in both cases the order of the addition of the reactants was changed (s. Scheme 4-4).



Scheme 4-8: General structure of the synthesized Menshutkin products; Product class A is based on pyridine and includes pyridinium bromide groups, product class B on 1-methyl-1*H*-imidazole (1-methylimidazolium bromide groups) and product class C on 1-butyl-1*H*-imidazole (1-butylimidazolium bromide groups).

The formed products **4.19** to **4.44** are summarized in Table A-17 (Appendix A5). In all cases, the products appeared as colorless or yellow to orange, clear to milky, high viscous, sticky liquids. Due to the stickiness, Viscosity measurements were not possible. Due to the liquid aggregate state of the

quaternized silicones, the here formed quaternized products can be named as polymerized ionic liquids (PIL) by definition.^[123]

From the previous chapter 4.2.1.1 it is known that the halosilated products contain a small amount of hydrosilylation by-products. At the beginning, it was checked whether both side-groups participate in the quaternization reaction or if one group is favored. The results of **4.19** are illustrated in Figure 4-8 as an example. The detected shifts and observations of **4.19** can represent all quaternized products **4.19** to **4.44**.

In the ^1H - ^{13}C -HSQC-NMR (Figure 4-8), the signals **i**, **l** and **k** belong to the pyridinium ring and prove the successful quaternization. Due to the change in the carbon's surrounding (signal **e**) from C-Br to C-NR₃⁺ the signal is downfield shifted to a higher extent than **b**. This proves the connection between the siloxane starting material and the amine. While **b** and **c** (located close to the silyl-oxy bond) barely show a change in their positions compared to the halosilated intermediate **4.1a**, signal **d** has also been slightly shifted to downfield. This results in a separation of the signals of the halosilated and hydrosilylated side-groups. Moreover **f** and **g** show slightly shifts to lower ppm (highfield) compared to the bromopropyl group. Probably this is due to the direct bonding to the silicon, so its effect cannot be shielded by the oxygen atom. The quaternization of the hydrosilylated side-group can be proven by the shift of signal **h**. In the ^1H -NMR the shift is not that big, but there is a big shift in the ^{13}C -NMR from 34.9 ppm to 67.3 ppm.

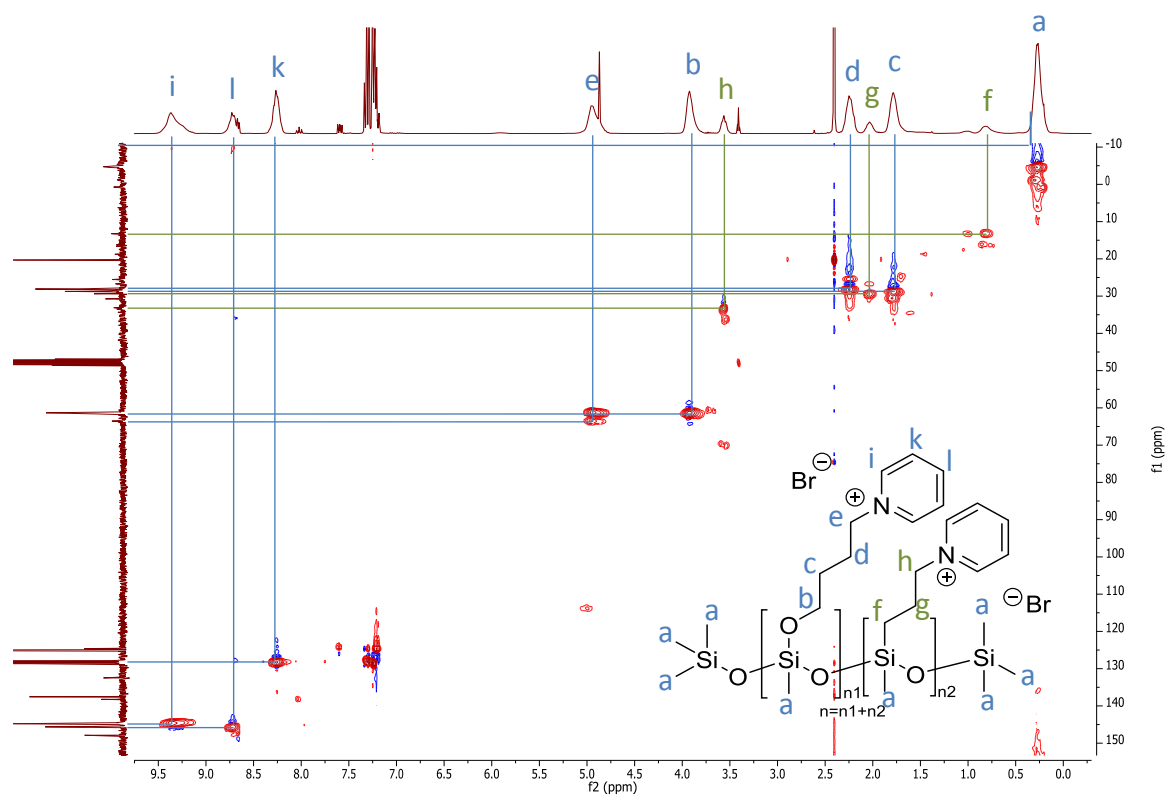


Figure 4-8: ^1H - ^{13}C -HSQC-NMR of **4.19** in deuterated chloroform (400 MHz, 25 °C); for reasons of simplification the methyl groups on the silicon have been grouped together as **a**.

The ^1H - ^{13}C -HSQC-NMR spectrum in Figure 4-8 shows not only the good correlation, but there is also the signal of the solvent visible (Toluene at ~ 7.25 and 2.40 ppm). This demonstrates one problem that has arisen during the synthesis work. Due to the stickiness and the high viscosities of the products, the removing of the solvent is difficult. Furthermore, the conversions differ depending on the siloxane starting material and the amine. The lower the concentration of brominated side-groups in the starting material, the more difficult it is to quantify the conversion via NMR. This is especially the case with SM-25, SM-15 and $\text{D}_3\text{D}^{\text{H}}$. Taken as a whole the samples converted with 1-butyl-1*H*-imidazole in toluene/ethanol (1:1) show the highest conversion with an average of 74.7 ± 5.0 %, followed by pyridinium bromide containing samples (72.7 ± 12.7 %). Samples based on 1-methyl-1*H*-imidazole show the lowest conversion with an average of 62.4 ± 11.8 %. 1-methyl-1*H*-imidazole also shows the biggest difficulties in the synthesis and removal of unreacted amine. Another reason for the non-quantitative conversion may be the size and bulkiness of the halosilated starting materials.

To determine the relationship between conversion of the product and purification (removing of the solvent and volatiles), a solvent-screening was performed. The results are summarized in Figure 4-9. The solvents are sorted by their polarities from nonpolar to polar (according to the elution strength). Overall, no significant difference in the reaction can be determined referred to the variation of the solvents. However, it is clear that 1-methyl-1*H*-imidazole has a much lower conversion in most cases. DMF seems to be the most suitable solvent which is also utilized in literature.^[107b] It promotes the highest conversion (95%) of product **4.21**. The complete removal of the solvent could not be reached in any case. The best results were obtained with acetonitrile, DMF and the mixture Toluene/EtOH, whereas alcohols should be preferred towards environmental issues.^[124]

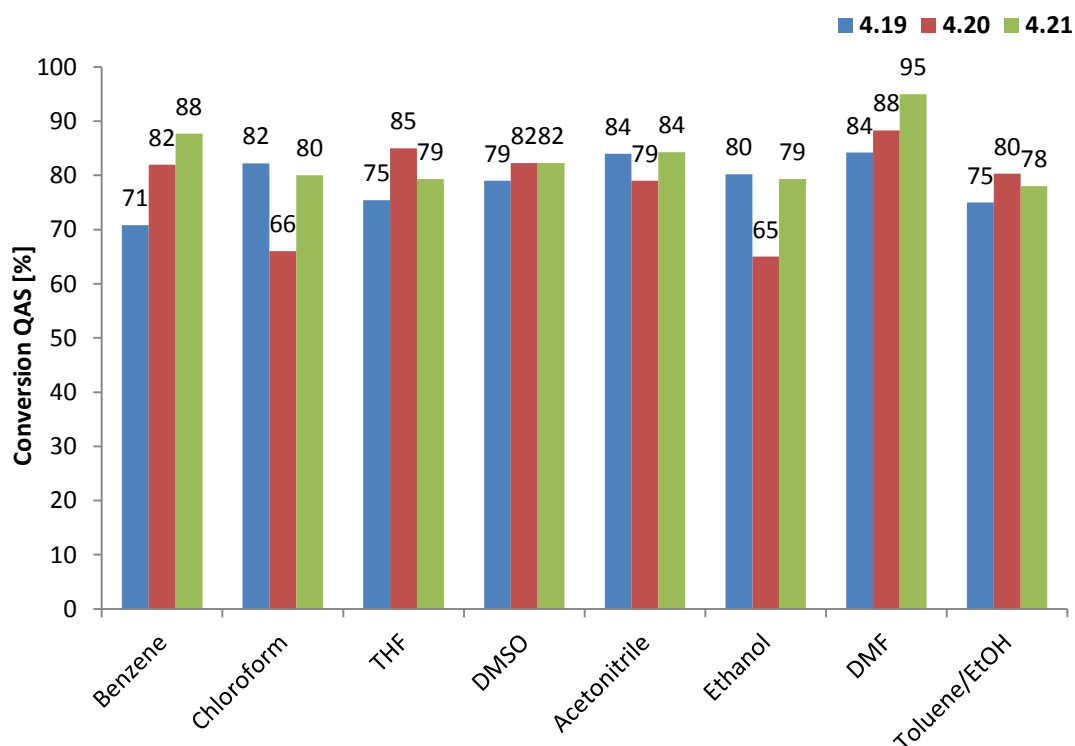


Figure 4-9: Solvent-screening of samples **4.19**, **4.20** and **4.21**; the solvents are arranged by their polarity (according to the elution strength).

Apart from the dependence of the conversion on the solvent, the solvent-screening also showed that the complete dissolution was not always achieved. This is also evident in the problem of determining the conversions via NMR for samples with smaller amounts of side groups as it was mentioned before (for example samples **4.33** to **4.41**, which are based on SM-25, SM-15 and D_3D^H). The siloxane backbone is soluble in deuterated chloroform, but the quaternized side-groups are soluble in polar solvents. In addition the determination of the molecular mass via GPC measurements is hardly possible. The products with increased numbers of side-groups (for example **4.19** to **4.32**) are not soluble in THF, which is utilized as eluent. Also, the samples appear to change their state of aggregation over time. The freshly produced liquid samples may become solid and waxy over time. Analytical results proved that this is not a decomposition or chemical reaction of the product. Probably the ionic structure of the products leads to an amphiphilic orientation as it was already mentioned by Novi *et.al.*^[30b] This orientation cannot be changed by solutions, heat or ultrasound afterwards.

To determine the problem of seemingly varying solubility, solubility tests of all samples were performed. In addition, the solubility of the halosilated products (**4.1a**, **4.2** to **4.5a**, **4.6**, **4.12** and **4.13**) and the starting materials were also determined. For reasons of clarity and comprehensibility only results of chosen products based on SM-100 and SM-15 are shown in Figure 4-10 and Figure 4-11. The other results and further information about the performance are shown in Appendix A5. Thereby it was taken into account, that the chosen products can represent all important observations.

The solvents in Figure 4-10 were sorted by their polarity from nonpolar to polar (according to the elution strength). The starting material SM-100 is soluble in nonpolar solvents. The halogenated samples **4.1a**, **4.12** and **4.13** are soluble in non-polar solvents too, whereas the highly non-polar solvents n-heptane and n-hexane are no longer suitable, but DMF is appropriate. The number of carbon atoms in the side-groups does not matter. However, once quaternary groups have been introduced into the silicone, the solubility shifts to the polar side. Again, the number of carbon atoms in the side-groups does not matter. Moreover the quaternized samples with the highest number of side-groups are soluble in water. However, the product precipitates after 24 hours (yellow fields).

	SM-100	4.1a	4.12	4.13	4.19	4.20	4.21	4.24	4.25	4.26	4.27	4.28	4.29
n-Hexane	Green	Red	Red	Red	Red	Red	Red	Red	Red	Red	Red	Red	Red
n-Heptane	Green	Red	Red	Red	Red	Red	Red	Red	Red	Red	Red	Red	Red
Toluene	Green	Green	Green	Green	Red	Red	Red	Red	Red	Red	Red	Red	Red
Benzene	Green	Green	Green	Green	Red	Red	Red	n/s	n/s	n/s	n/s	n/s	n/s
Chloroform	Green	Green	Green	Green	Red	Red	Red	Red	Red	Red	Red	Red	Red
THF	Green	Green	Green	Green	Red	Red	Red	Red	Red	Red	Red	Red	Red
Ethylacetate	Green	Green	Green	Green	Red	Red	Red	Red	Red	Red	Red	Red	Red
Acetone	Green	Green	Green	Green	Red	Red	Red	Red	Red	Red	Red	Red	Red
DMSO	Red	Red	Red	Red	Green	Green	Green	Green	Green	Green	Green	Green	Green
Acetonitrile	Red	Red	Red	Red	Red	Green	Green	n/s	n/s	n/s	n/s	n/s	n/s
EtOH	Green	Red	Red	Red	Green	Green	Green	Green	Green	Green	Green	Green	Green
MeOH	Red	Red	Red	Red	Green	Green	Green	Green	Green	Green	Green	Green	Green
DMF	Red	Green	Green	Green	Green	Green	Green	n/s	n/s	n/s	n/s	n/s	n/s
Water	Red	Red	Red	Red	Yellow	Yellow	Yellow	Yellow	Yellow	Yellow	Yellow	Yellow	Yellow

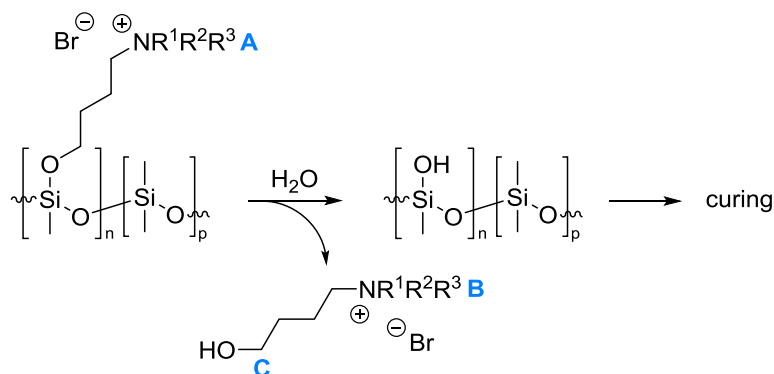
Figure 4-10: Solubility tests of SM-100 and SM-100 based samples; the green fields show solubility, the red fields show insolubility, and the yellow fields represents the change from solubility to precipitation over time or increasing in concentration; n/s = not specified.

Figure 4-11 shows the solubility-test results of the samples **4.4** and **4.36** to **4.38** which are based on SM-15. The starting material and the halosilated product show similar results to those presented in Figure 4-10, whereby **4.4** is more soluble in nonpolar solvents. The quaternized products show no longer such a strong change in polarity. The boundaries between polar and nonpolar blur. Here the influence of the siloxane backbones becomes clear. The siloxane backbone is responsible for the solubility in nonpolar solvents, whereas the quaternized side-groups are responsible for the solubility in polar solvents. The higher the amount of quaternized side-groups in the polymer, the more soluble is the sample in polar solvents. With the decreasing of these side-groups the solubility shifts back to the nonpolar solvents. This phenomenon can be observed over the different products (sorted according to the starting materials).

	SM-15	4.4	4.36	4.37	4.38
n-Hexane	Green	Green	Green	Green	Green
n-Heptane	Green	Green	Green	Green	Green
Toluene	Green	Green	Red	Green	Red
Benzene	Green	Green	Green	Green	Red
Chloroform	Green	Green	Green	Green	Green
THF	Green	Green	Red	Green	Green
Ethylacetate	Green	Green	Red	Red	Red
Acetone	Green	Green	Green	Green	Green
DMSO	Red	Red	Green	Green	Green
Acetonitrile	Red	Red	Red	Red	Red
EtOH	Red	Green	Green	Green	Green
MeOH	Red	Red	Green	Green	Green
DMF	Red	Yellow	Red	Green	Yellow
Water	Red	Red	Red	Red	Red

Figure 4-11: Solubility tests of SM-15 and SM-15 based samples; the green fields show solubility, the red fields show insolubility, and the yellow fields represents the change from solubility to precipitation over time or increasing in concentration.

Now it becomes clear why the solvent is so important in the synthesis. Optimally, it should dissolve both the halogenated intermediate and the quaternized product. In addition, storage of the products in dissolved form can prevent a change in the state of aggregation (solidification). However, the polarity of the solvent again plays a very important role. As it was mentioned before, a time-delayed precipitation of some quaternized samples could be overserved when they were diluted in water or some other polar solvents. This precipitation is caused by the instability of the silyl-oxy bond against hydrolysis. In the presence of water, the silyl-oxy bond is split as it is illustrated in Scheme 4-9. The low molecular weight quaternary ammonium salt remains soluble in the polar solvent while the silicone precipitates.



Scheme 4-9: Proposed hydrolysis process of the quaternized samples and further curing of the siloxane backbone; the blue letters mark the groups of **Figure 4-12** and **Figure 4-13**.

This hydrolysis could be visualized in time-resolved ^1H -NMR experiments of **4.19** (**Figure 4-12**) and **4.20** (**Figure 4-13**). These two samples stand exemplary for the possibility to hydrolyze both the pyridinium-functionalized and the imidazolium-functionalized silicones. **Figure 4-12** shows the temporal change of the ^1H -NMR spectrum of **4.19** over a period of 11 weeks. The broad signal **A** at 9.26 ppm decreases with time, which belongs to the QAS-group linked to the silicone through the silyl-oxy bond. At the same time, a narrow doublet **B** is created at 9.15 ppm and increases during time. This signal belongs to the quaternary group which is hydrolyzed (s. Scheme 4-9). Moreover a new triplet **C** is formed at 3.10 ppm, which belongs to the hydrogen atoms of the newly formed $-\text{CH}_2\text{-OH}$ group.

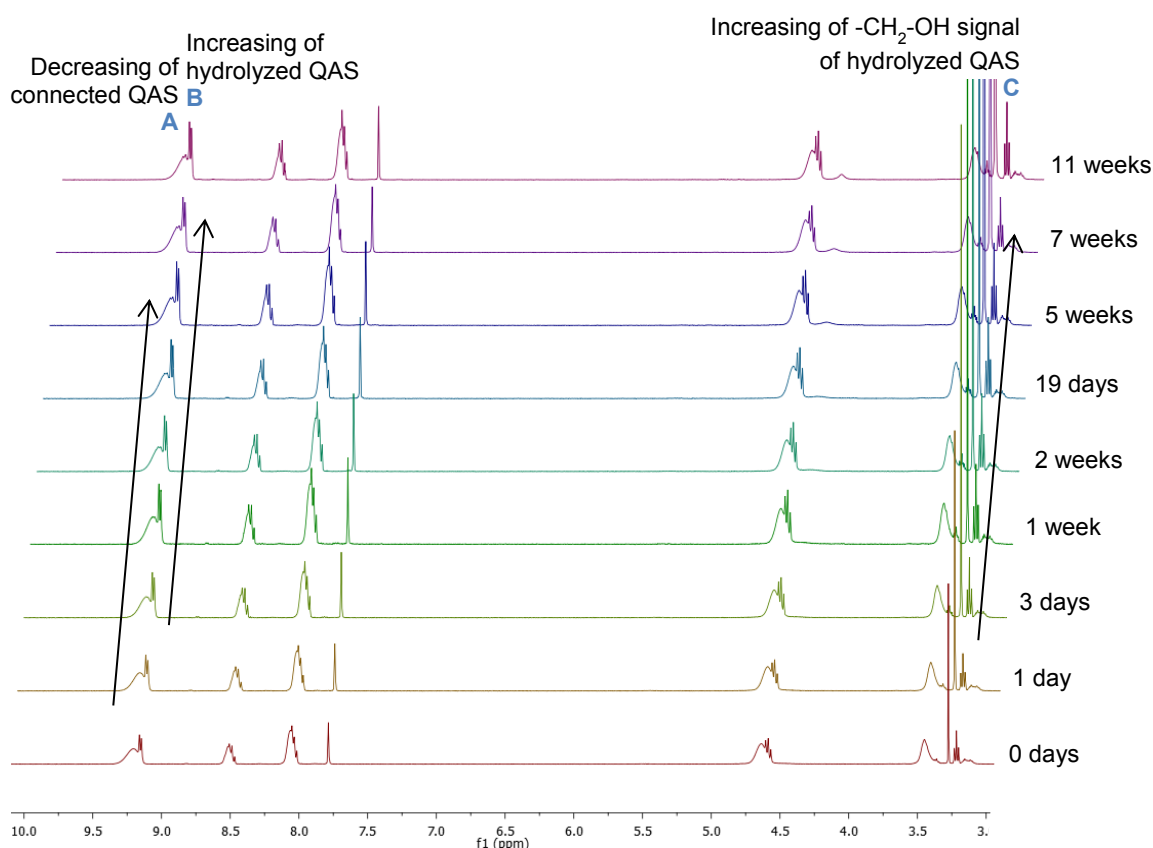


Figure 4-12: Time-resolved ^1H -NMR of **4.19** in deuterated DMSO (400 MHz, 26 °C); it is an example for the hydrolysis of the pyridinium-functionalized side-group.

In sample **4.20** (Figure 4-13) the hydrolysis over time can be followed as well. This is the hydrolysis of an imidazolium-functionalized side-group. In comparison to **4.19** the hydrolysis of imidazolium groups seems to be slower. The signals of the hydrolyzed QAS-containing leaving group (**B** at 9.25 ppm and **C** at 3.15 ppm) can be detected after one week. However, the quantification of the hydrolysis speed is difficult due to the overlap of the signals **A** and **B**.

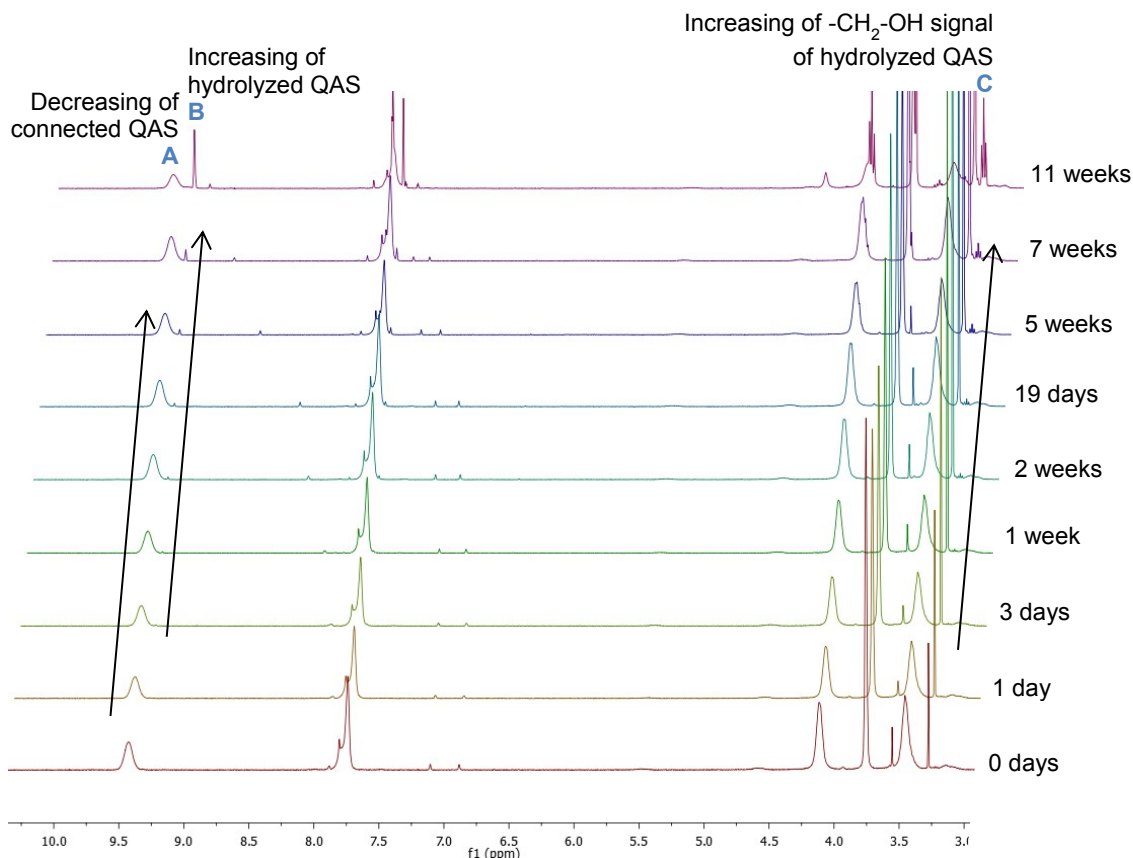


Figure 4-13: Time-resolved ^1H -NMR of **4.20** in deuterated DMSO (400 MHz, 26 °C); it is an example for the hydrolysis of the imidazolium-functionalized side-group.

With the help of the aforementioned results it could be shown that the halosilated products are quaternizable. Several products based on pyridine, 1-methyl-1*H*-imidazole and 1-butyl-1*H*-imidazole were produced. It could be shown that the conversion depends on the amine and the suitable solvent. In addition, the solubility changes with the introduction of the quaternary groups. Due to the orientation of the ions in the polymer during time^[30b] and the ability to hydrolyze the silyl-oxy bond, careful storage of the products is required. The time-resolved ^1H -NMR spectra proved the hydrolysis of the silyl-oxy bond to form QAS-containing leaving groups. The quantification of the ^1H -NMR spectra was not possible due to overlapping of the signals, but the influence of the QAS-group on the hydrolysis speed could be proved.

4.2.2.2 Kinetic Studies of Menshutkin Reaction

In order to determine possible optimization processes to improve conversion, kinetic studies were also carried out. The reaction order was calculated by integration of ^1H -NMR (further information, see Appendix A5). The evaluation of the reaction order is done with a linear regression. The experiments

were done with **4.19** (based on SM-100 and pyridine), since the partially strong overlap of the signals in the $^1\text{H-NMR}$ of **4.20** and **4.21** makes an evaluation of the kinetic data hardly possible without obtaining a very large error. In addition, only the formation of the quaternary compound can be monitored, since the signal **e** (C-Br, s. Figure 4-2) cannot be integrated separately.

As it is shown in Figure 4-14, the kinetic experiments of sample **4.19** take place at 65 °C, 75 °C and 85 °C. For the determination of the reaction order, the signals **e**, **i** and **l** (Figure 4-8) were averaged and their squared values were plotted against time reaction time. The overall reaction is expected to follow second order (the data are listed in Appendix A5, Table A-19). The second order kinetics can be confirmed by literature reports.^[125]

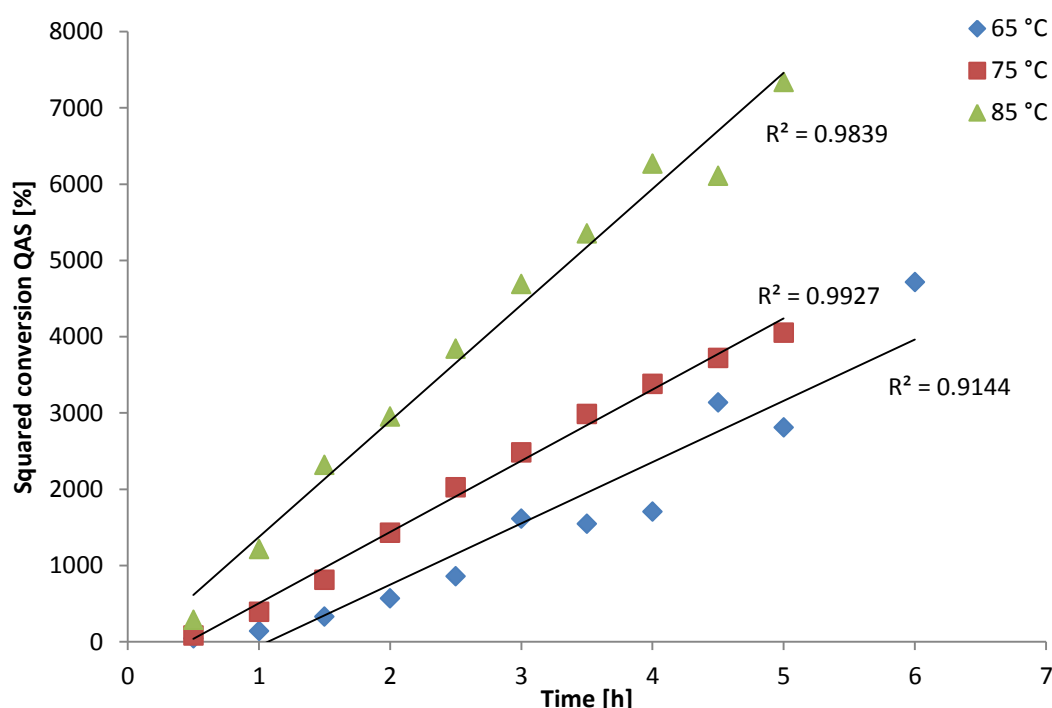


Figure 4-14: Kinetic studies of sample **4.19** at different temperatures; the overall reaction follows second order; the y-axis contains the squared data.

The kinetic measurements have shown that the Menshutkin quaternization is a second-order reaction. Thus, the reaction rate depends on both the silicone and the amine and is concentration-dependent. Probably the Menshutkin reaction reaches higher conversions with another type of reactor.^[126] Similar results were already reported by Selvamony.^[127]

4.2.2.3 Characterization

Besides the synthetic pathway, also the properties of the formed products were evaluated. As already mentioned due to the stickiness and changed solubility of the products, the general properties such as Viscosity or the molecular masses could not be determined. Instead, the glass transition temperature and, as before, the contact angles were measured.

The glass transition temperature was measured via DSC (Differential Scanning Calorimetry, further information s. Appendix A1). For comparison also the T_G of the starting materials, as well as the

halosilated intermediates **4.1a**, **4.2** to **4.5a**, **4.6**, **4.12** and **4.13** were measured. As it was already mentioned, siloxanes have a high torsional flexibility due to the differences between the Si-O-Si (145°) and O-Si-O (110°) bond angles. This difference causes a low bond torsional barrier around the Si-O bond (close to 0.0 kcal/mol). Due to the low bond torsional barrier glass transition temperatures (T_G) of polysiloxanes are often very low ($\sim -120^\circ\text{C}$) and they are amorphous at room temperature.^[8] The working range of the available instrument only goes down to -75°C . Therefore, the starting materials, the intermediates, as well as some quaternized products are outside the measurement scale.

The results are shown in Figure 4-15. It becomes clear that the quaternary side-groups can increase the glass transition temperature significantly. The increase depends both on the amount of the quaternary side-groups in the polymer and on the nature of the quaternary group, meaning the amine on which it is based. For example the samples containing pyridinium bromide groups (product class A) show the biggest increase of the glass transition temperature (blue bars). Although SM-100 and the halosilated intermediate 4.1a have glass transition temperatures lower than -75°C , the corresponding quaternized product **4.19** (left blue bar) shows an increase of minimum 40°C with a T_G of -32.2°C . This slope decreases with decreasing proportion of quaternary side groups (from left to right). **4.39** (pyridinium bromide functionalized $\text{D}_3\text{D}^{\text{H}}$) is again outside the measuring range. The product classes B (containing 1-methylimidazolium bromide groups) and C (containing 1-butylimidazolium bromide groups) show comparable trends. However, their T_G s are lower, which means that they can drop out of the measuring range even with higher amounts of QAS in the polymer.

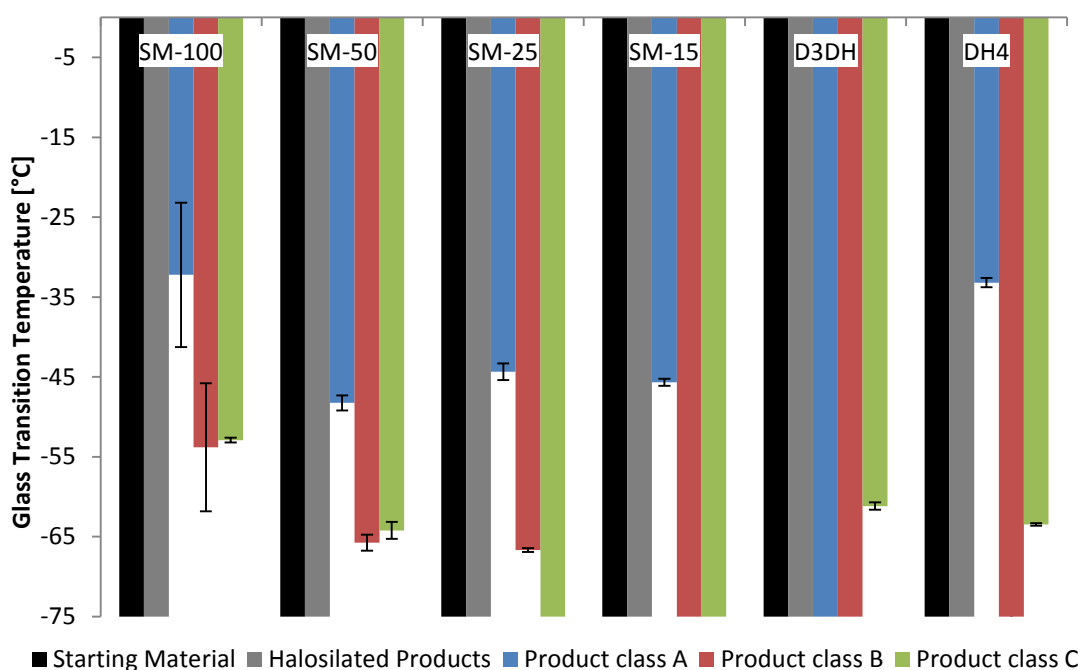


Figure 4-15: DSC measurements of the quaternized products; blue: product class A (including pyridinium bromide groups), red: product class B (including 1-methylimidazolium bromide groups), green: product class C (including 1-butylimidazolium bromide groups); the black bars are the starting materials and the grey bars are the corresponding halosilated intermediates; measured values in the lower part of the diagram are outside the measuring range (below -75°C); the standard deviations were calculated from two to three repetitions.

In addition to the general DSC measurements, the glass transition temperatures were also measured compared to the length of the alkyl chains. For this purpose, the samples **4.19** to **4.21** and **4.24** to **4.29** were measured, as well as their intermediates **4.1a**, **4.12** and **4.13**. All products are based on SM-100, but they differ in the length of the alkyl chain between the siloxane backbone and the quaternary ammonium groups, which can be a butoxy, pentoxy or hexyloxy group. The results are shown in Figure 4-16. As before, the halosilated intermediates are outside the measurement range. The quaternized products, on the other hand, again show strikingly increased glass transition temperatures. The products quaternized with pyridine again have the highest T_G (-37.6 to -28.4 °C). The other two product classes (red and green bars) show comparable results (-61.0 to -52.9 °C). Overall, neither the alkyl chain between silicone and quaternary group seems to have any influence on the glass transition, nor the terminal alkyl chain on the quaternary group itself.

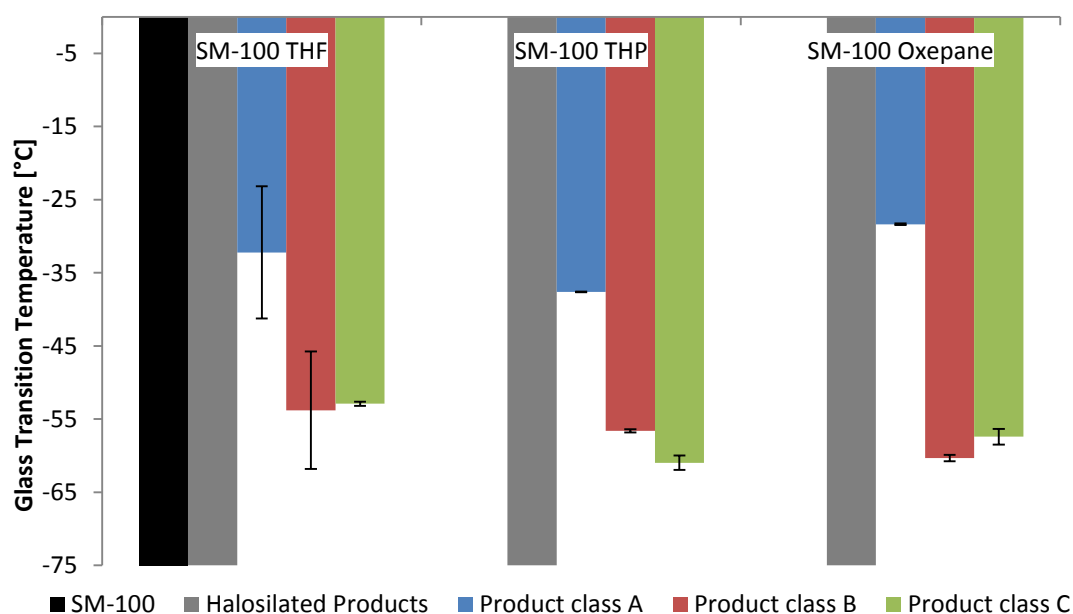


Figure 4-16: DSC measurements of the quaternized products based on SM-100; blue: product class A (**4.19**, **4.24**, **4.27**), red: product class B (**4.20**, **4.25**, **4.28**), green: product class C (**4.21**, **4.26**, **4.29**); the black bar is the starting material SM-100 and the grey bars are the corresponding halosilated intermediates **4.1a**, **4.12** and **4.13**, measured values in the lower part of the diagram are outside the measuring range (below -75 °C); the standard deviations were calculated from two to three repetitions.

Furthermore, contact angles (CA) of all samples **4.19** to **4.44** were measured. Since this part of the research should not have any direct influence on the surface energy, the measured values were only used as controls. As expected, the samples show no significant change in the contact angles. The results are listed in Table A-21 (Appendix A4).

In conclusion, the quaternization of the halosilated intermediates via Menshutkin reaction is possible and gives a variety of products with different amounts and structures of quaternary ammonium salt groups. The products have a big influence on the glass transition temperature, but probably little on the CA. Both the halosilated and the hydrosilylated by-products are equally quaternized. However, conversion and storing is affected by both the amine and the solvent.

4.3 Determination of Antimicrobial Properties

The introduction of antimicrobial (including antibacterial and antifungal) properties into polymeric matrices is an important topic nowadays. The culprit of antimicrobial activity is either hampering the growing of microorganisms^[32] or killing them.^[30-31, 33] Good antimicrobial activity depends on both, the structure and morphology of the material, although it can act very differently on different strains of bacteria/fungi. To this day, the structure-activity relationship of antimicrobial materials is not completely understood, so the activity prediction of newly developed compounds is not possible yet.

In this research, the introduction of brominated and quaternized ammonium side-groups into silicones is presented with the aim of achieving bactericidal and fungicidal properties. For testing the desired antimicrobial activity, the Kirby-Bauer Test, the ISO 22196 and the minimum inhibitory concentration (MIC) were utilized and evaluated. This gives an overview about the antimicrobial activity of the produced samples, as well as their strengths and weaknesses.

This part of the research was done in close collaboration with the Microbiological Department in Henkel Corporation in Dusseldorf. The antimicrobial tests were performed and recorded by the Microbiological Department.

4.3.1 Kirby-Bauer Test

The Kirby-Bauer Test is also known as Agar Diffusion Test and can be used for determination of antimicrobial activity in combination with diffusion properties.^[128] It determines the ability of an antimicrobial agent to inhibit the growth of microorganisms. The antimicrobial test substrate (preferably in the liquid phase) is applied to the center of an agar plate (prepared with the respective strain) onto a small filter paper. After a certain incubation time, the diameter of zone of inhibition is measured (further information s. Appendix A1).

The Kirby-Bauer test is a cheap quick test to get an initial statement about antimicrobial activity to all desired bacteria, yeasts or fungi. The samples can be used concentrated or dissolved in different solvents. However, the test does not clearly show whether the microorganisms were killed or only prevented from growing. In addition, the test can clearly show that the test substrate is antimicrobial active. However, a negative test result does not always equate to inactivity. Leaching and diffusion effects can influence the test results. An antimicrobial agent that leaches into the agar matrix has a larger contact area to the test strain than a solid, insoluble one. Therefore, the test substrate should be liquid.

Therefore, the test results should not be quantified and should generally be assessed with caution. The Kirby-Bauer Test is very well suited to get first trend-setting results quickly on which further tests can be built upon.

For reasons of clarity and comprehensibility, only results of chosen products based on polymeric starting materials are shown in Figure 4-17. The other results and further information about the performance are shown in Appendix A5. The products shown were chosen to represent all important observations. The utilized strains are *Aspergillus brasiliensis* (fungus), *Staphylococcus aureus* (gram-

positive bacterium) and *Exophiala dermatitidis* (black yeast). Methicillin-resistant *Staphylococcus aureus* (MRSA) is known as a hospital bug.

Besides the synthesized samples, some reference materials and starting substances were tested. 4-Bromo-1-butanol and 1-bromobutane represent the possible leaving groups after hydrolysis of the brominated intermediates. While 4-bromo-1-butanol shows strong activity, 1-bromobutane appears to be inactive. Since the quaternized samples were dissolved in DMSO in order to keep the influence of the diffusion as constant as possible, DMSO was also measured. It shows no antimicrobial activity. Bardac® is a disinfectant containing didecyl dimethylammonium chloride (DDAC). It shows antimicrobial activity depending on its concentration, although it is not used undiluted. At last, the amines were tested in pure form and diluted, showing only a certain activity in their pure form.

Since bromine is classified as toxic, first tests were already done with the halogenated intermediates (**4.1a** to **4.4**). Due to their insolubility in DMSO, these samples were measured in their pure form. They showed antimicrobial activity in some cases. This is dependent on the proportion of brominated side groups in the polymer.

The QAS-functionalized samples **4.19** to **4.38** show antimicrobial activities in all cases. These first test results prove the successful introduction of antimicrobial activity, which was the aim of this research. As already mentioned these samples change their aggregation state during time, so they were stored and measured in DMSO. The lower activity compared to **4.19** may be due to the lower concentration due to dilution. Moreover, the Kirby-Bauer Test should not be quantified. The zone of inhibition is comparable in all cases. The compounds work better against bacteria (*Staphylococcus aureus*) and black yeast (*Exophiala dermatitidis*) than against fungi (*Aspergillus brasiliensis*).

































































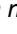
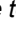
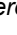

Zone of Inhibition [mm]			
(maximum 45 mm)			
Samples	<i>Aspergillus brasiliensis</i>	<i>Exophiala dermatitidis</i>	<i>Staphylococcus aureus</i>
4-Bromo-1-butanol	 9.0	 34.0	 21.0
Bromobutane	0.0	0.0	0.0
DMSO	0.0	0.0	n.d
Bardac®	 4.5	 11.4	 12.1
Bardac® 1:10	 2.0	 5.3	 8.0
Bardac® 1:100	 1.5	 4.3	 4.5
Pyridine	0.0	 1.0	 1.0
Pyridine 1:10	0.0	0.0	0.0
Pyridine 1:100	0.0	0.0	0.0
1-Methyl-1 <i>H</i> -imidazole	 3.5	 12.3	 6.5
1-Methyl-1 <i>H</i> -imidazole 1:10	0.0	0.0	0.0
1-Methyl-1 <i>H</i> -imidazole 1:100	0.0	0.0	0.0
1-Butyl-1 <i>H</i> -imidazole	 5.0	 15.0	 11.0
4.1a	0.0	 29.0	 17.0
4.2	0.0	 10.0	0.0
4.3	0.0	0.0	0.0
4.4	0.0	0.0	0.0
4.19	 1.0	 4.4	 2.0
4.20	 4.4	 8.8	 10.5
4.21	 3.5	 7.8	 9.0
4.24	0.0	 6.0	 6.0
4.25	0.0	 6.0	 7.0
4.26	 2.8	 8.3	 8.3
4.27	0.0	 7.0	 6.0
4.28	0.0	 9.0	 7.0
4.29	 1.8	 8.3	 8.0
4.30	0.0	 4.7	 8.5
4.31	 1.3	 8.0	 8.7
4.32	 3.0	 7.5	 7.0
4.33	0.0	 4.3	 7.0
4.34	 1.0	 5.7	 7.0
4.35	 1.3	 5.3	 6.0
4.36	0.0	 1.5	 4.0
4.37	0.0	 1.5	 4.0
4.38	0.0	 2.5	 4.0

Figure 4-17: Kirby-Bauer Test of brominated (**4.1a** to **4.4**) quaternized products (**4.19** to **4.38**); the red bars symbolize the zone of inhibition in which the maximum number can be 45 mm due to the diameter of the petri dishes; the slightly red highlighted substrates are references; Bardac® is a disinfectant containing Didecyl dimethyl ammonium chloride (DDAC).

The results of the Kirby-Bauer Test prove the successful introduction of antimicrobial activity via halosilation and quaternization of poly- and cyclosiloxanes. Although the test should not be quantified since it is biased by diffusion processes, the antimicrobial activity of the siloxanes containing QAS groups seems to be relatively independent on the type and number of side-groups. In conclusion, the Kirby-Bauer Test has clearly shown that further antimicrobial tests are necessary in order to determine the antimicrobial activity more clearly.

4.3.2 Minimum Inhibitory Concentration (MIC)

Minimum inhibitory concentration (MIC) is the lowest concentration of an antimicrobial agent that will inhibit the visible growth of a microorganism after overnight incubation. The MIC is an important factor in the classification and comparability of new substances. It is often used by diagnostic laboratories mainly to confirm resistance.^[47] The utilized strains are *Candida albicans* (pathogenic yeast), *Staphylococcus aureus* (gram-positive bacterium) and *Pseudomonas aeruginosa* (gram-negative bacterium). The MIC was done and recorded by the microbiological department of the Henkel Corporation in Dusseldorf. Methicillin-resistant *Staphylococcus aureus* (MRSA) and *Pseudomonas aeruginosa* are both known as hospital bugs.

For reasons of clarity and comprehensibility, only results of chosen products based on SM-50 and SM-15 are shown. The other results and further information about the performance are shown in Appendix A5. The products shown were chosen to represent all important observations.

The evaluation is done optically. The antimicrobial activity is given when the solution is still clear after the incubation time. As it is shown in Figure 4-18, the evaluation of the test is based on the test setup (triple determination). The green fields are clear solutions, meaning that the test substance is antimicrobially active. The yellow fields illustrate the beginning of growth and the red fields indicate growth of the molds and thus inactivity of the antimicrobial substance. As it was already mentioned, the samples were tested diluted in DMSO. The solvent was tested as blank and showed no detectable antimicrobial activity.

By contrast, the test series containing the synthesized QAS-functionalized silicones (**4.30**, **4.31** and **4.32**) show antimicrobial activity. It becomes clear that this activity depends not only on the quaternary ammonium group, but also on the strain which is tested. Pyridinium functionalized silicones (**4.30**) show the lowest antimicrobial activity. The limit against *Staphylococcus aureus* is reached at 313 ppm, while no activity is detectable (> 5000 ppm) against *Pseudomonas aeruginosa* and *Candida albicans*. With **4.31** (1-methylimidazolium functionalized) the activity limit drops to 156 ppm against *Staphylococcus aureus* and the activity limit against *Candida albicans* is in the measuring range (5000 ppm). The best results were shown by **4.32** (1-butylimidazolium functionalized). The MIC against *Staphylococcus aureus* was detected at 39 ppm. The values against *Pseudomonas aeruginosa* and *Candida albicans* are 2500 ppm and 313 ppm. The samples with the best MICs (13 ppm) in this work were sample **4.26** and **4.29**.

These measurements reflect the MIC for all samples. The smallest MIC can be measured for 1-butylimidazolium functionalized samples, whereas Pyridinium functionalized shows the lowest activity. The strain *Staphylococcus aureus* is the most sensitive, while *Pseudomonas aeruginosa* is the most robust.

		no growth		-
		1 to 5 germs		(-)
		begin of growth		(+)
		growth		+

	ppm	DMSO			4.30			4.31			4.32		
<i>Staphylococcus aureus</i>	5000	+	+	+	(+)	(+)	-	(+)	(+)	(+)	-	(+)	(-)
	2500	+	+	+	-	(+)	(-)	-	-	-	(-)	+	(+)
	1250	+	+	+	-	-	-	-	-	-	-	-	-
	625	+	+	+	-	-	-	-	-	(+)	-	-	-
	313	+	+	+	-	-	(-)	-	-	-	-	-	-
	156	+	+	+	+	+	+	-	-	(-)	(+)	-	-
	100	+	+	+	+	+	+	+	+	+	(+)	(+)	(+)
	78	+	+	+	+	+	+	+	+	+	-	-	-
	50	+	+	+	+	+	+	+	+	+	(+)	+	(+)
	39	+	+	+	+	+	+	+	+	+	-	-	-
<i>Pseudomonas aeruginosa</i>	25	+	+	+	+	+	+	+	+	+	+	+	+
	13	+	+	+	+	+	+	+	+	+	+	+	+
	5000	+	+	+	+	+	+	+	+	+	(-)	(+)	(+)
	2500	+	+	+	+	+	+	+	+	+	(-)	(+)	-
<i>Candida albicans</i>	1250	+	+	+	+	+	+	+	+	+	+	+	+
	625	+	+	+	+	+	+	+	+	+	+	+	+
	5000	+	+	+	+	+	+	+	(+)	(+)	-	-	(+)
	2500	+	+	+	+	+	+	+	+	+	-	(+)	(-)
	1250	+	+	+	+	+	+	+	+	+	-	-	-
	625	+	+	+	+	+	+	+	+	+	-	-	-
	313	+	+	+	+	+	+	+	+	+	(-)	(-)	-
	156	+	+	+	+	+	+	+	+	+	+	+	+
	78	+	+	+	+	+	+	+	+	+	+	+	+

Figure 4-18: Minimum Inhibition Concentration of SM-50 based samples **4.30**, **4.31** and **4.32**; DMSO is tested as blank; the green fields are clear solutions, so here the test substance is antimicrobially active; The yellow fields illustrate the beginning of growth and the red fields indicate growth of the molds and thus inactivity of the test substance.

It is well known that quaternary ammonium salts with long alkyl chains (C8-C18) often have better antimicrobial activity (for example DDAC).^[30h, 107b] The alkyl chain can act like a hinge, causing a faster interaction with the cell wall. This may be one reason why pyridinium based samples, unlike 1-butylimidazolium based samples, only works at higher MICs.

This trend can also be observed in Figure 4-19. Here the test results of MIC of SM-15 based samples **4.36**, **4.37** and **4.38** are given. Sample **4.38** (1-butylimidazolium functionalized) showed the only measurable effects against *Staphylococcus aureus* (456 ppm) and *Candida albicans* (1250 ppm). Thus, there is also a correlation between the amount of quaternary side-groups in the polymer and the antimicrobial activity. The higher the concentration in the polymer, the lower the MIC. Further results (s. Appendix A5) are between the measured values from Figure 4-18 and Figure 4-19.

	ppm	4.36			4.37			4.38		
<i>Staphylococcus aureus</i>	5000	+	+	+	+	+	+	(+)	-	(+)
	2500	+	+	+	+	+	+	-	(+)	(+)
	1250	+	+	+	+	+	+	(+)	-	-
	625	+	+	+	+	+	+	-	-	-
	313	+	+	+	+	+	+	(+)	-	(+)
	156	+	+	+	+	+	+	+	(+)	(+)
	78	+	+	+	+	+	+	+	+	+
	39	+	+	+	+	+	+	+	+	+
<i>Pseudomonas aeruginosa</i>	5000	+	+	+	+	+	+	+	+	+
	2500	+	+	+	+	+	+	+	+	+
<i>Candida albicans</i>	5000	+	+	+	+	+	+	-	-	-
	2500	+	+	+	+	+	+	-	(+)	-
	1250	+	+	+	+	+	+	-	-	(-)
	625	+	+	+	+	+	+	+	+	+
	313	+	+	+	+	+	+	+	+	+

Figure 4-19: Minimum Inhibition Concentration of SM-15 based samples **4.36**, **4.37** and **4.38**; the green fields are clear solutions, so the test substance is antimicrobially active; The yellow fields illustrate the beginning of growth and the red fields indicate growth of the molds and thus inactivity of the antimicrobial substance.

Well-known antifungals, such as amphotericin B, ketoconazole, miconazole, fluconazole or itraconazole have MICs between 0.8 to 50 ppm against *Candida albicans*.^[33b] The human beta-defensin-3 (belongs to the host-defense peptide family) shows an MIC of 0.2 ppm against *Staphylococcus aureus* and 25 ppm against *Candida albicans*.^[10c]

Silicone based materials which have comparable structure were analyzed by Mizerska *et. al.*^[34a, 107b] The compounds contain 1-octylimidazolium bromide, 1-octylimidazolium chloride and *tert*-butylammonium chloride groups which are connected to the silicone backbone via hydrosilylation. Antimicrobial tests against *staphylococcus aureus* showed MICs between 3 and 80 ppm, which is comparable to our results. The antimicrobial tests against *Pseudomonas aeruginosa* showed MICs between 20 and 510 ppm, resp. 5000 ppm, whereas our best test results were obtained with 2500 ppm against *Pseudomonas aeruginosa*.

However, there is also literature to which our results are not only comparable, but also show much better antimicrobial activity. Piecuch^[30i] reported MIC values between 5 to more than 800 ppm against *Staphylococcus aureus*. They synthesized derivatives *N,N,N',N'*-tetramethylethylenediamine with quaternary ammonium groups. Voo *et.al.*^[30k] produced PEG-co-P(MTC-FPM)₄ polymers (MTC-FPM: furan-protected maleimide monomers) which have a MIC of 250 ppm against *Staphylococcus aureus*.

In conclusion, the MIC analysis shows that all quaternized silicones produced in this research are antimicrobially effective. In addition, it is now possible to obtain a quantitative statement about this antimicrobial activity. In contrast to the Kirby-Bauer test, the samples can be differentiated according to their chemical composition and the correlated antimicrobial activity. The 1-butylimidazolium functionalized samples with a high ratio of these quaternary groups show the best (lowest) MICs. All samples show the best effect against *Staphylococcus aureus*. In comparison to literature based MIC

values, it could be proven, that the produced samples are not only comparable to the literature, but also show better antimicrobial activity in some cases.

4.3.3 ISO 22196:2011

The ISO 22196:2011, also called film contact test, is an international standard test method and was done and recorded by the microbiological department of the Henkel Corporation in Dusseldorf. The test gives quantitative results of the antimicrobial activity in a solid state after 24 and 48 hours incubation. The utilized strain is *Exophiala dermatitidis* (black yeast). The test piece is measured in solid form, so the different samples were cured into a PDMS standard formulation with an amount of 10% following the sample preparation in Appendix A2. The strain suspension is placed between the test substrate and a cover glass, incubated and subsequently evaluated via counting by means of plating on culture medium.

The reference is a PDMS standard formulation without any antimicrobial agents and was provided by the microbiological department. The test results are shown in Figure 4-20 (logarithmic plotted). For a better overview of the antimicrobial effect, the samples were sorted by the amines and in descending concentration of the side-groups. It can be seen that pyridinium-based samples have the strongest antimicrobial activity in solid state against *Exophiala dermatitidis*. The measured data are at the detection limit of the measurement. In the imidazolium-based samples **4.40** is an exception (very good antimicrobial activity). The other samples are partly in the area of the reference. Nevertheless, there are also samples (e.g. **4.37**, **4.32** and **4.38**) which have decreased the number of cells after 48 hours by one order of magnitude. These results are very good, considering that the samples are in solid form and thus can only act on the surface.

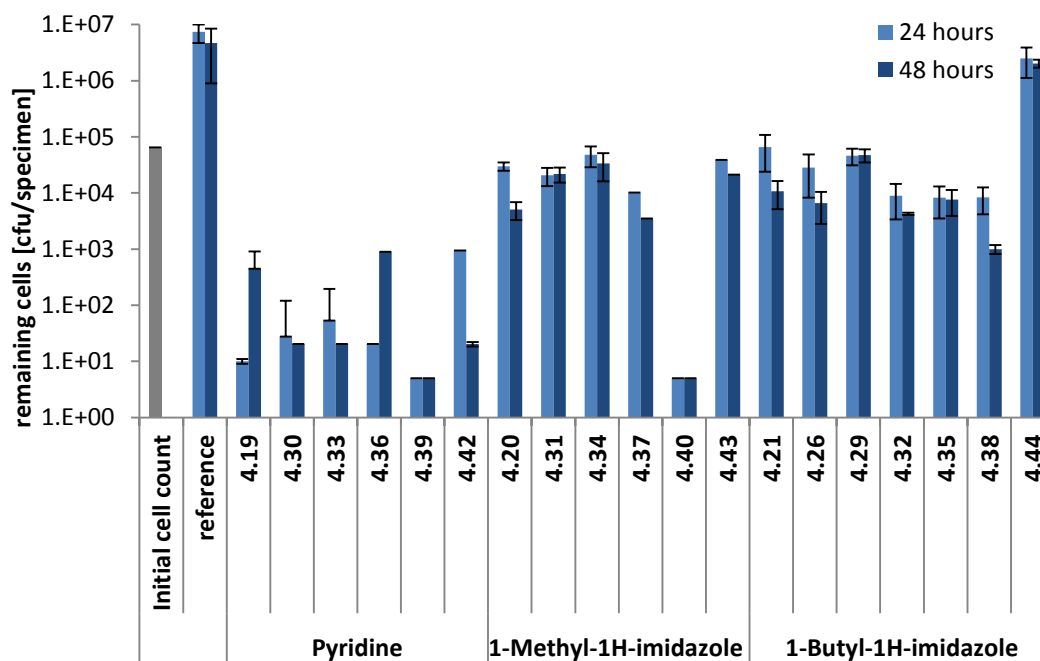


Figure 4-20: ISO 22196:2011 test for the measurement of antibacterial activity on plastics and other nonporous surfaces; the test is evaluated after 24 hours (light blue bars) and 48 hours (dark blue bars); the samples are sorted by amines and descending number of side-groups; the reference is a standard PDMS formulations; the standard deviations were calculated from three repetitions.

The ISO 22196:2011 shows how diverse the antimicrobial activity can be compared to the determination of the MIC. While the 1-butylimidazolium-functionalized samples were best at the MIC, the ISO 22196:2011 shows that the pyridinium-functionalized samples perform better here. On the one hand, this can be due to the solidification of the liquid sample (curing) during the test (mobility reasons). It may also be because another test strain was used here. However, the antimicrobial tests show that the antimicrobial activity depends not only on the chemical composition, but also on the targeted strain and the conditions *resp.* environment.

4.4 Conclusion and Outlook

The second part of this thesis dealt with the introduction of bactericidal and fungicidal properties into the silicone. For this purpose, the polymers were first halosilated and then quaternized.

In the beginning, a successful methodology for the synthesis of halogenalkyl functionalized products via Pt-catalyzed halosilation was established. For this purpose, the Pt-catalyzed halosilation was compared with the literature-known Pd-based methodology. In addition to a faster reaction time due to a concentration-independent reaction rate (zero order kinetic), the products have a higher level of purity and improved appearance. However, the Pt-based products have also hydrosilylated by-products.

The investigations in the replacement of the standard reactants (allyl bromide and THF) showed that there is a good possibility to expand the portfolio of reaction conditions and end products. Though this screening, the limits of the Pt-catalyzed halosilation reaction were also identified. The evaluation of the Viscosity results and contact angles of the halogenalkyl functionalized products also showed that their properties are suitable for consecutive reactions or further applications.

In the second part, the introduction of quaternary ammonium salt groups via Menshutkin reaction was established. Several products based on pyridine, 1-methyl-1*H*-imidazole and 1-butyl-1*H*-imidazole were produced successfully. It could be shown that the conversion depends on the amine and the solvent, as well as on the reaction order. Since the Menshutkin reaction is concentration-dependent, it probably might reach higher conversions in another type of reactor.^[126-127]

The antimicrobial tests proved that all QAS-containing samples show antimicrobial activity. Thus, the aim of the project has been clearly fulfilled. However, the tests have also shown that the antimicrobial effect depends very much on different parameters. While the 1-butylimidazolium-functionalized samples were best at the MIC, the ISO 22196:2011 shows that the pyridinium-functionalized samples perform better in the solid state. So the activity depends not only on the chemical composition, but also on the targeted strain and the measurement conditions.

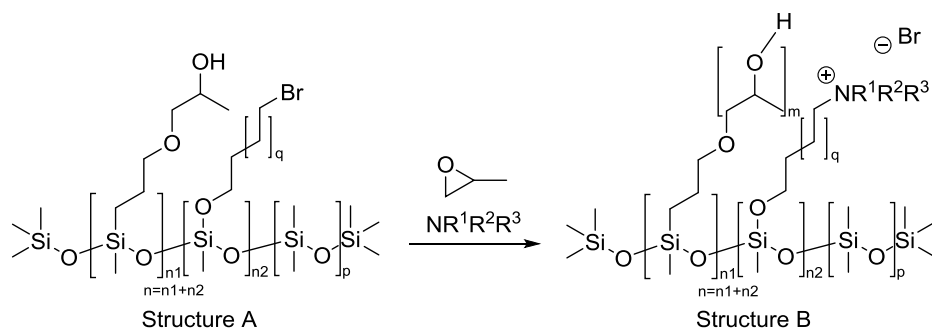
In comparison to literature based MIC values, it could be proven, that the produced samples are not only comparable to the literature, but also show better antimicrobial activity in some cases.

5 Part III: Successive Introduction of Hydrosilylated and Halosilated Side-Groups into Silicones

This part is focused on the combination of the aforementioned properties to offer the opportunity to produce bi-functional silicones containing both anti-adhesion and bactericidal/fungicidal properties. Therefore, the OH-functionalized samples of Part I will be combined with the halogenated products of Part II to obtain bi-functional silicones. In consultation with the cooperation partner, the focus of this research was set on Part I and Part II, since they provide the basis for the following one. Part III of this research explores the first bi-functionalization experiments. The synthesis and possible mutual disturbance of both functional groups (hydrosilylated and halosilated side-groups) are in focus. The research will be continued even after submitting the thesis.

5.1 Background

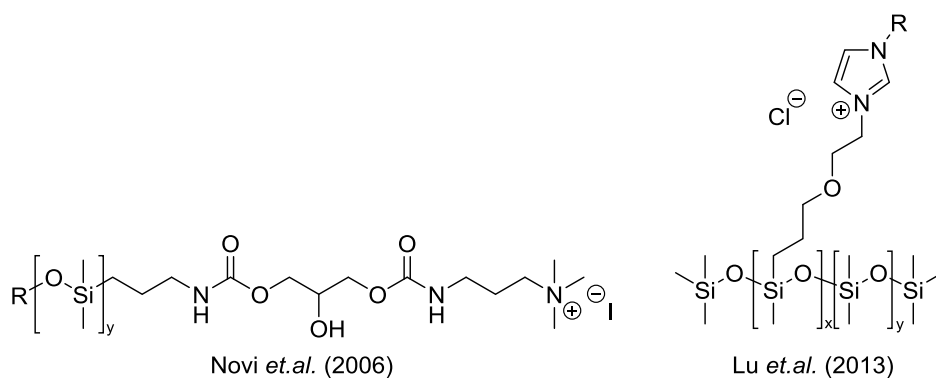
The desired bi-functionalization of silicones to obtain products with anti-adhesion and bactericidal/fungicidal properties can be split into a multi-stage synthesis. The first step is a hydrosilylation reaction to obtain partial converted polysiloxane propyleneglycol brush copolymers. The synthesis of these mono-functionalized samples is already described in chapter 3.2.3.3 (Part I). In a consecutive reaction of the left SiH groups, it is possible to integrate a second functional group into the system (s. structure A, Scheme 5-1). This bi-functionalization is achieved by a halosilation reaction, as described in chapter 4.2.1. Structure B can be obtained by further propoxylation and quaternization reactions like described previously.



Scheme 5-1: Structure A illustrates the bi-functionalized product after hydrosilylation and halosilation;
Structure B illustrates the general structure after consecutive propoxylation and quaternization.

To the best of our knowledge, there are no reports of silicones containing both hydrophilic polyalkylene glycol chains as well as halogenated or quaternized groups. As already shown, the two functional groups themselves represent novel compounds. The state of the art of these respective functional groups was already presented in chapter 3.1 and 4.1.

In some cases there are reports, which mention similar, but structurally different structures. For example, Novi *et al.* reported PDMS containing trimethylammonium end-groups which are connected via a hydroxyl functionalized carbamate bridge (s. Scheme 5–2).^[30b] Interestingly, they mention that this amphiphilic polymer possesses a self-emulsifying character in water and antibacterial properties. These observations support the working hypothesis of this research.



Scheme 5-2: left: polydimethylsiloxane backbone with hydroxyl functionalized carbamate and trimethylammonium iodide end-groups within the main chain; right: PDMS containing imidazolium chloride side-groups linked by ether bridge.

Furthermore, Nakamura *et al.* reported an antimicrobial composition including an ammonium group-containing polymer which is dispersed polydimethylsiloxane methacrylates.^[119a] These systems are used in medical applications.

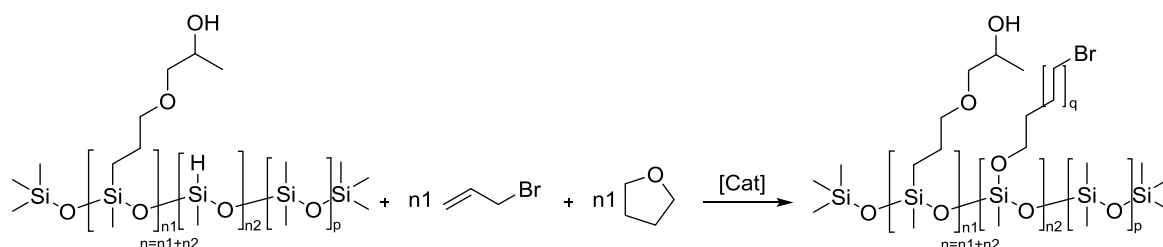
From the known systems, perhaps the one with the highest similarity to those presented here was reported by Lu *et al.* (Scheme 5–2).^[118] In there, an ether bridge is first introduced into the side groups by hydrosilylation and subsequently quaternized. However, this will not be described as bi-functionalization, because the ether bridge does not represent a second function such as a PEG chain.

5.2 Results and Discussion

The following part deals with the halogenation reaction of partial hydrosilylated samples, which were discussed in chapter 3.2.3.3. The synthesis and characterization of these bi-functionalized compounds is focused on the mutual disturbance of both functional groups in respect to their synthetic routes. Deeper investigations, further propoxylation and quaternization reactions and antimicrobial tests will be included in the outlook. Since this work was done as part of an industrial cooperation, the research will be continued even after submitting the thesis.

5.2.1 Synthesis

In the following, consecutive halosilation reactions are made with partial hydrosilylated sample **3.35** and its derivatives as it is shown in Scheme 5-3 (s. Table 3-3). **3.35** is made from SM-50 and contains approximately 50 % converted SiH groups.



Scheme 5-3: Consecutive halosilation of hydrosilylated PHMS with THF and allyl bromide.

The samples **5.1** to **5.7** with the desired bi-functionalization are summarized in Table 5-1. Unless otherwise indicated, the intended ratio between hydrosilylated and halosilated groups should be 1:1. The table also shows the obtained amounts of these groups. In sample **5.1** and **5.2** Platinum-catalysts were utilized. Unfortunately, these products were already cured during synthesis, so no halosilated product could be determined. Neither a C-Br band in IR, nor bromine could be detected in elemental analysis.

Table 5-1: Summary of the products **5.1** to **5.7**; unless otherwise indicated, the ratio $\text{SiCH}_2\text{:SiOR}$ is 1:1; the conversions and formed amounts were calculated by integration of $^1\text{H-NMR}$.

Sample	Starting Material	Catalyst	1 st Synthesis		2 nd Synthesis		Isolated Yield [%]
			Converted Amount SiH [%]	Formed Amount SiCH_2 [%]	Converted Amount SiH [%]	Formed Amount Si-OR [%]	
5.1	3.35	Karstedt	56	38.5	> 99	n/d	n/d
5.2	3.35	Pt@C	56	38.5	98	n/d	n/d
5.3	3.35	PdCl_2	56	38.5	99	9	56.3
5.4^a	3.35f	PdCl_2	43	19	93	83.5	47.9
5.5^b	3.35g	PdCl_2	82	60	> 99	7	50.2
5.6	3.35e	PdCl_2	10	6	80	13.5	40.1
5.7	SM-50	PdCl_2	-	n/d	> 99	83.5	75.4

^a ratio 1:3; ^b ratio 3:1.

After the catalyst was changed to palladium (PdCl_2), samples **5.3** to **5.7** were obtained. Pd-catalyzed samples show a C-Br band in IR, as well as bromine is detectable in elemental analysis. As an example, the 2D ^1H - ^{13}C -HSQC-NMR spectrum of product **5.3** is shown in Figure 5-1. The signals **b** to **h** belong to the hydrosilylated group and signal **i** to **m** belong to the halosilated one. Detailed descriptions of the signal correlations are given in chapter 3.2.1 and 4.2.1.1. All desired signals are present and can be assigned to the corresponding groups. The positions in both ^1H -NMR and ^{13}C -NMR are consistent with the positions of the mono-functionalized products, although a bigger overlapping of signals is observed. As it was already mentioned, the signals **d** and **e₂** of the hydrosilylated part are both at around 3.4 ppm in ^1H -NMR. Signal **m** is overlapped with this signal and can be detected with a 2D analysis. It is the same with the signals **c** and **k** at around 1.6 ppm. There is no clear answer yet whether the bromopropyl by-product is formed (hydrosilylated by-product of halosilation). A statement based on the signals in the given NMR-spectra is not possible.

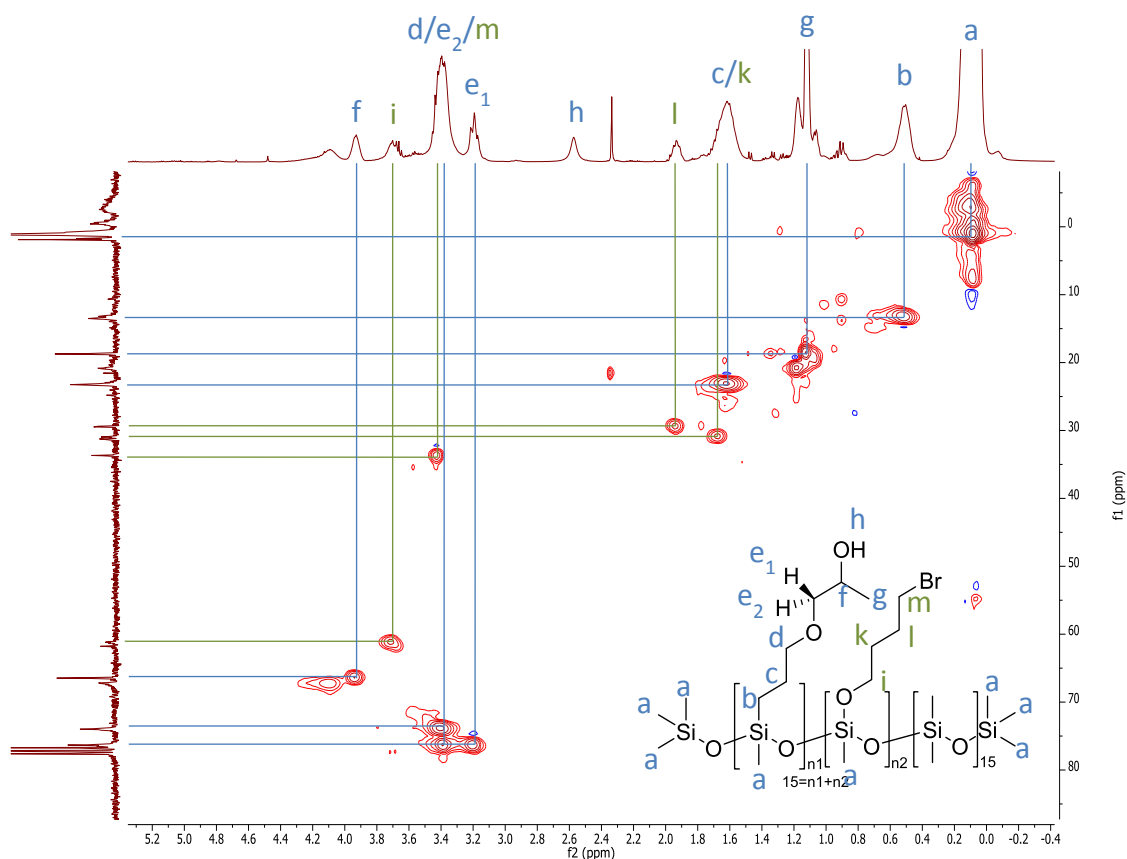


Figure 5-1: ^1H - ^{13}C -HSQC-NMR of **5.3** in deuterated chloroform (400 MHz, 25 °C); the overlapping of the signals of the halosilated and hydrosilylated products are shown; the methyl groups at silicon have been grouped together as **a**; signals **b** to **h** belong to the hydrosilylated group and signals **i** to **m** belong to the halosilated one.

The products, which were catalyzed by palladium, have the same appearance than the ones in chapter 4.2.1.1. The experiments were done in Rostock, where no equipment for measuring the yellowness index is available. However, Figure 5-2 illustrates the color changing during time (**5.7** is chosen as an example). The products look yellow in the beginning and their appearance gets darker

until it changes to a dark brown crumbly solid with a brown precipitation. Since samples **5.1** and **5.2** (Pt-catalyzed) show no discoloration, this has to be caused by palladium. In further investigations, the purification (removing of palladium) has to be optimized.

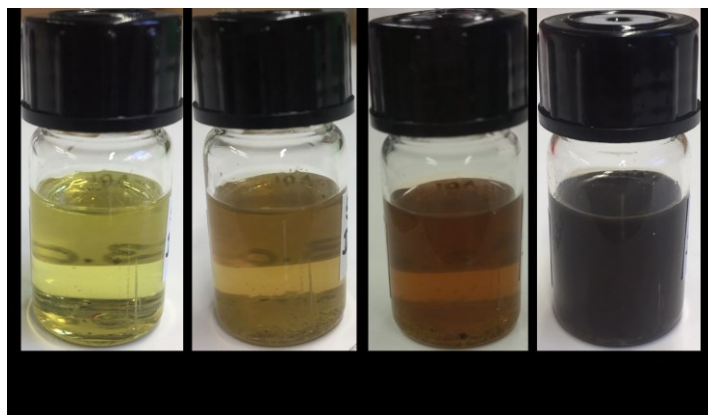


Figure 5-2: Pictures of sample **5.7** during storage; the product gets darker and precipitation is formed; the product is cured on day five.

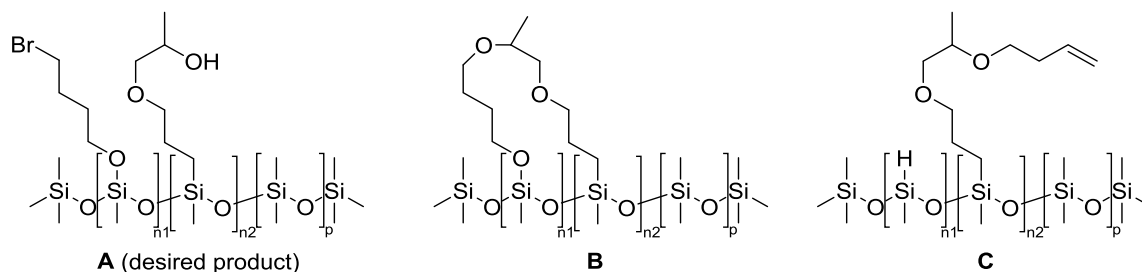
As already shown in Figure 5-1, the analytical data (NMR, IR, EA) prove the presence of both hydrosilylated and halosilated side-groups. However, the integrals of the halosilated groups in ^1H -NMR are smaller than expected. This means that less halosilated product was formed. Moreover the amount of bromine, which was measured in elemental analysis, is smaller than calculated as well. For example in sample **5.3** there are 3.55 % bromine detectable, although it should contain approximately 14.92 %. This leads to the assumption that not only the desired product can be formed during bi-functionalization. Possible products are shown in Scheme 5-4. Structure A illustrates the desired product, which presence is already proven in sample **5.3** to **5.6**.

Structure B can be formed, when the bromine group and the hydroxy-group of the desired product react with each other forming a network (most probably via nucleophilic substitution). After the bromine is removed by forming HBr, the two side-groups are connected via ether linkage. Whether this bond is formed cannot be proved yet. If structure B is present, signal **m** should be decreased and signal **f** should be increased (^1H -NMR, s. Figure 5-1). Due to the overlapping of signal **d**, **e₂** and **m**, there is no integration possible. Moreover, in ^{13}C -NMR signal **m** should be shifted from 33.68 ppm to around 67.25 – 76.26 ppm, because then it would be comparable to the signals **d**, **e₂** or **f**. Such shifting is not detectable. Samples **5.1** and **5.2** show no halosilated signals at all and samples **5.3** to **5.7** show the desired signal at around 34 ppm.

Structure C can be obtained when the free allyl bromide reacts with the hydroxyl group of the hydrosilylated side-group. THF does not participate in that reaction. The allylic group binds to the oxygen and HBr is released. In organic synthetic chemistry, allyl bromide is known as common reactant for allylic protection of alcohols and amines.^[129] Actually, the products contain signals of the allylic groups in the ^1H -NMR spectra except of **5.3** and **5.5**. Sample **5.1** and **5.2** could not be purified because of the curing processes. Here, the presence can also be caused by the remaining allyl bromide. Whether an ether formation took place, cannot be clarified clearly. On the one hand, it is not

expected that the SiH groups are converted. On the other hand, Palladium is known as suitable catalyst for the deprotection of *O*-allylphenols.^[130]

All in all, it is proven that the desired product is formed. However, it cannot be excluded yet, that some by-products, such as structure B or structure C are formed as well. The ratio between these structures seems to be controllable by the reaction conditions.



Scheme 5-4: Possible chemical structures that can be formed during bi-functionalization; A is the desired product, B illustrates a condensation of the formed functional groups and C shows the function of allylic groups as protection groups.

Sample **5.7** represents a synthetic pathway with special reaction conditions. Unlike **5.1** to **5.6**, both reactions took place simultaneously as the reactants were added together (reaction conditions are described in Appendix A6). The utilized catalyst was PdCl₂. Analytical results prove the presence of halosilated side-groups, although there are some signals of the hydrosilylated side-groups missing in ¹H-NMR. With the simultaneous addition of all reactants, halosilation appears to be the preferred reaction. Moreover, PdCl₂ seems to do not be a suitable catalyst for hydrosilylation reactions. This is already confirmed in the PdCl₂-catalyzed halosilation from chapter 4.2.1.1, although in general, Pd-catalyzed hydrosilylation reactions are known in literature.^[121, 131]

Figure 5-3 shows the measured molecular masses compared to the calculated ones. In addition, the polydispersities are shown as well. As it was already mentioned in chapter 3.2.1, the molecular masses differ from the calculated ones. In general the measured ones are smaller. This can be caused by the bulkiness of the branched products, which causes a smaller hydrodynamic volume compared to the linear GPC standard.^[99] It can be also caused by the lowered conversion of the desired groups as it is shown in Table 5-1. In general the formed hydrosilylated and halosilated groups do not reach a yield of 100 % in total compared to SiH groups expect of **5.4**, which has the lowest difference between calculated and measured molecular mass.

In addition to the molecular weights, the polydispersities are given as well. These are very large in some experiments. Product **5.3** has a PDI of 11.595 and **5.4** has a PDI of 13.112. In general, the products, which were synthesized in this research, reach PDIs between 1.0 and 6.5. However, the increased polydispersity can be attributed to the bi-functionalization. Because of the introduction of two different functionalities in two steps, the ratio of both functionalities can differ in the different polymer chains. This inhomogeneity can have an effect on the Viscosity.

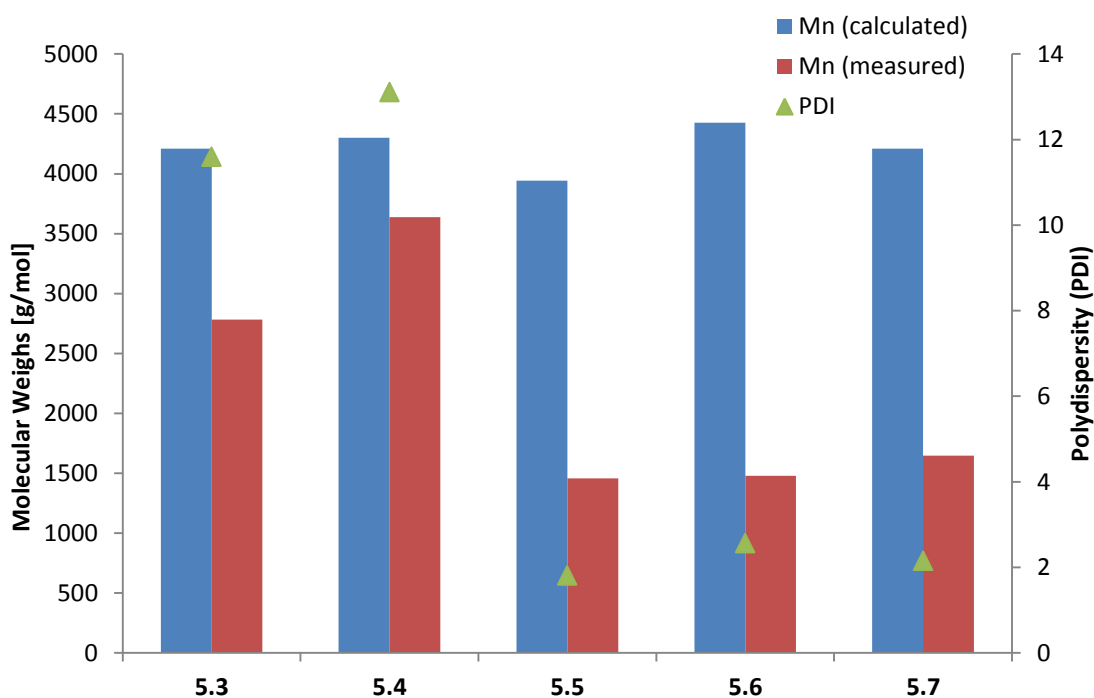


Figure 5-3: Molecular weights of bi-functionalized products; comparison of calculated and measured molecular weights M_n of **5.3** to **5.7**; the PDI is given as well.

In conclusion, the investigations in the bi-functionalization of polyhydrosiloxanes utilized a successful synthetic pathway to synthesize products with both hydrosilylated and halogenated side-groups. It shows clearly that the Pd-catalyzed halosilation is more suitable as a consecutive reaction than the Pt-catalyzed one. **5.3** shows all desired signals in the ^1H - ^{13}C -HSQC-NMR, while there is no bromine detectable in samples **5.1** and **5.2**. Unfortunately, it could not be proved yet whether there are any side-products in the polymers. The integrals of the signals are lower than expected, but the analytical results do not allow clear conclusions about the presence of by-products. Further investigations should include the optimization of the synthetic method, as well as the purification process to remove the Pd-catalyst and obtain purified products.

5.2.2 Characterization

The obtained products **5.1** to **5.7** contain the already mentioned and characterized hydrosilylated and halosilated side-groups. In the following part, the rheological behavior is assessed and it is determined whether it still matches with the properties of the mono-functionalized products or if it shows novel properties. Due to the small sample quantity, no contact angles could be determined.

The Viscosity results are summarized in Table 5-2. Rheological measurements of **5.1**, **5.2** and **5.4** were not possible because of curing of the sample. The samples **5.6** and **5.7** show viscosities comparable to those of the mono-functionalized products. They follow the behavior of Newtonian liquids as it is reported in literature.^[132] A Newtonian fluid is defined as a liquid whose shear stress τ is proportional to the shear rate $\dot{\gamma}$ in a laminar flow process. It corresponds to the Newtonian law of Viscosity.^[102, 133]

Table 5-2: Viscosity results of the samples 5.1 to 5.7; the sample 5.6 and 5.7 follow the behavior of Newtonian liquids; n/d = not detectable.

Sample	Viscosity [mPas]
5.1	n/d
5.2	n/d
5.3	non-Newtonian liquid
5.4	n/d
5.5	non-Newtonian liquid
5.6	0.0639
5.7	0.0766

However, the rheological measurements of Samples 5.3 and 5.5 show quite different behavior, which is non-Newtonian. Non-Newtonian liquids refer to fluids whose Viscosity does not remain constant when the shear rate is changed. Thus, they are no longer explainable with the Newtonian law of Viscosity.^[134] Materials, whose Viscosity decreases when the shear rate is increasing, are called pseudoplastic or shear-thinning (s. Figure 5-4). Their zero Viscosity (Viscosity at a shear rate zero) is infinitely high. Examples of pseudoplastic compounds are polymer melts or dispersions. In contrast, there are also shear-thickening *resp.* dilatant fluids, whose Viscosity increases with increasing shear rate. The most popular example is corn starch.^[135]

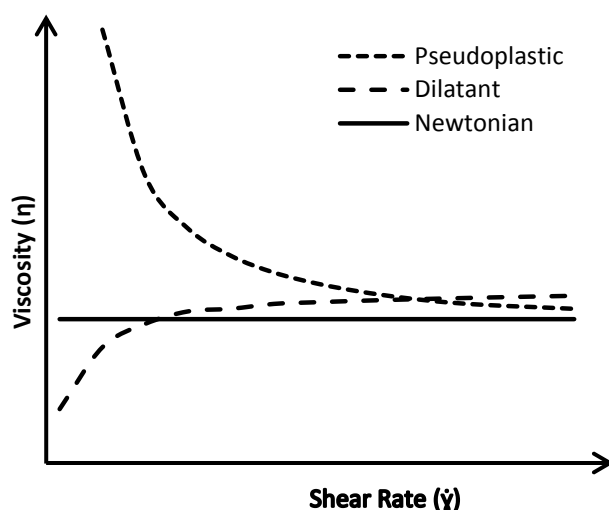


Figure 5-4: Rheological behavior of Newtonian and non-Newtonian fluids.

The viscosities of sample 5.3 and 5.5 decrease when the share rate is increased (Figure 5-5, the datasets are listed in Appendix A6). They belong to the shear-thinning non-Newtonian liquids. These are the only two samples in the entire research that have shown non-Newtonian behavior. It is hypothesized that the non-Newtonian behavior is caused by the interaction of the hydrosilylated and halosilated side-groups. The bromine can form hydrogen bonds with the hydrogen of the terminal hydroxy-group. This causes an increase in the Viscosity. By increasing shear rate, a stronger force is

applied on the system and the hydrogen bonds can be suppressed or broken. As a result, the interaction forces between the polymer chains decrease along with the Viscosity. Comparable observations were already described in literature. Briscoe et.al reports rheological properties of aqueous solutions of poly(vinylalcohol) as a function of the degree of e.g. polymer hydrolysis, temperature or pressure.^[136]

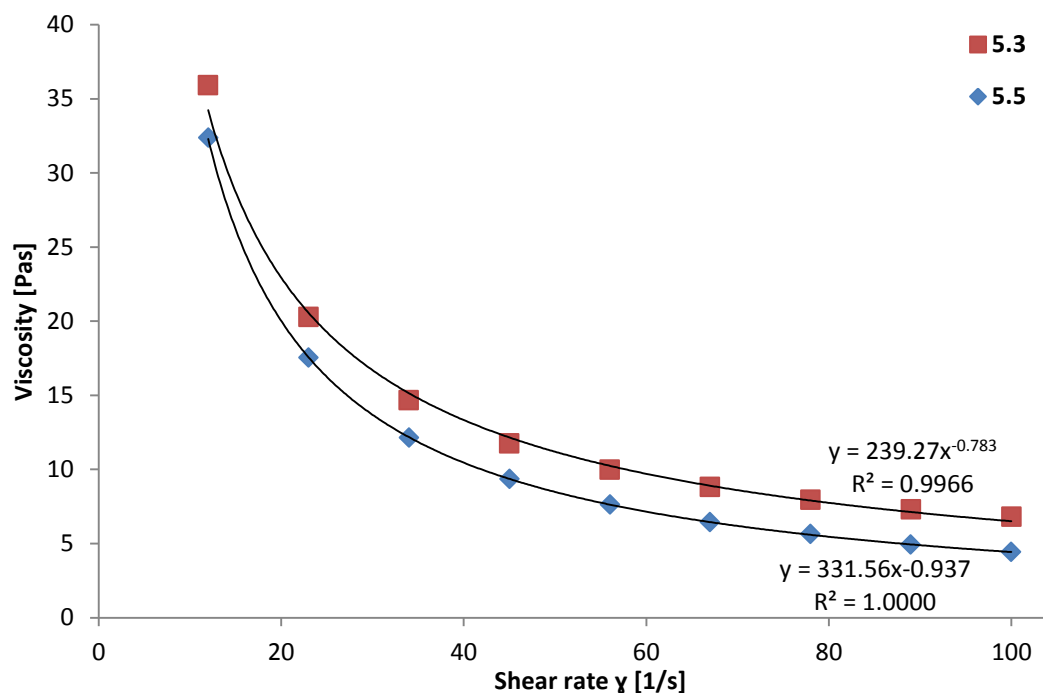


Figure 5-5: Viscosity results of sample 5.3 and 5.5; both samples have a non-Newtonian behavior; the trend line is calculated by a power function.

Unfortunately, it was not possible to clarify why samples 5.4 and 5.6 show no non-Newtonian behavior yet. These samples still contain some unreacted SiH-groups, and from previous results it is known that unconverted SiH groups in halosilated products cause curing of the product (s. chapter 4.2.1.2). Hence, it is assumed that the SiH groups left in the polymer can disturb the formation of hydrogen bonds, which causes inhibition of non-Newtonian behavior. The discussed rheological behavior shows, that two Newtonian compounds can be able to change the rheology of a system when they are combined.

5.3 Conclusion and Outlook

In this part of the research, the functional groups of Part I (hydrosilylation) and Part II (halosilation) were combined to obtain bi-functionalized products. The focus was set on the development of a synthetic methodology and study of the interactions between the two functional groups. It shows a first insight into the potential of this research, because it offers the opportunity to produce bi-functional silicones containing both anti-adhesion and bactericidal/fungicidal properties. Since this work was done as part of an industrial cooperation, the research will be continued even after submitting the thesis.

It was possible to develop a successful synthetic route introducing halosilated side-groups besides hydrosilylated ones. It has been shown that platinum (Karstedt) is less suitable as a catalyst than palladium(II) chloride, since the bromine is expelled from the product. The ^1H - ^{13}C -HSQC-NMR of **5.3** proves the conversion of both functional groups. However, the analytical results also show that the reaction can promote by-product formation, as well as crosslinking via ether bridges or the formation of allyl protecting groups. Further investigations should include the repetition of the experiments, as well as the optimization of the synthetic methodology. Since palladium-catalyzed products have a yellowing effect, it is also important to optimize their purification.

Rheological measurements have shown that fully-converted bi-functionalized products have a different rheological behavior than the mono-functionalized ones. The mono-functionalized samples are Newtonian liquids, while the bi-functionalized ones show non-Newtonian behavior. Their Viscosity decreases while the shear rate is increased. It is hypothesized that the non-Newtonian behavior is caused by the interaction of the hydrosilylated and halosilated side-groups. The bromine can form hydrogen bonds with the hydrogen of the terminal hydroxy-group causing an increase in the Viscosity. Further investigations, including the repetition of the rheological measurements, are necessary to clearly prove the hypothesis.

Finally, scale-up experiments have to be investigated. Higher sample quantities are important for further analyses such as CA measurements or the determination of antimicrobial activity. Moreover, consecutive propoxylation and quaternization reactions have to be tested. However, it would be best to first propoxylate the partial hydrosilylated products (s. chapter 3.2.3.3) and then halosilate and quaternize them. An influence of the terminated hydroxy-group is not expected, since the quaternization also takes place in alcohols as solvents. However, the scale-up could contain some problems due to the exothermic effect of hydrosilylation and propoxylation. A larger volume can cause a worse temperature control and this is an important factor in the partial hydrosilylation reaction.

So far, it could be proven that the synthesis of bi-functional products is possible. It has to be proven too, that they still possess the desired anti-adhesion and bactericidal/fungicidal properties. However, antimicrobial activity is expected since antimicrobial activity despite bi-functionalization is proven in literature.^[34a, 107b, 119b]

6 Outlook

The research represents a successful way to synthesize silicones containing two different kinds of antimicrobial active compounds. The results in this work can serve as a basis for industrial processes and can be applicable in different application fields (such as household, air conditioning systems or medical).

Therefore, it is very important to strengthen the already generated results and to prove resulting hypotheses.

Part I deals with the introduction of anti-adhesion properties into silicones via side-group hydrosilylation and consecutive propoxylation to form polysiloxane polypropyleneglycol brush copolymers. These copolymers were successfully synthesized, although further investigations on the extension of the siloxane starting materials are necessary in order to further determine the influence of exothermic effects, molar masses and number of side-groups. In this case, basic properties such as the molecular mass should be re-determined by further analytical methods (e.g. MALDI TOF measurements), to avoid the problem of deviating hydrodynamic volumes in the GPC.

Furthermore, it is known that the antimicrobial effect of the polysiloxane propyleneglycol brush copolymers is caused by the alkoxyated side-groups. Extension of the alkoxylation method to ethylene oxide or mixtures of PO/EO could improve the antimicrobial activity. In general, further anti-adhesion tests should be made in order to obtain a statistically reliable statement. Further measurements like dynamic contact angles (among others) shall be made to get a deeper understanding on the relationship between the morphology of the hydrophilic copolymer and its effect on the surface energy.

Part II presents the introduction of bactericidal and fungicidal properties into the silicone. The two-step synthesis includes the side-group halosilation and consecutive quaternization (Menshutkin reaction) to obtain halogenalkyl and QAS-functionalized siloxanes (quaternary ammonium salts). Although the halosylated products have already been used successfully as intermediates, there are still some unclarified mechanistic problems which have to be investigated. For this, it is necessary to produce low molecular weight products for analyzing them in e.g. MALDI TOF, GC or ESI-TOF/MS. Moreover, the synthesis of further derivatives would be possible through further reactant-screenings.

The replacement of the halogen by quaternary ammonium salt groups via Menshutkin reaction was successfully demonstrated with pyridine, 1-methyl-1*H*-imidazole and 1-butyl-1*H*-imidazole. The results have shown that the synthesis of these products is possible, and that their antimicrobial activity could be proved. Based on these results, investigations in the chemical structure of the QAS and their linkage to the silicone backbone should be done to determine their influence on the antimicrobial activity.

Furthermore, it is important to analyze the mentioned solidification (curing) of the polymeric products during time. For this purpose it is necessary to do a long-term study in which the samples (pure and dissolved in different solvents) are stored and characterized after defined time intervals. This would also provide information about the hydrolysis rate of the samples. It is already shown that the QAS-

functionalized silicones can hydrolyze on the silyl-oxy bond. Controlled hydrolysis offers the possibility of controlled delivery of antimicrobial agents. This can be applicable in e.g. medical application fields.

In Part III, the already mentioned functional groups were combined in a successive reaction to gain a bi-functionalized siloxane to offer the opportunity to produce bi-functional silicones containing both anti-adhesion and bactericidal/fungicidal properties. Preliminary tests showed that it is possible to synthesize hydrosilylated propyleneglycol side-groups and halosilated halogenalkyl side-groups on the same silicone backbone. While this part of the research can benefit from the results of the two previous parts, the results have to be checked for mutual influences/disturbances of both functional groups. Preliminary rheological measurements have shown that the rheological properties of the produced materials can be tailored.

Since the focus was set on the synthetic pathway, further analytical tests (such as contact angle determination, rheological measurements, anti-adhesion and antimicrobial tests) must be made. However, antimicrobial activity is expected since antimicrobial activity despite bi-functionalization is proven in literature.^[34a, 107b, 119b] Moreover consecutive propoxylation and quaternization reactions have to be tested.

Finally, scale-up experiments of the both mono-functionalized and bi-functionalized samples have to be investigated. The transfer of a laboratory scale into larger systems can pose further synthesis-related or technical difficulties which have to be addressed before a later industrial use. The exothermic effect of hydrosilylation and propoxylation reaction must be taken in account in the scale-up in order to control the conversion of the SiH-groups. It is of advantage that the propoxylation already takes place in a semi-batch process. Moreover the prices of the catalysts and reagents, as well as the catalyst-loading have to be checked for scale-ups. Palladium is currently much more expensive than platinum (28th of february 2019).^[137] The quaternization does not require any catalyst. But the removing of solvents and volatile contents is already challenging in small scales. In addition, the storage is currently only possible in solution. This means a larger use of solvents and a larger required space for scale-ups.

7 Summary

This thesis represents a successful way to synthesize silicones containing two different kinds of antimicrobial active compounds.

Part I: Introduction of Anti-Adhesion Properties into Silicones

- Successful synthesis of polysiloxane polypropyleneglycol brush copolymers containing anti-adhesion properties (hydrosilylation and propoxylation)
- Hydrosilylation shows a high selectivity towards the hydrosilylated α -product
- Propoxylation reaction (semi-batch process) shows a good proportionality between the desired chain-lengths of the PPG side-groups and the added volume of PO
- Product characterization determined a proportional correlation between the degree of polymerization and the rheological behavior
- CA measurements revealed a time-dependent decreasing effect of a water droplet
- Anti-Adhesion Assay proved the worsened adhesion of microbes
- Two patents were filed
 - Preparation of polysiloxane polyalkyleneglycol brush copolymers. European patent application EP 18210646.8, (Priority: 6th of December 2018)
 - Curable composition comprising polysiloxane polyalkyleneglycol brush copolymers. European patent application EP 18210647.6, (Priority: 6th of December 2018)

Part II: Introduction of Bactericidal and Fungicidal Properties into Silicones

- Successful development of Platinum-catalyzed halosilation reactions to form halogenalkyl functionalized polysiloxanes
- Pt-catalyzed halosilated products have a higher level of purity, improved appearance and changed reaction order compared to the literature
- Successful Menshutkin reaction to form QAS-functionalized siloxanes linked by silyl-oxy bond
- Investigations proved the conversion's dependence on the amine and the solvent, as well as on the reaction order
- The time-resolved ¹H-NMR spectra proved the hydrolysis of the silyl-oxy bond to form QAS-containing leaving groups
- The antimicrobial tests proved that all QAS-containing samples show antimicrobial activity
- One patent was filed
 - Process for the Preparation of Functionalized Polysiloxanes. European patent application EP 18209736.0, (Priority: 3rd of December 2018)

Part III: Successive Introduction of of Hydrosilylated and Halosilated Side-Groups into Silicones

- Successful synthetic route to gain a bi-functionalized siloxane containing both hydrosilylated and halosilated side-groups
- Rheological measurements show shear-thinning non-Newtonian behavior

„Wer nur an einer einzigen Sache arbeitet, entdeckt selten etwas Neues. Von demjenigen jedoch sind viele nützliche Entdeckungen zu erwarten, der ganz unterschiedlichen Fragen nachgeht und die Dinge untereinander zu verknüpfen versteht.“

Joachim Jungius (1587 – 1657)

8 References

- [1] J. J. Berzelius, *Ann. de Chimie et de Physique* **1824**, 27, 53.
- [2] M. Hermann, *Justus Liebigs Ann. Chem.* **1855**, 95, 211.
- [3] a) F. S. Kipping, *J. Chem. Soc., Trans.* **1907**, 91, 209; b) N. R. Thomas, *Silicon* **2010**, 2, 187; c) F. S. Kipping, *Proc. R. Soc. London* **1937**, 159, 139.
- [4] E. G. Rochow, *J. Am. Pharm. Assoc.* **1951**, 40, 593.
- [5] a) L. Rösch, P. John, R. Reitmeier, in *Ullmann's Encyclopedia of Industrial Chemistry*, Wiley-VCH Verlag GmbH & Co. KGaA, **2000**; b) R. Schliebs, J. Ackermann, *Chem. Unserer Zeit* **1987**, 21, 121; c) W. Kalchauer, B. Pachaly, in *Handbook of Heterogeneous Catalysis*, Wiley-VCH Verlag GmbH & Co. KGaA, **2008**; d) C. Elschenbroich, *Organometallics*, 3 ed., Wiley-VCH, Weinheim, **2006**.
- [6] a) S. Yilmaz, N. Floquet, J. L. Falconer, *Journal of Catalysis* **1996**, 159, 31; b) M. Okamoto, S. Onodera, T. Okano, E. Suzuki, Y. Ono, *Journal of Organometallic Chemistry* **1997**, 531, 67; c) T. C. Frank, K. B. Kester, J. L. Falconer, *Journal of Catalysis* **1985**, 91, 44; d) T. C. Frank, K. B. Kester, J. L. Falconer, *J. Catal.* **1985**, 95, 396.
- [7] J. R. Koe, in *Comprehensive Organometallic Chemistry III* (Eds.: H. C. Editors-in-Chief: Robert, D. M. P. Mingos), Elsevier, Oxford, **2007**, pp. 549.
- [8] A. Guerra-Contreras, A. Villegas, E. Ramírez-Oliva, J. Cervantes, *Silicon* **2017**, 9, 525.
- [9] a) B. Marciniec, in *Hydrosilylation, Vol. 1* (Ed.: B. Marciniec), Springer Netherlands, **2009**, pp. 3; b) B. Marciniec, J. Chojnowski, *Progress in Organosilicon Chemistry*, Gordon and Breach Publisher, Basel, **1995**; c) F. O. Stark, J. R. Falender, A. P. Wright, in *Comprehensive Organometallic Chemistry* (Eds.: W. Editors-in-Chief: Geoffrey, F. G. A. Stone, F. G. A. S. Edward W. Abel A2 - Editors-in-Chief: Geoffrey Wilkinson, W. A. Edward), Pergamon, Oxford, **1982**, pp. 305; d) S. J. Clarson, J. A. Semlyen, *Siloxane Polymers*, 1st ed., New Jersey, **1993**; e) H.-H. Moretto, M. Schulze, G. Wagner, in *Ullmann's Encyclopedia of Industrial Chemistry*, Wiley-VCH Verlag GmbH & Co. KGaA, **2000**; f) H.-H. Moretto, M. Schulze, G. Wagner, in *Ullmann's Encyclopedia of Industrial Chemistry*, Wiley-VCH Verlag GmbH & Co. KGaA, **2005**; g) M. H. Mazurek, in *Comprehensive Organometallic Chemistry III* (Eds.: H. C. Editors-in-Chief: Robert, D. M. P. Mingos), Elsevier, Oxford, **2007**, pp. 651.
- [10] a) D. J. Sheehan, C. A. Hitchcock, C. M. Sibley, *Clin. Microbiol. Rev.* **1999**, 12, 40; b) C. Cocuau, M.-H. Rodier, G. Daniault, C. Imbert, *J. Antimicrob. Chemother.* **2005**, 56, 507; c) Y. Shi, W. Song, Z. H. Feng, Y. T. Zhao, F. Li, et al., *Eur. J. Clin. Microbiol. Infect. Dis.* **2009**, 28, 415; d) A. L. Santos, C. L. Sodre, R. S. Valle, B. A. Silva, E. A. Abi-Chacra, et al., *Curr. Med. Chem.* **2012**, 19, 2715; e) M. Okada, S. Yasuda, T. Kimura, M. Iwasaki, S. Ito, et al., *J. Biomed. Mater. Res. A* **2006**, 76A, 95; f) H. Li, M. Fairfax R, F. Dubocq, R. O. Darouiche, A. Rajpurkar, et al., *J. Urol.* **1998**, 160, 1910; g) R. O. Darouiche, M. D. Mansouri, E. M. Kojic, *Clin. Microbiol. Infect.* **2006**, 12, 397; h) A. Salvarci, M. Koroglu, B. Erayman, *Urol.* **2016**, 88, 66; i) A. Colas, J. Curtis, in *Biomaterials Science (Third Edition)* (Eds.: A. S. Hoffman, F. J. Schoen, J. E. Lemons), Academic Press, **2013**, pp. 82.
- [11] a) A. Kottmann, E. Mejía, T. Hémerly, J. Klein, U. Kragl, *Chem. Asian J.* **2017**, 12, 1168 ; b) C. N. C. Richard A. Harvey, *Microbiology*, Third ed., LWW, **2012**.
- [12] J. O. Corliss, *J. Protozool.* **1975**, 22, 3.
- [13] S. Vander Hook, *Louis Pasteur : groundbreaking chemist & biologist*, ABDO Pub. Company, Edina, Minn., **2011**.
- [14] a) E. Buddecke, *Grundriss der Biochemie, Vol. 7*, Walter de Gruyter, Berlin, **1984**; b) A. L. Lehninger, *Prinzipien der Biochemie*, Walter der Gruyter, Berlin, **1987**; c) A. A. Kwaasi, in *Encyclopedia of Food Sciences and Nutrition (Second Edition)* (Ed.: B. Caballero), Academic Press, Oxford, **2003**, pp. 3877.
- [15] U. Kück, M. Nowrousian, B. Hoff, I. Engh, *Schimmelpilze: Lebensweise, Nutzen, Schaden, Bekämpfung*, 3. Aufl. ed., Springer, Berlin [u.a.], **2009**.
- [16] a) M. Forrest, *Food Contact Materials - Rubbers, Silicones, Coatings and Inks*, Smithers Rapra Technology, **2009**; b) *Guidance for Industry: Preparation of Premarket Submissions for Food Contact Substances: Chemistry Recommendations*, U.S. Department of Health and Human Services, **2007**; c) M. L. White, *Code of Federal Regulations Vol 21 Part 170 to 199, Vol. 21*, Office of the Federal Register National Archives and Records Administration, **2012**; d) *Guidance for Industry and FDA Staff: Saline, Silicone Gel, and Alternative Breast Implants*, U.S. Department of Health and Human Services, **2006**.
- [17] A. T. Wolf, *Durability of Building and Construction Sealants and Adhesives: (STP 1453)* ASTM International, **2004**.
- [18] W. B. Whitman, D. C. Coleman, W. J. Wiebe, *Proc. Natl. Acad. Sci.* **1998**, 95, 6578.

- [19] C. R. Woese, G. E. Fox, *Proc. Natl. Acad. Sci.* **1977**, *74*, 5088.
- [20] O. S. Andersen, I. Roger E. Koeppe, *Annu. Rev. Biophys. Biomol. Struct.* **2007**, *36*, 107.
- [21] a) Y. Liu, E. Breukink, *Antibiotics* **2016**, *5*, 28; b) A. J. Egan, R. M. Cleverley, K. Peters, R. J. Lewis, W. Vollmer, *FEBS J.* **2016**, 13959.
- [22] A. Muñoz-Bonilla, M. Fernández-García, *Prog. Polym. Sci.* **2012**, *37*, 281.
- [23] X. Zhang, L. Wang, E. Levanen, *RSC Adv.* **2013**, *3*, 12003.
- [24] a) E. Fadeeva, V. K. Truong, M. Stiesch, B. N. Chichkov, R. J. Crawford, et al., *Langmuir* **2011**, *27*, 3012; b) Y. Arima, H. Iwata, *Biomaterials* **2007**, *28*, 3074; c) J. H. Lee, G. Khang, J. W. Lee, H. B. Lee, *J. Colloid Interface Sci.* **1998**, *205*, 323.
- [25] E. A. Epstein, M. A. Reizian, M. R. Chapman, *J. Bacteriol.* **2009**, *191*, 608.
- [26] Klaus-Günter. Collatz, A. Bogenrieder, *Lexikon der Biologie: Allgemeine Biologie - Pflanzen - Tiere*, Herder **1984**.
- [27] S. M. Bowman, S. J. Free, *BioEssays* **2006**, *28*, 799.
- [28] M. D. André Bryskier, *Antimicrobial Agents: Antibacterials and Antifungals*, ASM Press, **2005**.
- [29] a) A. Kugel, S. Stafslie, B. J. Chisholm, *Prog. Org. Coat.* **2011**, *72*, 222; b) X.-M. Li, D. Reinhoudt, M. Crego-Calama, *Chem. Soc. Rev.* **2007**, *36*, 1350; c) A. B. G. S. Subhash Latthe, C. Shridhar Maruti and R. Shrikant Vhatkar, *J. Surf. Eng. Mater. Adv. Technol.* **2012**, *2*, 76; d) T. S. John, R. H. Scott, A. Tolga, *Rep. Prog. Phys.* **2015**, *78*, 086501.
- [30] a) G. Sauvet, S. Dupond, K. Kazmierski, J. Chojnowski, *J. Appl. Polym. Sci.* **2000**, *75*, 1005; b) C. Novi, A. Mourran, H. Keul, M. Möller, *Macromol. Chem. Phys.* **2006**, *207*, 273; c) J. J. H. Oosterhof, K. J. D. A. Buijsen, H. J. Busscher, B. F. A. M. van der Laan, H. C. van der Mei, *Appl. Environ. Microbiol.* **2006**, *72*, 3673; d) K. De Prijck, N. De Smet, T. Coenye, E. Schacht, H. J. Nelis, *Mycopathologia* **2010**, *170*, 213; e) A. Agarwal, K. M. Guthrie, C. J. Czuprynski, M. J. Schurr, J. F. McAnulty, et al., *Adv. Funct. Mater.* **2011**, *21*, 1863; f) Y. Lin, Q. Liu, L. Cheng, Y. Lei, A. Zhang, *React. Funct. Polym.* **2014**, *85*, 36; g) S.-B. Yeh, C.-S. Chen, W.-Y. Chen, C.-J. Huang, *Langmuir* **2014**, *30*, 11386; h) Y. Chen, Q. Han, Y. Wang, Q. Zhang, X. Qiao, *J. Appl. Polym. Sci.* **2015**, *132*, 41723; i) A. Piecuch, E. Obłąk, K. Guz-Regner, *J. Surfactants Deterg.* **2016**, *19*, 275; j) A. Vaterrodt, B. Thallinger, K. Daumann, D. Koch, G. M. Guebitz, et al., *Langmuir* **2016**, *32*, 1347; k) Z. X. Voo, M. Khan, Q. Xu, K. Narayanan, B. W. J. Ng, et al., *Polym. Chem.* **2016**, *7*, 656.
- [31] a) Y. Yao, Y. Ohko, Y. Sekiguchi, A. Fujishima, Y. Kubota, *J. Biomed. Mater. Res. B.* **2008**, *85B*, 453; b) P. Kaali, E. Strömberg, R. E. Aune, G. Czél, D. Momcilovic, et al., *Polym. Degrad. Stab.* **2010**, *95*, 1456; c) S. Perni, C. Piccirillo, A. Kafizas, M. Uppal, J. Pratten, et al., *J. Cluster Sci.* **2010**, *21*, 427; d) J. S. Shah, B. Girase, W. W. Thein-Han, R. D. K. Misra, *Adv. Eng. Mater.* **2011**, *13*, B41; e) C. Y. Tang, D.-z. Chen, K. Y. Y. Chan, K. M. Chu, P. C. Ng, et al., *Polym. Int.* **2011**, *60*, 1461; f) K. Taptim, N. Sombatsompop, *J. Vinyl Addit. Technol.* **2013**, *19*, 113; g) V. Jankauskaite, B. Abzalbekuly, A. Lisauskaite, I. Procycevas, E. Fataraitė, et al., *Mater. Sci. Eng.* **2014**, *20*, 42; h) C. G. Kumar, S. Pombala, *Nanotech.* **2014**, *25*, 325101; i) K. Taptim, A. Ansarifar, N. Sombatsompop, *Polym. Eng. Sci.* **2014**, *54*, 932; j) L. L. Wang, T. Sunb, S. Y. Zhoua, L. Q. Shaoa, *Acta Phys. Pol., A* **2014**, *125*; k) S. K. Sehmi, S. Noimark, J. Weiner, E. Allan, A. J. MacRobert, et al., *ACS Appl. Mater. Interfaces* **2015**, *7*, 22807; l) N. Tran, M. N. Kelley, P. A. Tran, D. R. Garcia, J. D. Jarrell, et al., *J. Mater. Sci. Eng.* **2015**, *49*, 201; m) A. Groza, C. Ciobanu, C. Popa, S. Iconaru, P. Chapon, et al., *Polymers* **2016**, *8*, 131; n) T. G. Peñaflor Galindo, T. Kataoka, S. Fujii, M. Okuda, M. Tagaya, *Colloid Interface Sci. Commun.* **2016**, *10–11*, 15.
- [32] a) H. Sawada, Y. Ikematsu, T. Kawase, Y. Hayakawa, *Langmuir* **1996**, *12*, 3529; b) L. Xu, W. Chen, A. Mulchandani, Y. Yan, *Angew. Chem., Int. Ed.* **2005**, *44*, 6009; c) A. W. Hassel, S. Milenkovic, U. Schürmann, H. Greve, V. Zaporotchenko, et al., *Langmuir* **2007**, *23*, 2091; d) B. Bhushan, K. Koch, Y. C. Jung, *Appl. Phys. Lett.* **2008**, *93*, 093101; e) A. Okada, T. Nikaido, M. Ikeda, K. Okada, J. Yamauchi, et al., *Dent. Mater. J.* **2008**, *27*, 565; f) J. Ji, W. Zhang, *J. Biomed. Mater. Res. A* **2009**, *88A*, 448; g) J.-S. Lee, Y.-S. Lee, M.-S. Kim, S.-K. Hyun, C.-H. Kang, et al., *Adv. Mater. Sci. Eng.* **2013**, *2013*, 4; h) M. W. Thielke, E. P. Bruckner, D. L. Wong, P. Theato, *Polymer* **2014**, *55*, 5596; i) J. Zhang, A. Wang, S. Seeger, *Polym. Chem.* **2014**, *5*, 1132; j) M. Obaid, N. A. M. Barakat, O. A. Fadali, S. Al-Meer, K. Elsaid, et al., *Polymer* **2015**, *72*, 125; k) M. Ashraf, P. Champagne, C. Campagne, A. Perwuelz, F. Dumont, et al., *J. Ind. Text.* **2016**, *45*, 1440; l) J. Ou, Z. Wang, F. Wang, M. Xue, W. Li, et al., *Appl. Surf. Sci.* **2016**, *364*, 81; m) F. Zhang, S. Gao, Y. Zhu, J. Jin, *J. Membr. Sci.* **2016**, *513*, 67.
- [33] a) R. Van Noort, R. Bayston, *J. Biomed. Mater. Res. A* **1979**, *13*, 623; b) A. V. Kalya, D. G. Ahearn, *J. Ind. Microbiol. Biotechnol.* **1995**, *14*, 451; c) C. A. Kauffman, P. L. Carver, *Drugs* **1997**, *53*, 539; d) K. Sato, H. Tomioka, T. Akaki, S. Kawahara, *Int. J. Antimicrob. Agents* **2000**, *16*, 25; e) D. M. Kuhn, T. George, J. Chandra, P. K. Mukherjee, M. A. Ghannoum, *Antimicrob. Agents Chemother.* **2002**, *46*, 1773; f) A. Katragkou, A. Chatzimoschou, M. Simitsopoulou, M.

- Dalakiouridou, E. Diza-Mataftsi, et al., *Antimicrob. Agents Chemother.* **2008**, 52, 357; g) C. R. Pusateri, E. A. Monaco, M. Edgerton, *Arch. Oral Biol.* **2009**, 54, 588; h) N. O. Hübner, R. Matthes, I. Koban, C. Rändler, G. Müller, et al., *Skin Pharmacol. Physiol.* **2010**, 23(suppl 1), 28; i) A. Katragkou, A. Chatzimoschou, M. Simitsopoulou, E. Georgiadou, E. Roilides, *J. Antimicrob. Chemother.* **2011**, 66, 588; j) D. Toulet, C. Debarre, C. Imbert, *J. Antimicrob. Chemother.* **2012**, 67, 430; k) M. Chan, G. Hidalgo, B. Asadishad, S. Almeida, N. Muja, et al., *Colloids Surf., B* **2013**, 110, 275; l) C.-M. Phan, L. N. Subbaraman, L. Jones, *J. Biomater. Sci., Polym. Ed.* **2014**, 25, 1907; m) C. Dong, Z. Lu, F. Zhang, *Mater. Lett.* **2015**, 142, 35; n) S. Jebors, C. Pinese, B. Nottelet, K. Parra, M. Amblard, et al., *J. Pept. Sci.* **2015**, 21, 243; o) M. F. Khan, L. Zepeda-Velazquez, M. A. Brook, *Colloids Surf., B* **2015**, 132, 216; p) S. L. Steffensen, M. H. Vestergaard, M. Groenning, M. Alm, H. Franzyk, et al., *Eur. J. Pharm. Biopharm.* **2015**, 94, 305.
- [34] a) U. Mizerska, W. Fortuniak, J. Chojnowski, K. Turecka, A. Konopacka, et al., *J. Inorg. Organomet. Polym. Mater.* **2010**, 20, 554; b) S. Ye, P. Majumdar, B. Chisholm, S. Stafslie, Z. Chen, *Langmuir* **2010**, 26, 16455.
- [35] S. Belkhair, M. Kinninmonth, L. Fisher, B. Gasharova, C. M. Liauw, et al., *RSC Adv.* **2015**, 5, 40932.
- [36] a) M. Gosau, R. Bürgers, T. Vollkommer, T. Holzmann, L. Prantl, *J. Biomater. Appl.* **2013**, 28, 187; b) M. Gosau, L. Prantl, M. Feldmann, A. Kokott, S. Hahnel, et al., *Biofouling* **2010**, 26, 359.
- [37] A. Goyal, A. Kumar, P. K. Patra, S. Mahendra, S. Tabatabaei, et al., *Macromol. Rapid Commun.* **2009**, 30, 1116.
- [38] a) D. Depan, R. D. K. Misra, *J. Mater. Sci. Eng.* **2014**, 34, 221; b) O. Girshevitz, Y. Nitzan, C. N. Sukenik, *Chem. Mater.* **2008**, 20, 1390.
- [39] a) E. Ozkan, E. Allan, I. P. Parkin, *RSC Adv.* **2014**, 4, 51711; b) E. Ozkan, F. T. Ozkan, E. Allan, I. P. Parkin, *RSC Adv.* **2015**, 5, 8806.
- [40] B. J. Nablo, H. L. Prichard, R. D. Butler, B. Klitzman, M. H. Schoenfisch, *Biomaterials* **2005**, 26, 6984.
- [41] a) E. Bovero, K. E. A. Magee, E. C. Young, C. Menon, *Macromol. React. Eng.* **2013**, 7, 624; b) M. Cazacu, C. Racles, A. Airinei, A. Vlad, I. Stoica, *Polym. Adv. Technol.* **2012**, 23, 122; c) R. Dastjerdi, M. Montazer, S. Shahsavan, *Colloids Surf., A* **2009**, 345, 202.
- [42] K. Lim, R. R. Y. Chua, B. Ho, P. A. Tambyah, K. Hadinoto, et al., *Acta Biomater.* **2015**, 15, 127.
- [43] a) B. E. De Pauw, *Int. J. Antimicrob. Agents* **2000**, 16, 147; b) J. R. Graybill, *Eur. J. Clin. Microbiol. Infect. Dis.* **1989**, 8, 402.
- [44] a) J. H. Chang, I. W. Hunter, *Macromol. Rapid Commun.* **2011**, 32, 718; b) J. Yang, Z. Zhang, X. Xu, X. Zhu, X. Men, et al., *J. Mater. Chem.* **2012**, 22, 2834; c) C. González-Obeso, W. L. Song, M. A. Rodríguez-Pérez, J. F. Mano, *Mater. Sci. Forum* **2013**, 730-732, 44; d) S. Chernyy, M. Järn, K. Shimizu, A. Swerin, S. U. Pedersen, et al., *ACS Appl. Mater. Interfaces* **2014**, 6, 6487; e) A. de Leon, R. C. Advincula, *ACS Appl. Mater. Interfaces* **2014**, 6, 22666; f) M. Obaid, O. A. Fadali, B.-H. Lim, H. Fouad, N. A. M. Barakat, *Mater. Lett.* **2015**, 138, 196; g) V. F. Cardoso, A. R. Machado, V. C. Pinto, P. J. Sousa, G. Botelho, et al., *J. Polym. Sci. B* **2016**, 54, 1802.
- [45] A. Lafuma, D. Quéré, *Nature Materials* **2003**, 2, 457.
- [46] a) W. C. White, J. M. Olderman, *Proc. INDA* **1982**; b) M. Feoktistova, P. Geserick, M. Leverkus, *Cold Spring Harb. Protoc.* **2016**, 2016, 343; c) M. J. Humphries, *Methods Mol. Biol.* **2009**, 522, 203; d) S. A. Seyedmehdi, H. Zhang, J. Zhu, *Appl. Surf. Sci.* **2012**, 258, 2972; e) Y. Yuan, T. R. Lee, in *Surface Science Techniques* (Eds.: G. Bracco, B. Holst), Springer Berlin Heidelberg, Berlin, Heidelberg, **2013**, pp. 3.
- [47] J. M. Andrews, *J. Antimicrob. Chemother* **2001**, 48 Suppl 1, 5.
- [48] ISO 22196:2011(E), Measurement of antibacterial activity on plastics and other nonporous Surfaces.
- [49] EN ISO 846:1997, Plastics: Evaluation of the action of microorganisms on plastics.
- [50] a) T. Bahners, L. Prager, S. Kriehn, J. S. Gutmann, *Appl. Surf. Sci.* **2012**, 259, 847; b) O. Norihiko, A. Hirohito, T. Yuichi, W. Hiroko, *Base material having hydrophilic layer*, WO2013001894, **2013**.
- [51] F. C. Whitmore, E. W. Pietrusza, L. H. Sommer, *J. Am. Chem. Soc.* **1947**, 69, 2108.
- [52] J. L. Speier, J. A. Webster, G. H. Barnes, *J. Am. Chem. Soc.* **1957**, 79, 974.
- [53] a) A. J. Chalk, J. F. Harrod, *J. Am. Chem. Soc.* **1965**, 87, 16; b) M. A. Schroeder, M. S. Wrighton, *J. Organomet. Chem.* **1977**, 128, 345.
- [54] T. I. Gountchev, T. D. Tilley, *Organometallics* **1999**, 18, 5661.

- [55] a) V.B. Pukhnarevich, E. Lukevics, L.T. Kopylova, M. G. Voronkov, Riga, Latvia, **1992**; b) M. J. K. Thomas, *Polym. Int.* **2001**, 50, 256; c) B. Marcinić, *Hydrosilylation*, Vol. 1, Springer Netherlands, **2009**.
- [56] a) I. Ojima, in *The Chemistry of Organic Silicon Compounds, Volume 2, Parts 1, 2, and 3* (Ed.: S. Patai), Wiley, **1998**; b) B. Marcinić, H. Maciejewski, C. Pietraszuk, P. Pawluc, J. Gulinski, in *Encyclopedia of Catalysis*, John Wiley & Sons, Inc., **2002**.
- [57] a) B. Marcinić, H. Maciejewski, J. Mirecki, *J. Organomet. Chem.* **1991**, 418, 61; b) B. Marcinić, H. Maciejewski, *J. Organomet. Chem.* **1993**, 454, 45; c) B. Marcinić, H. Maciejewski, U. Rosenthal, *J. Organomet. Chem.* **1994**, 484, 147; d) B. Marcinić, H. Maciejewski, J. Guliński, B. Maciejewska, W. Duczmal, *J. Organomet. Chem.* **1996**, 521, 245.
- [58] a) C. Naoto, K. Tamotsu, K. Yasuteru, M. Hidetatsu, K. Fumitoshi, et al., *Chem. Lett.* **2000**, 29, 14; b) M. Brookhart, B. E. Grant, *J. Am. Chem. Soc.* **1993**, 115, 2151.
- [59] S. C. Bart, E. Lobkovsky, P. J. Chirik, *J. Am. Chem. Soc.* **2004**, 126, 13794.
- [60] Y. Nakajima, S. Shimada, *RSC Adv.* **2015**, 5, 20603.
- [61] a) J. F. Harrod, A. J. Chalk, *J. Am. Chem. Soc.* **1964**, 86, 1776; b) P. Magnus, *J. Am. Chem. Soc.* **2001**, 123, 781.
- [62] a) L. N. Lewis, C. A. Sumpter, M. Davis, *J. Inorg. Organomet. Polym.* **1995**, 5, 377; b) L. N. Lewis, C. A. Sumpter, J. Stein, *J. Inorg. Organomet. Polym.* **1996**, 6, 123.
- [63] H. M. Bank, G. T. Decker; Dow Silicones Corp.; *Unsaturated alcohols as accelerators for hydrosilylation*, US5486637, **1995**.
- [64] H. M. Bank, A. K. Roy; Dow Silicones Corp.; *Unsaturated accelerators for hydrosilylation*, US5756795, **1996**.
- [65] H. M. Bank; Dow Silicones Corp.; *Method for maintaining catalytic activity during a hydrosilylation reaction*, US5359113A, **1993**.
- [66] A. Hopf, K. H. Dötz, *J. Mol. Catal. A: Chem.* **2000**, 164, 191.
- [67] B. Karstedt; General Electric Co; *Platinum complexes of unsaturated siloxanes and platinum containing organopolysiloxanes*, US3775452, **1971**.
- [68] X. Cui, K. Junge, X. Dai, C. Kreyenschulte, M.-M. Pohl, et al., *ACS Cent. Sci.* **2017**, 3, 580.
- [69] H. Aneetha, W. Wu, J. G. Verkade, *Organometallics* **2005**, 24, 2590.
- [70] a) O. Buisine, G. Berthon-Gelloz, J.-F. Brière, S. Stérin, G. Mignani, et al., *Chem. Commun.* **2005**, 3856; b) G. Berthon-Gelloz, O. Buisine, J.-F. Brière, G. Michaud, S. Stérin, et al., *J. Organomet. Chem.* **2005**, 690, 6156; c) I. E. Markó, S. Stérin, O. Buisine, G. Berthon, G. Michaud, et al., *Adv. Synth. Catal.* **2004**, 346, 1429; d) G. De Bo, G. Berthon-Gelloz, B. Tinant, I. E. Markó, *Organometallics* **2006**, 25, 1881.
- [71] J. W. Sprengers, M. J. Agerbeek, C. J. Elsevier, H. Kooijman, A. L. Spek, *Organometallics* **2004**, 23, 3117.
- [72] a) Jeroen W. Sprengers, M. de Greef, Marcel A. Duin, Cornelis J. Elsevier, *Eur. J. Inorg. Chem.* **2003**, 2003, 3811; b) C. R. Baar, L. P. Carbray, M. C. Jennings, R. J. Puddephatt, *J. Am. Chem. Soc.* **2000**, 122, 176.
- [73] N. D. Jones, G. Lin, R. A. Gossage, R. McDonald, R. G. Cavell, *Organometallics* **2003**, 22, 2832.
- [74] H. Kricheldorf, *Silicon in Polymer Synthesis*, **1996**.
- [75] M. Zaranek, P. Pawluc, *ACS Catal.* **2018**, 8, 9865.
- [76] a) M. Rutnakornpituk, *Eur. Polym. J.* **2005**, 41, 1043; b) C. Racles, M. Cazacu, B. Fischer, D. M. Opris, *Smart Mater. Struct.* **2013**, 22; c) C. Racles, M. Alexandru, A. Bele, V. E. Musteata, M. Cazacu, et al., *RSC Adv.* **2014**, 4, 37620; d) M. Khachidze, T. Tatrishvili, N. Jalagonia, K. Gelashvili, E. Markarashvili, et al., *Oxid. Commun.* **2015**, 38, 13.
- [77] A. W. A. D. McNaught, *IUPAC. Compendium of Chemical Terminology*, 2nd ed., Oxford, **1997**.
- [78] a) K. Kuciński, M. Jankowska-Wajda, T. Ratajczak, S. Bałabańska-Trybuś, A. Schulmann, et al., *ACS Omega* **2018**, 3, 5931; b) J. E. Gómez, F. H. Navarro, J. E. Sandoval, *Electrophoresis* **2014**, 35, 2579; c) G. Hreczycho, *Eur. J. Inorg. Chem.* **2015**, 2015, 67.
- [79] a) Norbert Adam, Geza Avar, Herbert Blankenheim, Wolfgang Friederichs, Manfred Giersig, et al., in *Ullmann's Encyclopedia of Industrial Chemistry*, **2005**; b) Wilfried Umbach, W. Stein, *J. Am. Oil Chem. Soc.* **1971**, 48, 394.
- [80] A. Wurtz, *Ann. Chim. Phys.* **1863**, 69, 330.
- [81] P. Dubois, O. Coulembier, J.-M. Raquez, *Handbook of Ring-Opening Polymerization*, Wiley VCH, Weinheim, **2009**.
- [82] J. R. Ebdon, *Polym. Int.* **1994**, 33, 233.
- [83] a) H. Staudinger, O. Schweitzer, *Ber. Dtsch. Chem. Ges.* **1929**, 62, 2395; b) H. N. Stokes, *Am. Chem. J.* **1897**, 19, 782.
- [84] C. Schoeller, M. Wittwer; IG Farbenindustrie AG; *Assistants for the textile and related industries*, US1970578, **1930**.

- [85] a) D. Ovidiu, C. Constantin; Henkel AG and Co KGaA; *Catalytic alkoxylation of fatty alcohol(s) and other fat derivs. - by passing down falling-film reactor in contact with parallel stream of alkylene oxide, esp. ethylene oxide*, DE4128827, **1991**; b) G. M. Leuteritz, *Fat Sci. Technol.* **1991**, 93, 383; c) R. Braun, A. Schönbucher, *Chem. Ing. Tech.* **2001**, 73, 536; d) J.-L. Gustin, *Safety of ethoxylation reactions*, Vol. 157, **2001**; e) E. Salzano, M. Di Serio, E. Santacesaria, *J. Loss Prev. Process Ind.* **2007**, 20, 238.
- [86] J. Delaval, P. Guinet, J. Morel, R. Puthet; Rhone Poulenc Sa; *Novel polysiloxane-polyalkylene copolymers*, US3564037, **1971**.
- [87] H. R. Johnston; Continental Tire Americas LLC; *Method of making a polyether using a double metal cyanide complex compound*, US3278459, **1963**.
- [88] a) H. van der Hulst, G. A. Pogany, J. Kuyper; BASF; *Catalysts for the polymerization of epoxides and process for the preparation of such catalysts*, US4477589, **1982**; b) J. Kuyper, G. Boxhoorn, *J. Catal.* **1987**, 105, 163.
- [89] a) R. J. Herold, R. A. Livigni, in *Polymerization Kinetics and Technology*, Vol. 128, AMERICAN CHEMICAL SOCIETY, **1973**, pp. 208; b) Y.-J. Huang, G.-R. Qi, Y.-H. Wang, *J. Polym. Sci. A* **2002**, 40, 1142; c) I. Kim, J.-T. Ahn, C. S. Ha, C. S. Yang, I. Park, *Polymer* **2003**, 44, 3417; d) L.-C. Wu, A.-F. Yu, M. Zhang, B.-H. Liu, L.-B. Chen, *J. Appl. Polym. Sci.* **2004**, 92, 1302; e) I. Kim, S. H. Byun, C.-S. Ha, *J. Polym. Sci. A* **2005**, 43, 4393; f) C. G. Rodriguez, R. C. Ferrier, A. Helenic, N. A. Lynd, *Macromolecules* **2017**, 50, 3121; g) F. S. Kipping, L. L. Lloyd, *J. Chem. Soc., Trans.* **1901**, 79, 449.
- [90] a) S. Chen, G.-R. Qi, Z.-J. Hua, H.-Q. Yan, *J. Polym. Sci. A* **2004**, 42, 5284; b) M. J. Yi, S.-H. Byun, C.-S. Ha, D.-W. Park, I. Kim, *Solid State Ionics* **2004**, 172, 139; c) A. Cambón, A. Rey-Rico, S. Barbosa, J. F. A. Soltero, S. G. Yeates, et al., *J. Controlled Release* **2013**, 167, 68.
- [91] A. Raghuraman, D. Babb, M. Miller, M. Paradkar, B. Smith, et al., *Macromolecules* **2016**, 49, 6790.
- [92] a) E. Santacesaria, M. Di Serio, L. Lisi, D. Gelosa, *Ind. Eng. Chem. Res.* **1990**, 29, 719; b) E. Santacesaria, R. Tesser, M. Di Serio, *Chin. J. Chem. Eng.* **2018**.
- [93] a) G. Rossmly, G. Koerner; Goldschmidt AG; *Polysiloxane-polyalkyleneglycol block copolymers suitable as foam stabilizers in the manufacture of polyurethane foams* US3723491, **1973**; b) M. Winterberg, A. Dietrich, M. Woznicka, E. Mejía, U. Kragl, et al.; Henkel AG Co KGaA; *Process for the preparation of hydroxyl-functionalized polysiloxanes*, EP20160204752, **2016**.
- [94] K. W. Haider, J. Chung, J. F. Dormish, R. V. Starcher, I. L. Yano, et al.; Covestro LLC; *Polyether-polysiloxane polyols*, US20080171829, **2008**.
- [95] N. Hadjichristidis, S. Pispas, M. Pitsikalis, H. Iatrou, D. J. Lohse, in *Encyclopedia of Polymer Science and Technology*, John Wiley & Sons, Inc., **2002**.
- [96] a) S. Lentsch, M. Sopha, V. Man; Ecolab Inc.; *Rinse aid for plasticware* EP0875556, **1998**; b) T. Iimura, A. Hayashi, H. Furukawa; Dow Corning Toray Co.; *Cosmetic and topical skin preparation comprising higher alcohol-modified silicone*, WO2011136389, **2011**; c) K. M. Lee, L. J. Petroff, W. J. S. Jr.; Dow Corning; *Method of making silicone polyether copolymers having reduced odor*, US6162888, **2000**; d) X. Tang, Y. Sun, Z. Luo, J. Shen, T. Chen; Jiangsu Maysta Chemical Co., Ltd., Peop. Rep. China *Olefine acid ester contained organic silicon polyether copolymer and preparing method thereof*, CN103665385A, **2014**.
- [97] D. C. Webster, R. B. Bodkhe; NDSU RES Foundation; *Functionalized silicones with polyalkylene oxide side chains*, WO 2013052181, **2013**.
- [98] L. Pricop, V. Hamciuc, M. Marcu, A. Ioanid, S. Alazaroaie, *High Perform. Polym.* **2005**, 17, 303.
- [99] T. G. Scholte, N. L. J. Meijerink, *Br. Polym. J.* **1977**, 9, 133.
- [100] A. Ranowsky, **2016**, <https://www.cscscientific.com/csc-scientific-blog/how-does-contact-angle-relate-to-surface-tension> (01.02.2019)
- [101] T. A. Coney, W. J. Masica, *Effect of flow rate on the dynamic contact angle for wetting liquids*, **1969**.
- [102] P. W. Atkins, J. de Paula, *Physikalische Chemie*, Vol. 5, Wiley-VCH, Weinheim, **2013**.
- [103] Q. Yu, H. Yin, *Chin. J. Chem. Eng.* **2006**, 14, 555.
- [104] O. Mukbaniani, T. Tatrishvili, G. Titvinidze, N. Mukbaniani, L. Lezhava, et al., *J. Appl. Polym. Sci.* **2006**, 100, 2511.
- [105] Ł. Szyc, J. Guo, M. Yang, J. Dreyer, P. M. Tolstoy, et al., *The Journal of Physical Chemistry A* **2010**, 114, 7749.
- [106] a) Z. Lyu, C. Dong, Q. Li, F. Wang; University Qingdao; *Preparation of phosphorus-containing flame-retardant silicone oil*, CN20141470957, **2014**; b) C. Dong, Z. Lyu, F. Zhang, P. Zhu; *Method for preparing water-repellent flame-retardant additive*, CN104177618, **2014**; c) C.

- Dong, Z. Lu, F. Zhang, P. Zhu, L. Zhang, et al., *Mater. Lett.* **2015**, 152, 276; d) C. Dong, Z. Lu, F. Zhang, P. Zhu, P. Wang, et al., *J. Therm. Anal. Calorim.* **2016**, 123, 535.
- [107] a) J. Chojnowski, W. Fortuniak, P. Rościszewski, W. Werel, J. Łukasiak, et al., *J. Inorg. Organomet. Polym. Mater.* **2006**, 16, 219; b) U. Mizerska, W. Fortuniak, J. Chojnowski, R. Hałas, A. Konopacka, et al., *Eur. Polym. J.* **2009**, 45, 779; c) W. Fortuniak, U. Mizerska, J. Chojnowski, T. Basinska, S. Slomkowski, et al., *J. Inorg. Organomet. Polym. Mater.* **2011**, 21, 576.
- [108] P. Liu, Q. Chen, B. Yuan, M. Chen, S. Wu, et al., *Materials Science and Engineering: C* **2013**, 33, 3865.
- [109] R. N. Haszeldine, M. J. Newlands, J. B. Plumb, *J. Chem. Soc.* **1965**, 2101.
- [110] J. Ohshita, A. Iwata, F. Kanetani, A. Kunai, Y. Yamamoto, et al., *J. Org. Chem.* **1999**, 64, 8024.
- [111] a) A. Iwata, J. Ohshita, H. Tang, A. Kunai, Y. Yamamoto, et al., *J. Org. Chem.* **2002**, 67, 3927; b) J. Ohshita, Y. Izumi, Z. Lu, J. Ikada, A. Kunai, *J. Organomet. Chem.* **2006**, 691, 1907; c) J. Ohshita, K. Inata, Y. Izumi, A. Kunai, *J. Organomet. Chem.* **2007**, 692, 3526; d) Z. Lu, J. Ohshita, T. Mizumo, *J. Organomet. Chem.* **2012**, 697, 51; e) C. Dong, Z. Lv, P. Zhu; *Preparation method of novel organic silicone oil water repellent agent used for cotton fabric*, CN102408570, **2012**; f) C. H. L. Dong, Zhou; Zhu, Ping; Wang, Lei *Adv. Mater. Res.* **2014**, 998-999, 15; g) C. L. Dong, Zhou; Zhu, Ping; Wang, Lei; Zhang, Fengjun *J. Eng. Fibers Fabr.* **2015**, 10, 171.
- [112] C.-I. L. Fan, Si-feng; Yang, Qing-jing; Zeng, Chao-yuan; Huang, Chao; Fan, Bao-min *Yunnan Minzu Daxue Xuebao, Ziran Kexueban* **2013**, 22.
- [113] a) N. Menshutkin, *Z. physik. Chem.* **1890**, 5U, 589; b) N. Menshutkin, *Z. physik. Chem.* **1890**, 6U, 41.
- [114] W. R. Brasen, C. R. Hauser, *Org. Synth.* **1954**, 34, 58.
- [115] V. Caló, A. Nacci, A. Monopoli, A. Fanizzi, *Org Lett* **2002**, 4, 2561.
- [116] a) K. Maeda, S. Iwasa, K. Nakano, E. Hasegawa; NEC Corporation; *Polymer having silicon atoms and sulfonium salt units and photoresist compositions containing the same*, US5747622, **1993**; b) Y. Chenghua, G. Yuliang, X. Longhe, B. Liang, C. Zufen; Dymatic Chemicals Inc.; *Preparation method of dication-type organic silicon modified waterborne polyurethane color fixing agent*, CN201711286021, **2018**.
- [117] a) M. A. Appeaning, M. A. Boulos, D. J. Kinning, G. Teverovskiy, M. L. Steiner, et al.; 3M Innovative Properties Co; *Adhesive article and method of making the same*, WO2017US38491, **2018**; b) K. Okazaki; Mitsui Chemicals, Inc.; *Modified acrylic resin cured product, and laminate therefor, and production methods therefor* JPWO2016136811, **2017**.
- [118] G. Lu, D. Ahn, C. Wong; Dow Corning; *Silicone-based ionic liquids and applications thereof*, WO2013096211, **2013**.
- [119] a) M. Nakamura, K. Fujisawa, T. Goshima; Tory Industries, Inc.; *Antibacterial composition for medical use and medical device*, EP2275154, **2009**; b) J. Jońca, C. Tukaj, W. Werel, U. Mizerska, W. Fortuniak, et al., *J. Mater. Sci.: Mater. Med.* **2016**, 27, 1.
- [120] H. X. Wang Yanlin, Yang Jian, *Petrochem. Technol.* **2013**, 42, 1137.
- [121] S. Rendler, R. Fröhlich, M. Keller, M. Oestreich, *Eur. J. Org. Chem.* **2008**, 2008, 2582.
- [122] a) O. Moreau, C. Portella, F. Massicot, J. M. Herry, A. M. Riquet, *Surf. Coat. Technol.* **2007**, 201, 5994; b) E. Haladjova, G. Mountrichas, S. Pispas, S. Rangelov, *J. Org. Chem.* **2016**, 120, 2586.
- [123] a) W. Kunz, H. J. Gores, in *Encyclopedia of Applied Electrochemistry*, Vol. 3rd Edition (Eds.: G. Kreysa, K.-i. Ota, R. F. Savinell), Springer Reference, New York, **2014**, pp. 1106 ; b) N. Matsumi, K. Sugai, M. Miyake, H. Ohno, *Macromolecules* **2006**, 39, 6924; c) H. Ohno, *Bull. Chem. Soc. Jpn.* **2006**, 79, 1665.
- [124] F. P. Byrne, S. Jin, G. Paggiola, T. H. M. Petchey, J. H. Clark, et al., *Sustain. Chem. Process.* **2016**, 4, 7.
- [125] a) M. S. C. S. Santos, E. F. G. Barbosa, *J. Mol. Catal. A: Chem.* **2009**, 306, 82; b) J. Wang, X.-z. Yang, G.-s. Li, Y.-y. Shi, *Riyong Huaxue Gongye* **2007**, 37, 235.
- [126] D. S. Christen, in *Praxiswissen der chemischen Verfahrenstechnik*, Springer, Berlin, Heidelberg, **2010**.
- [127] S. C. B. Selvamony, *ISRN Chemical Engineering* **2013**, 2013.
- [128] P. H. J. Chandrakant Kokate, *Textbook of Pharmaceutical Biotechnology*, 1st ed., Elsevier, **2011**.
- [129] S. N. Khattab, R. Subirós-Funosas, A. El-Faham, F. Albericio, *Eur. J. Org. Chem.* **2010**, 2010, 3275.
- [130] M. Ishizaki, M. Yamada, S.-i. Watanabe, O. Hoshino, K. Nishitani, et al., *Tetrahedron* **2004**, 60, 7973.

- [131] Z. D. Miller, R. Dorel, J. Montgomery, *Angew. Chem., Int. Ed.* **2015**, *54*, 9088.
- [132] S. S. Soni, N. V. Sastry, V. K. Aswal, P. S. Goyal, *J. Org. Chem.* **2002**, *106*, 2606.
- [133] G. K. Batchelor, *An Introduction to Fluid Dynamics (Cambridge Mathematical Library)*, 2. ed., Cambridge University Press, Cambridge, **2000**.
- [134] B. D. Coleman, H. Markovitz, W. Noll, *Viscometric Flows of Non-Newtonian Fluids*, 1. ed., Springer Tracts in Natural Philosophy Pittsburgh, **1966**.
- [135] I. L. Herceg, A. Režek Jambrak, D. Šubarić, M. Brncic, S. Rimac, et al., *Czech J. Food Sci.* **2018**, *28*, 83.
- [136] B. Briscoe, P. Luckham, S. Zhu, *Polymer* **2000**, *41*, 3851.
- [137] W. Ernhöfer, **2019**, <https://www.process.vogel.de/rohstoffpreise-ziehen-weiter-an-a-807474/> (11.03.2019)
- [138] a) K. L. Guyer, K. M. Lewis, S. Umapathy, A. Saxena, Y.-F. Wang; Momentive Performance Materials Inc. (Waterford, NY, US); *Hydrophilic silicone monomers, process for their preparation and thin films containing the same*, WO 2013142060, **2014**; b) C. D. Juengst, W. P. Weber, G. Manuel, *J. Organomet. Chem.* **1986**, *308*, 187.
- [139] E. C. Steiner, R. O. Trucks, *J. Am. Chem. Soc.* **1968**, *90*, 720.

Appendix

A1. Equipment and Testing methods

Equipment:

Unless otherwise indicated, the reactions were performed under moisture free conditions and under argon atmosphere using conventional Schlenk techniques. Argon was dried by passing it through a phosphorous pentoxide filled column. The equipment was oven-dried and flushed with argon before getting in contact with the sensitive substances.

The pressures for distillations and evacuations were measured by CVC 3000 Vacuubrand pressure sensors. The standard vacuum pressure (oil pump) was ≥ 0.01 mbar.

NMR-Spectroscopy:

All NMR measurements were done on a Bruker 300 MHz and 400 MHz instrument with deuterated solvents. All the samples were measured at room temperature (297 K). The chemical shifts are given in ppm. The calibration of the chemical shifts in ^1H , ^{13}C , dept and IG^{29}Si spectra was carried out by using the shifts of the deuterated solvents (CDCl_3 , δH 7.26, 77.0; DMSO-d_6 , δH 2.49, 39.7; CD_3OD , δH 3.31, 49.0).

GPC:

Gel permeation chromatography was carried out using HP1090 II Chromatography with DAD detector (HEWLETT PACKARD) at 40 °C. Tetrahydrofuran (THF) was used as an eluent. THF was passed through three PSS SDV gel columns with molecular weight ranges of 102, 103 and 104 $\text{g}\cdot\text{mol}^{-1}$ with a flow rate of $0.9\text{ ml}\cdot\text{min}^{-1}$. The calibration of the device was carried out using polystyrene standards.

Elemental Analysis:

Elemental analyses were recorded by the analytic department of the Leibniz Institute for Catalysis with a Flash EA 1112 analyzer by Thermo Quest or with a C/H/N/S-micro analyzer TruSpec-932 by Leco. Elemental analyses of platinum and palladium were performed on a flame atomic absorption spectrometer Perkin-Elmer Analyst 300. The determination of halogens was done with a potentiometric titration (analytical titration TIM 580 und TIM 870). Detection of silicon was done via atomic absorption spectrometry with Perkin-Elmer AAnalyst 300.

Infrared Spectroscopy:

Infrared spectra of the samples were measured in ATR technique (attenuated total reflection) on Bruker Alpha FT-IR-Spektrometer. Liquid samples were measured solvent-free in a film and solid samples were pressed directly on to the IR-detector window. Adsorption bands are given in wave numbers (cm^{-1}) and were measured in the range from $7500 - 375\text{ cm}^{-1}$ (wavelength $1.3 - 27\text{ nm}$).

Viscosimetry:

Rheological properties of the samples were measured by RheoStress 1 with CR-Mode (controlled rate mode) at 25.00 °C. All measurements were performed in neat conditions using cone plate "C35/1° Ti

L" from Thermo Scientific. Instrument was calibrated with Thermo Scientific S1000 and S100000. Each measurement consisted of 10 single measurements, whereas the average is calculated.

DSC (Differential Scanning Calorimetry):

Thermal properties were determined with a differential scanning calorimetry DSC 1 STARe System (400 W) from Mettler Toledo. A FRS5 sensor and the dynamic temperature system IntraCooler TC100 RC from HUBER were used. For all measurements sample pans with pin and lid were employed. As reference an empty sample pan was used. The lid was penetrated with a needle and the pan was closed through cold welding. The measurements were performed at atmospheric pressure under inert conditions. For each sample, one full heating and cooling cycle was measured prior to the actual measurements.

Contact angle measuring system Dataphysics OCA 40 Micro:

Contact angles were measured with instrument OCA 40 Micro from the Company DataPhysics at the department of Fluid Technology and microfluidics (University of Rostock) via sessile drop method. The samples were cured in a defined PDMS formulation during sample preparation and were measured with a defined droplet of distilled water at the beginning and after 30, 60 and 90 seconds. The parameters of the environment are not controlled, neither detected, which can cause measuring variations.

Samples from Part I are prepared following Scheme A-1 and Scheme A-2, whereas samples from Part II are only prepared following Scheme A-2.

Hazen Factor and Yellowness Index:

The color values were measured with a LCS III from BYK. The LCS III is a VIS spectrophotometer with a wavelength range of 320 to 1100 nm. The Hazen color value (ISO 6271, also known as "AHPA-method" or Platinum-Cobalt Scale) is defined as mg of platinum per 1 liter of solution. The Yellowness Index is calculated and displayed in accordance with ASTM D 1925 for illuminant C and a 2 ° standard observer. The instrument was calibrated with distilled water.

Anti-Adhesion Assay:

The Anti-Adhesion Assay is a test method to determine the adhesive properties of a sealant surface towards fungal cells. The method can be used with either yeast cells or mold spores. The utilized strain is *Exophiala dermatitidis* (isolate). The Assay was done and recorded by the microbiological department of the Henkel Corporation in Dusseldorf. Each sample (solid aggregation state) is cut into 20x20mm pieces and put in a standard six-well plate (s. Figure A-1). The wells were filled with cell suspension ensuring that the specimens were completely overlaid. The plates were incubated at RT for 60 min to let cells sediment and adhere to the surface. After the sedimentation and adhesion phase, the test surfaces are washed and the remaining cells are washed and counted by means of plating on culture medium.

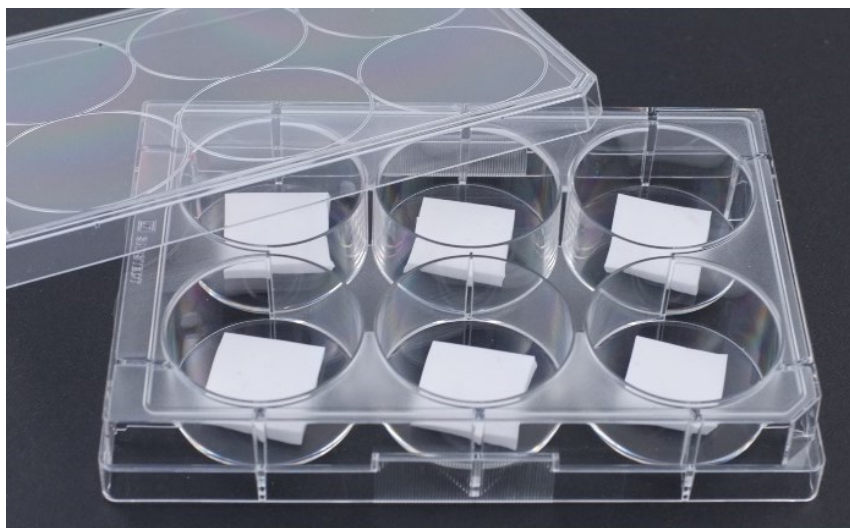


Figure A-1: Standard six-well plate with test material for the Anti-Adhesion Assay; the picture is adapted from Henkel Corporation Dusseldorf (microbiological department).

Kirby-Bauer Test (Zone of inhibition):

The Kirby-Bauer Test is also known as Agar Diffusion Test and can be used for determination of antimicrobial activity in combination with diffusion properties.^[128] The utilized strains are *Aspergillus brasiliensis* (ATCC 16404), *Staphylococcus aureus* (ATCC 6538) and *Exophiala dermatitidis* (isolate). The Kirby-Bauer Test was done and recorded by the microbiological department of the Henkel Corporation in Dusseldorf.

A suspension of the bacterial or fungal strain of interest is spread evenly over the face of a sterile agar plate. The antimicrobial test substrate (preferential liquid aggregation state) is applied to the center of the agar plate onto a small filter paper. The agar plate is incubated for a defined time at a temperature suitable for the test microorganisms. The evaluation of the Kirby-Bauer Test is shown in Figure A-2. If the test substrate leaches from the filter paper into the agar and it further contains antimicrobial activity, a zone of inhibition is formed around the filter paper.

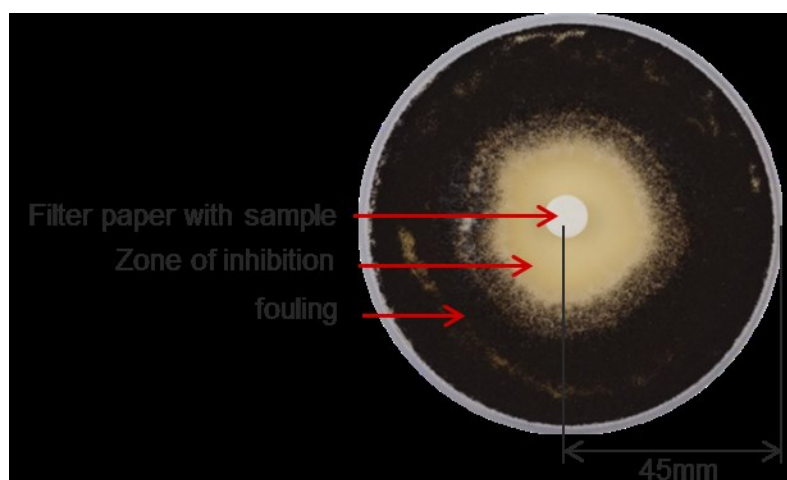


Figure A-2: Illustration of the Kirby-Bauer Test and its evaluation; the picture is adapted from Henkel Corporation Dusseldorf (microbiological department).

Minimum Inhibitory Concentration (MIC).^[47]

The MIC is an antimicrobial testing method to detect the lowest concentration of an antimicrobial agent that prevents visible growth of bacteria or molds. The utilized strains are *Candida albicans* (ATCC 10231), *Staphylococcus aureus* (ATCC 6538) and *Pseudomonas aeruginosa* (DSMZ 939). The MIC was done and recorded by the microbiological department of the Henkel Corporation in Dusseldorf.

The evaluation is done optically (for example see Figure A-3). The antimicrobial activity is given when the solution is still clear. The concentrations appear from a serial dilution.

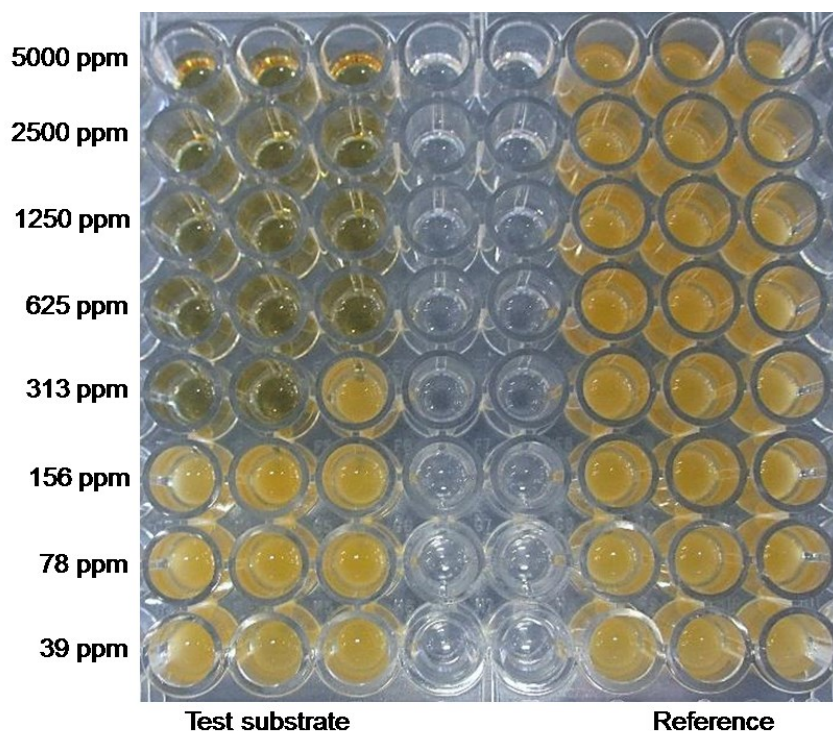


Figure A-3: Test equipment with test substrate (left) and reference (right) for the MIC; clear vials represent concentrations, in which the test substrate is antimicrobial active; the picture is adapted from Henkel Corporation Dusseldorf (microbiological department).

ISO 22196:2011.^[48]

ISO 22196:2011 (Measurement of antibacterial activity on plastics and other nonporous Surfaces) is an international standard test method and was done and recorded by the microbiological department of the Henkel Corporation in Dusseldorf. The utilized strain is *Exophiala dermatitidis* (isolate).

A2. Materials

Unless otherwise indicated, all reagents were obtained from commercial suppliers and were used without further purification. The solvents were used as commercial p.a. and HPLC quality.

Following solvents were purchased from Acros Organics and utilized for synthetic, storage or stabilization purposes: acetone, acetonitrile, benzene, chloroform, dimethylformamide (DMF), dimethylsulfoxide (DMSO), ethanol, ethyl acetate, methanol, n-heptane, n-hexane, pentane, tetrahydrofuran (THF), dried THF (stored over molecular sieves), toluene, dried toluene (stored over molecular sieves).

The deuterated solvents chloroform, DMSO and methanol were ordered from Deutero and Eurisotop.

Allyl cyanide, dioctyltin dilaurate (DOTL), 1,3,5,7-Tetramethylcyclotetrasiloxane (D^H_4) and platinum-divinyltetramethyldisiloxane complex in xylene (2.1-2.4 % Pt, trade name Karstedt), were purchased from ABCR.

Activated charcoal, bromobutane, ϵ -caprolactone, 1-methyl-1*H*-imidazole, platinum (10% supported on charcoal, in short Pt@C), pyridine, tetrahydropyran (THP), and thiolane were ordered from Alfa Aesar.

Allylchloride, 1-butyl-1*H*-imidazole, hexamethylene oxide (Oxepane), palladium(II)chloride ($PdCl_2$) and trimethylamine (~28 % ~4.3 mol/L in water) were obtained from TCI Chemicals.

Allylbromide, 3-bromo-1-phenyl-1-propene, celite® S filter aid, chlorobutane and trimethylamine were purchased from Sigma Aldrich.

The PPG references Acclaim® 6300, Acclaim® 8200 and Acclaim® 12200 were purchased from Covestro.

Propylene oxide was ordered from Acros Organics.

3-Isocyanatopropyltrimethoxysilane (trade name Geniosil GF40) was obtained from Wacker Silicones.

Double metal-cyanide complex (DMC), toluene-2,4-diisocyanate (TDI) and the linear PDMS standard formulation were provided by Henkel Corporation Dusseldorf.

1,3,3',5,5',7,7'-Heptamethylcyclotetrasiloxane (D_3D^H)^[138] and 1-(allyloxy)propan-2-ol were synthesized in our own laboratories.^[139]

PHMS starting materials:

Trimethylsilylterminated poly(methylhydro)siloxane (ca. 1900 g/mol, short: SM-100)) was purchased from Alfa Aesar, trimethylsilylterminated (15-18% methylhydrosiloxane)-dimethylsiloxane copolymer (ca. 2900 g/mol, short: SM-15), trimethylsilylterminated (25-35% methylhydrosiloxane)-dimethylsiloxane copolymer (ca. 3800 g/mol, short: SM-25) and trimethylsilylterminated (50-55% methylhydrosiloxane)-dimethylsiloxane copolymer (ca. 2200 g/mol, short: SM-50) were purchased from ABCR.

The PHMS starting materials contain dimethylsiloxane units in the backbone, as well as hydridomethylsiloxane units (SiH). The ratio between SiH groups and Si-CH₃ groups can be varied (Table A-1).

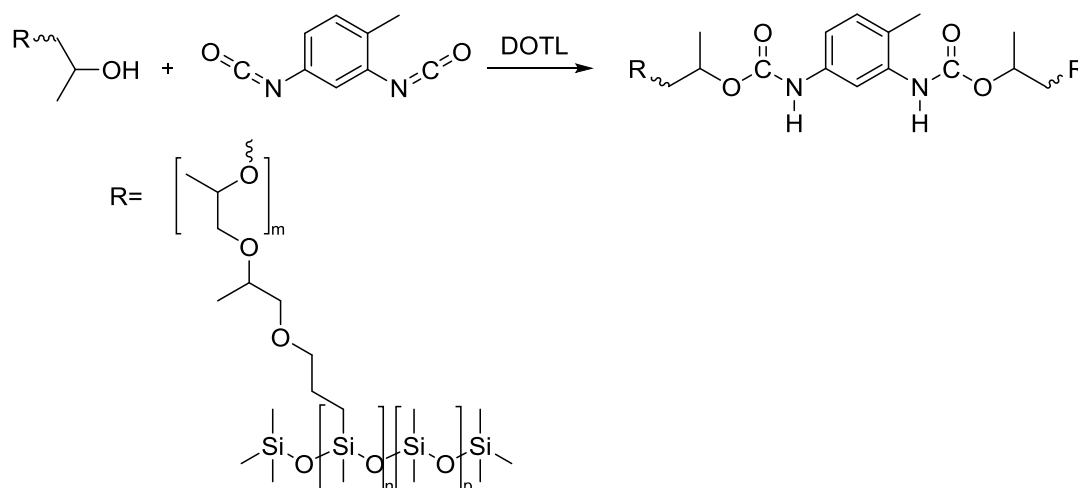
Table A-1: Summary of the PHMS starting materials; the molecular masses, viscosities and ratio of hydridomethyl siloxane units and dimethyl siloxane units in different polysiloxane is given; the numbers are calculated by the molecular mass and arithmetically averaged.

Type PHMS	Hydridomethyl siloxane units	Dimethyl siloxane units	Mn [g/mol]	Viscosity [mPas]
SM-100	29.0	0	1900	0.021
SM-50	15.2	15.2	2200	0.013
SM-25	18.2	34.3	3800	0.025
SM-15	6.7	31.4	2900	0.024

Sample preparation:

A: Curing of Polysiloxane Polyalkyleneglycol Brush Copolymers with Toluol-2,4-diisocyanat (TDI):

The homogeneous curing of polysiloxane polyalkyleneglycol brush copolymers with TDI is shown in Scheme A-1. It is a polyaddition in which urethane groups are formed by the reaction of the NCO-group of TDI and the secondary OH-group of the sample. The polyaddition is catalyzed by 1 wt-% of dioctyltin dilaurate (DOTL). The amount of TDI is calculated so, that at least one but maximally two OH-groups of a polymer are reacted to keep free brush-like polymer arms. After mixing under argon atmosphere, the sample is cured at 70 °C.

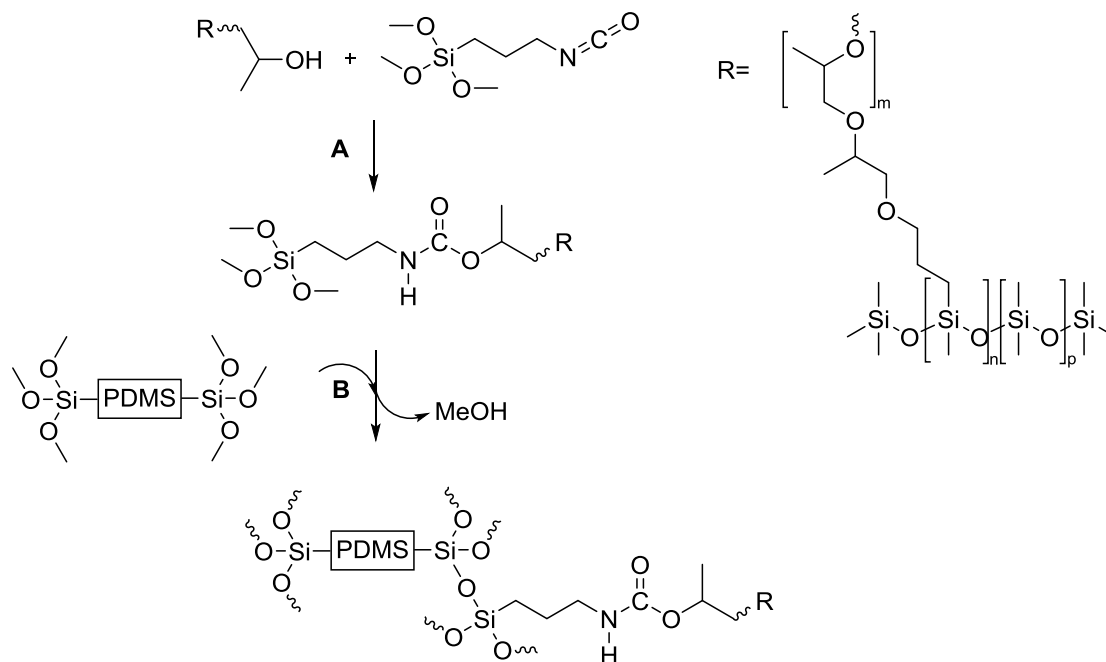


Scheme A-1: Curing of Polysiloxane Polyalkyleneglycol Brush Copolymers via polyurethane synthesis.

B: Curing of Polysiloxane Polyalkyleneglycol embedded in standard PDMS formulation:

The curing of polysiloxane polyalkyleneglycol brush copolymers with 3-isocyanatopropyltrimethoxysilane (Geniosil GF40) embedded in a standard PDMS formulation is shown in Scheme A-2. In step A the secondary OH-group forms a urethane group with the Geniosil

GF40 to get trimethoxysilyl terminated polymers. The amount of Geniosil GF 40 is calculated so, that at least one but maximally two OH-groups of a polymer are reacted to keep free brush-like polymer arms. The curing is a polycondensation reaction (step B) between the linear PDMS standard and the polymer sample. It is catalyzed by 1 wt-% of DOTL. The amount of polymer sample in the PDMS formulation ranges from 0.5 to 80 wt-%. Unless otherwise indicated, 10 wt-% are utilized. The mixture is spread on a clear film with an area around 10x10cm and cured at RT for several days.



Scheme A-2: Curing of Polysiloxane Polyalkyleneglycol Brush Copolymers via polyurethane synthesis (A) and consecutive polycondensation (B) embedded in standard PDMS formulation.

A3. Appendix to Part I

Synthesis of full-converted Polysiloxane Propyleneglycol Copolymers:

Table A-2: Summary of the products **3.1a** to **3.3a**; unless otherwise indicated, the desired conversion is 100% and the general reaction time is 24 hours; the yields are calculated from the average of several experiments.

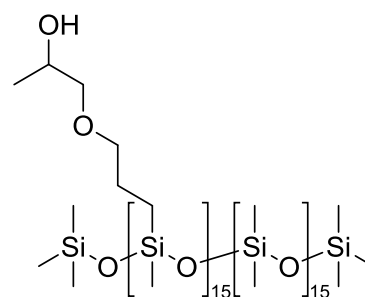
Sample	Starting Material	Catalyst	PPG [wt-%]	Conversion [%]	Isolated Yield [%]	Viscosity [Pas]
3.1a	SM-50	Karstedt	44.5	>99	55 - 80	1.474 ± 0.626
3.1b		Pt@C		81	32	0.711
3.2a	SM-25	Karstedt	35.7	>99	80 - 90	0.630
3.2b		Pt@C		84	46	0.368
3.3a	SM-15	Karstedt	21.1	>99	80 - 99	0.291 ± 0.091
3.3b		Pt@C		85	55	0.095

Synthesis of poly(3-(2-hydroxypropoxy)propyl)methylsiloxane-co-polydimethylsiloxane (3.1a):**Representative procedure A:**

0.1 mol% Karstedt (2 % of Pt in the catalyst) compared to siloxane starting material and 30 mL toluene were added into the evacuated flask and stirred at room temperature (20°C) for a couple of minutes under argon atmosphere. 2.16 mL 1-(allyloxy)propan-2-ol (17.05 mmol) and 2.49 mL SM-50 (1.14mmol) were added dropwise. The mixture was stirred and refluxed (oil bath temperature: 120 °C) under inert atmosphere (Ar) until complete conversion of the Si-H groups was achieved (the reaction was followed by ¹H-NMR). The mixture (when necessary) was decolorized by adding activated carbon and an excess of pentane and stirred for 16 h at room temperature. The crude was filtrated trough celite, and the solvents and volatiles were filtered off using Schlenk technique. The obtained product (yield 55 – 80 %) was a colorless, transparent viscous liquid.

¹H-NMR (300 MHz, CDCl₃, 24 °C, ppm) δ = 3.91 – 3.86 (m, 1H, O-CH₂-CH(CH₃)-OH), 3.39 – 3.32 (m, 3H, CH₂-O-CH₂-CH(CH₃)-OH), 3.19 – 3.14 (t, 1H, -O-CH₂-CH-), 2.93 (s, 1H, -OH), 1.62 – 1.56 (p, 2H, -Si-CH₂-CH₂-), 1.09 – 1.07 (d, 3H, CH₃-CH-), 0.49 – 0.44 (t, 2H, -Si-CH₂-), 0.04 – 0.02 (s, 3H, -Si-CH₃). **¹³C-NMR** (300 MHz, CDCl₃, 24 °C, ppm) δ = 76.82 (-O-CH₂-CH-), 74.25 (-Si-CH₂-CH₂-CH₂-), 66.65 (-O-CH₂-CH-), 23.49 (-Si-CH₂-CH₂-), 19.00 (CH₃-CH-), 13.79 (-Si-CH₂-), 1.49 (-Si-CH₃).

²⁹Si-NMR (300 MHz, CDCl₃, 24 °C, ppm): δ = 7.43 (-Si(CH₃)₃), -21.49 – -22.80 (O-Si-O). **EA** (% , measured (calculated)), repeating unit C₉H₂₂O₄Si₂: C 41.68 (34.71), H 9.248 (8.93), Si 13.75 (37.87). **IR** (ATR, 32 scans, cm⁻¹): 3427.7, 2961.3, 1411.5, 1374.0, 1257.8, 1009.3, 908.5, 841.1, 793.3, 685.9. **GPC** (THF, 40 °C, g/mol): M_n=5017, M_w=6157, PDI=1.666.



Synthesis of poly(3-(2-hydroxypropoxy)propyl)methylsiloxane-co-polydimethylsiloxane (3.1b):

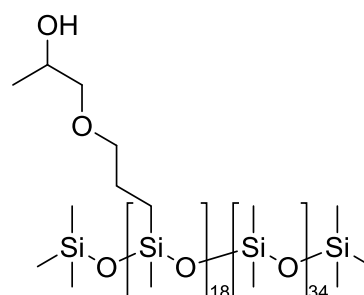
Product **3.1b** was synthesized (32 % yield) according to the representative procedure A, using 0.5 mol% Pt supported on charcoal compared to siloxane starting material (10 % of Pt in the catalyst) and 10mL toluene. The mixture was stirred for 24hours (oil bath temperature: 90 °C) under inert atmosphere (Ar). 81 % conversion was obtained.

¹H-NMR (300 MHz, CDCl₃, 24 °C, ppm) δ = 4.69 – 4.67 (s, 1H, SiH), 3.96 – 3.90 (m, 1H, O-CH₂-CH(CH₃)-OH), 3.44 – 3.35 (m, 3H, CH₂-O-CH₂-CH(CH₃)-OH), 3.23 – 3.17 (t, 1H, -O-CH₂-CH-), 2.77 (s, 1H, -OH), 1.67 – 1.56 (p, 2H, -Si-CH₂-CH₂-), 1.13 – 1.11 (d, 3H, CH₃-CH-), 0.53 – 0.47 (t, 2H, -Si-CH₂-), 0.11 – 0.03 (s, 3H, -Si-CH₃). **¹³C-NMR** (300 MHz, CDCl₃, 24 °C, ppm) δ = 76.74 (-O-CH₂-CH-), 74.00 (-Si-CH₂-CH₂-CH₂-), 66.45 (-O-CH₂-CH-), 23.25 (-Si-CH₂-CH₂-), 18.71 (CH₃-CH-), 13.53 (-Si-CH₂-), 1.23 (-Si-CH₃). **²⁹Si-NMR** (300 MHz, CDCl₃, 24 °C, ppm): δ = -20.50 - -22.53 (O-Si-O), -37.57 (SiH). **EA** (% , measured (calculated)), repeating unit C₉H₂₂O₄Si₂: C 37.325 (34.71), H 8.751 (8.93), Si 13.35 (37.87). **IR** (ATR, 32 scans, cm⁻¹): 2961.6, 2150.6, 1411.7, 1374.2, 1257.9, 1010.9, 908.3, 793.0, 686.5. **GPC** (THF, 40 °C, g/mol): M_n=4065, M_w= 7390, PDI=1.819.

Synthesis of poly(3-(2-hydroxypropoxy)propyl)methylsiloxane-co-polydimethylsiloxane (3.2a):

Product **3.2a** was synthesized (80 – 90 % yield) according to the representative procedure A, using 100 mL toluene, 15.02 mL 1-(allyloxy)propan-2-ol (118.40 mmol) and 25.51 mL SM-25 (6.50 mmol).

¹H-NMR (CDCl₃, 400 MHz, 24 °C, ppm): δ = 3.93 (m, 1H, -OCH₂CH(CH₃)OH), 3.39 (m, 3H, -CH₂OCH₂CHOH), 3.19 (m, 2H, -OCH₂CH(CH₃)OH), 2.73 (s, 1H, -OH), 1.61 (m, 2H, -SiCH₂CH₂CH₂O), 1.12(m, 3H, -OCH₂CH(CH₃)OH), 0.50 (m, 2H, -SiCH₂CH₂O), 0.05 (m, 3H, -SiCH₃). **¹³C-NMR** (CDCl₃, 300 MHz, 25 °C, ppm): δ = 72.29 (t, OCH₂CH(CH₃)OH), 72.85 (s, -CH₂OCH₂), 65.27 (s, -OCH₂CH(CH₃)OH), 26.28 (s, -SiCH₂CH₂O), 17.52 (s, -CH₂CH(CH₃)OH), 6.94 (s, -SiCH₂CH₂O), 0.00 (s, Si-CH₃). **²⁹Si-NMR** (CDCl₃, 400 MHz, 24°C, ppm): δ = 7.27 (s, Si-CH₃), -21.91 (s, O-Si-O). **IR** (ATR, 32 scans, cm⁻¹): 3431.7, 2961.5, 1412.2, 1257.7, 1008.8, 842.1, 791.4, 686.1. **EA** (% , measured (calculated)), repeating unit C₁₁H₂₈O₅Si₃: C 35.53 (35.63), H 7.693 (9.24), Si 15.57 (37.78). **GPC** (THF, 40 °C, g/mol): M_n=5261, M_w=11506, PD=2.187.

Synthesis of poly(3-(2-hydroxypropoxy)propyl)methylsiloxane-co-polydimethylsiloxane (3.2b):

Product **3.2b** was synthesized (46 % yield) according to the representative procedure A, using 0.5 mol% Pt supported on charcoal compared to siloxane starting material (10 % of Pt in the catalyst), 10 mL toluene, 1.42 mL 1-(allyloxy)propan-2-ol (11.18 mmol) and 2.55 mL SM-25 (0.66 mmol). The mixture was stirred for 24 hours (oil bath temperature: 90 °C) under inert atmosphere (Ar). 84 % conversion was obtained.

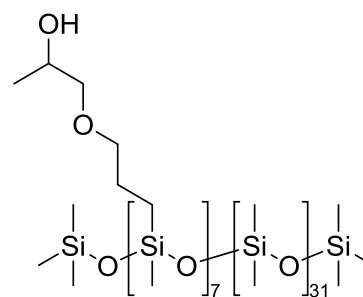
¹H-NMR (300 MHz, CDCl₃, 24 °C, ppm) δ = 4.62 – 4.61 (s, 1H, SiH), 3.92 – 3.82 (m, 1H, O-CH₂-CH(CH₃)-OH), 3.41 – 3.28 (m, 3H, CH₂-O-CH₂-CH(CH₃)-OH), 3.17 – 3.11 (t, 1H, -O-CH₂-CH-), 2.69 (s, 1H, -OH), 1.59 – 1.51 (p, 2H, -Si-CH₂-CH₂-), 1.07 – 1.05 (d, 3H, CH₃-CH-), 0.49 – 0.38 (t, 2H, -Si-CH₂-), 0.12 – 0.04 – 0.03 (s, 3H, -Si-CH₃). **¹³C-NMR** (300 MHz, CDCl₃, 24 °C, ppm) δ = 76.33 (-O-

$\underline{\text{CH}}_2\text{-CH-}$), 74.02 ($-\text{Si-CH}_2\text{-CH}_2\text{-}\underline{\text{CH}}_2\text{-}$), 66.46 ($-\text{O-CH}_2\text{-}\underline{\text{CH-}}$), 23.24 ($-\text{Si-CH}_2\text{-}\underline{\text{CH}}_2\text{-}$), 18.70 ($\underline{\text{CH}}_3\text{-CH-}$), 13.53 ($-\text{Si-}\underline{\text{CH}}_2\text{-}$), 1.49 – 0.89 ($-\text{Si-}\underline{\text{CH}}_3$). **$^{29}\text{Si-NMR}$** (300 MHz, CDCl_3 , 24 °C, ppm): δ = 7.28 ($-\underline{\text{Si}}(\text{CH})_3$), -20.53 – -22.63 (O-Si-O), -37.58 (SiH). **EA** (% , measured (calculated)), repeating unit $\text{C}_{11}\text{H}_{28}\text{O}_5\text{Si}_3$: C 36.53 (35.63), H 8.166 (9.24), Si 12.00 (37.78). **IR** (ATR, 32 scans, cm^{-1}): 2961.7, 1411.6, 1257.8, 1009.9, 910.2, 791.3, 686.9, 504.7. **GPC** (THF, 40 °C, g/mol): $M_n=5142$, $M_w=9930$, PDI=1.931.

Synthesis of poly(3-(2-hydroxypropoxy)propyl)methylsiloxane-co-polydimethylsiloxane (3.3a):

Product **3.3a** was synthesized (80 – 99 % yield) according to the representative procedure A, using 10 mL toluene, 0.72 mL 1-(allyloxy)propan-2-ol (5.64 mmol) and 2.60 mL SM-15 (0.86 mmol).

$^1\text{H-NMR}$ (400 MHz, CDCl_3 , 24 °C, ppm) δ = 3.99 – 3.89 (m, 1H, O- $\underline{\text{CH}}_2\text{-CH}(\text{CH}_3)\text{-OH}$), 3.43 – 3.38 (m, 3H, $\underline{\text{CH}}_2\text{-O-CH}_2\text{-CH}(\text{CH}_3)\text{-OH}$), 3.22 – 3.17 (t, 1H, -O- $\underline{\text{CH}}_2\text{-CH-}$), 2.47 (s, 1H, -OH), 1.68 – 1.55 (p, 2H, -Si- $\underline{\text{CH}}_2\text{-CH}_2\text{-}$), 1.14 – 1.12 (d, 3H, $\underline{\text{CH}}_3\text{-CH-}$), 0.53 – 0.47 (t, 2H, -Si- $\underline{\text{CH}}_2\text{-}$), 0.12 – 0.04 (s, 3H, -Si- $\underline{\text{CH}}_3$). **$^{13}\text{C-NMR}$** (400 MHz, CDCl_3 , 24 °C, ppm) δ = 76.33 ($-\text{O-}\underline{\text{CH}}_2\text{-CH-}$), 74.05 ($-\text{Si-CH}_2\text{-CH}_2\text{-}\underline{\text{CH}}_2\text{-}$), 66.52 ($-\text{O-CH}_2\text{-}\underline{\text{CH-}}$), 23.28 ($-\text{Si-CH}_2\text{-}\underline{\text{CH}}_2\text{-}$), 18.69 ($\underline{\text{CH}}_3\text{-CH-}$), 13.55 ($-\text{Si-}\underline{\text{CH}}_2\text{-}$), 1.25 ($-\text{Si-}\underline{\text{CH}}_3$). **$^{29}\text{Si-NMR}$** (400 MHz, CDCl_3 , 24 °C, ppm): δ = 7.24 ($-\underline{\text{Si}}(\text{CH})_3$), -21.43 – -22.73 (O-Si-O). **EA** (% , measured (calculated)), repeating unit $\text{C}_{17}\text{H}_{46}\text{O}_8\text{Si}_6$: C 37.095 (37.32), H 8.3385 (8.48), Si 12.457 (30.8). **IR** (ATR, 32 scans, cm^{-1}): 2961.29, 2903.26, 1411.55, 1257.49, 1012.39, 841.41, 793.33, 686.78. **GPC** (THF, 40 °C, g/mol): $M_n=4933$, $M_w=10584$, PDI=2.677.



Synthesis of poly(3-(2-hydroxypropoxy)propyl)methylsiloxane-co-polydimethylsiloxane (3.3b):

Product **3.3b** was synthesized (55 % yield) according to the representative procedure A, using 0.5 mol% Pt supported on charcoal compared to siloxane starting material (10 % of Pt in the catalyst), 10 mL toluene, 0.72 mL 1-(allyloxy)propan-2-ol (5.64 mmol) and 2.60 mL SM-15 (0.86 mmol). The mixture was stirred for 24 hours (oil bath temperature: 90 °C) under inert atmosphere (Ar). 85 % conversion was obtained.

$^1\text{H-NMR}$ (400 MHz, CDCl_3 , 24 °C, ppm) δ = 4.70 – 4.67 (s, 1H, SiH), 3.98 – 3.90 (m, 1H, O- $\underline{\text{CH}}_2\text{-CH}(\text{CH}_3)\text{-OH}$), 3.42 – 3.37 (m, 3H, $\underline{\text{CH}}_2\text{-O-CH}_2\text{-CH}(\text{CH}_3)\text{-OH}$), 3.22 – 3.17 (t, 1H, -O- $\underline{\text{CH}}_2\text{-CH-}$), 2.45 (s, 1H, -OH), 1.66 – 1.59 (p, 2H, -Si- $\underline{\text{CH}}_2\text{-CH}_2\text{-}$), 1.13 – 1.11 (d, 3H, $\underline{\text{CH}}_3\text{-CH-}$), 0.53 – 0.48 (t, 2H, -Si- $\underline{\text{CH}}_2\text{-}$), 0.14 – 0.04 (s, 3H, -Si- $\underline{\text{CH}}_3$). **$^{13}\text{C-NMR}$** (400 MHz, CDCl_3 , 24 °C, ppm) δ = 76.36 ($-\text{O-}\underline{\text{CH}}_2\text{-CH-}$), 74.06 ($-\text{Si-CH}_2\text{-CH}_2\text{-}\underline{\text{CH}}_2\text{-}$), 66.52 ($-\text{O-CH}_2\text{-}\underline{\text{CH-}}$), 23.29 ($-\text{Si-CH}_2\text{-}\underline{\text{CH}}_2\text{-}$), 18.72 ($\underline{\text{CH}}_3\text{-CH-}$), 13.57 ($-\text{Si-}\underline{\text{CH}}_2\text{-}$), 1.18 ($-\text{Si-}\underline{\text{CH}}_3$). **$^{29}\text{Si-NMR}$** (400 MHz, CDCl_3 , 24 °C, ppm): δ = 7.30 ($-\underline{\text{Si}}(\text{CH})_3$), -20.50 – -22.64 (O-Si-O), -37.52 (SiH). **EA** (% , measured (calculated)), repeating unit $\text{C}_{17}\text{H}_{46}\text{O}_8\text{Si}_6$: C 33.02 (37.32), H 8.0985 (8.48), Si 10.175 (30.8). **IR** (ATR, 32 scans, cm^{-1}): 2961.7, 1412.2, 1257.6, 1010.1, 910.7, 789.4, 686.5, 505.1. **GPC** (THF, 40 °C, g/mol): $M_n=3930$, $M_w=6215$, PDI=1.581.

Synthesis of full-converted Polysiloxane Polypropyleneglycol Copolymers:**Table A-3:** Summary of the products **3.4** to **3.32**; starting material, PPG wt-%, theoretically and experimental monomer unit, isolated yield and the Viscosity are listed; the yields are calculated from the average of several experiments.

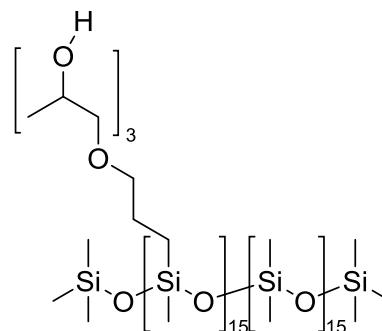
Sample	Starting Material	PPG [wt-%]	Monomer Unit (theor.)	Monomer Unit (exp.)	Isolated Yield [%]	Viscosity [Pas]
3.4	3.1a	64.9	2.61	2.89 ± 0.071	80 - 95	2.231 ± 0.6215
3.5		74.3	5.22	5.24	95	3.024
3.6		79.8	7.82	9.83 ± 3.465	93 - 97	9.342 ± 5.7926
3.7		83.3	10.43	11.15 ± 2.383	80 - 95	9.179 ± 0.4731
3.8	3.2a	59.3	3.25	3.61 ± 0.283	90 - 95	0.748 ± 0.1082
3.9		70.3	6.50	7.43 ± 0.177	90 - 97	1.348 ± 0.1655
3.10		76.6	9.75	10.51 ± 0.403	95 - 96	1.395 ± 0.1513
3.11		80.7	13.00	13.95 ± 0.099	93 - 95	1.938 ± 2.1397
3.12	3.3a	27.2	1.78	1.80 ± 0.064	91 - 94	0.269 ± 0.0183
3.13		32.4	2.57	2.18 ± 0.088	91 - 92	0.549 ± 0.0194
3.14		36.9	3.35	2.84 ± 0.057	89	0.494 ± 0.3354
3.15		40.8	4.14	4.25 ± 0.460	87 - 92	0.330 ± 0.0463
3.16		44.3	4.92	4.19 ± 0.240	89 - 94	1.271 ± 0.0574
3.17		47.4	5.71	5.76 ± 0.028	87 - 92	1.769 ± 0.3810
3.18		50.1	6.49	6.13 ± 0.910	76 - 99	1.579 ± 0.9912
3.19		58.8	9.63	9.47 ± 0.057	90 - 91	3.180 ± 1.0607
3.20		63.5	11.98	10.97 ± 0.603	80 - 92	1.863 ± 1.0428
3.21		67.3	14.33	14.24 ± 0.141	87 - 92	2.234 ± 0.2297
3.22		71.3	17.47	19.04 ± 0.027	66 - 98	6.520 ± 2.8281
3.23		73.6	19.82	19.96 ± 0.672	83 - 88	4.595 ± 0.8652
3.24		76.3	22.96	24.30 ± 0.759	86 - 96	3.461 ± 0.6107
3.25		77.9	25.31	28.13 ± 3.804	84 - 94	1.841 ± 0.8813
3.26		80.6	30.02	34.67 ± 5.339	80 - 90	12.665 ± 10.6985
3.27		81.7	32.37	37.28 ± 2.942	83 - 92	2.600
3.28		85.6	43.35	46.16 ± 0.021	91	16.735 ± 3.3022
3.29		88.1	54.33	53.18 ± 6.307	90 - 94	8.095 ± 5.8902
3.30		89.9	65.31	67.95 ± 4.511	89 - 90	22.590 ± 17.7342
3.31		91.2	76.29	80.02 ± 7.616	90 - 92	14.775 ± 14.6442
3.32		92.2	87.28	98.94 ± 13.782	91 - 93	11.930 ± 2.3617

Synthesis of poly((hydroxyl)-polypropyleneglycol)methylsiloxane-co-polydimethylsiloxane (3.4):

Representative procedure B:

5.0 g of **3.1a** (1.27 mmol) were mixed together with 500 ppm DMC catalyst referring to the OH-number in starting material and 20 g heptane in a 100 mL- stirring Autoclave. The reaction mixture was stirred at room temperature with constant stirring at 350 RPM for several minutes under vacuum (0.001 bar) and argon atmosphere (1 bar). Reaction temperature was increased to 110 °C and after reaching this, 3.5 mL of propylene oxide (50.02 mmol) were added to the reaction mixture and stirred constantly at 350 RPM until reaction takes place. After cooling down, solvent and volatile contents were filtered off using Schlenk technique. The obtained product (yield 80 - 95 %) was a white, milky, viscous liquid.

¹H-NMR (CDCl₃, 400 MHz, 24 °C, ppm): δ = 3.96 – 3.89 (m, 2H, first monomer unit OCH₂CH(CH₃)OH), 3.72 – 3.49 (m, 3H, CH₂-O-CH₂-CH(CH₃)-OH), 3.55 – 3.49 (m, 2H, side-chain -O-CH₂-CH-), 3.44 – 3.33 (m, 2H, side-chain -OCH₂CH(CH₃)OH), 3.20 - 3.17 (m, 2H, first monomer unit -OCH₂CH(CH₃)OH), 1.96 (s, 1H, OH), 1.61 (m, 2H, -SiCH₂CH₂CH₂O), 1.20 – 1.18 (d, 3H, first monomer unit CH₃-CH-), 1.11 (m, 3H, side-chain -OCH₂CH(CH₃)OH), 0.53 (m, 2H, -SiCH₂CH₂O), 0.06 (m, 3H, -SiCH₃). **¹³C-NMR** (CDCl₃, 300 MHz, 25 °C, ppm): δ = 76.08 (-Si-CH₂-CH₂-CH₂-), 74.43 (side-group -O-CH₂-CH-), 73.94 (side-chain -O-CH₂-CH-), 73.46 (first monomer unit -O-CH₂-CH-), 66.87 (first monomer unit -OCH₂CH(CH₃)OH), 23.63 (-SiCH₂CH₂O), 18.03 (first monomer unit -CH₂CH(CH₃)OH), 17.90 (side-chain CH₃-CH-), 14.06 (-SiCH₂CH₂O), 1.23 (Si-CH₃). **²⁹Si-NMR** (CDCl₃, 400 MHz, 24 °C, ppm): δ = 2.92(s, Si-CH₃), -21.90 (O-Si-O). **EA** (% , measured (calculated)), C₁₈H₄₆O₆Si₄: C 46.96 (45.91), H 9.10 (9.85), Si 12.46 (23.86). **IR** (ATR, 32 scans, cm⁻¹): 2965.3, 2869.8, 1453.7, 1373.8, 1258.3, 1082.1, 1010.9, 907.4, 841.0, 795.0, 687.2. **GPC** (THF, 40 °C, g/mol): M_n=3737, M_w=17114, PDI=6.319.



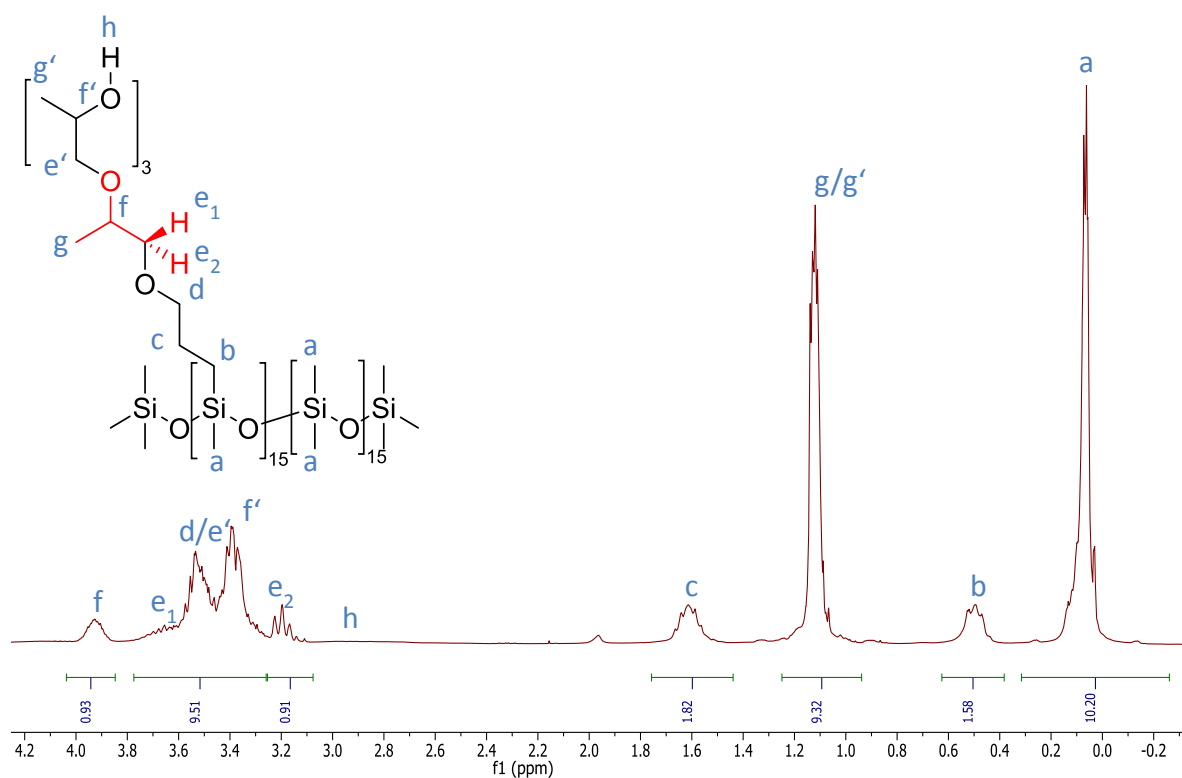


Figure A-4: ^1H -NMR of **3.4** in deuterated chloroform (400 MHz, 24 °C); the separated signals from the first monomer unit are shown.

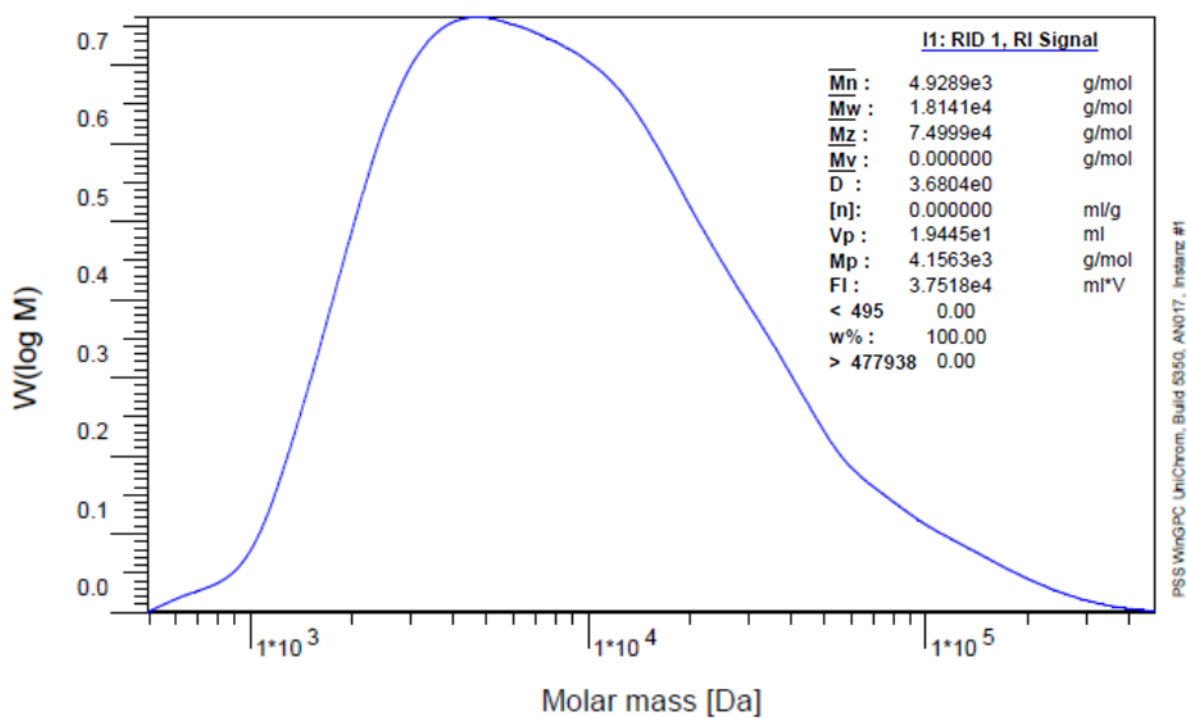


Figure A-5: GPC result of **3.4** in THF (shown GPC results are an average of two measurements).

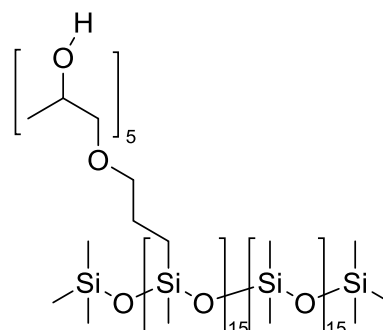
Synthesis of poly((hydroxyl)-polypropyleneglycol)methylsiloxane-co-polydimethylsiloxane (3.5):

Product **3.5** was synthesized (95 % yield) according to the representative procedure B, using 7.0 mL of propylene oxide (100.03 mmol).

¹H-NMR (CDCl₃, 400 MHz, 24 °C, ppm): δ = 4.67 (s, 1H, -SiH), 3.95 – 3.90 (m, 2H, OCH₂CH(CH₃)OH), 3.73 – 3.64 (m, 3H, CH₂-O-CH₂-CH(CH₃)-OH), 3.55 – 3.50 (m, 2H, -O-CH₂-CH-), 3.40 – 3.37 (m, 2H, -OCH₂CH(CH₃)OH), 3.20 (m, 2H, -OCH₂CH(CH₃)OH), 1.19 (s, 1H, OH), 1.61 (m, 2H, -SiCH₂CH₂CH₂O), 1.28 (m, 3H, CH₃-CH-), 1.11 (d, 3H, -OCH₂CH(CH₃)OH), 0.50 (m, 2H, -SiCH₂CH₂O), 0.06 (m, 3H, -SiCH₃).

¹³C-NMR (CDCl₃, 300 MHz, 25 °C, ppm): δ = 75.64 (-Si-CH₂-CH₂-CH₂-), 74.00 (-O-CH₂-CH-), 73.52 (-O-CH₂-CH-), 73.02 (-O-CH₂-CH-), 66.43 (-OCH₂CH(CH₃)OH), 23.30 (-SiCH₂CH₂O), 18.70 (-CH₂CH(CH₃)OH), 17.61 (CH₃-CH-), 13.52 (-SiCH₂CH₂O), 1.26 (Si-CH₃).

²⁹Si-NMR (CDCl₃, 400 MHz, 24 °C, ppm): δ = 7.50 (Si-CH₃), -21.91 (O-Si-O). **EA** (% , measured (calculated)), C₅₉H₁₂₈O₂₀Si₄: C 46.96 (55.80), H 9.10 (10.16), Si 12.46 (8.85). **IR** (ATR, 32 scans, cm⁻¹): 3455.6, 2968.6, 2868.2, 1453.5, 1372.8, 1258.8, 1086.2, 1012.3, 926.6, 841.5, 798.7, 686.2. **GPC** (THF, 40 °C, g/mol): M_n=5124, M_w=14364, PDI=2.804.

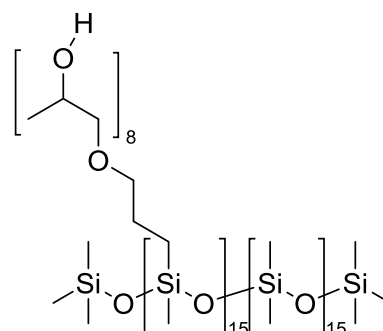
Synthesis of poly((hydroxyl)-polypropyleneglycol)methylsiloxane-co-polydimethylsiloxane (3.6):

Product **3.6** was synthesized (93 - 97% yield) according to the representative procedure B, using 10.5 mL of propylene oxide (150.05 mmol).

¹H-NMR (CDCl₃, 400 MHz, 24 °C, ppm): δ = 3.95 – 3.92 (m, 2H, OCH₂CH(CH₃)OH), 3.71 – 3.66 (m, 3H, CH₂-O-CH₂-CH(CH₃)-OH), 3.57 – 3.47 (m, 2H, -O-CH₂-CH-), 3.41 – 3.36 (m, 2H, -OCH₂CH(CH₃)OH), 3.20 (m, 2H, -OCH₂CH(CH₃)OH), 1.82 (s, 1H, OH), 1.62 (m, 2H, -SiCH₂CH₂CH₂O), 1.28 (m, 3H, CH₃-CH-), 1.13 (m, 3H, -OCH₂CH(CH₃)OH), 0.50 (m, 2H, -SiCH₂CH₂O), 0.06 (m, 3H, -SiCH₃).

¹³C-NMR (CDCl₃, 300 MHz, 25 °C, ppm): δ = 75.66 (-Si-CH₂-CH₂-CH₂-), 75.25 (-O-CH₂-CH-), 73.53 (-O-CH₂-CH-), 73.03 (-O-CH₂-CH-), 66.47 (-OCH₂CH(CH₃)OH), 23.31 (-SiCH₂CH₂O), 18.70 (-CH₂CH(CH₃)OH), 17.61 (CH₃-CH-), 13.59 (-SiCH₂CH₂O), 1.21 (Si-CH₃).

²⁹Si-NMR (CDCl₃, 400 MHz, 24 °C, ppm): δ = 7.29 (Si-CH₃), -21.93 (O-Si-O). **EA** (% , measured (calculated)), C₅₉H₁₂₈O₂₀Si₄: C 52.67 (52.77), H 9.36 (10.09), Si 6.77 (13.71). **IR** (ATR, 32 scans, cm⁻¹): 2969.1, 2867.8, 1453.1, 1372.8, 1343.8, 1296.5, 1259.2, 1087.3, 1013.4, 908.4, 799.4, 666.5. **GPC** (THF, 40 °C, g/mol): M_n=8080, M_w=35076.0, PDI=4.278.



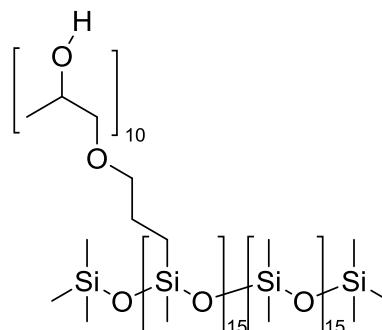
Synthesis of poly((hydroxyl)-polypropyleneglycol)methylsiloxane-co-polydimethylsiloxane (3.7):

Product **3.7** was synthesized (95 % yield) according to the representative procedure B, using 14.0 mL of propylene oxide (200.07 mmol).

¹H-NMR (CDCl₃, 400 MHz, 24 °C, ppm): δ = 3.96 – 3.88 (m, 2H, OCH₂CH(CH₃)OH), 3.73 – 3.60 (m, 3H, CH₂-O-CH₂-CH(CH₃)-OH), 3.55 – 3.47 (m, 2H, -O-CH₂-CH-), 3.43 – 3.32 (m, 2H, -OCH₂CH(CH₃)OH), 3.20 (m, 2H, -OCH₂CH(CH₃)OH), 1.91 (s, 1H, OH), 1.62 (m, 2H, -SiCH₂CH₂CH₂O), 1.34 – 1.30 (m, 3H, CH₃-CH-), 1.14 (m, 3H, -OCH₂CH(CH₃)OH), 0.50 (m, 2H, -SiCH₂CH₂O), 0.06 (m, 3H, -SiCH₃).

¹³C-NMR (CDCl₃, 300 MHz, 25 °C, ppm): δ = 75.64 (-Si-CH₂-CH₂-CH₂-), 74.21 (-O-CH₂-CH-), 73.51 (-O-CH₂-CH-), 73.05 (-O-CH₂-CH-

), 66.15 (-OCH₂CH(CH₃)OH), 23.03 (-SiCH₂CH₂O), 18.70 (-CH₂CH(CH₃)OH), 17.47 (CH₃-CH-), 8.18 (-SiCH₂CH₂O), 1.02 (Si-CH₃). **²⁹Si-NMR** (CDCl₃, 400 MHz, 24 °C, ppm): δ = 7.88 (Si-CH₃), -22.60 (O-Si-O). **EA** (% , measured (calculated)), C₄₂H₉₄O₁₄Si₄: C 57.01 (53.92), H 9.64 (10.13), Si 6.22 (12.01). **IR** (ATR, 32 scans, cm⁻¹): 2969.3, 2867.9, 1453.0, 1372.7, 1343.9, 1296.5, 1259.4, 1088.6, 1013.4, 925.6, 800.0, 668.4. **GPC** (THF, 40 °C, g/mol): M_n=8232, M_w=32003, PDI=3.883.

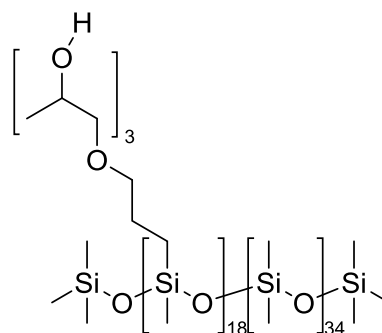
Synthesis of poly((hydroxyl)-polypropyleneglycol)methylsiloxane-co-polydimethylsiloxane (3.8):

Product **3.8** was synthesized (90 - 95% yield) according to the representative procedure B, using 5.0 g of **3.2a** (0.87 mmol) and 3.5 mL of propylene oxide (50.02 mmol).

¹H-NMR (CDCl₃, 400 MHz, 24 °C, ppm): δ = 3.95 – 3.89 (m, 2H, OCH₂CH(CH₃)OH), 3.72 – 3.64 (m, 3H, CH₂-O-CH₂-CH(CH₃)-OH), 3.58 – 3.48 (m, 2H, -O-CH₂-CH-), 3.46 – 3.33 (m, 2H, -OCH₂CH(CH₃)OH), 3.23 – 3.17 (m, 2H, -OCH₂CH(CH₃)OH), 1.60 (m, 2H, -SiCH₂CH₂CH₂O), 1.35 – 1.31 (m, 3H, CH₃-CH-), 1.11 (m, 3H, -OCH₂CH(CH₃)OH), 0.49 (m, 2H, -SiCH₂CH₂O), 0.05 (m, 3H, -SiCH₃).

¹³C-NMR (CDCl₃, 300 MHz, 25 °C, ppm): δ = 75.53 (-Si-CH₂-CH₂-CH₂-), 75.12 (-O-CH₂-CH-), 73.39 (-O-CH₂-CH-), 72.90 (-O-

CH₂-CH-), 66.15 (-OCH₂CH(CH₃)OH), 23.18 (-SiCH₂CH₂O), 18.58 (-CH₂CH(CH₃)OH), 17.48 (CH₃-CH-), 13.36 (-SiCH₂CH₂O), 1.11 (Si-CH₃). **²⁹Si-NMR** (CDCl₃, 400 MHz, 24 °C, ppm): δ = 7.52 (Si-CH₃), -21.90 (O-Si-O). **EA** (% , measured (calculated)), C₂₄H₆₀O₈Si₅: C 46.66 (46.71), H 8.87 (9.80), Si 8.55 (22.75). **IR** (ATR, 32 scans, cm⁻¹): 2965.3, 2870.1, 1453.2, 1373.6, 1258.4, 1082.5, 1009.9, 841.8, 794.6, 686.3. **GPC** (THF, 40 °C, g/mol): M_n=3470, M_w=9312, PDI=2.779.



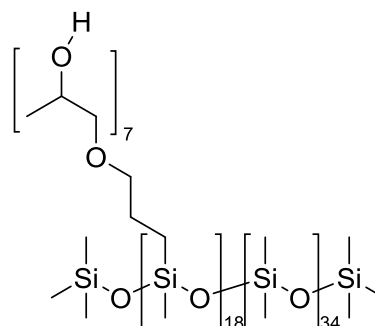
Synthesis of poly((hydroxyl)-polypropyleneglycol)methylsiloxane-co-polydimethylsiloxane (3.9):

Product **3.9** was synthesized (90 - 97% yield) according to the representative procedure B, using 5.0 g of **3.2a** (0.87 mmol) and 7.0 mL of propylene oxide (100.03 mmol).

¹H-NMR (CDCl₃, 400 MHz, 24 °C, ppm): δ = 3.93 – 3.91 (m, 2H, OCH₂CH(CH₃)OH), 3.68 (m, 3H, CH₂-O-CH₂-CH(CH₃)-OH), 3.55 – 3.50 (m, 2H, -O-CH₂-CH-), 3.40 – 3.37 (m, 2H, -OCH₂CH(CH₃)OH), 3.22 – 3.12 (m, 2H, -OCH₂CH(CH₃)OH), 2.70 (s, 1H, OH), 1.59 (m, 2H, -SiCH₂CH₂CH₂O), 1.33 (m, 3H, CH₃-CH-), 1.11 (m, 3H, -OCH₂CH(CH₃)OH), 0.48 (m, 2H, -SiCH₂CH₂O), 0.03 (m, 3H, -SiCH₃).

¹³C-NMR (CDCl₃, 300 MHz, 25 °C, ppm): δ = 73.86 (-Si-CH₂-CH₂-CH₂-), 72.22 (-O-CH₂-CH-), 71.45 (-O-CH₂-CH-), 71.52 (-O-CH₂-CH-), 64.73 (-OCH₂CH(CH₃)OH), 21.56 (-SiCH₂CH₂O), 21.45 (-CH₂CH(CH₃)OH), 16.90 (CH₃-CH-), 15.41 (-SiCH₂CH₂O), 0.68 (Si-CH₃).

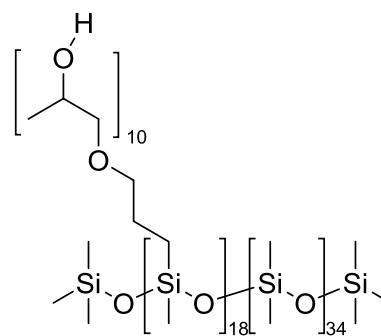
²⁹Si-NMR (CDCl₃, 400 MHz, 24 °C, ppm): δ = -6.97 (Si-CH₃), -21.89 (O-Si-O). **EA** (% , measured (calculated)), C₃₆H₈₄O₁₂Si₅: C 51.21 (50.90), H 9.31 (9.97), Si 4.79 (16.53). **IR** (ATR, 32 scans, cm⁻¹): 2968.3, 2868.7, 1453.0, 1373.0, 1344.0, 1259.0, 1085.7, 1011.3, 927.4, 797.2, 686.5. **GPC** (THF, 40 °C, g/mol): M_n=5134, M_w=11372, PDI=2.284.

Synthesis of poly((hydroxyl)-polypropyleneglycol)methylsiloxane-co-polydimethylsiloxane (3.10):

Product **3.10** was synthesized (95 - 96% yield) according to the representative procedure B, using 5.0 g of **3.2a** (0.87 mmol) and 10.5 mL of propylene oxide (150.05 mmol).

¹H-NMR (CDCl₃, 400 MHz, 24 °C, ppm): δ = 3.94 – 3.89 (m, 2H, OCH₂CH(CH₃)OH), 3.70 – 3.63 (m, 3H, CH₂-O-CH₂-CH(CH₃)-OH), 3.55 – 3.48 (m, 2H, -O-CH₂-CH-), 3.41 – 3.36 (m, 2H, -OCH₂CH(CH₃)OH), 3.21 – 3.13 (m, 2H, -OCH₂CH(CH₃)OH), 2.12 (s, 1H, OH), 1.61 (m, 2H, -SiCH₂CH₂CH₂O), 1.27 (m, 3H, CH₃-CH-), 1.12 (m, 3H, -OCH₂CH(CH₃)OH), 0.49 (m, 2H, -SiCH₂CH₂O), 0.05 (m, 3H, -SiCH₃).

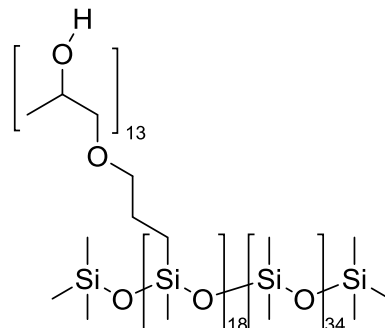
¹³C-NMR (CDCl₃, 300 MHz, 25 °C, ppm): δ = 74.46 (-Si-CH₂-CH₂-CH₂-), 72.82 (-O-CH₂-CH-), 72.33 (-O-CH₂-CH-), 71.77 (-O-CH₂-CH-), 65.27 (-OCH₂CH(CH₃)OH), 22.06 (-SiCH₂CH₂O), 17.50 (-CH₂CH(CH₃)OH), 17.06 (CH₃-CH-), 16.29 (-SiCH₂CH₂O), 0.05 (Si-CH₃). **²⁹Si-NMR** (CDCl₃, 400 MHz, 24 °C, ppm): δ = 7.30 (Si-CH₃), -21.92 (O-Si-O). **EA** (% , measured (calculated)), C₄₅H₁₀₂O₁₅Si₅: C 53.37 (52.80), H 9.34 (10.04), Si 8.59 (13.72). **IR** (ATR, 32 scans, cm⁻¹): 2968.8, 2868.1, 1452.7, 1372.9, 1344.0, 1259.2, 1087.1, 1011.7, 926.8, 798.2, 686.8. **GPC** (THF, 40 °C, g/mol): M_n=5352, M_w=12913, PDI=2.412.



Synthesis of poly((hydroxyl)-polypropyleneglycol)methylsiloxane-co-polydimethylsiloxane (3.11):

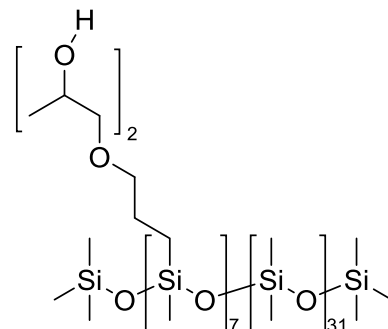
Product **3.11** was synthesized (93 – 95 % yield) according to the representative procedure B, using 5.0 g of **3.2a** (0.87 mmol) and 14.0 mL of propylene oxide (200.07 mmol).

¹H-NMR (CDCl₃, 400 MHz, 24 °C, ppm): δ = 3.93 – 3.90 (m, 2H, OCH₂CH(CH₃)OH), 3.70 – 3.65 (m, 3H, CH₂-O-CH₂-CH(CH₃)-OH), 3.56 – 3.43 (m, 2H, -O-CH₂-CH-), 3.40 – 3.35 (m, 2H, -OCH₂CH(CH₃)OH), 3.18 (m, 2H, -OCH₂CH(CH₃)OH), 2.16 (s, 1H, OH), 1.58 (m, 2H, -SiCH₂CH₂CH₂O), 1.28 – 1.24 (m, 3H, CH₃-CH-), 1.11 (m, 3H, -OCH₂CH(CH₃)OH), 0.47 (m, 2H, -SiCH₂CH₂O), 0.05 (m, 3H, -SiCH₃). **¹³C-NMR** (CDCl₃, 300 MHz, 25 °C, ppm): δ = 75.62 (-Si-CH₂-CH₂-CH₂-), 75.10 (-O-CH₂-CH-), 73.45 (-O-CH₂-CH-), 73.01 (-O-CH₂-CH-), 66.41 (-OCH₂CH(CH₃)OH), 23.24 (-SiCH₂CH₂O), 17.58 (-CH₂CH(CH₃)OH), 17.45 (CH₃-CH-), 13.52 (-SiCH₂CH₂O), 1.16 (Si-CH₃). **²⁹Si-NMR** (CDCl₃, 400 MHz, 24 °C, ppm): δ = 6.18 (Si-CH₃), -21.94 (O-Si-O). **EA** (% , measured (calculated)), C₅₄H₁₂₀O₁₈Si₅: C 54.93 (54.14), H 9.48 (10.10), Si 6.96 (11.72). **IR** (ATR, 32 scans, cm⁻¹): 2969.2, 2868.9, 1453.1, 1372.9, 1344.0, 1296.7, 1259.3, 1087.1, 1011.8, 926.6, 798.9, 685.1. **GPC** (THF, 40 °C, g/mol): M_n=6784, M_w=19211, PDI=3.082.

Synthesis of poly((hydroxyl)-polypropyleneglycol)methylsiloxane-co-polydimethylsiloxane (3.12):

Product **3.12** was synthesized (91 - 94% yield) according to the representative procedure B, using 35.3 g of **3.3a** (9.82 mmol) and 3.5 mL of propylene oxide (50.02 mmol).

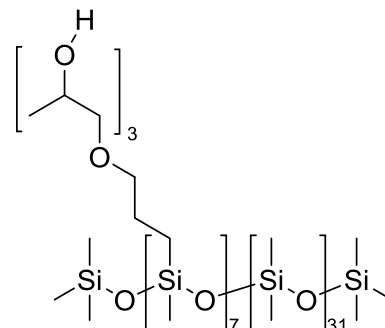
¹H-NMR (CDCl₃, 400 MHz, 24 °C, ppm): δ = 3.99 – 3.91 (m, 2H, OCH₂CH(CH₃)OH), 3.60 – 3.58 (m, 3H, CH₂-O-CH₂-CH(CH₃)-OH), 3.57 – 3.48 (m, 2H, -O-CH₂-CH-), 3.44 – 3.37 (m, 2H, -OCH₂CH), 3.23 – 3.17 (m, 2H, -OCH₂CH), 2.52 (s, 1H, OH), 1.60 (m, 2H, -SiCH₂CH₂CH₂O), 1.33 – 1.31 – 1.24 (m, 3H, CH₃-CH-), 1.11 (m, 3H, -OCH₂CH(CH₃)OH), 0.86 (m, 2H, -SiCH₂CH₂O), 0.05 (m, 3H, -SiCH₃). **¹³C-NMR** (CDCl₃, 300 MHz, 25 °C, ppm): δ = 76.07 (-Si-CH₂-CH₂-CH₂-), 75.25 (-O-CH₂-CH-), 75.08 (-O-CH₂-CH-), 73.63 (-O-CH₂-CH-), 66.39 (-OCH₂CH(CH₃)OH), 22.80 (-SiCH₂CH₂O), 18.27 (-CH₂CH(CH₃)OH), 17.05 (CH₃-CH-), 14.24 (-SiCH₂CH₂O), 1.16 (Si-CH₃). **²⁹Si-NMR** (CDCl₃, 400 MHz, 24 °C, ppm): δ = -21.94 (O-Si-O). **EA** (% , measured (calculated)), C₁₈H₄₆O₆Si₄: 32.99 (45.91), 7.889 (9.85), 10.68 (23.86). **IR** (ATR, 32 scans, cm⁻¹): 2961.8, 1411.6, 1257.7, 1009.3, 841.6, 790.3, 686.5, 505.0. **GPC** (THF, 40 °C, g/mol): M_n=4757, M_w=14693, PDI=3.103.



Synthesis of poly((hydroxyl)-polypropyleneglycol)methylsiloxane-co-polydimethylsiloxane (3.13):

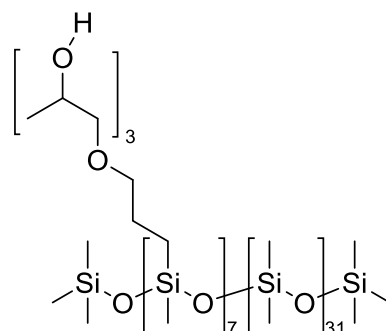
Product **3.13** was synthesized (91 - 92 % yield) according to the representative procedure B, using 12.6 g of **3.3a** (3.50 mmol) and 2.5 mL of propylene oxide (35.73 mmol).

¹H-NMR (CDCl₃, 400 MHz, 24 °C, ppm): δ = 3.96 – 3.92 (m, 2H, OCH₂CH(CH₃)OH), 3.68 – 3.61 (m, 3H, CH₂-O-CH₂-CH(CH₃)-OH), 3.57 – 3.52 (m, 2H, -O-CH₂-CH-), 3.42 – 3.38 (m, 2H, -OCH₂CH), 3.21 – 3.17 (m, 2H, -OCH₂CH), 1.62 (m, 2H, -SiCH₂CH₂CH₂O), 1.20 – 1.19 (m, 3H, CH₃-CH-), 1.13 (m, 3H, -OCH₂CH(CH₃)OH), 0.50 (m, 2H, -SiCH₂CH₂O), 0.06 (m, 3H, -SiCH₃). **¹³C-NMR** (CDCl₃, 300 MHz, 25 °C, ppm): δ = 76.64 (-Si-CH₂-CH₂-CH₂-), 75.99 (-O-CH₂-CH-), 74.37 (-O-CH₂-CH-), 73.86 (-O-CH₂-CH-), 66.84 (-OCH₂CH(CH₃)OH), 23.59 (-SiCH₂CH₂O), 19.01 (-CH₂CH(CH₃)OH), 17.81 (CH₃-CH-), 13.86 (-SiCH₂CH₂O), 1.51 (Si-CH₃). **²⁹Si-NMR** (CDCl₃, 400 MHz, 24 °C, ppm): δ = -21.93 (s, O-Si-O). **EA** (% , measured (calculated)), C₂₁H₅₂O₇Si₄: C 36.125 (38.00), H 7.927 (8.99), Si 9.866 (32.31). **IR** (ATR, 32 scans, cm⁻¹): 2962.0, 1411.5, 1257.7, 1009.8, 790.2, 686.6, 503.9. **GPC** (THF, 40 °C, g/mol): M_n=5199, M_w=26495, PDI=5.095.

Synthesis of poly((hydroxyl)-polypropyleneglycol)methylsiloxane-co-polydimethylsiloxane (3.14):

Product **3.14** was synthesized (89 % yield) according to the representative procedure B, using 10.2 g of **3.3a** (2.84 mmol) and 3.0 mL of propylene oxide (42.87 mmol).

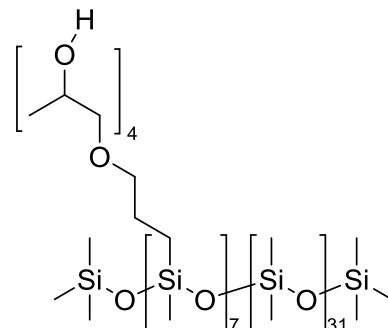
¹H-NMR (CDCl₃, 400 MHz, 24 °C, ppm): δ = 3.94 – 3.91 (m, 2H, OCH₂CH(CH₃)OH), 3.70 – 3.63 (m, 3H, CH₂-O-CH₂-CH(CH₃)-OH), 3.57 – 3.49 (m, 2H, -O-CH₂-CH-), 3.43 – 3.34 (m, 2H, -OCH₂CH), 3.22 – 3.16 (m, 2H, -OCH₂CH), 2.43 (s, 1H, OH), 1.59 (m, 2H, -SiCH₂CH₂CH₂O), 1.34 – 1.33 (m, 3H, CH₃-CH-), 1.13 (m, 3H, -OCH₂CH(CH₃)OH), 0.49 (m, 2H, -SiCH₂CH₂O), 0.06 (m, 3H, -SiCH₃). **¹³C-NMR** (CDCl₃, 300 MHz, 25 °C, ppm): δ = 75.90 (-Si-CH₂-CH₂-CH₂-), 75.24 (-O-CH₂-CH-), 73.62 (-O-CH₂-CH-), 73.10 (-O-CH₂-CH-), 66.07 (-OCH₂CH(CH₃)OH), 22.88 (-SiCH₂CH₂O), 18.27 (-CH₂CH(CH₃)OH), 17.06 (CH₃-CH-), 13.05 (-SiCH₂CH₂O), 0.75 (Si-CH₃). **²⁹Si-NMR** (CDCl₃, 400 MHz, 24 °C, ppm): δ = -21.94 (O-Si-O). **EA** (% , measured (calculated)), C₃₃H₈₄O₁₂Si₈: C 39.035 (39.85), H 9.3715 (9.10), Si 8.6385 (29.82). **IR** (ATR, 32 scans, cm⁻¹): 2962.0, 1374.1, 1257.8, 1009.4, 841.5, 790.4, 686.4. **GPC** (THF, 40 °C, g/mol): M_n=4861, M_w=16561, PDI=3.325.



Synthesis of poly((hydroxyl)-polypropyleneglycol)methylsiloxane-co-polydimethylsiloxane (3.15):

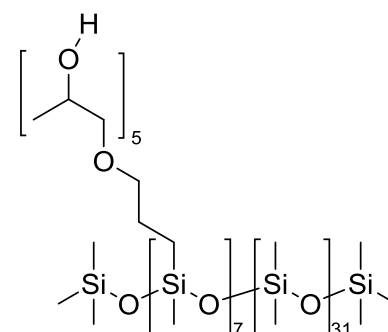
Product **3.15** was synthesized (87 - 92% yield) according to the representative procedure B, using 10.0 g of **3.3a** (2.78 mmol) and 4.0 mL of propylene oxide (57.16 mmol).

¹H-NMR (CDCl₃, 400 MHz, 24 °C, ppm): δ = 3.95 – 3.91 (m, 2H, OCH₂CH(CH₃)OH), 3.71 – 3.60 (m, 3H, CH₂-O-CH₂-CH(CH₃)-OH), 3.57 – 3.49 (m, 2H, -O-CH₂-CH-), 3.45 – 3.36 (m, 2H, -OCH₂CH), 3.21 – 3.13 (m, 2H, -OCH₂CH), 2.61 (s, 1H, OH), 1.62 (m, 2H, -SiCH₂CH₂CH₂O), 1.27 (m, 3H, CH₃-CH-), 1.12 (m, 3H, -OCH₂CH(CH₃)OH), 0.49 (m, 2H, -SiCH₂CH₂O), 0.06 (m, 3H, -SiCH₃). **¹³C-NMR** (CDCl₃, 300 MHz, 25 °C, ppm): δ = 75.99 (-Si-CH₂-CH₂-CH₂-), 75.18 (-O-CH₂-CH-), 73.72 (-O-CH₂-CH-), 73.20 (-O-CH₂-CH-), 66.19 (-OCH₂CH(CH₃)OH), 22.94 (-SiCH₂CH₂O), 18.37 (-CH₂CH(CH₃)OH), 17.17 (CH₃-CH-), 13.21 (-SiCH₂CH₂O), 0.86 (Si-CH₃). **²⁹Si-NMR** (CDCl₃, 400 MHz, 24 °C, ppm): δ = -21.90 (O-Si-O). **EA** (%), measured (calculated)), C₃₃H₈₄O₁₂Si₈: C 38.08 (41.44), H 8.631 (9.19), Si 9.8525 (27.68). **IR** (ATR, 32 scans, cm⁻¹): 2962.0, 1374.1, 1257.8, 1009.4, 841.6, 790.5, 686.5, 503.5. **GPC** (THF, 40 °C, g/mol): M_n=4914, M_w=11288, PDI=2.297.

Synthesis of poly((hydroxyl)-polypropyleneglycol)methylsiloxane-co-polydimethylsiloxane (3.16):

Product **3.16** was synthesized (89 - 94% yield) according to the representative procedure B, using 9.0 g of **3.3a** (2.50 mmol) and 4.5 mL of propylene oxide (64.31 mmol).

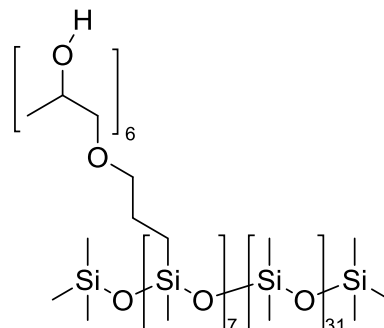
¹H-NMR (CDCl₃, 400 MHz, 24 °C, ppm): δ = 3.95 – 3.92 (m, 2H, OCH₂CH(CH₃)OH), 3.70 – 3.66 (m, 3H, CH₂-O-CH₂-CH(CH₃)-OH), 3.57 – 3.46 (m, 2H, -O-CH₂-CH-), 3.41 – 3.38 (m, 2H, -OCH₂CH), 3.21 – 3.12 (m, -OCH₂CH), 2.53 (s, 1H, OH), 1.62 (m, 2H, -SiCH₂CH₂CH₂O), 1.20 – 1.19 (m, 3H, CH₃-CH-), 1.13 (m, 3H, -OCH₂CH(CH₃)OH), 0.50 (m, 2H, -SiCH₂CH₂O), 0.06 (m, 3H, -SiCH₃). **¹³C-NMR** (CDCl₃, 300 MHz, 25 °C, ppm): δ = 76.64 (-Si-CH₂-CH₂-CH₂-), 75.98 (-O-CH₂-CH-), 74.37 (-O-CH₂-CH-), 73.84 (-O-CH₂-CH-), 66.80 (-OCH₂CH(CH₃)OH), 23.58 (-SiCH₂CH₂O), 19.00 (-CH₂CH(CH₃)OH), 17.94 (CH₃-CH-), 13.86 (-SiCH₂CH₂O), 1.50 (Si-CH₃). **²⁹Si-NMR** (CDCl₃, 400 MHz, 24 °C, ppm): δ = -21.91 (O-Si-O). **EA** (%), measured (calculated)), C₃₆H₉₀O₁₃Si₈: C 42.03 (42.82), H 8.8165 (9.27), Si 9.833 (25.84). **IR** (ATR, 32 scans, cm⁻¹): 2962.0, 1374.4, 1257.8, 1010.2, 790.6, 687.0. **GPC** (THF, 40 °C, g/mol): M_n=5218, M_w=251189, PDI=4.829.



Synthesis of poly((hydroxyl)-polypropyleneglycol)methylsiloxane-co-polydimethylsiloxane (3.17):

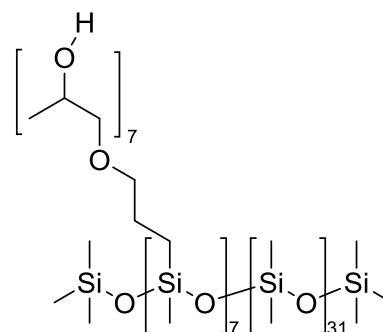
Product **3.17** was synthesized (87 - 92 % yield) according to the representative procedure B, using 8.3 g of **3.3a** (2.31 mmol) and 5.0 mL of propylene oxide (71.45 mmol).

¹H-NMR (CDCl₃, 400 MHz, 24 °C, ppm): δ = 3.95 – 3.93 (m, 2H, OCH₂CH(CH₃)OH), 3.72 – 3.64 (m, 3H, CH₂-O-CH₂-CH(CH₃)-OH), 3.56 – 3.51 (m, 2H, -O-CH₂-CH-), 3.41 – 3.38 (m, 2H, -OCH₂CH), 3.19 (m, 2H, -OCH₂CH), 2.36 (s, 1H, OH), 1.62 (m, 2H, -SiCH₂CH₂CH₂O), 1.30 – 1.25 (m, 3H, CH₃-CH-), 1.13 (m, 3H, -OCH₂CH(CH₃)OH), 0.50 (m, 2H, -SiCH₂CH₂O), 0.06 (m, 3H, -SiCH₃). **¹³C-NMR** (CDCl₃, 300 MHz, 25 °C, ppm): δ = 75.35 (-Si-CH₂-CH₂-CH₂-), 74.94 (-O-CH₂-CH-), 73.25 (-O-CH₂-CH-), 72.66 (-O-CH₂-CH-), 66.19 (-OCH₂CH(CH₃)OH), 23.00 (-SiCH₂CH₂O), 18.36 (-CH₂CH(CH₃)OH), 17.18 (CH₃-CH-), 13.22 (-SiCH₂CH₂O), 0.87 (Si-CH₃). **²⁹Si-NMR** (CDCl₃, 400 MHz, 24 °C, ppm): δ = -21.92 (O-Si-O). **EA** (% , measured (calculated)), C₂₉H₆₈O₁₀Si₄: C 48.545 (45.00), H 9.149 (9.41), Si 6.557 (22.79). **IR** (ATR, 32 scans, cm⁻¹): 2962.8, 1374.1, 1257.9, 1010.1, 791.2, 686.8. **GPC** (THF, 40 °C, g/mol): M_n=6383, M_w=28243, PDI=4.517.

Synthesis of poly((hydroxyl)-polypropyleneglycol)methylsiloxane-co-polydimethylsiloxane (3.18):

Product **3.18** was synthesized (76 - 99 % yield) according to the representative procedure B, using 5.0 g of **3.3a** (1.39 mmol) and 3.5 mL of propylene oxide (50.02 mmol).

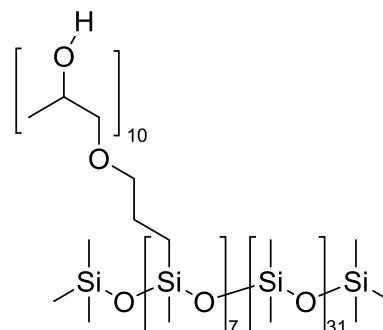
¹H-NMR (CDCl₃, 400 MHz, 24 °C, ppm): δ = 3.92 – 3.87 (m, 1H, OCH₂CH(CH₃)OH), 3.70 – 3.61 (m, 3H, CH₂-O-CH₂-CH(CH₃)-OH), 3.55 – 3.45 (m, 2H, -O-CH₂-CH-), 3.43 – 3.30 (m, 2H, -OCH₂CH(CH₃)OH), 3.20 – 3.13 (m, 2H, -OCH₂CH), 2.71 (s, 1H, OH), 1.59 (m, 2H, -SiCH₂CH₂CH₂O), 1.32 – 1.29 (m, 3H, CH₃-CH-), 1.09 (m, 3H, -OCH₂CH(CH₃)OH), 0.47 (m, 2H, -SiCH₂CH₂O), 0.00 (m, 3H, -SiCH₃). **¹³C-NMR** (CDCl₃, 300 MHz, 25 °C, ppm): δ = 75.16 (-Si-CH₂-CH₂-CH₂-), 73.54 (-O-CH₂-CH-), 73.02 (-O-CH₂-CH-), 72.51 (-O-CH₂-CH-), 65.98 (-OCH₂CH(CH₃)OH), 22.76 (-SiCH₂CH₂O), 18.24 (-CH₂CH(CH₃)OH), 17.12 (CH₃-CH-), 13.04 (-SiCH₂CH₂O), 0.68 (Si-CH₃). **²⁹Si-NMR** (CDCl₃, 400 MHz, 24 °C, ppm): δ = -21.07 (O-Si-O). **EA** (% , measured (calculated)), C₂₆H₆₂O₁₇Si₄: C 48.65 (45.00), H 9.9 (9.41), Si 5.648 (22.79). **IR** (ATR, 32 scans, cm⁻¹): 2961.9, 1412.1, 1257.8, 1009.7, 790.5, 686.9. **GPC** (THF, 40 °C, g/mol): M_n=7174, M_w=17584, PD=2.455.



Synthesis of poly((hydroxyl)-polypropyleneglycol)methylsiloxane-co-polydimethylsiloxane (3.19):

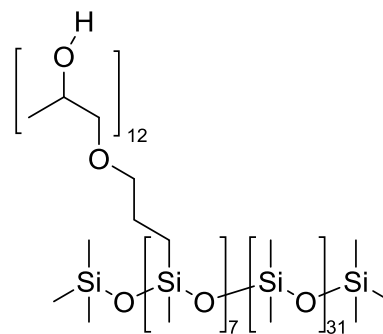
Product **3.19** was synthesized (90 - 91 % yield) according to the representative procedure B, using 5.1 g of **3.3a** (1.42 mmol) and 5.5 mL of propylene oxide (78.60 mmol).

¹H-NMR (CDCl₃, 400 MHz, 24 °C, ppm): δ = 3.94 – 3.90 (m, 2H, OCH₂CH(CH₃)OH), 3.71 – 3.62 (m, 3H, CH₂-O-CH₂-CH(CH₃)-OH), 3.56 – 3.47 (m, 2H, -O-CH₂-CH-), 3.40 – 3.37 (m, 2H, -OCH₂CH), 3.21 – 3.11 (m, 2H, -OCH₂CH), 2.59 (1H, OH), 1.61 (m, 2H, -SiCH₂CH₂CH₂O), 1.29 – 1.22 (m, 3H, CH₃-CH-), 1.12 (m, 3H, -OCH₂CH(CH₃)OH), 0.49 (m, 2H, -SiCH₂CH₂O), 0.07 (m, 3H, -SiCH₃). **¹³C-NMR** (CDCl₃, 300 MHz, 25 °C, ppm): δ = 75.32 (-Si-CH₂-CH₂-CH₂-), 74.81 (-O-CH₂-CH-), 73.20 (-O-CH₂-CH-), 72.72 (-O-CH₂-CH-), 66.13 (-OCH₂CH(CH₃)OH), 22.92 (-SiCH₂CH₂O), 18.35 (-CH₂CH(CH₃)OH), 17.15 (CH₃-CH-), 13.19 (-SiCH₂CH₂O), 0.94 (Si-CH₃). **²⁹Si-NMR** (CDCl₃, 400 MHz, 24 °C, ppm): δ = -21.94 (O-Si-O). **EA** (%), measured (calculated)), C₄₅H₁₀₂O₁₅Si₄: C 52.2 (49.31), H 9.1635 (9.94), Si 8.315 (18.44). **IR** (ATR, 32 scans, cm⁻¹): 2969.6, 2869.3, 1726.6, 1452.8, 1373.1, 1344.3, 1259.3, 1086.8, 1013.2, 926.6, 799.1, 666.2. **GPC** (THF, 40 °C, g/mol): M_n=6411, M_w=13013, PDI=2.029.

Synthesis of poly((hydroxyl)-polypropyleneglycol)methylsiloxane-co-polydimethylsiloxane (3.20):

Product **3.20** was synthesized (80 - 92 % yield) according to the representative procedure B, using 5.0 g of **3.3a** (1.39 mmol) and 7.0 mL of propylene oxide (100.03 mmol).

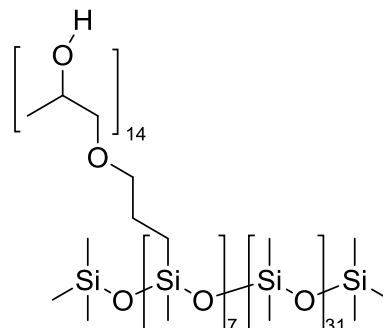
¹H-NMR (CDCl₃, 400 MHz, 24 °C, ppm): δ = 3.95 – 3.92 (m, 2H, OCH₂CH(CH₃)OH), 3.74 – 3.71 (m, 3H, CH₂-O-CH₂-CH(CH₃)-OH), 3.54 – 3.53 (m, 2H, -O-CH₂-CH-), 3.41 – 3.37 (m, 2H, -OCH₂CH), 3.22 – 3.19 (m, 2H, -OCH₂CH), 2.70 (s, 1H, OH), 1.61 (m, 2H, -SiCH₂CH₂CH₂O), 1.29 – 1.28 (m, 3H, CH₃-CH-), 1.11 (m, 3H, -OCH₂CH(CH₃)OH), 0.48 (m, 2H, -SiCH₂CH₂O), 0.06 (m, 3H, -SiCH₃). **¹³C-NMR** (CDCl₃, 300 MHz, 25 °C, ppm): δ = 75.65 (-Si-CH₂-CH₂-CH₂-), 74.04 (-O-CH₂-CH-), 73.51 (-O-CH₂-CH-), 73.02 (-O-CH₂-CH-), 66.14 (-OCH₂CH(CH₃)OH), 22.90 (-SiCH₂CH₂O), 18.69 (-CH₂CH(CH₃)OH), 17.48 (CH₃-CH-), 13.19 (-SiCH₂CH₂O), 0.83 (Si-CH₃). **²⁹Si-NMR** (CDCl₃, 400 MHz, 24 °C, ppm): δ = -21.94 (O-Si-O). **EA** (%), measured (calculated)), C₆₂H₁₃₆O₂₁Si₄: C 54.18 (50.18), H 9.175 (9.9), Si 8.127 (16.47). **IR** (ATR, 32 scans, cm⁻¹): 2968.9, 2868.1, 1452.6, 1372.8, 1344.0, 1296.5, 1259.0, 1088.0, 1011.8, 927.5, 795.2, 687.2. **GPC** (THF, 40 °C, g/mol): M_n=7746, M_w=18792, PDI=2.430.



Synthesis of poly((hydroxyl)-polypropyleneglycol)methylsiloxane-co-polydimethylsiloxane (3.21):

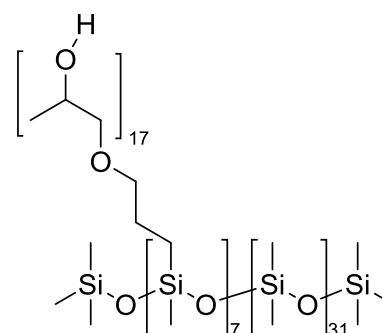
Product **3.21** was synthesized (87 - 92 % yield) according to the representative procedure B, using 5.1 g of **3.3a** (1.42 mmol) and 8.5 mL of propylene oxide (121.47 mmol).

¹H-NMR (CDCl₃, 400 MHz, 24 °C, ppm): δ = 3.93 – 3.90 (m, 2H, OCH₂CH(CH₃)OH), 3.70 – 3.60 (m, 3H, CH₂-O-CH₂-CH(CH₃)-OH), 3.56 – 3.47 (m, 2H, -O-CH₂-CH-), 3.40 – 3.35 (m, 2H, -OCH₂CH), 3.18 – 3.11 (m, 2H, -OCH₂CH), 2.13 (s, 1H, OH), 1.59 (m, 2H, -SiCH₂CH₂CH₂O), 1.28 – 1.20 (m, 3H, CH₃-CH-), 1.14 (m, 3H, -OCH₂CH(CH₃)OH), 0.50 (m, 2H, -SiCH₂CH₂O), 0.06 (m, 3H, -SiCH₃). **¹³C-NMR** (CDCl₃, 300 MHz, 25 °C, ppm): δ = 75.64 (-Si-CH₂-CH₂-CH₂-), 74.91 (-O-CH₂-CH-), 73.16 (-O-CH₂-CH-), 72.63 (-O-CH₂-CH-), 68.26 (-OCH₂CH(CH₃)OH), 22.30 (-SiCH₂CH₂O), 18.35 (-CH₂CH(CH₃)OH), 17.15 (CH₃-CH-), 10.65 (-SiCH₂CH₂O), 1.19 (Si-CH₃). **²⁹Si-NMR** (CDCl₃, 400 MHz, 24 °C, ppm): δ = -21.92 (O-Si-O). **EA** (% , measured (calculated)), C₆₂H₁₃₆O₂₁Si₄: C 54.32 (51.11), H 9.248 (9.94), Si 4.939 (15.18). **GPC** (THF, 40 °C, g/mol): M_n=7819, M_w=15867, PDI=2.020.

Synthesis of poly((hydroxyl)-polypropyleneglycol)methylsiloxane-co-polydimethylsiloxane (3.22):

Product **3.22** was synthesized (66 - 98 % yield) according to the representative procedure B, using 5.0 g of **3.3a** (1.39 mmol) and 10.5 mL of propylene oxide (150.05 mmol).

¹H-NMR (CDCl₃, 400 MHz, 24 °C, ppm): δ = 3.93 – 3.86 (m, 2H, OCH₂CH(CH₃)OH), 3.69 – 3.62 (m, 3H, CH₂-O-CH₂-CH(CH₃)-OH), 3.55 – 3.47 (m, 2H, -O-CH₂-CH-), 3.39 – 3.34 (m, 2H, -OCH₂CH(CH₃)OH), 3.19 – 3.12 (m, 2H, -OCH₂CH(CH₃)OH), 2.70 (s, 1H, OH), 1.57 (m, 2H, -SiCH₂CH₂CH₂O), 1.27 – 1.18 (m, 3H, CH₃-CH-), 1.10 (m, 3H, -OCH₂CH(CH₃)OH), 0.46 (m, 2H, -SiCH₂CH₂O), 0.0 (m, 3H, -SiCH₃). **¹³C-NMR** (CDCl₃, 300 MHz, 25 °C, ppm): δ = 75.32 (-Si-CH₂-CH₂-CH₂-), 74.87 (-O-CH₂-CH-), 73.13 (-O-CH₂-CH-), 72.69 (-O-CH₂-CH-), 66.11 (-OCH₂CH(CH₃)OH), 22.87 (-SiCH₂CH₂O), 18.31 (-CH₂CH(CH₃)OH), 17.11 (CH₃-CH-), 13.15 (-SiCH₂CH₂O), 0.80 (Si-CH₃). **²⁹Si-NMR** (CDCl₃, 400 MHz, 24 °C, ppm): δ = -21.97 (O-Si-O). **EA** (% , measured (calculated)), C₆₈H₁₄₆O₂₃Si₄: C 56.625 (52.59), H 9.355 (10.00), Si 3.80 (13.12). **IR** (ATR, 32 scans, cm⁻¹): 2967.9, 2868.2, 1452.6, 1372.1, 1343.9, 1259.0, 1086.3, 1012.9, 927.0, 796.0, 687.7. **GPC** (THF, 40 °C, g/mol): M_n=12025, M_w=31019, PDI=2.491.



Product **3.23** was synthesized (83 - 88 % yield) according to the representative procedure B, using 5.1 g of **3.3a** (1.42 mmol) and 12.0 mL of propylene oxide (171.49 mmol).

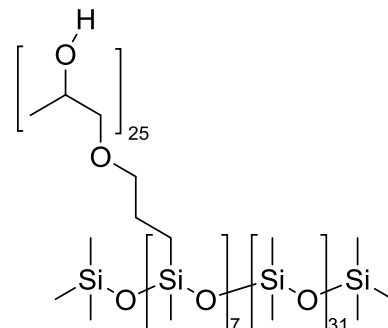
[illegible]

Product **3.24** was synthesized (86 - 96% yield) according to the representative procedure B, using 5.0 g of **3.3a** (1.39 mmol) and 14.0 mL of propylene oxide (200.07 mmol).

Synthesis of poly((hydroxyl)-polypropyleneglycol)methylsiloxane-co-polydimethylsiloxane (3.25):

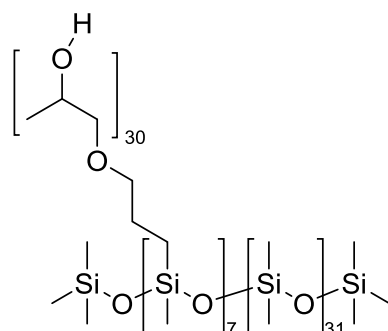
Product **3.25** was synthesized (84 - 94 % yield) according to the representative procedure B, using 3.8 g of **3.3a** (1.06 mmol) and 12.0 mL of propylene oxide (171.49 mmol).

¹H-NMR (CDCl₃, 400 MHz, 24 °C, ppm): δ = 3.91 (m, 2H, OCH₂CH(CH₃)OH), 3.71 – 3.62 (m, 3H, CH₂-O-CH₂-CH(CH₃)-OH), 3.56 – 3.47 (m, 2H, -O-CH₂-CH-), 3.40 – 3.35 (m, 2H, -OCH₂CH), 3.20 – 3.13 (m, 2H, -OCH₂CH), 1.6 (m, 2H, -SiCH₂CH₂CH₂O), 1.32 – 1.26 (m, 3H, CH₃-CH-), 1.10 (m, 3H, -OCH₂CH(CH₃)OH), 0.47 (m, 2H, -SiCH₂CH₂O), 0.04 (m, 3H, -SiCH₃). **¹³C-NMR** (CDCl₃, 300 MHz, 25 °C, ppm): δ = 75.18 (-Si-CH₂-CH₂-CH₂-), 74.54 (-O-CH₂-CH-), 73.03 (-O-CH₂-CH-), 72.53 (-O-CH₂-CH-), 65.91 (-OCH₂CH(CH₃)OH), 22.36 (-SiCH₂CH₂O), 17.12 (-CH₂CH(CH₃)OH), 16.90 (CH₃-CH-), 12.91 (-SiCH₂CH₂O), 0.44 (Si-CH₃). **²⁹Si-NMR** (CDCl₃, 400 MHz, 24 °C, ppm): δ = -21.97 (O-Si-O). **EA** (% , measured (calculated)), C₉₉H₂₁₆O₃₄Si₄: C 57.45 (54.52), H 9.817 (9.95), Si 2.418 (10.46 **IR** (ATR, 32 scans, cm⁻¹): 2966.6, 2868.0, 1452.1, 1372.7, 1258.5, 1084.5, 1012.2, 926.6, 796.0, 686.6. **GPC** (THF, 40 °C, g/mol): M_n=11553, M_w=30812, PDI=2.580.

Synthesis of poly((hydroxyl)-polypropyleneglycol)methylsiloxane-co-polydimethylsiloxane (3.26):

Product **3.26** was synthesized (80 - 90 % yield) according to the representative procedure B, using 3.2 g of **3.3a** (0.89 mmol) and 12.0 mL of propylene oxide (171.49 mmol).

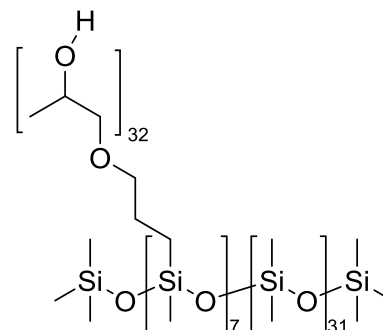
¹H-NMR (CDCl₃, 400 MHz, 24 °C, ppm): δ = 3.97 – 3.88 (m, 2H OCH₂CH(CH₃)OH), 3.71 – 3.64 (m, 3H, CH₂-O-CH₂-CH(CH₃)-OH), 3.58 – 3.45 (m, 2H, -O-CH₂-CH-), 3.41 – 3.30 (m, 2H, -OCH₂CH), 3.21 – 3.12 (m, 2H, -OCH₂CH), 2.53 (s, 1H, OH), 1.60 (m, 2H, -SiCH₂CH₂CH₂O), 1.22 – 1.18 (m, 3H, CH₃-CH-), 1.11 (m, 3H, -OCH₂CH(CH₃)OH), 0.86 (m, 2H, -SiCH₂CH₂O), 0.05 (m, 3H, -SiCH₃). **¹³C-NMR** (CDCl₃, 300 MHz, 25 °C, ppm): δ = 75.33 (-Si-CH₂-CH₂-CH₂-), 74.81 (-O-CH₂-CH-), 73.20 (-O-CH₂-CH-), 72.64 (-O-CH₂-CH-), 66.39 (-OCH₂CH(CH₃)OH), 22.80 (-SiCH₂CH₂O), 17.29 (-CH₂CH(CH₃)OH), 17.16 (CH₃-CH-), 14.24 (-SiCH₂CH₂O), 1.16 (-SiCH₃). **²⁹Si-NMR** (CDCl₃, 400 MHz, 24 °C, ppm): δ = -21.94 (O-Si-O). **EA** (% , measured (calculated)), C₁₀₉H₂₃₂O₃₉Si₇: C 55.5 (55.39), H 9.829 (9.89), Si 7.385 (8.32 **IR** (ATR, 32 scans, cm⁻¹): 2969.6, 2868.0, 1452.7, 1372.7, 1343.8, 1296.6, 1259.5, 1089.7, 1013.0, 926.2, 798.6, 666.1. **GPC** (THF, 40 °C, g/mol): M_n=11290, M_w=45473, PDI= 3.814.



Synthesis of poly((hydroxyl)-polypropyleneglycol)methylsiloxane-co-polydimethylsiloxane (3.27):

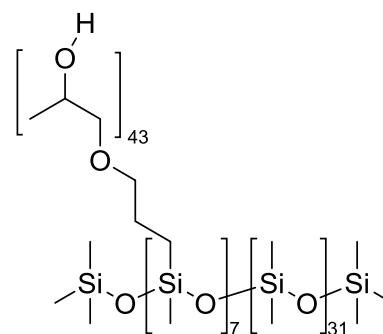
Product **3.27** was synthesized (83 - 92 % yield) according to the representative procedure B, using 2.6 g of **3.3a** (0.72 mmol) and 10.0 mL of propylene oxide (142.91 mmol).

¹H-NMR (CDCl₃, 400 MHz, 24 °C, ppm): δ = 3.86 (m, 2H, OCH₂CH(CH₃)OH), 3.68 – 3.60 (m, 3H, CH₂-O-CH₂-CH(CH₃)-OH), 3.53 – 3.39 (m, 2H, -O-CH₂-CH-), 3.36 – 3.33 (m, 2H, -OCH₂CH), 3.16 – 3.07 (m, 2H, -OCH₂CH), 1.58 (m, 2H, -SiCH₂CH₂CH₂O), 1.23 – 1.20 (m, 3H, CH₃-CH-), 1.08 (m, 3H, -OCH₂CH(CH₃)OH), 0.45 (m, 2H, -SiCH₂CH₂O), 0.02 (m, 3H, -SiCH₃). **¹³C-NMR** (CDCl₃, 300 MHz, 25 °C, ppm): δ = 75.51 (-Si-CH₂-CH₂-CH₂-), 75.12 (-O-CH₂-CH-), 73.37 (-O-CH₂-CH-), 72.95 (-O-CH₂-CH-), 66.68 (-OCH₂CH(CH₃)OH), 23.02 (-SiCH₂CH₂O), 17.49 (-CH₂CH(CH₃)OH), 17.26 (CH₃-CH-), 14.45 (-SiCH₂CH₂O), 1.39 (Si-CH₃). **²⁹Si-NMR** (CDCl₃, 400 MHz, 24 °C, ppm): δ = -21.99 (O-Si-O). **EA** (% , measured (calculated)), C₁₁₆H₂₄₈O₄₁Si₇: C 57.32 (55.78), H 10.51 (10.04), Si 3.40 (8.41). **IR** (ATR, 32 scans, cm⁻¹): 2969.6, 2868.1, 1452.9, 1372.6, 1343.8, 1296.6, 1259.6, 1089.4, 1013.1, 926.1, 799.9, 668.4. **GPC** (THF, 40 °C, g/mol): M_n=12241, M_w=42605, PDI= 3.069.

Synthesis of poly((hydroxyl)-polypropyleneglycol)methylsiloxane-co-polydimethylsiloxane (3.28):

Product **3.28** was synthesized (91 % yield) according to the representative procedure B, using 2.3 g of **3.3a** (0.64 mmol) and 12.0 mL of propylene oxide (171.49 mmol).

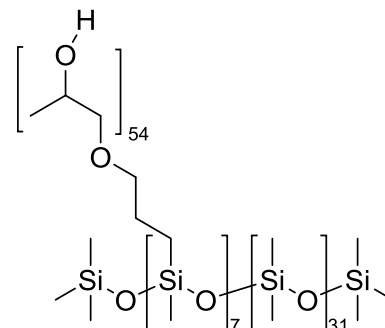
¹H-NMR (CDCl₃, 400 MHz, 24 °C, ppm): δ = 3.92 – 3.88 (m, 2H, OCH₂CH(CH₃)OH), 3.70 – 3.63 (m, 3H, CH₂-O-CH₂-CH(CH₃)-OH), 3.53 – 3.48 (m, 2H, -O-CH₂-CH-), 3.38 – 3.35 (m, 2H, -OCH₂CH), 3.19 – 3.10 (m, 2H, -OCH₂CH), 1.57 (m, 2H, -SiCH₂CH₂CH₂O), 1.27 – 1.26 (m, 3H, CH₃-CH-), 1.09 (m, 3H, -OCH₂CH(CH₃)OH), 0.47 (m, 2H, -SiCH₂CH₂O), 0.03 (m, 3H, -SiCH₃). **¹³C-NMR** (CDCl₃, 300 MHz, 25 °C, ppm): δ = 75.63 (-Si-CH₂-CH₂-CH₂-), 75.07 (-O-CH₂-CH-), 73.44 (-O-CH₂-CH-), 72.91 (-O-CH₂-CH-), 66.50 (-OCH₂CH(CH₃)OH), 23.20 (-SiCH₂CH₂O), 17.56 (-CH₂CH(CH₃)OH), 17.43 (CH₃-CH-), 13.46 (-SiCH₂CH₂O), 1.11 (-SiCH₃). **²⁹Si-NMR** (CDCl₃, 400 MHz, 24 °C, ppm): δ = -21.95 (O-Si-O). **EA** (% , measured (calculated)), C₁₄₉H₃₁₄O₅₂Si₇: C 58.48 (56.71), H 10.565 (10.10), Si 2.103 (7.17). **IR** (ATR, 32 scans, cm⁻¹): 2969.6, 2867.6, 1452.7, 1372.5, 1343.7, 1296.4, 1259.7, 1090.1, 1013.2, 925.8, 800.4, 666.4. **GPC** (THF, 40 °C, g/mol): M_n=14833, M_w=55327, PDI=3.527.



Synthesis of poly((hydroxyl)-polypropylenglycol)methylsiloxane-co-polydimethylsiloxane (3.29):

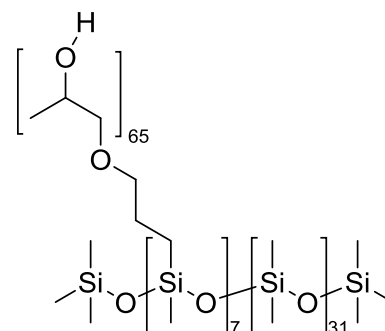
Product **3.29** was synthesized (90 - 94% yield) according to the representative procedure B, using 2.0 g of **3.3a** (0.56 mmol) and 12.0 mL of propylene oxide (171.49 mmol).

¹H-NMR (CDCl₃, 400 MHz, 24 °C, ppm): δ = 3.94 – 3.92 (m, 2H, OCH₂CH(CH₃)OH), 3.72 – 3.65 (m, 3H, CH₂-O-CH₂-CH(CH₃)-OH), 3.57 – 3.50 (m, 2H, -O-CH₂-CH-), 3.42 – 3.37 (m, 2H, -OCH₂CH), 3.21 – 3.17 (m, 2H, -OCH₂CH), 1.91 (s, 1H, -OH), 1.60 (m, 2H, -SiCH₂CH₂CH₂O), 1.31 – 1.24 (m, 3H, CH₃-CH-), 1.13 (m, 3H, -OCH₂CH(CH₃)OH), 0.43 (m, 2H, -SiCH₂CH₂O), 0.06 (m, 3H, -SiCH₃). **¹³C-NMR** (CDCl₃, 300 MHz, 25 °C, ppm): δ = 75.67 (-Si-CH₂-CH₂-CH₂-), 75.26 (-O-CH₂-CH-), 73.53 (-O-CH₂-CH-), 72.97 (-O-CH₂-CH-), 66.95 (-OCH₂CH(CH₃)OH), 22.96 (-SiCH₂CH₂O), 17.63 (-CH₂CH(CH₃)OH), 17.50 (CH₃-CH-), 15.22 (-SiCH₂CH₂O), 0.86 (-SiCH₃). **²⁹Si-NMR** (CDCl₃, 400 MHz, 24 °C, ppm): δ = -24.99 (O-Si-O). **EA** (%), measured (calculated)), C₁₈₂H₃₈₀O₆₃Si₇: C 58.265 (57.68), H 9.847 (10.15), Si 2.715 (5.86). **IR** (ATR, 32 scans, cm⁻¹): 2970.0, 2868.2, 1727.0, 1452.9, 1372.7, 1343.7, 1296.7, 1259.7, 1089.5, 1013.6, 925.8, 803.2, 666.2. **GPC** (THF, 40 °C, g/mol): M_n=11295, M_w=52276, PDI=4.237.

Synthesis of poly((hydroxyl)-polypropylenglycol)methylsiloxane-co-polydimethylsiloxane (3.30):

Product **3.30** was synthesized (89 - 90 % yield) according to the representative procedure B, using 1.5 g of **3.3a** (0.42 mmol) and 12.0 mL of propylene oxide (171.49 mmol).

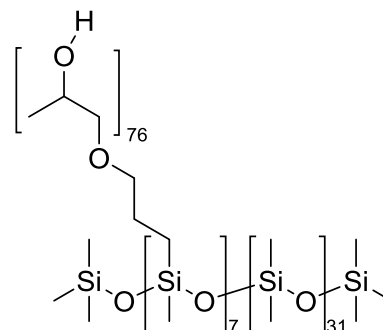
¹H-NMR (CDCl₃, 400 MHz, 24 °C, ppm): δ = 3.95 – 3.90 (m, 2H, OCH₂CH(CH₃)OH), 3.73 – 3.67 (m, 3H, CH₂-O-CH₂-CH(CH₃)-OH), 3.56 – 3.51 (m, 2H, -O-CH₂-CH-), 3.41 – 3.38 (m, 2H, -OCH₂CH), 3.22 – 3.13 (m, 2H, -OCH₂CH), 1.78 (m, 2H, -OCH₂CH), 1.64 (m, 2H, -SiCH₂CH₂CH₂O), 1.30 – 1.23 (m, 3H, CH₃-CH-), 1.12 (m, 3H, -OCH₂CH(CH₃)OH), 0.48 (m, 2H, -SiCH₂CH₂O), 0.07 (m, 3H, -SiCH₃). **¹³C-NMR** (CDCl₃, 300 MHz, 25 °C, ppm): δ = 75.36 (-Si-CH₂-CH₂-CH₂-), 74.94 (-O-CH₂-CH-), 73.22 (-O-CH₂-CH-), 72.75 (-O-CH₂-CH-), 66.37 (-OCH₂CH(CH₃)OH), 22.73 (-SiCH₂CH₂O), 17.32 (-CH₂CH(CH₃)OH), 17.18 (CH₃-CH-), 7.70 (-SiCH₂CH₂O), 0.89 (-SiCH₃). **²⁹Si-NMR** (CDCl₃, 400 MHz, 24 °C, ppm): δ = -21.24 (O-Si-O). **EA** (%), measured (calculated)), C₂₁₅H₄₄₆O₇₄Si₇: C 58.416 (58.37), H 10.075 (10.075). **IR** (ATR, 32 scans, cm⁻¹): 2969.7, 2867.6, 1453.1, 1372.5, 1343.6, 1296.4, 1259.8, 1090.5, 1013.5, 925.8, 800.8, 669.0. **GPC** (THF, 40 °C, g/mol): M_n=13824, M_w=51363, PDI=3.584.



Synthesis of poly((hydroxyl)-polypropyleneglycol)methylsiloxane-co-polydimethylsiloxane (3.31):

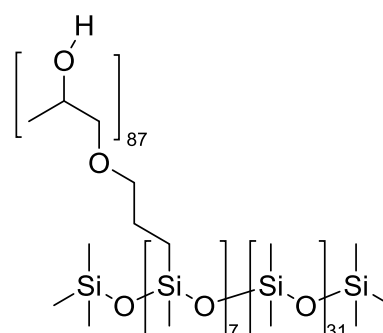
Product **3.31** was synthesized (90 - 92 % yield) according to the representative procedure B, using 1.3 g of **3.3a** (0.36 mmol) and 12.0 mL of propylene oxide (171.49 mmol).

¹H-NMR (CDCl₃, 400 MHz, 24 °C, ppm): δ = 3.95 – 3.88 (m, 2H, OCH₂CH(CH₃)OH), 3.71 – 3.65 (m, 3H, CH₂-O-CH₂-CH(CH₃)-OH), 3.58 – 3.44 (m, 2H, -O-CH₂-CH-), 3.41 – 3.29 (m, 2H, -OCH₂CH), 3.18 – 3.12 (m, 2H, -OCH₂CH), 1.63 (m, 2H, -SiCH₂CH₂CH₂O), 1.28 – 1.25 (m, 3H, CH₃-CH-), 1.11 (m, 3H, -OCH₂CH(CH₃)OH), 0.46 (m, 2H, -SiCH₂CH₂O), 0.07 (m, 3H, -SiCH₃). **¹³C-NMR** (CDCl₃, 300 MHz, 25 °C, ppm): δ = 75.65 (-Si-CH₂-CH₂-CH₂-), 74.24 (-O-CH₂-CH-), 73.49 (-O-CH₂-CH-), 73.00 (-O-CH₂-CH-), 67.49 (-OCH₂CH(CH₃)OH), 23.61 (-SiCH₂CH₂O), 17.60 (-CH₂CH(CH₃)OH), 17.38 (CH₃-CH-), 13.27 (-SiCH₂CH₂O), 1.49 (-SiCH₃). **²⁹Si-NMR** (CDCl₃, 400 MHz, 24 °C, ppm): δ = -21.92 (O-Si-O). **EA** (% , measured (calculated)), C₂₄₈H₅₁₂O₈₅Si₇: C 59.07 (59.08), H 9.837 (10.25), Si 2.545 (4.14). **IR** (ATR, 32 scans, cm⁻¹): 2969.9, 2867.8, 1726.3, 1452.8, 1372.5, 1343.6, 1296.5, 1259.8, 1090.3, 1013.4, 925.6, 803.2. **GPC** (THF, 40 °C, g/mol): M_n=15039, M_w=53152, PDI=3.373.

Synthesis of poly((hydroxyl)-polypropyleneglycol)methylsiloxane-co-polydimethylsiloxane (3.32):

Product **3.32** was synthesized (91 - 93 % yield) according to the representative procedure B, using 1.0 g of **3.3a** (0.28 mmol) and 12.0 mL of propylene oxide (171.49 mmol).

¹H-NMR (CDCl₃, 400 MHz, 24 °C, ppm): δ = 3.93 (m, 2H, OCH₂CH(CH₃)OH), 3.73 – 3.69 (m, 3H, CH₂-O-CH₂-CH(CH₃)-OH), 3.59 – 3.50 (m, 2H, -O-CH₂-CH-), 3.40 – 3.30 (m, 2H, -OCH₂CH), 3.22 – 3.12 (m, 2H, -OCH₂CH), 1.61 (s, 1H, -OH), 1.30 – 1.22 (m, 3H, CH₃-CH-), 1.14 (m, 3H, -OCH₂CH(CH₃)OH), 0.52 (m, 2H, -SiCH₂CH₂O), 0.06 (m, 3H, -SiCH₃). **¹³C-NMR** (CDCl₃, 300 MHz, 25 °C, ppm): δ = 75.36 (-Si-CH₂-CH₂-CH₂-), 74.95 (-O-CH₂-CH-), 73.22 (-O-CH₂-CH-), 72.64 (-O-CH₂-CH-), 65.06 (-OCH₂CH(CH₃)OH), 21.09 (-SiCH₂CH₂O), 17.31 (-CH₂CH(CH₃)OH), 17.18 (CH₃-CH-), 14.64 (-SiCH₂CH₂O), 0.88 (-SiCH₃). **²⁹Si-NMR** (CDCl₃, 400 MHz, 24 °C, ppm): δ = -24.98 (O-Si-O). **EA** (% , measured (calculated)), C₂₈₁H₅₇₈O₉₆Si₇: C 59.69 (59.42), H 10.135 (10.27), Si 2.505 (3.67). **IR** (ATR, 32 scans, cm⁻¹): 2696.8, 2867.9, 1726.2, 1452.8, 1372.5, 1343.6, 1296.4, 1259.9, 1090.6, 1013.6, 925.8, 802.8. **GPC** (THF, 40 °C, g/mol): M_n=14054, M_w=66490, PDI=4.765.



Contact Angles measurements of fully-conv. Polysiloxane Polypropyleneglycol Copolymers:

Table A-4: Summary of the contact angles of the products **3.1a** to **3.32**; standard PDMS and PPG are added for comparison reasons; samples were cured into a standard PDMS formulation with an amount of 10% (s. Scheme A-2); the standard deviations were calculated from two to three repetitions.

Sample	PPG [wt-%]	CA t(0sec) [deg]	CA t(30sec) [deg]	CA t(60sec) [deg]	CA t(90sec) [deg]
PDMS		103.9 ± 8.27	106.4 ± 9.55	104.8 ± 9.90	104.6 ± 9.26
PPG		95.2 ± 4.24	93.6 ± 3.75	92.7 ± 3.82	92.3 ± 2.19
3.1a	30.95	104.1 ± 2.01	106.0 ± 2.10	102.7 ± 1.55	93.3 ± 2.90
3.2a	26.45	108.1 ± 3.04	89.4 ± 0.64	84.5 ± 0.71	83.5 ± 0.28
3.3a	16.32	92.5 ± 3.75	78.4 ± 4.45	77.5 ± 3.96	76.5 ± 3.46
3.4	50.72	98.6 ± 5.92	90.2 ± 4.39	87.7 ± 3.57	85.6 ± 3.48
3.5	61.68	100.6 ± 2.10	95.3 ± 0.50	91.1 ± 0.98	88.8 ± 0.65
3.6	68.66	102.0 ± 1.97	90.6 ± 1.86	86.6 ± 2.21	84.7 ± 2.00
3.7	72.97	109.3 ± 0.78	98.2 ± 1.98	94.1 ± 1.41	91.4 ± 3.54
3.8	48.47	108.2 ± 5.72	99.6 ± 3.24	94.0 ± 4.97	89.4 ± 4.81
3.9	60.34	106.1 ± 4.06	96.5 ± 2.70	91.5 ± 3.23	88.4 ± 3.40
3.10	67.77	107.0 ± 0.14	92.3 ± 4.60	88.8 ± 4.53	85.8 ± 2.90
3.11	72.85	97.6 ± 0.14	89.5 ± 0.71	84.3 ± 0.57	82.2 ± 0.21
3.12	22.77	102.1 ± 2.05	82.0 ± 1.70	79.9 ± 0.99	77.4 ± 0.28
3.13	27.32	86.1 ± 0.85	78.8 ± 0.00	74.3 ± 0.71	72.4 ± 0.35
3.14	31.45	94.4 ± 3.12	88.4 ± 2.19	83.2 ± 4.96	81.4 ± 4.09
3.15	35.14	72.7 ± 8.70	65.6 ± 4.53	64.9 ± 4.10	64.0 ± 3.46
3.16	38.46	81.6 ± 0.14	77.7 ± 0.57	72.4 ± 2.26	70.6 ± 2.12
3.17	41.45	81.9 ± 2.61	79.3 ± 1.65	76.9 ± 1.96	75.3 ± 3.01
3.18	44.13	107.9 ± 0.28	82.6 ± 6.86	80.2 ± 5.73	78.9 ± 5.87
3.19	52.89	81.0 ± 0.14	72.3 ± 4.03	65.1 ± 5.73	62.0 ± 5.44
3.20	57.84	102.4 ± 2.83	89.4 ± 2.47	84.9 ± 4.45	80.7 ± 3.89
3.21	61.84	94.7 ± 7.14	84.1 ± 4.74	78.7 ± 4.24	76.4 ± 3.04
3.22	66.13	105.0 ± 4.10	97.7 ± 3.82	88.9 ± 2.55	84.4 ± 2.55
3.23	68.76	104.9 ± 1.70	97.8 ± 0.99	92.8 ± 0.42	89.2 ± 0.64
3.24	71.70	95.3 ± 0.07	86.6 ± 0.64	80.6 ± 0.85	76.5 ± 0.64
3.25	72.01	103.1 ± 2.60	98.0 ± 2.60	94.6 ± 2.75	90.6 ± 5.38
3.26	76.64	82.5 ± 0.57	80.1 ± 1.91	77.9 ± 2.19	76.2 ± 2.33
3.27	77.92	101.4 ± 0.28	94.2 ± 3.46	91.6 ± 0.57	90.6 ± 0.99
3.28	82.43	103.1 ± 0.14	104.0 ± 0.64	104.2 ± 0.71	103.6 ± 0.14
3.29	85.40	98.6 ± 1.27	99.5 ± 1.48	98.7 ± 0.57	98.4 ± 0.64
3.30	87.52	100.1 ± 1.41	102.1 ± 1.70	101.6 ± 1.34	101.0 ± 0.78
3.31	89.10	99.2 ± 0.85	99.7 ± 1.41	98.9 ± 1.48	98.9 ± 2.19
3.32	90.32	99.4 ± 1.41	100.0 ± 1.34	100.5 ± 0.14	99.0 ± 0.14

Table A-5: Summary of the contact angles of the products **3.1a** to **3.32**; samples were cured in a homogeneous pure film (s. Scheme A-1); the standard deviations were calculated from two to three repetitions.

Sample	PPG [wt-%]	CA t(0sec) [deg]	CA t(30sec) [deg]	CA t(60sec) [deg]	CA t(90sec) [deg]
3.1a	30.95	102.8 ± 0.14	95.9 ± 4.74	91.8 ± 7.28	89.5 ± 8.56
3.2a	26.45	100.7 ± 6.15	71.7 ± 0.21	67.2 ± 0.71	65.9 ± 0.57
3.3a	16.32	99.8 ± 3.25	75.9 ± 0.49	71.9 ± 1.41	70.0 ± 1.67
3.4	50.72	83.7 ± 0.78	75.3 ± 0.07	73.4 ± 0.21	70.9 ± 1.41
3.5	61.68	74.1 ± 0.07	69.8 ± 2.40	68.7 ± 2.62	68.3 ± 2.62
3.6	68.66	89.7 ± 1.41	79.5 ± 1.77	77.6 ± 0.85	75.8 ± 0.92
3.7	72.97	99.8 ± 1.27	84.7 ± 3.82	78.8 ± 3.39	76.0 ± 4.45
3.8	48.47	92.4 ± 0.60	84.3 ± 1.84	79.6 ± 0.07	75.9 ± 0.71
3.9	60.34	104.2 ± 2.90	90.4 ± 3.46	76.2 ± 9.62	66.9 ± 4.81
3.10	67.77	97.6 ± 0.42	76.8 ± 1.13	69.7 ± 1.91	66.8 ± 1.77
3.11	72.85	99.5 ± 0.35	81.3 ± 9.12	74.9 ± 9.83	70.7 ± 7.64
3.12	22.77	94.0 ± 2.26	78.8 ± 1.56	73.3 ± 0.57	71.3 ± 0.00
3.13	27.32	76.7 ± 1.27	64.3 ± 0.21	61.0 ± 2.12	59.4 ± 1.56
3.14	31.45	82.3 ± 3.46	64.6 ± 1.48	61.0 ± 1.41	59.6 ± 0.99
3.15	35.14	74.0 ± 4.17	59.9 ± 0.57	55.2 ± 2.55	53.7 ± 2.40
3.16	38.46	66.6 ± 0.35	61.3 ± 4.38	58.9 ± 3.96	58.2 ± 4.24
3.17	41.45	71.4 ± 4.31	67.6 ± 2.83	65.3 ± 1.84	64.5 ± 0.92
3.18	44.13	87.7 ± 8.91	71.3 ± 5.80	66.2 ± 5.02	63.6 ± 6.79
3.19	52.89	84.7 ± 3.25	70.4 ± 2.40	66.4 ± 1.84	64.0 ± 0.92
3.20	57.84	86.4 ± 18.67	87.0 ± 1.91	81.4 ± 0.28	77.1 ± 1.41
3.21	61.84	88.0 ± 4.74	75.7 ± 3.68	69.8 ± 2.55	66.0 ± 0.21
3.22	66.13	110.8 ± 3.39	111.2 ± 3.18	108.0 ± 0.57	103.9 ± 0.92
3.23	68.76	79.2 ± 2.12	72.3 ± 3.25	71.3 ± 3.25	70.3 ± 3.39
3.24	71.70	77.6 ± 0.07	68.6 ± 1.77	66.1 ± 2.19	65.2 ± 1.56
3.25	72.01	88.8 ± 4.38	77.5 ± 5.30	71.8 ± 1.92	68.9 ± 3.68
3.26	76.64	72.0 ± 1.72	70.2 ± 2.19	67.5 ± 2.62	65.8 ± 1.91
3.27	77.92	85.1 ± 4.44	75.4 ± 3.54	72.4 ± 1.20	69.9 ± 0.78
3.28	82.43	96.8 ± 1.48	87.9 ± 3.04	82.5 ± 2.69	79.4 ± 1.34
3.29	85.40	93.0 ± 2.12	94.4 ± 1.91	94.3 ± 1.84	94.3 ± 2.76
3.30	87.52	93.7 ± 0.07	93.9 ± 0.07	93.8 ± 0.99	93.8 ± 0.85
3.31	89.10	94.4 ± 5.80	94.6 ± 5.73	94.3 ± 5.80	94.2 ± 6.86
3.32	90.32	99.8 ± 3.25	75.9 ± 0.49	71.9 ± 1.41	70.0 ± 1.63

Kinetic Studies of fully-converted Polysiloxane Propyleneglycol Copolymers:

Experiments were done made from SM-50 starting material to get optimized ratios of the different integrals. This correlates with products **3.1a**. The disappearance of the SiH function was followed by NMR. Samples withdrawn from the reaction medium with a syringe were cooled by adding cooled deuterated chloroform. The calibration of the chemical shifts in ^1H spectra was carried out by using the shifts of CDCl_3 (δH 7.26 ppm). The following data are the integrals compared to the integral of the Si- CH_3 signal at 0ppm and they are directly transferable to the percentage of unreacted SiH groups. Unfilled rows were not measured due to the individual monitoring at each temperature. The integrals of the formed product were measured, but due to the influence of the exothermic behavior the determination was not possible. Therefore, the data are not listed.

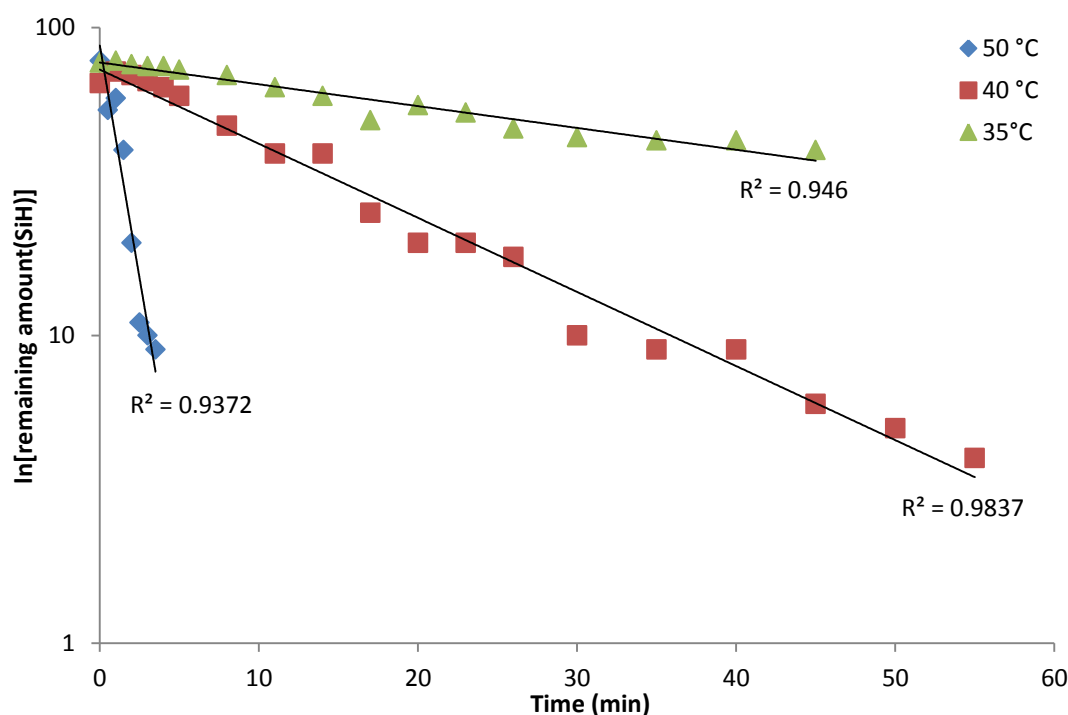


Figure A-6: Logarithmic-plotted diagram of time-resolved kinetic studies of hydrosilylation. The activation energy is about 206.7 ± 7.9 [kJ/(mol)].

Table A-6: Data of the kinetic studies of **3.1a** were calculated via integration of the ^1H -NMR analytics; unfilled rows were not measured due to the individual monitoring at each temperature, the equations are based on the slope of the trend line of the logarithmic plotted diagram (s. Figure 3-9).

Time [min]	Integral SiH (T=50 °C)	Integral SiH (T=40 °C)	Integral SiH (T=35 °C)
0	78	66	77
0.5	54	-	-
1	59	72	78
1.5	40	-	-
2	20	70	76
2.5	11	-	-
3	10	67	75
3.5	9	-	-
4	9	64	75
4.5	9	-	-
5	9	60	73
8	-	48	70
11	-	39	64
14	-	39	60
17	-	25	50
20	-	20	56
23	-	20	53
26	-	18	47
30	7	10	44
35	-	9	43
40	-	9	43
45	-	6	40
50	-	5	n/d
55	-	4	n/d
60	5	5	32
75	-	4	n/d
90	-	5	23
Equation	$y = 87.419e^{-0.697x}$	$y = 72.974e^{-0.055x}$	$y = 77.012e^{-0.016x}$

Anti-Adhesion Assay of full-converted Polysiloxane Propyleneglycol Copolymers:

The test results of the Anti-Adhesion Assay should be seen as trend-setting, but for a clear statement, further repetitions should be done. Table A-7 shows the data of sample **3.20** which was cured into a PDMS standard formulation with different amounts ranges from 0.5 to 80 %. Table A-8 summarizes the results of the samples which were cured into a PDMS standard formulation with an amount of 10 %.

Table A-7: Data of the Anti-Adhesion Assay of sample **3.20** which was cured into a PDMS standard formulation with different amounts ranges from 0.5 to 80%.

Sample Amount [%]	Germination Number Compared to Reference [%]
3.20 (0.5)	5
3.20 (1)	59
3.20 (10)	42 ± 39.42
3.20 (20)	66
3.20 (30)	81
3.20 (40)	92
3.20 (50)	68
3.20 (60)	104
3.20 (70)	179
3.20 (80)	996

Table A-8: Data of the Anti-Adhesion Assay of samples which were cured into a PDMS standard formulation with an amount of 10 %; n/s = not specified; the standard deviations were calculated from three repetitions.

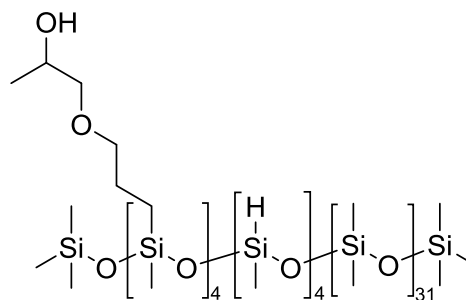
Sample	Germination Number Compared to Reference
	[%]
Reference	100.0 ± 3.80
3.1a	48.0
3.2a	9.0
3.3a	58.7 ± 36.91
3.4	37.5 ± 0.71
3.5	38.0 ± 9.90
3.6	37.09 ± 7.07
3.7	40.5 ± 13.44
3.8	24.3 ± 13.58
3.9	33.0 ± 10.44
3.10	23.3 ± 3.79
3.11	51.3 ± 18.58
3.12	n/s
3.13	n/s
3.14	n/s
3.15	n/s
3.16	n/s
3.17	n/s
3.18	51.0 ± 25.79
3.19	n/s
3.20	42.0 ± 39.43
3.21	n/s
3.22	70.3 ± 60.17
3.23	n/s
3.24	23.0 ± 3.00
3.25	n/s
3.26	n/s
3.27	75.0
3.28	128.0
3.29	83.0
3.30	100.0
3.31	70.5 ± 10.61
3.32	n/s

Synthesis of Polysiloxane Propyleneglycol Brush Copolymers with controlled partially Conversion:

Synthesis of poly(3-(2-hydroxypropoxy)propyl)methylsiloxane-co-polyhydridomethylsiloxane-co-polydimethylsiloxane (3.33a):

Product **3.33a** was synthesized (71 % yield) according to the representative procedure A, using 15 mL toluene, 0.6 mL 1-(allyloxy)propan-2-ol (5.17 mmol) and 5.0 mL SM-15 (2.27 mmol). 74 % conversion was obtained.

¹H-NMR (CDCl₃, 400 MHz, 24 °C, ppm): δ = 4.68 (s, 1H, SiH), 3.96 – 3.92 (m, 1H, -OCH₂CH(CH₃)OH), 3.45 – 3.35 (m, 3H, -CH₂OCH₂CHOH), 3.22 – 3.17 (m, 2H, -OCH₂CH(CH₃)OH), 2.39 (s, 1H, -OH), 1.67 – 1.58 (m, 2H, -SiCH₂CH₂CH₂O), 1.15 – 1.12 (d, 3H, -OCH₂CH(CH₃)OH), 0.56 – 0.46 (m, 2H, -SiCH₂CH₂O), 0.14 – 0.04 (m, 3H, -SiCH₃). **¹³C-NMR** (CDCl₃, 400 MHz, 25 °C, ppm): δ = 76.65

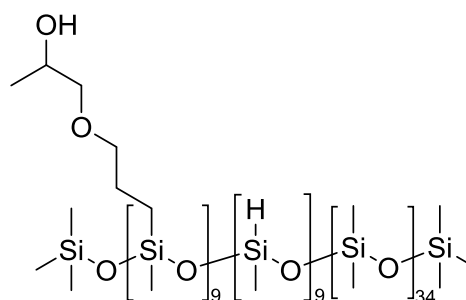


(OCH₂CH(CH₃)OH), 74.37 (-CH₂OCH₂), 66.86 (-OCH₂CH(CH₃)OH), 23.60 (-SiCH₂CH₂O), 19.00 (-CH₂CH(CH₃)OH), 13.88 (-SiCH₂CH₂O), 1.51 (Si-CH₃). **²⁹Si-NMR** (CDCl₃, 400 MHz, 24 °C, ppm): δ = 7.31 (-Si(CH₃)₃), -21.92 (O-Si-O), -37.65 (SiH). **IR** (ATR, 32 scans, cm⁻¹): 2961.8, 1412.3, 1257.7, 1011.1, 910.7, 789.4, 686.7. **GPC** (THF, 40 °C, g/mol): M_n=8172, M_w=69303, PD=8.481.

Synthesis of poly(3-(2-hydroxypropoxy)propyl)methylsiloxane-co-polyhydridomethylsiloxane-co-polydimethylsiloxane (3.34):

Product **3.34** was synthesized (65 % yield) according to the representative procedure A, using 0.5 mol% Pt supported on charcoal compared to siloxane starting material (10 % of Pt in the catalyst), 10 mL toluene, 0.72 mL 1-(allyloxy)propan-2-ol (5.64 mmol) and 2.5 mL SM-25 (0.66 mmol). The mixture was stirred for 24 hours (oil bath temperature: 90 °C) under inert atmosphere (Ar). 46 % conversion was obtained.

¹H-NMR (CDCl₃, 400 MHz, 24 °C, ppm): δ = 4.79 - 4.78 (s, 1H, SiH), 4.05 – 4.02 (m, 1H, -OCH₂CH(CH₃)OH), 3.54 – 3.45 (m, 3H, -CH₂OCH₂CHOH), 3.32 – 3.28 (t, 2H, -OCH₂CH(CH₃)OH), 2.89 (s, 1H, -OH), 1.75 – 1.69 (p, 2H, -SiCH₂CH₂CH₂O), 1.24 – 1.21 (d, 3H, -OCH₂CH(CH₃)OH), 0.65 – 0.59 (m, 2H, -SiCH₂CH₂O), 0.26 – 0.14 (m, 3H, -SiCH₃). **¹³C-NMR** (CDCl₃, 400 MHz, 25 °C, ppm): δ = 76.36

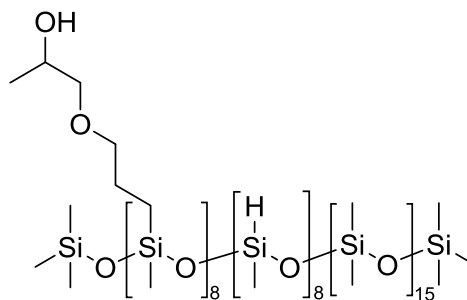


(-OCH₂CH(CH₃)OH), 74.03 (-CH₂OCH₂), 66.48 (-OCH₂CH(CH₃)OH), 23.26 (-SiCH₂CH₂O), 18.73 (-CH₂CH(CH₃)OH), 13.54 (-SiCH₂CH₂O), 1.16 (Si-CH₃). **²⁹Si-NMR** (CDCl₃, 400 MHz, 24 °C, ppm): δ = 7.32 (-Si(CH₃)₃), -21.21 - -22.55 (O-Si-O), -37.46 (SiH). **IR** (ATR, 32 scans, cm⁻¹): 2962.0, 2149.9, 1411.9, 1257.8, 1011.6, 909.5, 790.1, 701.3, 504.6. **GPC** (THF, 40 °C, g/mol): M_n=6109, M_w=11264, PD=1.844.

Synthesis of poly(3-(2-hydroxypropoxy)propyl)methylsiloxane-co-polyhydridomethylsiloxane-co-polydimethylsiloxane (3.35):

Product **3.35** was synthesized (88 % yield) according to the representative procedure A, using 0.5 mol% Pt supported on charcoal compared to siloxane starting material (10 % of Pt in the catalyst), 40 mL toluene, 2.16 mL 1-(allyloxy)propan-2-ol (17.05 mmol) and 4.97 mL SM-50 (2.27 mmol). The mixture was stirred for 24 hours (oil bath temperature: 90 °C) under inert atmosphere (Ar). 56 % conversion was obtained.

¹H-NMR (CDCl₃, 300 MHz, 24 °C, ppm): δ = 4.61 – 4.59 (s, 1H, SiH), 3.89 – 3.81 (m, 1H, -OCH₂CH(CH₃)OH), 3.39 – 3.24 (m, 3H, -CH₂OCH₂CHOH), 3.14 – 3.08 (t, 2H, -OCH₂CH(CH₃)OH), 2.58 (s, 1H, -OH), 1.60 – 1.46 (m, 2H, -SiCH₂CH₂CH₂O), 1.05 – 1.03 (d, 3H, -OCH₂CH(CH₃)OH), 0.47 – 0.37 (m, 2H, -SiCH₂CH₂O), 0.10 – 0.05 (m, 3H, -SiCH₃). **¹³C-NMR** (CDCl₃, 300 MHz, 25 °C, ppm): δ = 76.35



(-OCH₂CH(CH₃)OH), 73.98 (-CH₂OCH₂), 66.47 (-OCH₂CH(CH₃)OH), 23.24 (-SiCH₂CH₂O), 18.71 (-CH₂CH(CH₃)OH), 13.51 (-SiCH₂CH₂O), 1.18 (Si-CH₃). **²⁹Si-NMR** (CDCl₃, 300 MHz, 24 °C, ppm): δ = -20.90 (O-Si-O), -37.33 (SiH). **IR** (ATR, 32 scans, cm⁻¹): 2962.2, 2153.8, 1411.2, 1258.0, 1014.2, 907.0, 792.3, 756.3, 704.1. **GPC** (THF, 40 °C, g/mol): M_n=8280, M_w=48226, PD=5.824.

Table A-9: Summary of the parameter settings for the optimized synthetic pathway of half-converted polysiloxane propyleneglycol brush copolymers; unless otherwise indicated, the desired conversion is 50 % and the general reaction time is 24 hours.

Sample	Starting Material	c(SiH) [mol/L]	Solvent	Catalyst	Ratio SiH:C=C	Temperature [°C]	Converted Amount SiH [%]	Formed Amount SiCH ₂ [%]
3.33a	SM-15	0.5641	toluene	Karstedt	2:1	100	74.0	37.6
3.33b		0.3372	toluene	Karstedt	2:1	100	77.0	33.5
3.33c		0.1836	toluene	Karstedt	2:1	100	74.0	39.0
3.33d		0.1705	toluene	Karstedt	2:1	100	68.0	39.0
3.33e		0.1142	toluene	Karstedt	2:1	100	64.0	33.5
3.33f		0.0747	toluene	Karstedt	2:1	100	39.6	32.5
3.33g		0.0565	toluene	Karstedt	2:1	100	67.0	44.5
3.33h		0.0565	toluene	Karstedt	2:1	35	50.2	36.6
3.33i		0.0565	toluene	Karstedt	2:1	50	57.0	36.3
3.33j		0.0565	toluene	Karstedt	2:1	60	71.0	35.8
3.33k		0.0565	toluene	Karstedt	2:1	80	70.1	35.5
3.33l		0.0565	heptane	Karstedt	2:1	35	13.2	n.d.
3.33m		0.0565	THF	Karstedt	2:1	35	71.4	37.7
3.33n		0.3372	THF	Karstedt	2:1	100	70.9	43.1
3.33o		0.3372	toluene	Pt@C	2:1	100	47.0	35.4
3.34	SM-25	0.9057	toluene	Pt@C	2:1	120	46.0	78.0
3.34a		0.9057	toluene	Karstedt	2:1	120	77.0	71.0
3.34b		0.3767	toluene	Karstedt	2:1	120	77.0	77.0
3.34c		0.3604	toluene	Karstedt	2:1	120	51.0	77.0
3.34d		0.5159	toluene	Pt@C	2:1	100	64.0	37.5
3.35	SM-50	0.7325	toluene	Pt@C	2:1	90	56.0	38.5
3.35a		0.3224	toluene	Karstedt	2:1	35	71.0	33.5
3.35b		1.2719	toluene	Pt@C	2:1	100	53.0	35.5
3.35c		1.2719	toluene	Pt@C	2:1	100	62.0	38.0
3.35d		0.7325	toluene	Pt@C	2:1	100	59.0	36.5
3.35e ^a		0.7325	toluene	Pt@C	2:1	90	10.0	6.0
3.35f		0.7497	toluene	Pt@C	4:1	90	43.0	19.0
3.35g		0.7497	toluene	Pt@C	4:3	90	82.0	60.0

^a The reaction time was shortened to one hour.

Synthesis of half-converted Polysiloxane Polypropyleneglycol Copolymers:**Table A-10:** Summary of the products **3.36** to **3.39** made from **3.34** (SM-25), PPG wt-%, theoretically and experimental monomer unit, isolated yield and the Viscosity are listed; the results will be compared to products **3.8** to **3.11**; the standard deviations were calculated from two to three repetitions.

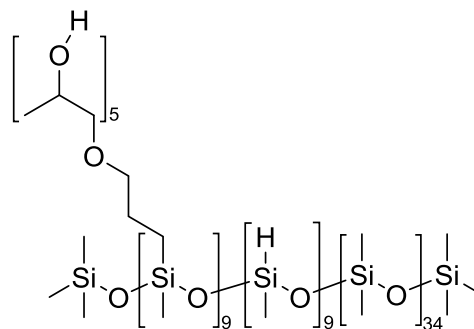
Sample	Starting Material	PPG [wt-%]	Monomer Unit (theor.)	Monomer Unit (exp.)	Isolated Yield [%]	Viscosity [Pas]
3.8	3.2a	59.34	3.25	3.61 ± 0.283	90 - 95	0.748 ± 0.1082
3.9		70.27	6.50	7.43 ± 0.177	90 - 97	1.348 ± 0.1655
3.10		76.56	9.75	10.51 ± 0.403	95 - 96	1.395 ± 0.1513
3.11		80.66	13.00	13.95 ± 0.099	93 - 95	1.938 ± 2.1397
3.36	3.34	50.50	5.34	3.17	89	2.939
3.37		63.80	10.68	5.78	95	9.590
3.38		71.47	16.01	8.72	93	11.500
3.39		76.46	21.35	11.91	95	8.289

Synthesis of poly((hydroxyl)-polypropyleneglycol)methylsiloxane-co-polyhydridomethylsiloxane-co-polydimethylsiloxane (3.36):

Product **3.36** was synthesized (89 % yield) according to the representative procedure B, using 5.0 g of **3.34** (1.044 mmol) and 3.5 mL of propylene oxide (50.02 mmol).

¹H-NMR (CDCl₃, 300 MHz, 24 °C, ppm): δ = 4.66 – 4.64 (s, 1H, SiH), 3.91 – 3.87 (m, 1H, O-CH₂-CH(CH₃)-OH), 3.70 – 3.61 (m, 3H, CH₂-O-CH₂-CH(CH₃)-OH), 3.55 – 3.44 (m, 2H, -O-CH₂-CH-), 3.38 – 3.33 (m, 1H, O-CH₂-CH(CH₃)-OH), 3.18 (t, 1H, -O-CH₂-CH-), 2.45 (s, 1H, -OH), 1.61 – 1.55 (m, 2H, -Si-CH₂-CH₂-), 1.15 (d, 3H, CH₃-CH-), 1.11 – 1.04 (d, 3H, CH₃-CH-), 0.50 – 0.44 (t, 2H, -Si-CH₂-), 0.12 – 0.00 (s, 3H, -Si-CH₃). **¹³C-NMR** (CDCl₃, 300 MHz, 25 °C, ppm): δ = 75.96

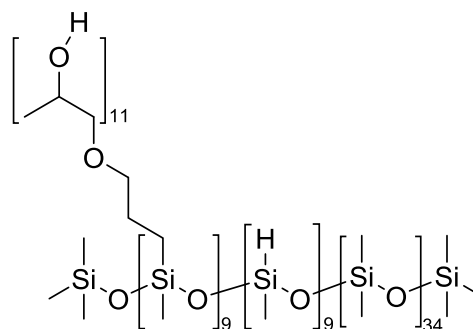
– 75.51 (-Si-CH₂-CH₂-CH₂-), 74.26 – 74.20 (-O-CH₂-CH-), 73.75 - 73.39 (-O-CH₂-CH-), 66.69 (-O-CH₂-CH-), 23.49 (-Si-CH₂-CH₂-), 18.98 (CH₃-CH-), 17.86 – 17.63 (CH₃-CH-), 13.78 (-Si-CH₂-), 1.47 – 1.15 (-Si-CH₃). **²⁹Si-NMR** (CDCl₃, 300 MHz, 24 °C, ppm): δ = -7.20 (-Si(CH₃)₃), -19.20 – -22.27 (O-Si-O), -37.53 (SiH). **GPC** (THF, 40 °C, g/mol): M_n=8500, M_w=31633, PDI=3.722.



Synthesis of poly((hydroxyl)-polypropyleneglycol)methylsiloxane-co-polyhydridomethylsiloxane-co-polydimethylsiloxane (3.37):

Product **3.37** was synthesized (95 % yield) according to the representative procedure B, using 5.0 g **3.34** (1.044 mmol) and 7.0 mL of propylene oxide (100.03 mmol).

¹H-NMR (CDCl₃, 300 MHz, 24 °C, ppm): δ = 4.61 (s, 1H, SiH), 3.87 – 3.83 (m, 1H, O-CH₂-CH(CH₃)-OH), 3.66 – 3.60 (m, 3H, CH₂-O-CH₂-CH(CH₃)-OH), 3.51 – 3.42 (m, 2H, -O-CH₂-CH-), 3.34 – 3.30 (m, 1H, O-CH₂-CH(CH₃)-OH), 3.13 (t, 1H, -O-CH₂-CH-), 2.49 (s, 1H, -OH), 1.58 – 1.52 (m, 2H, -Si-CH₂-CH₂-), 1.18 (d, 3H, CH₃-CH-), 1.07 – 1.04 (d, 3H, CH₃-CH-), 0.46 – 0.41 (t, 2H, -Si-CH₂-), 0.06 – -0.04 (s, 3H, -Si-CH₃). **¹³C-NMR** (CDCl₃, 300 MHz, 25 °C, ppm): δ =

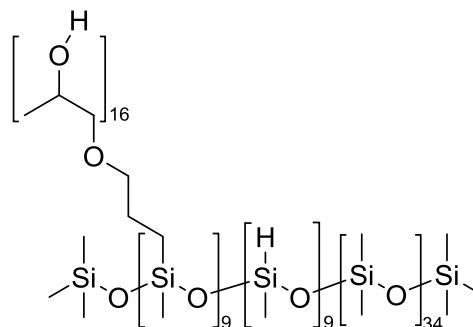


75.56 – 75.10 (-Si-CH₂-CH₂-CH₂-), 73.35 (-O-CH₂-CH-), 72.99 – 72.86 (-O-CH₂-CH-), 66.24 (-O-CH₂-CH-), 23.08 (-Si-CH₂-CH₂-), 18.30 (CH₃-CH-), 17.44 – 17.25 (CH₃-CH-), 14.08 (-Si-CH₂-), 1.75 – 0.74 (-Si-CH₃). **²⁹Si-NMR** (CDCl₃, 300 MHz, 24 °C, ppm): δ = -7.12 (-Si(CH₃)₃), -19.26 – -22.05 (O-Si-O), -37.69 (SiH). **GPC** (THF, 40 °C, g/mol): M_n=8252, M_w=29754, PDI=3.606.

Synthesis of poly((hydroxyl)-polypropyleneglycol)methylsiloxane-co-polyhydridomethylsiloxane-co-polydimethylsiloxane (3.38):

Product **3.38** was synthesized (93 % yield) according to the representative procedure B, using 5.0 g **3.34** (1.044 mmol) and 10.5 mL of propylene oxide (150.05 mmol).

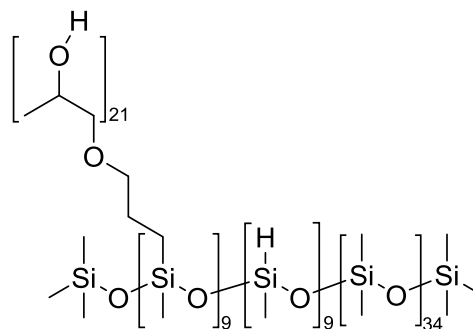
¹H-NMR (CDCl₃, 300 MHz, 24 °C, ppm): δ = 4.63 – 4.62 (s, 1H, SiH), 3.89 – 3.85 (m, 1H, O-CH₂-CH(CH₃)-OH), 3.66 – 3.56 (m, 3H, CH₂-O-CH₂-CH(CH₃)-OH), 3.50 – 3.44 (m, 2H, -O-CH₂-CH-), 3.38 – 3.28 (m, 1H, O-CH₂-CH(CH₃)-OH), 3.15 (t, 1H, -O-CH₂-CH-), 2.43 (s, 1H, -OH), 1.60 – 1.54 (m, 2H, -Si-CH₂-CH₂-), 1.30 – 1.27 (d, 3H, CH₃-CH-), 1.14 – 1.02 (d, 3H, CH₃-CH-), 0.48 – 0.45 (t, 2H, -Si-CH₂-), 0.09 – -0.02 (s, 3H, -Si-CH₃). **¹³C-NMR** (CDCl₃, 300 MHz, 25 °C, ppm): δ = 75.87 – 75.02 (-Si-CH₂-CH₂-CH₂-), 73.55 – 73.01 (-O-CH₂-CH-), 72.87 (-O-CH₂-CH-), 66.33 (-O-CH₂-CH-), 23.12 (-Si-CH₂-CH₂-), 18.56 (CH₃-CH-), 17.48 – 17.26 (CH₃-CH-), 13.41 (-Si-CH₂-), 1.4780 – 0.87 (-Si-CH₃). **²⁹Si-NMR** (CDCl₃, 300 MHz, 24 °C, ppm): δ = -7.18 (-Si(CH₃)₃), -20.62 – -22.14 (O-Si-O), -37.65 (SiH). **GPC** (THF, 40 °C, g/mol): M_n=9014, M_w=27471, PDI=3.048.



Synthesis of poly((hydroxyl)-polypropyleneglycol)methylsiloxane-co-polyhydridomethylsiloxane-co-polydimethylsiloxane (3.39):

Product **3.39** was synthesized (95 % yield) according to the representative procedure B, using 5.0 g **3.34** (1.044 mmol) and 14.0 mL of propylene oxide (200.07 mmol).

¹H-NMR (CDCl₃, 300 MHz, 24 °C, ppm): δ = 4.68 – 4.63 (s, 1H, SiH), 3.92 – 3.85 (m, 1H, O-CH₂-CH(CH₃)-OH), 3.67 – 3.61 (m, 3H, CH₂-O-CH₂-CH(CH₃)-OH), 3.57 – 3.44 (m, 2H, -O-CH₂-CH-), 3.39 – 3.28 (m, 1H, O-CH₂-CH(CH₃)-OH), 3.19 – 3.08 (t, 1H, -O-CH₂-CH-), 2.35 (s, 1H, -OH), 1.64 – 1.52 (m, 2H, -Si-CH₂-CH₂-), 1.32 – 1.27 (d, 3H, CH₃-CH-), 1.11 – 1.04 (d, 3H, CH₃-CH-), 0.52 – 0.41 (t, 2H, -Si-CH₂-), 0.10 – 0.00 (s, 3H, -Si-CH₃). **¹³C-NMR** (CDCl₃, 300 MHz,



25 °C, ppm): δ = 75.62 – 75.17 (-Si-CH₂-CH₂-CH₂-), 73.42 – 73.03 (-O-CH₂-CH-), 72.89 (-O-CH₂-CH-), 66.37 (-O-CH₂-CH-), 23.16 (-Si-CH₂-CH₂-), 18.16 (CH₃-CH-), 17.52 – 17.30 (CH₃-CH-), 13.45 (-Si-CH₂-), 1.09 – 0.92 (-Si-CH₃). **²⁹Si-NMR** (CDCl₃, 300 MHz, 24 °C, ppm): δ = -7.20 (-Si(CH₃)₃), -20.58 – -21.97 (O-Si-O), -37.63 (SiH). **GPC** (THF, 40 °C, g/mol): M_n=8459, M_w=23775, PDI=2.811.

A4. Appendix to Part IIa

Synthesis of Halogenalkyl functionalized Siloxanes:

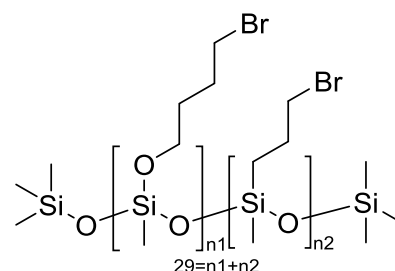
Table A-11: Summary of the products **4.1a** to **4.6**; unless otherwise indicated, the desired conversion of SiH groups is 100 % and the general reaction time is 24 hours; the yields are calculated from the average of several experiments.

Sample	Starting Material	Catalyst	Yield Halosilation [%]	Yield Hydrosilylation [%]	Isolated Yield [%]	Viscosity [Pas]
4.1a	SM-100	Karstedt	83.5 ± 4.84	16.7 ± 0.36	71 - 93	0.644 ± 0.196
4.1b		PdCl ₂	104.5 ± 2.90	0.0	87 - 95	2.031
4.2	SM-50	Karstedt	92.0 ± 0.52	9.4 ± 1.71	82 - 88	0.145 ± 0.007
4.3	SM-25	Karstedt	85.3 ± 1.34	4.4 ± 0.56	75 - 82	0.119 ± 0.015
4.4	SM-15	Karstedt	98.5 ± 1.61	2.4 ± 0.49	79 - 90	0.062 ± 0.005
4.5a	D ₃ D ^H	Karstedt	92.0 ± 5.14	0.0	57 - 84	0.008 ± 0.001
4.5b		PdCl ₂	82.2 ± 3.39	0.0	65 - 83	0.007
4.6	D ^H ₄	Karstedt	71.2 ± 0.93	13.8 ± 0.50	63 - 79	0.221 ± 0.039

Synthesis of poly(4-bromobutoxy)methylsiloxane (4.1a):**Representative procedure C:**

200 µL of Karstedt (2 % of Pt in the catalyst, 0.1 % mol in the mixture, 0.45 mmol) and 50 mL dried toluene were added into the flask under argon atmosphere and stirred at room temperature (20 °C) for a couple of minutes. Then dried THF (18.5 mL, 228.72 mmol) and allyl bromide (19.8 mL, 228.81 mmol) were added into the system. SM-100 (14.9 mL, 7.89 mmol, Mn 1900 g/mol) were added dropwise. The mixture was stirred and refluxed (oil bath temperature: 120 °C) under inert atmosphere (Ar) until complete conversion of the Si-H groups was achieved (the reaction was followed by ¹H-NMR). The mixture (when necessary) was decolorized by adding activated carbon and an excess of pentane and stirred for 16 h at room temperature. The crude was filtrated trough celite, and the solvents and volatiles were filtered off using Schlenk technique. The obtained product (yield 80-90 %, 7.15 mmol) was a colorless, transparent viscous liquid.

¹H-NMR (400 MHz, CDCl₃, 25 °C, ppm): δ = 3.75 – 3.64 (t, 2H, -O-CH₂-), 3.46 – 3.32 (m, 4H, -CH₂-Br, -CH₂-CH₂-CH₂-Br), 1.96 – 1.83 (p, 4H, -CH₂-CH₂-Br, -CH₂-CH₂-CH₂-Br), 1.71 – 1.64 (m, 2H, -O-CH₂-CH₂-), 0.69 (m, 2H, -CH₂-CH₂-CH₂-Br), 0.14 – 0.07 (s, 3H; -CH₃). **¹³C-NMR** (400 MHz, CDCl₃, 25 °C, ppm): δ = 61.36 (-O-CH₂-), 36.74 (-CH₂-CH₂-CH₂-Br), 33.72 (-CH₂-Br), 30.97 (-O-CH₂-CH₂-), 29.45 (-CH₂-CH₂-Br), 28.48 (-CH₂-CH₂-CH₂-Br), 26.8 (-CH₂-CH₂-CH₂-Br), -4.00 (-CH₃). **²⁹Si-NMR** (400 MHz, CDCl₃, 24 °C, ppm): δ = 9.13 (-Si(CH₃)₃), -58.84 (-O-Si(Me)-O_{2/2}).



774.04, 645.53, 560.81, 433.80. **EA** (% , measured (calculated)), repeating unit $C_5H_{11}BrO_2Si$: C 28.28 (28.2), H 6.22 (6.2), Br 33.2025 (37.5), Si 14.319 (13.2). **GPC** (THF, 40 °C, g/mol): $M_n=3238$, $M_w=10782$, PDI=3.386.

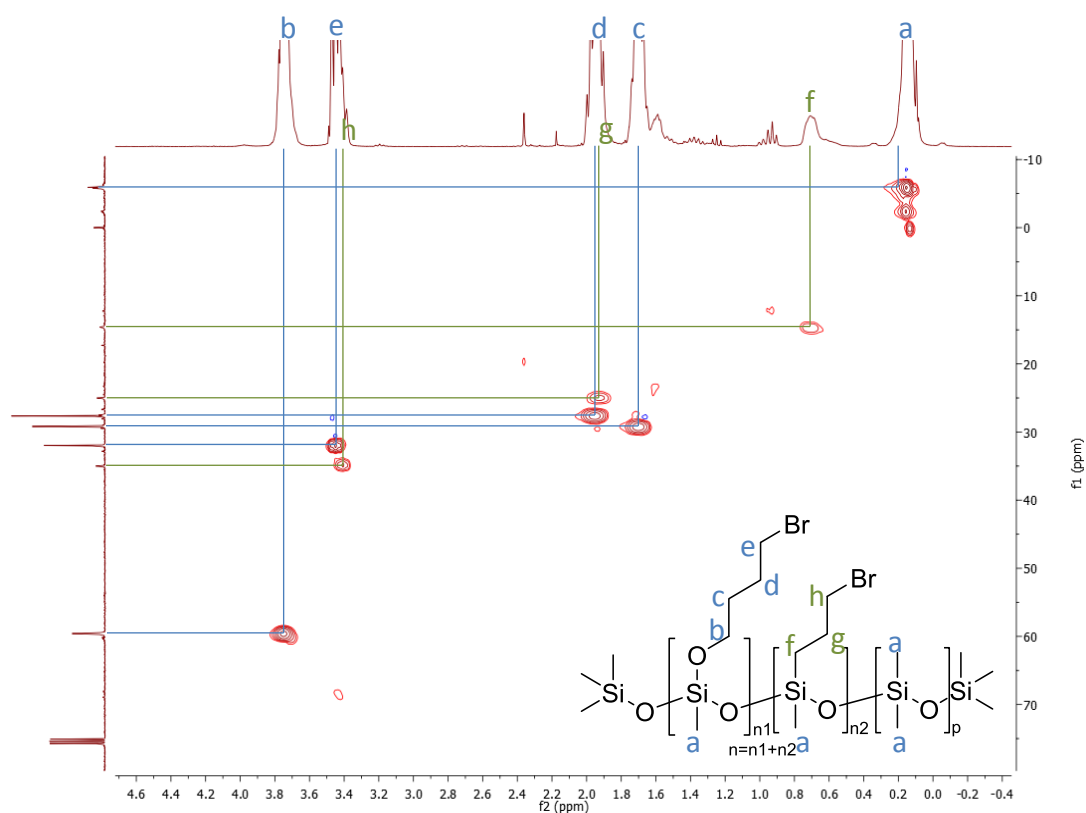


Figure A-7: 1H - ^{13}C -HSQC-NMR of **4.1a** in deuterated chloroform (400 MHz, 24 °C); the overlapping of the signals of the halosilated and hydrosilylated products are shown.

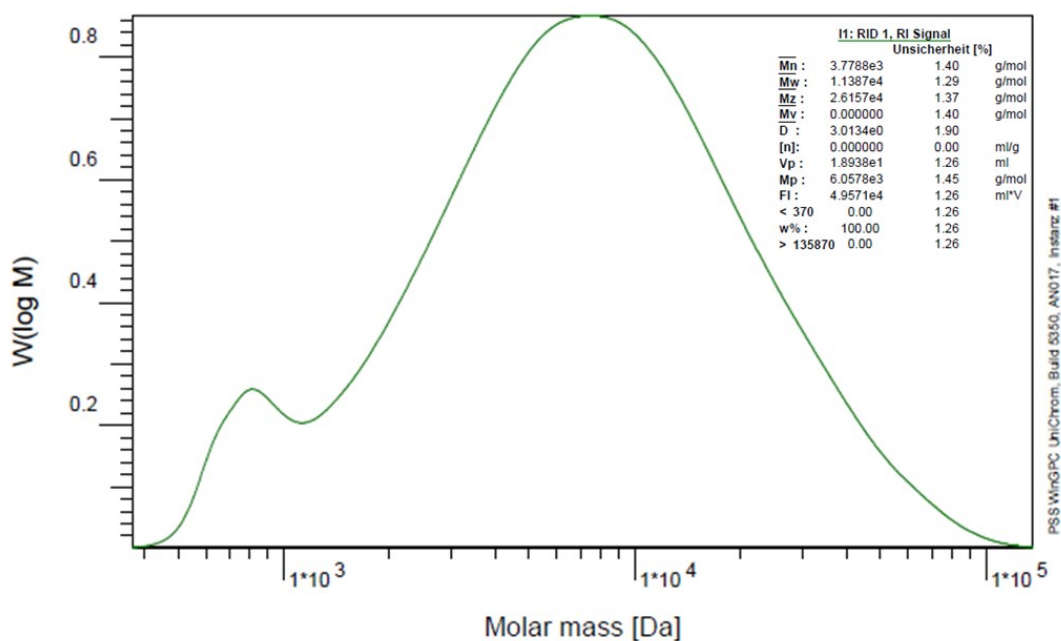


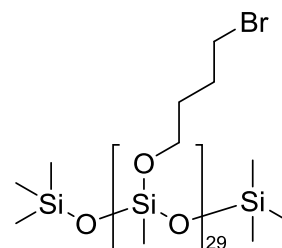
Figure A-8: GPC result of **4.1a** in THF (shown GPC results are an average of two measurements).

Synthesis of poly(4-bromobutoxy)methylsiloxane (**4.1b**):

Representative procedure D.^[111d]

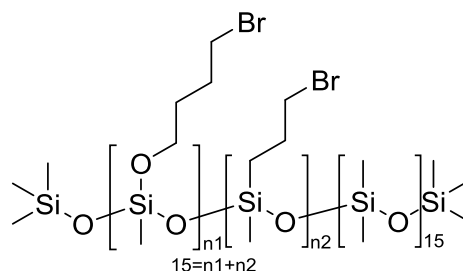
PdCl₂ (417 mg, 1.6 mol-% in the mixture, 2.35 mmol) and dried THF (37.1 mL, 168.61 mmol) were added into the flask under argon atmosphere and stirred at room temperature (20 °C) for a couple of minutes. Then allyl bromide (7.29 mL, 457.63 mmol) was added into the system. SM-100 (9.9 mL, 5.26 mmol, Mn 1900 g/mol) were added dropwise. The mixture was stirred (oil bath temperature: 50 °C) under inert atmosphere (Ar) for 24 hours. The mixture (when necessary) was decolorized by adding activated carbon and an excess of pentane and stirred for 16 h at room temperature. The crude was filtrated through celite, and the solvents and volatiles were evaporated under vacuum. The obtained product (yield 70 %; 4.63 mmol) was a yellow to black viscous liquid with precipitation.

¹H-NMR (400 MHz, CDCl₃, 24 °C, ppm): δ = 3.63 – 3.58 (m, 2H, -O-CH₂-), 3.33 – 3.28 (m, 2H, -CH₂-Br), 1.86 – 1.76 (p, 2H, -CH₂-CH₂-Br), 1.61 – 1.52 (m, 2H, -O-CH₂-CH₂-), 0.08 – 0.06 (s, 3H; -CH₃). **¹³C-NMR** (400 MHz, CDCl₃, 24 °C, ppm): δ = 61.39 (-O-CH₂-), 33.77 (-CH₂-Br), 30.98 (-O-CH₂-CH₂-), 29.45 (-CH₂-CH₂-Br), -4.15 (-CH₃). **²⁹Si-NMR** (400 MHz, CDCl₃, 24 °C, ppm): δ = -58.68 (-O-Si(Me)-O_{2/2}). **IR** (ATR, 32 scans, cm⁻¹): 2940.3, 2874.4, 1439.4, 1267.4, 1250.3, 1020.6, 971.4, 846.5, 772.2, 644.4, 560.0. **EA** (% , measured (calculated)), repeating unit C₅H₁₁BrO₂Si: C 28.3 (28.2), H 5.80 (6.2), Br 32.49 (37.5). **GPC** (THF, 40 °C, g/mol): M_n=4804, M_w=11998, PDI=2.505.

Synthesis of poly(4-bromobutoxy)methylsiloxane-co-polydimethylsiloxane (4.2):

Product **4.2** was synthesized (82-88 % yield, 8.01 mmol) according to the representative procedure C, using 20.0g of SM-50 (9.09 mmol, Mn 2200 g/mol), 40.0 mL dried THF (493.7 mmol), 11.8 mL allyl bromide (136.34 mmol) and 270 μL Karstedt (0.61 mmol). The reaction was carried out in dried THF.

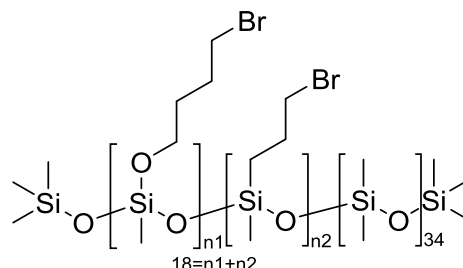
¹H-NMR (300 MHz, CDCl₃, 24 °C, ppm): δ = 3.65 – 3.55 (t, 2H, -O-CH₂-), 3.34 – 3.25 (m, 4H, -CH₂-Br, -CH₂-CH₂-CH₂-Br), 1.87 – 1.78 (p, 4H, -CH₂-CH₂-Br, -CH₂-CH₂-CH₂-Br), 1.61 – 1.48 (p, 2H, -O-CH₂-CH₂-), 0.57 – 0.52 (m, 2H, -CH₂-CH₂-CH₂-Br), 0.03 – 0.07 (s, 3H; -CH₃). **¹³C-NMR** (300 MHz, CDCl₃, 24 °C, ppm): δ = 61.24 (-O-CH₂-), 34.65 (-CH₂-CH₂-CH₂-Br), 33.79 (-CH₂-Br), 30.99 (-O-CH₂-CH₂-), 29.49 (-CH₂-CH₂-Br), 28.50 (-CH₂-CH₂-CH₂-Br), 26.31 (-CH₂-CH₂-CH₂-Br), 1.19, -4.00 (-CH₃). **²⁹Si-NMR** (300 MHz, CDCl₃, 24 °C, ppm): δ = -21.30 (-O-Si(Me)₂-O-), -58.85 (-O-Si(Me)-O_{2/2}). **IR** (ATR, 32 scans, cm⁻¹): 2960.5, 1440.4, 1259.1, 1014.1, 841.7, 780.2, 646.6, 561.5. **EA** (% , measured (calculated)), repeating unit C₇H₁₇BrO₃Si₂: C 29.86 (29.47), H 6.127 (6.01), Br 24.724 (28.01). **GPC** (THF, 40 °C, g/mol): M_n=2882, M_w=6166, PDI=1.896.



Synthesis of poly(4-bromobutoxy)methylsiloxane-co-polydimethylsiloxane (4.3):

Product **4.3** was synthesized (75-82 % yield, 4.01 mmol) according to the representative procedure C, using 20.0 g of SM-25 (5.26 mmol, Mn 3800 g/mol), 35.0 mL dried THF (432.0 mmol), 7.7 mL allyl bromide (89.48 mmol) and 130 μ L Karstedt (0.19 mmol). The reaction was carried out in dried THF.

¹H-NMR (300 MHz, CDCl₃, 24 °C, ppm): δ = 3.75 – 3.69 (t, 2H, -O-CH₂-), 3.45 – 3.41 (t, 4H, -CH₂-Br, -CH₂-CH₂-CH₂-Br), 1.99 – 1.89 (p, 4H, -CH₂-CH₂-Br, -CH₂-CH₂-CH₂-Br), 1.72 – 1.63 (p, 2H, -O-CH₂-CH₂-), 0.69 – 0.612 (m, 2H, -CH₂-CH₂-CH₂-Br), 0.14 – 0.04 (s, 3H; -CH₃). **¹³C-NMR**



(300 MHz, CDCl₃, 24 °C, ppm): δ = 61.23 (-O-CH₂-), 33.83 (-CH₂-Br), 31.02 (-O-CH₂-CH₂-), 29.51 (-CH₂-CH₂-Br),

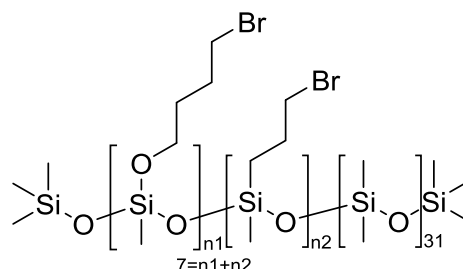
1.20, -3.80 (-CH₃). **²⁹Si-NMR** (300 MHz, CDCl₃, 24 °C, ppm): δ = -21.20 – -21.90 (-O-Si(Me)₂-O-), -58.70 (-O-Si(Me)-O_{2/2}). **IR** (ATR, 32 scans, cm⁻¹): 2961.3, 1411.3, 1258.1, 1011.2, 789.9, 701.8, 562.7.

EA (% , measured (calculated)), repeating unit C₉H₂₃BrO₄Si₃: C 29.165 (30.53), H 6.417 (6.64), Br 17.47 (20.68). **GPC** (THF, 40 °C, g/mol): M_n=4438, M_w=20763, PDI=2.085.

Synthesis of poly(4-bromobutoxy)methylsiloxane-co-polydimethylsiloxane (4.4):

Product **4.4** was synthesized (79-90 % yield, 7.15 mmol) according to the representative procedure C, using 25.0 g of SM-15 (8.62 mmol, Mn 2900 g/mol), 30.0 mL dried THF (370.3 mmol), 4.47 mL allyl bromide (51.72 mmol) and 180 μ L Karstedt (0.40 mmol). The reaction was carried out in dried THF.

¹H-NMR (400 MHz, CDCl₃, 24 °C, ppm): δ = 3.73 – 3.70 (t, 2H, -O-CH₂-), 3.45 – 3.41 (t, 4H, -CH₂-Br, -CH₂-CH₂-CH₂-Br), 1.96 – 1.91 (p, 4H, -CH₂-CH₂-Br, -CH₂-CH₂-CH₂-Br), 1.71 – 1.66 (p, 2H, -O-CH₂-CH₂-), 0.65 – 0.63 (m, 2H, -CH₂-CH₂-CH₂-Br), 0.13 – 0.05 (s, 3H; -CH₃). **¹³C-NMR**



(400 MHz, CDCl₃, 24 °C, ppm): δ = 61.19 (-O-CH₂-), 34.72 (-CH₂-CH₂-CH₂-Br), 33.76 (-CH₂-Br), 31.03 (-O-CH₂-CH₂-),

29.54 (-CH₂-CH₂-Br), 1.94 – 0.83, -3.79 (-CH₃). **²⁹Si-NMR** (400 MHz, CDCl₃, 24 °C, ppm): δ = -7.22 (-Si(CH₃)₃), -21.02 – -22.09 (-O-Si(Me)₂-O-), -58.86 – 58.91 (-O-Si(Me)-O_{2/2}). **IR** (ATR, 32 scans, cm⁻¹): 2961.5, 1411.8, 1257.7, 1010.5, 787.0, 687.2, 563.4.

EA (% , measured (calculated)), repeating unit C₁₇H₄₇BrO₈Si₇: C 29.875 (31.12), H 6.381 (7.22), Br 17.44 (12.18). **GPC** (THF, 40 °C, g/mol): M_n=3762, M_w=6417, PDI=1.711.

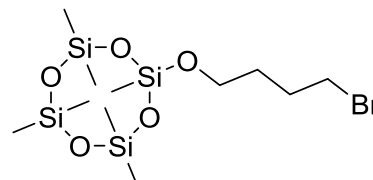
Synthesis of 1-(4-bromobutoxy)-1',3,3',5,5',7,7'-Heptamethylcyclotetrasiloxane (4.5a):

Product **4.5a** was synthesized (84 % yield, 42.46 mmol) according to the representative procedure C, using 15.8 mL of D₃D^H (53.18 mmol), dried THF (20 mL, 246.85 mmol), allyl bromide (4.59 mL, 53.16 mmol) and 400 μ L Karstedt (0.90 mmol). The reaction was carried out in dried THF.

¹H-NMR (400 MHz, CDCl₃, 24 °C, ppm): δ = 3.65 – 3.62 (t, 2H, -O-CH₂-), 3.35 – 3.32 (t, 2H, -CH₂-Br), 1.89 – 1.81 (p, 2H, -CH₂-CH₂-Br), 1.63 – 1.55 (p, 2H, -O-CH₂-CH₂-), 0.02 – 0.00 (s, 3H; -CH₃).

¹³C-NMR (400 MHz, CDCl₃, 24 °C, ppm): δ = 61.64 (-O-CH₂-), 34.12 (-CH₂-Br), 31.31 (-O-CH₂-CH₂-), 29.80 (-CH₂-CH₂-Br), -1.56 –

-1.03 (-CH₃), -3.64. ²⁹Si-NMR (400 MHz, CDCl₃, 24 °C, ppm): δ = -18.24 – -19.31 (Si(Me)₂-O_{2/2}), -56.93 (-O-Si(Me)-O_{2/2}). IR (ATR, 32 scans, cm⁻¹): 2962.5, 1409.7, 1259.2, 1051.2, 798.4, 699.2, 665.6, 559.9. EA (% , measured (calculated)), repeating unit C₁₁H₂₉BrO₅Si₄: C 27.31 (30.47), H 6.15 (6.74), Br 15.81 (18.43), Si 10.36 (25.91). GPC (THF, 40 °C, g/mol): M_n=438, M_w=467, PDI=1.066.

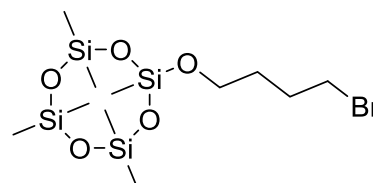
Synthesis of 1-(4-bromobutoxy)-1',3,3',5,5',7,7'-Heptamethylcyclotetrasiloxane (4.5b):

Product **4.5b** was synthesized (65-83 % yield, 7.40 mmol) according to the representative procedure C, using 2.5 mL of D₃D^H (8.86 mmol), dried THF (5.0 mL, 61.71 mmol), allyl bromide (0.84 mL, 9.74 mmol) and 24 mg PdCl₂ (0.14 mmol).

¹H-NMR (400 MHz, CDCl₃, 24 °C, ppm): δ = 3.75 – 3.72 (t, 2H, -O-CH₂-), 3.45 – 3.41 (t, 2H, -CH₂-Br), 1.98 – 1.91 (p, 2H, -CH₂-CH₂-Br), 1.72 – 1.65 (p, 2H, -O-CH₂-CH₂-), 0.14 – 0.07 (s, 3H; -CH₃).

¹³C-NMR (400 MHz, CDCl₃, 24 °C, ppm): δ = 61.65 (-O-CH₂-), 34.09 (-CH₂-Br), 31.31 (-O-CH₂-CH₂-), 29.80 (-CH₂-CH₂-Br), -1.53 –

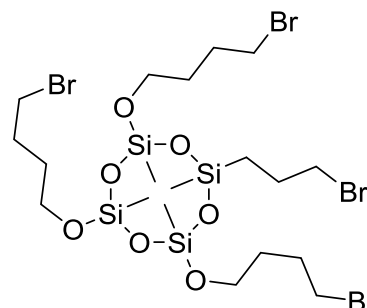
0.66 (-CH₃), -3.80. ²⁹Si-NMR (400 MHz, CDCl₃, 24 °C, ppm): δ = -18.55 – -21.26 (Si(Me)₂-O_{2/2}), -56.92 (-O-Si(Me)-O_{2/2}). IR (ATR, 32 scans, cm⁻¹): 2962.7, 1410.0, 1259.3, 1051.2, 799.0, 698.9, 665.1, 647.1, 559.5. EA (% , measured (calculated)), repeating unit C₁₁H₂₉BrO₅Si₄: C 24.07 (30.47), H 6.048 (6.74), Br 13.67 (18.43), Si 7.46 (25.91). GPC (THF, 40 °C, g/mol): M_n=384, M_w=410, PDI=1.075.



Synthesis of 1,3,5,7-Tetra(4-bromobutoxy)-1',3',5',7'-Tetramethylcyclotetrasiloxane (4.6):

Product **4.6** was synthesized (63-79% yield, 49.89 mmol) according to the representative procedure C, using 15.1 mL of D^H₄ (623.50 mmol), dried THF (50.0 mL, 617.11 mmol), allyl bromide (21.60 mL, 249.99 mmol) and 1000 µL Karstedt (2.24 mmol). The reaction was carried out in dried THF.

¹H-NMR (400 MHz, CDCl₃, 24 °C, ppm): δ = 4.83 – 4.75 (s, 1H, SiH), 3.68 – 3.54 (t, 2H, -O-CH₂-), 3.33 – 3.25 (m, 2H, -CH₂-Br), 1.84 – 1.74 (m, 2H, -CH₂-CH₂-Br), 1.61 – 1.52 (p, 2H, -O-CH₂-CH₂-), 0.07 – -0.10 (s, 3H; -CH₃). **¹³C-NMR** (400 MHz, CDCl₃, 24 °C, ppm): δ = 62.45 (-O-CH₂-), 33.72 (-CH₂-Br), 30.92 (-O-CH₂-CH₂-), 29.36 (-CH₂-CH₂-Br), -4.16 (-CH₃). **²⁹Si-NMR** (400 MHz, CDCl₃, 24 °C, ppm): δ = -58.49 - -59.12 (-O-Si(Me)-O_{2/2}). **IR** (ATR, 32 scans, cm⁻¹): 2939.0, 2872.3, 1437.1, 1266.5, 1024.4, 848.6, 769.5, 645.3, 560.3. **EA** (% , measured (calculated)), repeating unit C₂₀H₄₄Br₄O₈Si₄: C 29.77 (28.44), 6.43 (5.25), Br 32.34 (37.85), Si 13.67 (13.3). **GPC** (THF, 40 °C, g/mol): M_n=384, M_w=410, PDI=1.075.



Kinetic Studies of Halogenalkyl functionalized Siloxanes:

Experiments were done based on SM-100 starting material to get optimized ratios of the different integrals. The experiments correlate with products **4.1a** and **4.1b**. The disappearance of the SiH functionality as well as the forming of the halosilated product were followed by NMR. Samples withdrawn from the reaction medium with a syringe (0.1 mL) were cooled by adding cooled deuterated chloroform (0.5 mL). The calibration of the chemical shifts in ^1H spectra was carried out by using the shifts of CDCl_3 (δH 7.26 ppm). The following data are the integrals compared to the integral of the Si- CH_3 signal at 0ppm and they are directly transferable to the percentage of unreacted SiH groups *resp.* the formed Si-O-R signals.

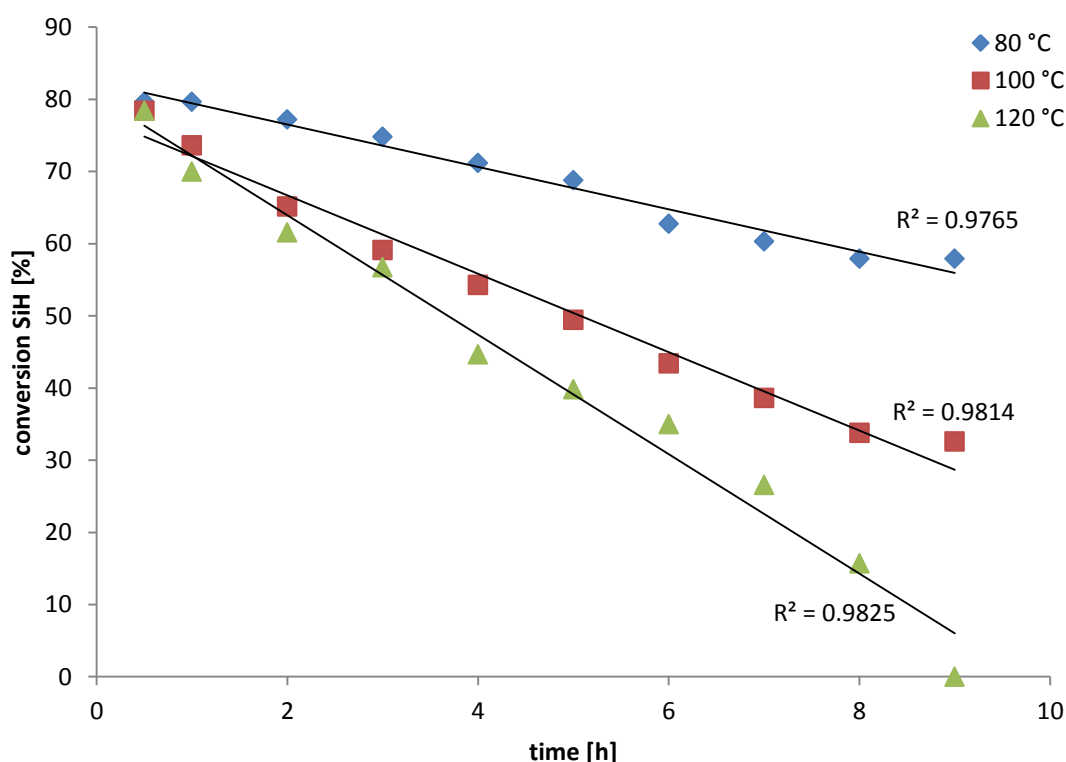


Figure A-9: Kinetic studies of sample **4.1a** at different temperatures; the reaction follows zero order depending on the siloxane. The activation energy is about 47.4 ± 2.2 kJ/(mol).

Table A-12: Data of the kinetic studies of **4.1a** calculated by integration of the $^1\text{H-NMR}$ analytics; the equations are based on the slope of the trend line (s. Figure A-9).

Time [h]	Integral SiH (T=120 °C)	Integral Si-OR (T=120 °C)	Integral SiH (T=100 °C)	Integral Si-OR (T=100 °C)	Integral SiH (T=80 °C)	Integral Si-OR (T=80 °C)
0.5	78.4	7.2	78.4	5.4	79.6	2.4
1	70.0	13.3	73.6	10.9	79.6	4.8
2	61.5	22.9	65.2	21.1	77.2	8.4
3	56.7	31.4	59.1	28.4	74.8	11.5
4	44.6	39.2	54.3	35.6	71.2	15.7
5	39.8	48.9	49.5	41.0	68.8	18.7
6	35.0	56.1	43.4	47.1	62.7	22.9
7	26.5	65.8	38.6	52.5	60.3	27.2
8	15.7	76.6	33.8	57.3	57.9	30.8
9	0.0	86.9	32.6	60.9	57.9	32.6
24	0.0	88.1	4.8	95.9	35.0	59.1
Equation	$y = -8.280x + 80.509$		$y = -5.436x + 77.586$		$y = -2.940x + 82.399$	

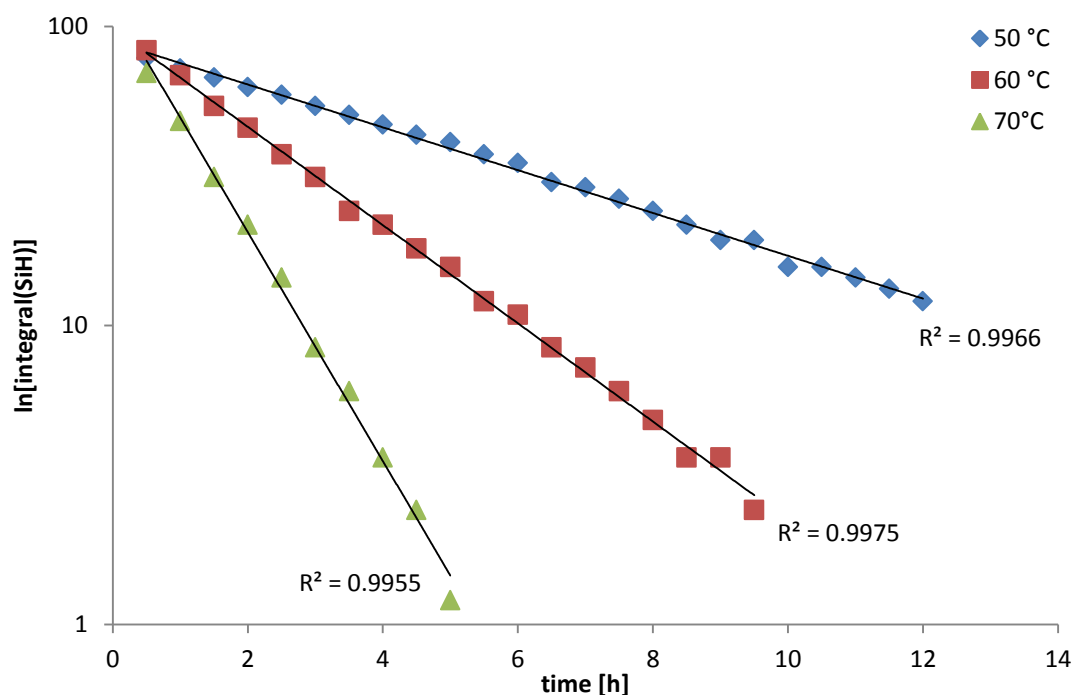


Figure A-10: Kinetic studies of sample **4.1b** at different temperatures; the reaction follows first order depending on the siloxane; the diagram is logarithmic plotted. The activation energy is about $80.4 \pm 3.1 \text{ kJ/(mol)}$.

Table A-13: Data of the kinetic studies of **4.1b** calculated by integration of the $^1\text{H-NMR}$ analytics; the equations are based on the slope of the trend line of the logarithmic plotted diagram (Figure A-10).

Time [h]	Integral SiH (T=70 °C)	Integral Si-OR (T=70 °C)	Integral SiH (T=60 °C)	Integral Si-OR (T=60 °C)	Integral SiH (T=50 °C)	Integral Si-OR (T=50 °C)
0.5	70.0	32.0	83.3	18.7	78.4	18.1
1	48.3	53.7	68.8	34.4	72.4	27.2
1.5	31.4	74.8	54.3	47.1	67.6	36.8
2	21.7	83.9	45.9	59.1	62.7	38.0
2.5	14.5	92.3	37.4	67.6	59.1	44.0
3	8.4	98.9	31.4	73.6	54.3	48.9
3.5	6.0	102.0	24.1	81.5	50.7	54.3
4	3.6	107.4	21.7	85.1	47.1	56.1
4.5	2.4	105.6	18.1	86.3	43.4	59.1
5	1.2	107.4	15.7	91.1	41.0	62.7
5.5	0.0	108.6	12.1	97.7	37.4	67.6
6	1.2	106.8	10.9	97.7	35.0	69.4
6.5	0.0	108.0	8.4	100.8	30.2	73.6
7	0.0	108.6	7.2	102.0	29.0	75.4
7.5	0.0	109.2	6.0	103.2	26.5	77.2
8	0.0	109.2	4.8	104.4	24.1	82.1
8.5	0.0	107.4	3.6	104.4	21.7	83.9
9	0.0	110.4	3.6	105.6	19.3	88.1
9.5	0.0	111.0	2.4	106.8	19.3	88.1
10	0.0	109.2	3.6	105.0	15.7	90.5
10.5	0.0	109.8	1.2	108.0	15.7	90.5
11	0.0	108.6	1.2	111.0	14.5	89.9
11.5	0.0	108.6	1.2	108.0	13.3	92.9
12	0.0	108.6	1.2	108.0	12.1	91.1
24	0.0	107.4	0.0	110.4	1.2	107.4
Equation	$y = -119.580e^{-0.881x}$		$y = 98.467e^{-0.378x}$		$y = 89.029e^{-0.165x}$	

Contact Angle measurements of Halogenalkyl functionalized Siloxanes:

The CA samples have to be solid to determine the solid-liquid-CA between the sample and the water droplet. Due to the fact that these products do not contain any groups to form urethane groups, the products were only embedded with an amount of 10% into the PDMS standard formulation without any networking. Further details are shown in Scheme A-2 (Appendix A2).

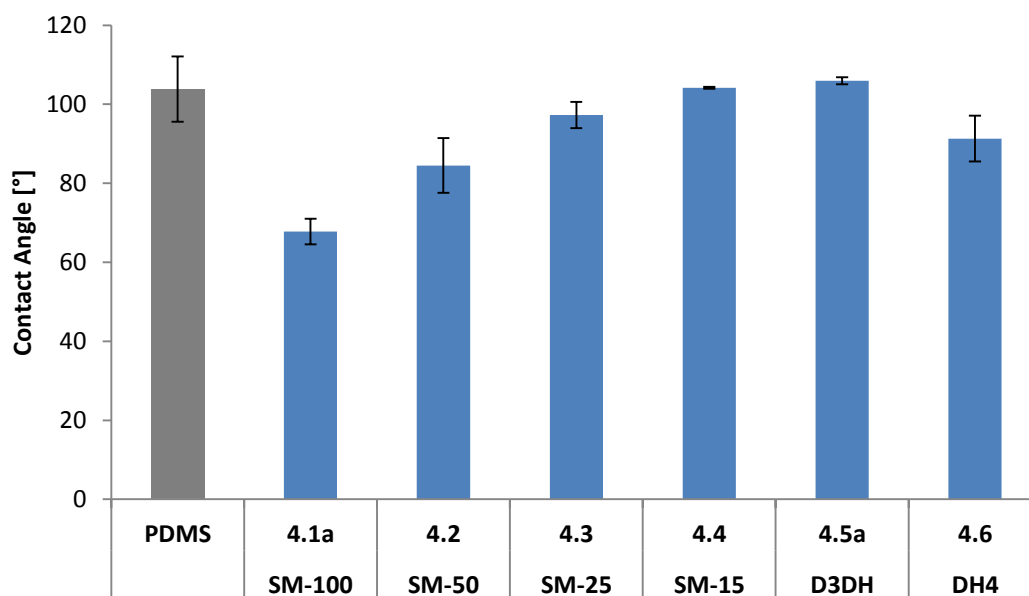


Figure A-11: Static contact angles of platinum-catalyzed halosilation products **4.1a** to **4.6** and reference material (standard PDMS formulation).

Table A-14: Summary of the contact angles of the products **4.1a** to **4.6**; standard PDMS is added for comparison reasons; samples were cured into a standard PDMS formulation with an amount of 10 % (Scheme A-2).

Sample	CA t(0 sec) [deg]
PDMS	103.9 ± 8.27
4.1a	67.8 ± 3.25
4.2	84.5 ± 6.93
4.3	97.3 ± 3.32
4.4	104.2 ± 0.21
4.5a	106.0 ± 0.92
4.6	91.3 ± 5.80

Synthesis of Halogenalkyl functionalized Siloxanes with varied Halogen Source:**Table A-15:** Summary of the products **4.7** to **4.11** in which the halogen source is varied; unless otherwise indicated, siloxane starting material is SM-100, the cyclic ether is THF and the general reaction conditions were used.

Sample	Halogene Source	Conversion SiH [%]	Yield Halosilation [%]	Yield Hydrosilylation [%]	Isolated Yield [%]	Viscosity [Pas]
4.7	3-Bromo-1-phenyl-1-propene	>99	69.5	16.5	83	n/s
4.8	4-Bromobutane	12	25.9	0.0	26	n/s
4.9^a	Allyl chloride	>99	13.0	47.8	56	1.885
4.10	4-Chlorobutane	23	86.2	not evaluable	64	n/s
4.11	Allyl cyanide	43	0.0	43.0	36	0.451

^a Experiment was done with SM-50.**Synthesis of poly(4-bromobutoxy)methylsiloxane (4.7):**

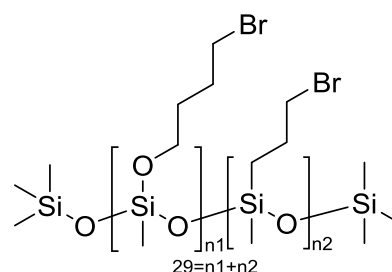
Product **4.7** was synthesized (83 % yield, 0.44 mmol) according to the representative procedure C, using 1.0 g of SM-100 (0.53 mmol, M_n 1900 g/mol), 1.24 mL dried THF (15.25 mmol), 2.26 mL 3-bromo-1-phenyl-1-propene (15.25 mmol) and 10 μ L Karstedt (0.03 mmol). The obtained product was a dark orange to brown, clear viscous liquid.

¹H-NMR (400 MHz, CDCl₃, 24 °C, ppm): δ = 7.25 – 7.01, 6.49 – 5.78, 4.95 – 4.88, 4.79 – 4.65, 4.01 – 3.97, 3.65 – 3.34 (t, 2H, -O-CH₂-), 3.37 – 3.18 (m, 4H, -CH₂-Br, -CH₂-CH₂-CH₂-Br), 1.84 – 1.70 (m, 4H, -CH₂-CH₂-Br, -CH₂-CH₂-CH₂-Br), 1.60 – 1.47 (m, 2H, -O-CH₂-CH₂-), 0.52 – 0.40 (m, 2H, -CH₂-CH₂-CH₂-Br), 0.11 – 0.09 (s, 3H; -CH₃). ¹³C-NMR (400 MHz, CDCl₃, 24 °C, ppm): δ = 142.66 – 125.57, 61.63 (-O-CH₂-), 38.05 (-CH₂-CH₂-CH₂-Br),

33.84 (-CH₂-Br), 31.23 (-O-CH₂-CH₂-), 29.68 (-CH₂-CH₂-Br), 25.24 (-CH₂-CH₂-CH₂-Br), -3.84 (-CH₃).

²⁹Si-NMR (400 MHz, CDCl₃, 24 °C, ppm): δ = -58.76 (-O-Si(Me)-O_{2/2}). IR (ATR, 32 scans, cm⁻¹): 3026.2, 2933.8, 2873.3, 1599.3, 1494.7, 1451.7, 1267.4, 1023.1, 964.2, 844.7, 744.9, 694.5, 560.5.

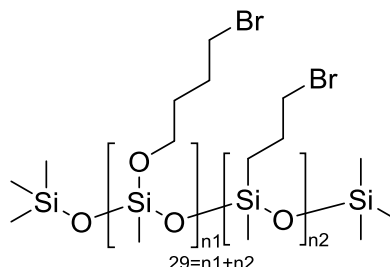
GPC (THF, 40 °C, g/mol): M_n =1494, M_w =3392, PDI=2.270.



Synthesis of poly(4-bromobutoxy)methylsiloxane (4.8):

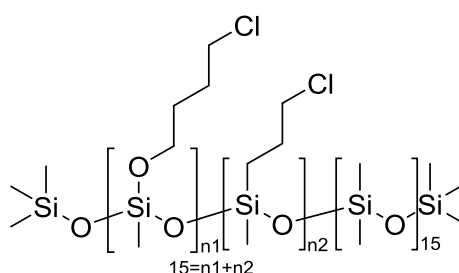
Product **4.8** was synthesized (26 % yield, 0.69 mmol) according to the representative procedure C, using 5.0 g of SM-100 (2.63 mmol, M_n 1900 g/mol), 6.18 mL dried THF (76.27 mmol), 8.19 mL bromobutane (76.24 mmol) and 70 μ L Karstedt (0.15 mmol). The obtained product was a brown, clear, high viscous liquid.

$^1\text{H-NMR}$ (300 MHz, CDCl_3 , 24 °C, ppm): δ = 4.73 – 4.71 (s, 1H, SiH), 3.75 – 3.73 (m, 2H, $-\text{O}-\text{CH}_2-$), 3.49 – 3.40 (m, 2H, $-\text{CH}_2-\text{Br}$), 1.59 – 1.55 (m, 2H, $-\text{O}-\text{CH}_2-\text{CH}_2-$), 0.21 – 0.11 (s, 3H; $-\text{CH}_3$). **$^{13}\text{C-NMR}$** (300 MHz, CDCl_3 , 24 °C, ppm): δ = 1.77 – 0.99 ($-\text{CH}_3$). **$^{29}\text{Si-NMR}$** (300 MHz, CDCl_3 , 24 °C, ppm): δ = 10.12 ($-\text{Si}(\text{CH}_3)_3$), -34.66 – -35.60 (SiH). **GPC** (THF, 40 °C, g/mol): M_n =9953, M_w =2861850, PDI=287.57.

Synthesis of poly(4-chlorobutoxy)methylsiloxane-co-polydimethylsiloxane (4.9):

Product **4.9** was synthesized (56 % yield, 1.08 mmol) according to the representative procedure C, using 5.0 g of SM-50 (2.63 mmol, M_n 2200 g/mol), 10.0 mL dried THF (123.42 mmol), 2.78 mL allyl chloride (34.09 mmol) and 70 μ L Karstedt (0.15 mmol). The reaction was carried out in dried THF. The obtained product was a clear, colorless, viscous liquid.

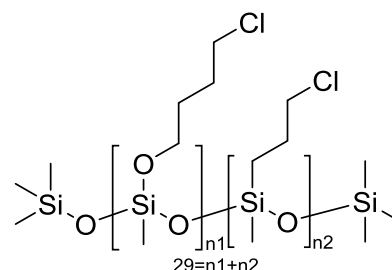
$^1\text{H-NMR}$ (400 MHz, CDCl_3 , 24 °C, ppm): δ = 3.76 – 3.70 (m, 2H, $-\text{O}-\text{CH}_2-$), 3.58 – 3.54 (t, 2H, $-\text{CH}_2-\text{Cl}$), 3.52 – 3.48 (m, 2H, $-\text{CH}_2-\text{CH}_2-\text{CH}_2-\text{Cl}$), 1.87 – 1.79 (p, 2H, $-\text{CH}_2-\text{CH}_2-\text{CH}_2-\text{Cl}$), 1.71 – 1.67 (m, 2H, $-\text{CH}_2-\text{CH}_2-\text{Cl}$), 1.39 – 1.38 (m, 2H, $-\text{O}-\text{CH}_2-\text{CH}_2-$), 0.97 – 0.93, 0.72 – 0.62 (m, 2H, $-\text{CH}_2-\text{CH}_2-\text{CH}_2-\text{Cl}$), 0.50 – 0.39, 0.22 – 0.05 (s, 3H; $-\text{CH}_3$). **$^{13}\text{C-NMR}$** (400 MHz, CDCl_3 , 24 °C, ppm): δ = 48.03, 45.33, 30.78, 30.09, 29.52, 27.12, 26.90, 18.41, 15.37, 2.37 – 1.01 ($-\text{CH}_3$). **$^{29}\text{Si-NMR}$** (400 MHz, CDCl_3 , 24 °C, ppm): δ = -21.05 ($-\text{O}-\text{Si}(\text{Me})_2-\text{O}-$), -46.46 ($-\text{O}-\text{Si}(\text{Me})-\text{O}_{2/2}$). **IR** (ATR, 32 scans, cm^{-1}): 2961.4, 1410.9, 1259.3, 1014.6, 843.8, 790.6, 690.5. **EA** (% , measured (calculated)), repeating unit $\text{C}_5\text{H}_{11}\text{ClO}_2\text{Si}$: C 29.20 (34.91), H 7.255 (7.12), Cl 10.965 (14.72), Si 31.34 (23.32). **GPC** (THF, 40 °C, g/mol): M_n =3009, M_w =11924, PDI=3.963.



Synthesis of poly(4-chlorobutoxy)methylsiloxane (4.10):

Product **4.10** was synthesized (64 % yield, 1.88 mmol) according to the representative procedure C, using 5.0 g of SM-100 (2.63 mmol, Mn 1900 g/mol), 6.5 mL dried THF (76.27 mmol), 7.93 mL chlorobutane (76.27 mmol) and 70 μ L Karstedt (0.15 mmol). The obtained product was a crumbly, white solid.

¹H-NMR (300 MHz, CDCl₃, 24 °C, ppm): δ = 4.59 – 4.56 (s, 1H, SiH), 3.50 – 3.44 (m, 2H, -O-CH₂-), 3.24 – 3.19 (t, 2H, -CH₂-Cl), 1.49 – 1.41 (m, 2H, -CH₂-CH₂-Cl), 1.26 – 1.15 (m, 2H, -O-CH₂-CH₂-), 0.73 – 0.64, 0.03 – 0.09 (s, 3H; -CH₃). **IR** (ATR, 32 scans, cm⁻¹): 2965.0, 2162.3, 1604.5, 1495.4, 1407.1, 1259.1, 1032.2, 835.3, 802.9, 763.6, 727.5, 693.6, 463.8. **EA** (% , measured (calculated)), repeating unit C₅H₁₁ClO₂Si: C 6.351 (34.91), H 3.297 (7.12), Cl n/d (14.72). **GPC** (THF, 40 °C, g/mol): M_n=5118, M_w=10435, PDI=2.039.

Synthesis of poly(4-cyanobutoxy)methylsiloxane (4.11):

Product **4.11** was synthesized (36 % yield, 1.06 mmol) according to the representative procedure C, using 5.0 g of SM-100 (2.63 mmol, Mn 1900 g/mol), 6.5 mL dried THF (76.27 mmol), 6.32 mL allyl cyanide (76.24 mmol) and 70 μ L Karstedt (0.15 mmol). The obtained product was a clear, slightly yellow, low viscous liquid.

No halosilation product was obtained.

Synthesis of Halogenalkyl functionalized Siloxanes with varied Heterocyclic Compounds:

Table A-16: Summary of the products **4.12** to **4.18** in which the heterocyclic compounds are varied; unless otherwise indicated, siloxane starting material is SM-100, the halogen source is allyl bromide and the general reaction conditions were used.

Sample	Heterocyclic Compounds	Conversion	Yield	Yield	Isolated	Viscosity [Pas]
		SiH [%]	Halosilation [%]	Hydrosilylation [%]	Yield [%]	
4.12	THP	99	56.9	23.0	40 - 44	1.879
4.13	Oxepane	96	60.9	22.5	59	2.454
4.14	ϵ -Caprolactone	>99	n/d	n/d	n/d	n/s
4.15	1,4-Dioxane	>99	0.0	27.5	37	n/s
4.16	Thiolane ^a	89	n/d	not evaluable	30	n/s
4.17^b	THP	>99	84.9	0.0	83	0.013
4.18^b	Oxepane	>99	88.8	0.0	82	0.008

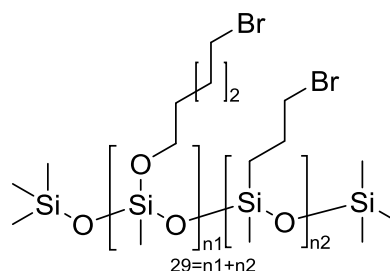
^a Thiolane is a sulfur analog to THF.

^b Experiments were done with D₃D^H.

Synthesis of poly(3-(4-bromopentoxymethyl)dimethylsiloxane (4.12):

Product **4.12** was synthesized (40-44% yield, 1.60 mmol) according to the representative procedure C, using 5.0 g of SM-100 (2.63 mmol, Mn 1900 g/mol), 7.5 mL tetrahydropyran (76.25 mmol), 6.59 mL allyl bromide (76.24 mmol) and 70 μ L Karstedt (0.15 mmol).

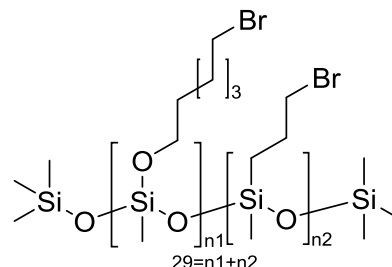
¹H-NMR (400 MHz, CDCl₃, 24 °C, ppm): δ = 3.70 – 3.64 (t, 2H, -O-CH₂-), 3.38 – 3.35 (m, 4H, -CH₂-Br, -CH₂-CH₂-CH₂-Br), 1.91 – 1.80 (p, 4H, -CH₂-CH₂-Br, -CH₂-CH₂-CH₂-Br), 1.56 – 1.50 (p, 2H, -O-CH₂-CH₂-), 1.48 – 1.42 (m, 2H, -O-CH₂-CH₂-CH₂-), 0.685 (m, 2H, -CH₂-CH₂-CH₂-Br), 0.17 – 0.06 (s, 3H; -CH₃). ¹³C-NMR (400 MHz, CDCl₃, 24 °C, ppm): δ = 62.98 (-O-CH₂-), 33.77 (-CH₂-Br), 32.61 (-O-CH₂-CH₂-), 31.56 (-CH₂-CH₂-Br), 24.59 (-O-CH₂-CH₂-CH₂-), -4.16 (-CH₃). ²⁹Si-NMR (400 MHz, CDCl₃, 24 °C, ppm): δ = 8.78 (-Si(CH₃)₃), -58.09 – -59.16 (-O-Si(Me)-O_{2/2}). IR (ATR, 32 scans, cm⁻¹): 2934.8, 2862.8, 1432.5, 1265.5, 1016.5, 931.5, 843.9, 772.3, 644.6, 561.2. EA (%), measured (calculated), repeating unit C₆H₁₃BrO₂Si: C 25.32 (32.01), H 5.80 (5.82), Br 29.61 (35.49), Si 16.75 (12.47). GPC (THF, 40 °C, g/mol): Mn=3295, Mw=21201, PDI=3.368.



Synthesis of (3-(4-bromohexyloxy)methylsiloxane (4.13):

Product **4.13** was synthesized (59% yield, 0.77 mmol) according to the representative procedure C, using 2.5 g of SM-100 (1.32 mmol, Mn 1900 g/mol), 4.24 mL oxepane (38.12 mmol), 3.29 mL allyl bromide (38.12 mmol) and 30 μ L Karstedt (0.07 mmol).

$^1\text{H-NMR}$ (400 MHz, CDCl_3 , 24 $^\circ\text{C}$, ppm): δ = 3.70 – 3.64 (t, 2H, -O-CH₂-), 3.38 – 3.35 (m, 4H, -CH₂-Br, -CH₂-CH₂-CH₂-Br), 1.91 – 1.80 (p, 4H, -CH₂-CH₂-Br, -CH₂-CH₂-CH₂-Br), 1.56 – 1.50 (p, 2H, -O-CH₂-CH₂-), 1.48 – 1.42 (m, 2H, -O-CH₂-CH₂-CH₂-), 0.685 (m, 2H, -CH₂-CH₂-CH₂-Br), 0.17 – 0.06 (s, 3H; -CH₃). **$^{13}\text{C-NMR}$**



(400 MHz, CDCl_3 , 24 $^\circ\text{C}$, ppm): δ = 62.98 (-O-CH₂-), 33.77 (-CH₂-Br), 32.61 (-O-CH₂-CH₂-), 31.56 (-CH₂-CH₂-Br), 24.59 (-O-CH₂-CH₂-CH₂-), -4.16 (-CH₃). **$^{29}\text{Si-NMR}$** (400 MHz, CDCl_3 , 24 $^\circ\text{C}$, ppm): δ = 8.78 (-Si(CH₃)₃), -58.09 – -59.16 (-O-Si(Me)-O_{2/2}). **IR** (ATR, 32 scans, cm^{-1}): 2934.8, 2862.8, 1432.5, 1265.5, 1016.5, 931.5, 843.9, 772.3, 644.6, 561.2. **EA** (% , measured (calculated)), repeating unit C₆H₁₃BrO₂Si: C 25.32 (32.01), H 5.80 (5.82), Br 29.61 (35.49), Si 16.75 (12.47). **GPC** (THF, 40 $^\circ\text{C}$, g/mol): M_n=3261, M_w=11663, PDI=3.576.

Synthesis of poly(6-bromohexanoate)methylsiloxane (4.14):

Product **4.14** was synthesized (0 % yield) according to the representative procedure C, using 2.5 g of SM-100 (1.32 mmol, Mn 1900 g/mol), 4.22 mL ϵ -caprolactone (38.12 mmol), 3.29 mL allyl bromide (38.12 mmol) and 30 μ L Karstedt (0.07 mmol).

No halosilation product was obtained.

Synthesis of poly(5-bromopent-1,5-dioxy)methylsiloxane (4.15):

Product **4.15** was synthesized (0 % yield) according to the representative procedure C, using 2.5 g of SM-100 (1.32 mmol, Mn 1900 g/mol), 3.25 mL 1,4-dioxane (38.12 mmol), 3.29 mL allyl bromide (38.12 mmol) and 30 μ L Karstedt (0.07 mmol).

No halosilation product was obtained.

Synthesis of poly((4-bromobutyl)thio)methylsiloxane (4.16):

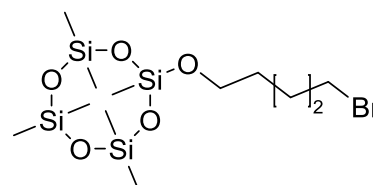
Product **4.16** was synthesized (0 % yield) according to the representative procedure C, using 2.5 g of SM-100 (1.32 mmol, Mn 1900 g/mol), 3.36 mL thiolane (38.12 mmol), 3.29 mL allyl bromide (38.12 mmol) and 30 μ L Karstedt (0.07 mmol).

No halosilation product was obtained.

Synthesis of 1-(4-bromopentoxo)-1',3,3',5,5',7,7'-Heptamethylcyclotetrasiloxane (4.17):

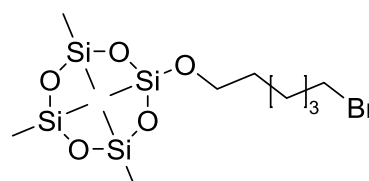
Product **4.17** was synthesized (83% yield, 9.85 mmol) according to the representative procedure C, using 3.51 mL of D₃D^H (11.81 mmol), tetrahydropyran (1.15 mL, 11.82 mmol), allyl bromide (1.02 mL, 11.82 mmol) and 260 µL Karstedt (0.59 mmol).

¹H-NMR (300 MHz, CDCl₃, 24 °C, ppm): δ = 3.62 – 3.59 (t, 2H, -O-CH₂-), 3.33 – 3.26 (t, 2H, -CH₂-Br), 1.81 – 1.74 (p, 2H, -CH₂-CH₂-Br), 1.52 – 1.46 (p, 2H, -O-CH₂-CH₂-), 1.45 – 1.35 (p, 2H, -O-CH₂-CH₂-CH₂-), 0.05 – 0.03 (s, 3H; -CH₃). **¹³C-NMR** (300 MHz, CDCl₃, 24 °C, ppm): δ = 62.07 (-O-CH₂-), 33.78 (-CH₂-Br), 32.73 (-CH₂-CH₂-Br), 31.60 (-O-CH₂-CH₂-), 24.71 (-O-CH₂-CH₂-CH₂-), 0.72 (-CH₃), -4.16. **²⁹Si-NMR** (300 MHz, CDCl₃, 24 °C, ppm): δ = -18.53 - -19.18 (Si(Me)₂-O_{2/2}), -56.97 (-O-Si(Me)-O_{2/2}). **IR** (ATR, 32 scans, cm⁻¹): 2962.4, 1410.0, 1259.1, 1051.2, 799.4, 698.8, 665.2, 645.4, 560.4. **EA** (%), measured (calculated)), repeating unit C₁₂H₃₁BrO₅Si₄: C 24.92 (32.2), H 5.82 (6.98), Br 13.85 (17.85), Si 7.44 (25.1). **GPC** (THF, 40 °C, g/mol): M_n=442, M_w=471, PDI=1.067.

**Synthesis of 1-(4-bromohexyloxy)-1',3,3',5,5',7,7'-Heptamethylcyclotetrasiloxane (4.18):**

Product **4.18** was synthesized (82% yield, 9.65 mmol) according to the representative procedure C, using 3.51 mL of D₃D^H (11.81 mmol), oxepane (1.31 mL, 11.82 mmol), allyl bromide (1.02 mL, 11.82 mmol) and 260 µL Karstedt (0.59 mmol).

¹H-NMR (400 MHz, CDCl₃, 24 °C, ppm): δ = 3.72 – 3.68 (t, 2H, -O-CH₂-), 3.41 – 3.38 (t, 2H, -CH₂-Br), 1.90 – 1.83 (p, 2H, -CH₂-CH₂-Br), 1.60 – 1.55 (p, 2H, -O-CH₂-CH₂-), 1.48 – 1.42 (p, 2H, -O-CH₂-CH₂-CH₂-), 1.41 – 1.35 (p, 2H, -O-CH₂-CH₂-CH₂-CH₂-), 0.13 – 0.07 (s, 3H; -CH₃). **¹³C-NMR** (400 MHz, CDCl₃, 24 °C, ppm): δ = 61.93 (-O-CH₂-), 33.54 (-CH₂-Br), 32.621 (-CH₂-CH₂-Br), 31.97 (-O-CH₂-CH₂-), 27.77 (-O-CH₂-CH₂-CH₂-), 24.84 (-O-CH₂-CH₂-CH₂-CH₂-), 0.15 (-CH₃), -4.40. **²⁹Si-NMR** (300 MHz, CDCl₃, 24 °C, ppm): δ = -18.84 (Si(Me)₂-O_{2/2}), -57.00 (-O-Si(Me)-O_{2/2}). **IR** (ATR, 32 scans, cm⁻¹): 2962.2, 1409.8, 1259.2, 1051.8, 799.9, 698.0, 664.9, 646.5, 560.4. **EA** (%), measured (calculated)), repeating unit C₁₃H₃₃BrO₅Si₄: C 30.13 (33.82), H 6.90 (7.21), Br 14.93 (17.31), Si 5.72 (24.33). **GPC** (THF, 40 °C, g/mol): M_n=444, M_w=467, PDI=1.052.



A5. Appendix to Part IIb

Synthesis of Siloxanes functionalized with Quaternary Ammonium Groups (QAS):

Table A-17: Summary of the products **4.19** to **4.44**; unless otherwise indicated, the starting materials were made with THF and the general reaction time is 24 hours; 1-methyl-1H-imidazole and 1-butyl-1H-imidazole are shortened to Me-Imi and Bu-Imi; the yields were calculated from several repetitions.

Sample	Starting Material	Amine	Conversion QAS [%]	Isolated Yield [%] ^a
4.19		Pyridine	76.4 ± 7.61	100.6 ± 8.19
4.20	4.1a	Me-Imi	62.5 ± 6.47	102.9 ± 2.63
4.21		Bu-Imi	78.0	102.8
4.22	4.1b	Pyridine	73.2	100.8
4.23		Me-Imi	63.5	102
4.24		Pyridine	75.0	102.3
4.25	4.12	Me-Imi	79.7	105.3
4.26		Bu-Imi	80.0	100.6
4.27		Pyridine	82.2	100.8
4.28	4.13	Me-Imi	65.7	111.5
4.29		Bu-Imi	72.3	100.4
4.30		Pyridine	74.4 ± 10.83	99.8 ± 14.23
4.31	4.2	Me-Imi	60.4 ± 14.58	102.3 ± 2.79
4.32		Bu-Imi	75.0	100.6
4.33		Pyridine	48.3 ± 15.70	92.8 ± 4.59
4.34	4.3	Me-Imi	56.9 ± 7.40	98.4 ± 1.31
4.35		Bu-Imi	75.0	98.2
4.36		Pyridine	66.6 ± 17.18	92.0 ± 2.05
4.37	4.4	Me-Imi	60.6 ± 15.61	97.8 ± 2.41
4.38		Bu-Imi	65.0	95.3
4.39		Pyridine	n/d	82.0 ± 3.04
4.40	4.5a	Me-Imi	n/d	61.5 ± 5.30
4.41		Bu-Imi	n/d	93.7
4.42		Pyridine	82.2 ± 9.05	98.0 ± 1.84
4.43	4.6	Me-Imi	75.2 ± 14.35	100.2 ± 0.57
4.44		Bu-Imi	77.7	92.8

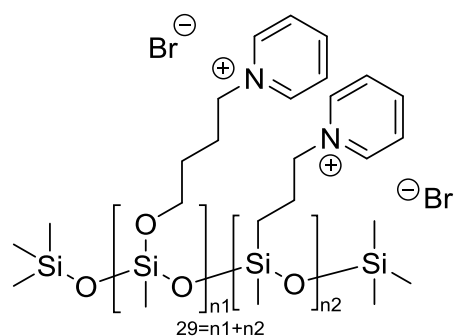
^a the isolated yields are calculated by integration of ¹H-NMR; the numbers higher than 100% belong to the mistake of calculations and left solvent/volatiles.

Synthesis of (4-(polymethylsiloxane)butoxy) pyridinium bromide (4.19):Representative procedure E:

30 mL DMF and 20.0 g of **4.1a** (3.2 mmol) were added into the flask under argon atmosphere and stirred at room temperature (20 °C) for a couple of minutes. Then pyridine (7.47 mL, 92.79 mmol) was added into the system. The mixture was stirred (oil bath temperature: 75°C) under inert atmosphere (Ar) for 24 hours (the reaction was followed by ¹H-NMR). The solvents and volatiles were evaporated under vacuum. The obtained product (yield 101 %, 0.33 mmol) was a yellow, milky, high viscous, sticky liquid.

¹H-NMR (300 MHz, CD₃OD, 24 °C, ppm): δ = 9.36 (m, 2H, arom.), 8.83 – 8.74 (m, 1H, arom.), 8.38 – 8.26 (m, 2H; arom.), 4.98 (m, 2H, -CH₂-N), 3.98 – 3.86 (m, 2H, -O-CH₂-), 3.60 – 3.54 (m, 2H, -CH₂-CH₂-CH₂-N), 2.32 – 2.20 (m, 2H, -CH₂-CH₂-N), 2.06 – 1.98 (m, 2H, -CH₂-CH₂-CH₂-N), 1.82 – 1.69 (m, 2H, -O-CH₂-CH₂-), 0.81 (m, 2H, -CH₂-CH₂-CH₂-N), 0.32 – 0.18 (s, 3H; -CH₃). **¹³C-NMR** (300 MHz, CD₃OD, 24 °C, ppm): δ = 146.97 (arom.), 146.00 (arom.), 129.55

(arom.), 62.67 (-CH₂-N), 61.79 (-O-CH₂-), 33.12 (-CH₂-CH₂-CH₂-N), 30.73 (-CH₂-CH₂-CH₂-N), 29.79 (-O-CH₂-CH₂-), 29.30 (-CH₂-CH₂-N), 13.25 (-CH₂-CH₂-CH₂-N), -3.62 (-CH₃). **²⁹Si-NMR** (300 MHz, CD₃OD, 25 °C, ppm): δ = 9.39 (-Si(CH₃)₃), -21.91 (-O-Si(Me)₂-O-), -58.42 (-O-Si(Me)-O_{2/2}). **IR** (ATR, 32 scans, cm⁻¹): 3335.75, 3127.21, 3024.17, 2963.65, 2935.12, 2871.83, 2060.64, 1632.52, 1485.37, 1266.96, 1017.33, 768.95, 680.95, 426.81. **EA** (% , measured (calculated)), repeating unit C₁₀H₁₆BrNO₂Si: C 41.625 (41.38), H 5.749 (5.56), Br 23.526 (27.53), N 3.493 (4.83), Si 9.536 (9.68).



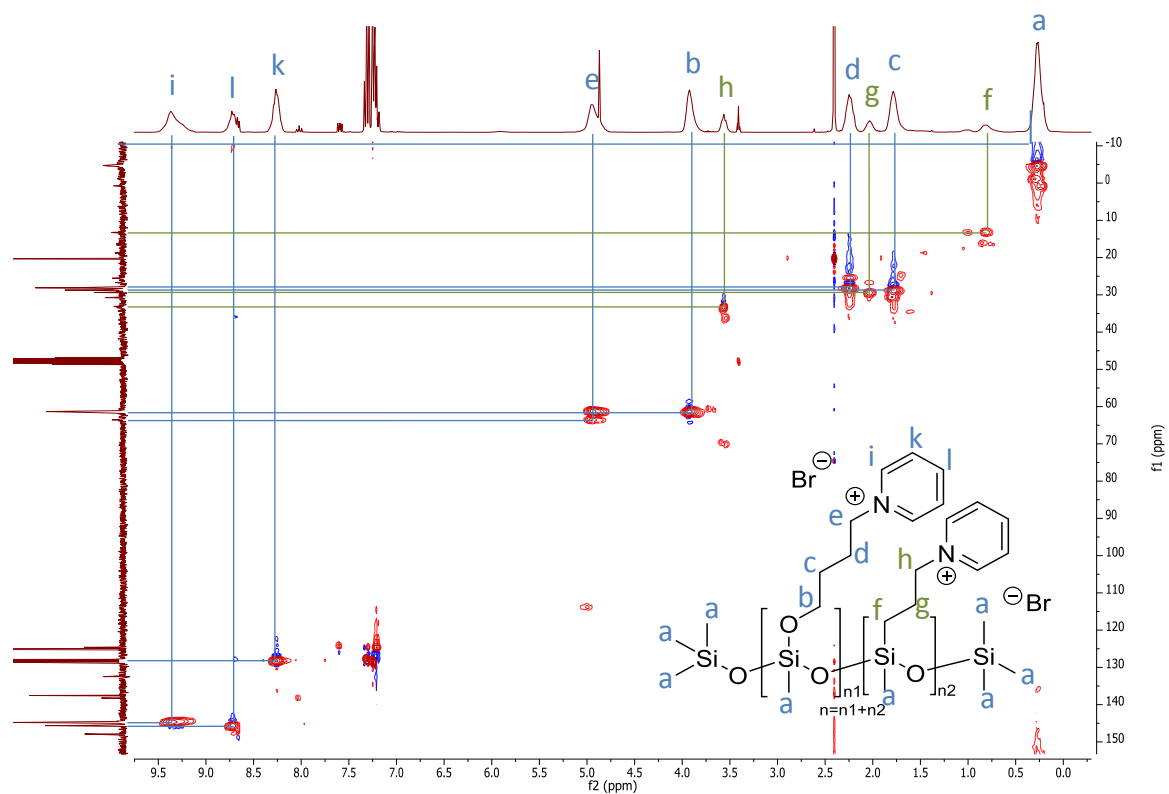


Figure A-12: ^1H - ^{13}C -HSQC-NMR of **4.19** in deuterated chloroform (300 MHz, 24 °C); the shifting of the signals promotes a separation of the signals; for reasons of simplification the methyl groups on the silicon have been grouped together as **a**.

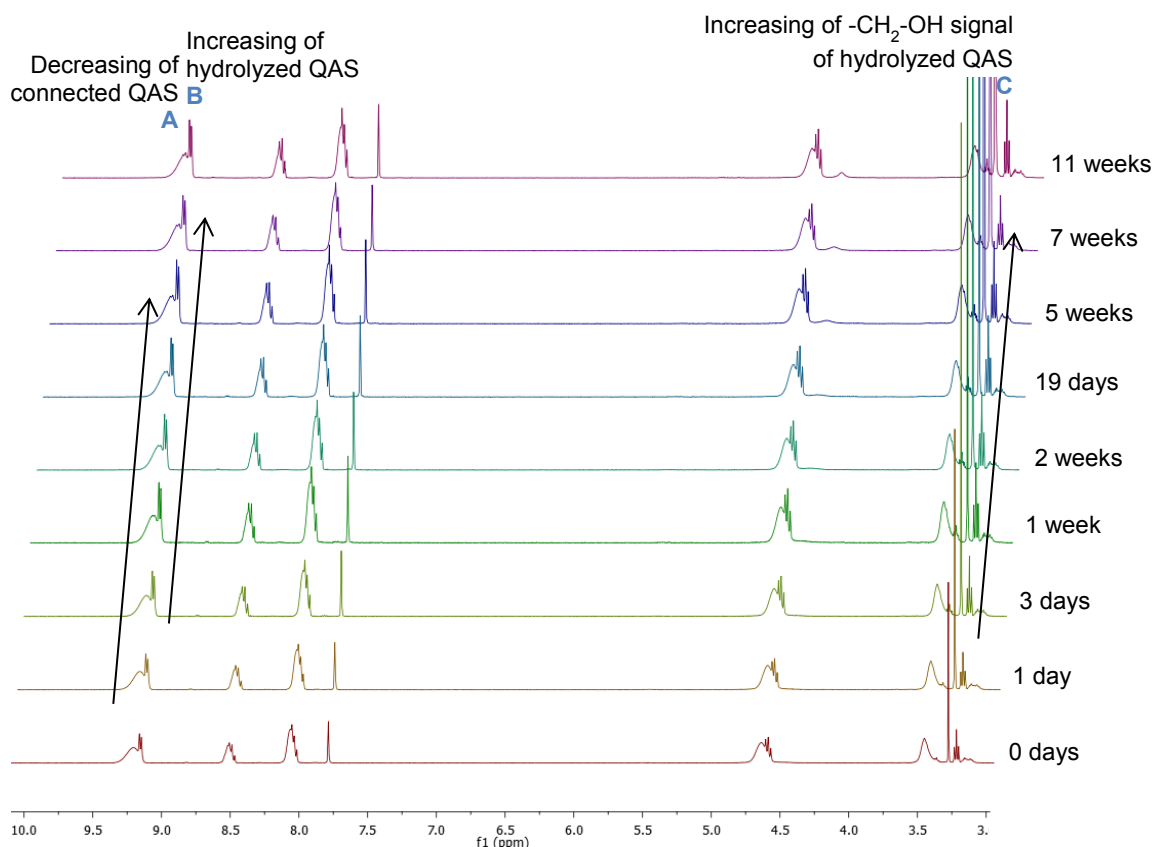
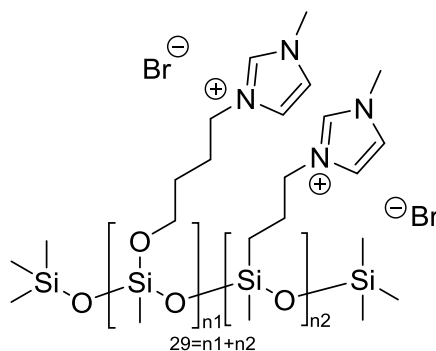


Figure A-13: Time-resolved ^1H -NMR of **4.19** in deuterated DMSO (400 MHz, 26 °C); it is an example for the hydrolysis of the pyridinium-functionalized side-group.

Synthesis of (4-(polymethylsiloxane)butoxy) 1-methyl-1H-imidazol-3-ium bromide (4.20**):**

Product **4.20** was synthesized (103 % yield, 0.81 mmol) according to the representative procedure E, using 5 mL EtOH, 5 mL dried Toluene, 5.0 g of **4.1a** (0.80 mmol) and 1.85 mL 1-methyl-1H-imidazole (23.20 mmol). The obtained product was a transparent, yellow, sticky, high viscous liquid.

^1H -NMR (300 MHz, CD_3OD , 25 °C, ppm): δ = 9.21 (s, $\text{N}=\text{CH}-\text{N}$), 7.77 – 7.76 (d, $\text{N}-\text{CH}=\text{CH}-\text{N}(\text{Me})$), 7.69 – 7.68 (d, $\text{N}-\text{CH}=\text{CH}-\text{N}(\text{Me})$), 4.37 (m, 2H, $-\text{CH}_2-\text{N}$), 4.05 (s, $\text{N}-\text{CH}_3$), 3.87 (m, 2H, $-\text{O}-\text{CH}_2-$), 3.57 – 3.51 (m, 2H, $-\text{CH}_2-\text{CH}_2-\text{CH}_2-\text{N}$), 2.05 (m, 2H, $-\text{CH}_2-\text{CH}_2-\text{N}$), 1.66 (m, 2H, $-\text{O}-\text{CH}_2-\text{CH}_2-$), 0.70 (m, 2H, $-\text{CH}_2-\text{CH}_2-\text{CH}_2-\text{N}$), 0.22 (s, 3H; $-\text{CH}_3$). **^{13}C -NMR** (300 MHz, CD_3OD , 25 °C, ppm): δ = 137.87 ($\text{N}=\text{CH}-\text{N}$), 124.92 ($\text{N}-\text{CH}=\text{CH}-\text{N}(\text{Me})$), 123.63 ($\text{N}-\text{CH}=\text{CH}-\text{N}(\text{Me})$), 61.92 ($-\text{O}-\text{CH}_2-$), 50.63 ($-\text{CH}_2-\text{N}$), 36.63 ($\text{N}-\text{CH}_3$), 35.21 ($-\text{CH}_2-\text{CH}_2-\text{CH}_2-\text{N}$), 29.97 ($-\text{CH}_2-\text{CH}_2-\text{N}$), 27.92 ($-\text{O}-\text{CH}_2-\text{CH}_2-$), 25.29 ($-\text{CH}_2-\text{CH}_2-\text{CH}_2-\text{N}$), 18.45 ($-\text{CH}_2-\text{CH}_2-\text{CH}_2-\text{N}$), -3.59 ($-\text{CH}_3$). **^{29}Si -NMR** (300 MHz, CD_3OD , 25 °C, ppm): δ = -21.29 ($-\text{O}-\text{Si}(\text{Me})_2-\text{O}-$), -58.71 ($-\text{O}-\text{Si}(\text{Me})-\text{O}_{2/2}$). **IR** (ATR, 32 scans, cm^{-1}): 3335.5, 3069.1, 2965.1, 1571.0, 1450.9, 1267.3, 1165.5, 1015.7, 765.3, 650.1, 618.9. **EA** (%), measured (calculated)), repeating unit $\text{C}_9\text{H}_{17}\text{BrN}_2\text{O}_2\text{Si}$: C 34.535 (36.86), H 6.215 (5.84), Br 23.434 (27.25), N 8.517 (9.55), Si 9.658 (9.58).



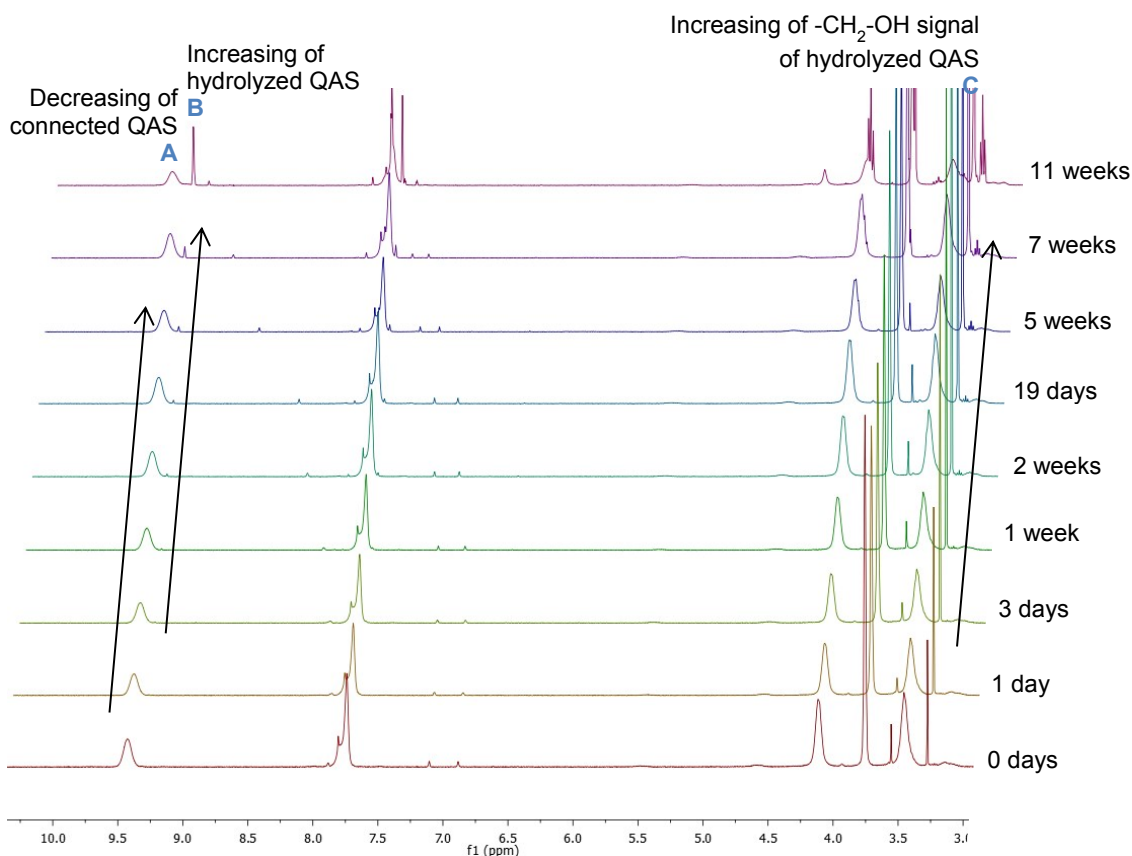
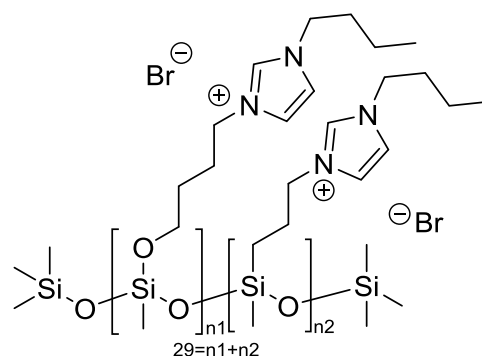


Figure A-14: Time-resolved ^1H -NMR of **4.20** in deuterated DMSO (400 MHz, 26 °C); it is an example for the hydrolysis of the imidazolium-functionalized side-group.

Synthesis of (4-(polymethylsiloxane)butoxy) 1-butyl-1H-imidazol-3-ium bromide (**4.21**):

Product **4.21** was synthesized (103 % yield, 0.82 mmol) according to the representative procedure E, using 5 mL EtOH, 5 mL dried Toluene, 5.0 g of **4.1a** (0.80 mmol) and 3.05 mL 1-butyl-1*H*-imidazole (23.20 mmol). The obtained product was a colorless, slightly milky, sticky, viscous liquid.

^1H -NMR (400 MHz, DMSO- d_6 , 25 °C, ppm): δ = 9.73 (s, N=CH-N), 7.96 – 7.91 (m, 2H, N-CH=CH-N(Bu)), 4.28 – 4.177 (t, 2H, -CH₂-N), 4.09 – 4.05 (t, -CH₂-CH₂-CH₂-CH₃), 3.71 – 3.61 (m, 2H, -O-CH₂-), 3.36 – 3.30 (m, 2H, -CH₂-CH₂-CH₂-N), 1.72 – 1.67 (m, 2H, -CH₂-CH₂-CH₂-N), 1.88 – 1.75 (p, 2H, -CH₂-CH₂-N), 1.73 – 1.67 (p, 2H, CH₂-CH₂-CH₃), 1.48 – 1.40 (m, 2H, -O-CH₂-CH₂-), 1.28 – 1.18 (p, 2H, CH₂-CH₃), 0.90 – 0.84 (3H, CH₂-CH₃), 0.45 (m, 2H, -CH₂-CH₂-CH₂-N), 0.10 – 0.00 (s, 3H; Si-CH₃). **^{13}C -NMR**



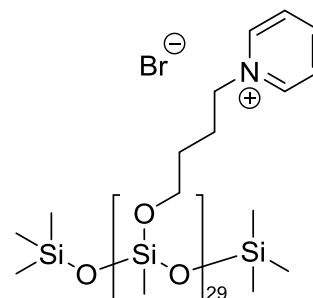
(400 MHz, DMSO- d_6 , 25 °C, ppm): δ = 136.09 (N=CH-N), 122.41 (N-CH=CH-N(Me)), 61.052 (-O-CH₂-), 48.503 (-CH₂-N), 46.75 (-CH₂-CH₂-CH₂-CH₃), 32.07 (CH₂-CH₂-CH₃), 31.29 (-CH₂-CH₂-N), 28.80 (-O-CH₂-CH₂-), 23.47 (-CH₂-CH₂-CH₂-N), 18.76 (CH₂-CH₃), 18.02 (-CH₂-CH₂-CH₂-N), 13.32 (CH₂-CH₃), -4.38 (Si-CH₃). **^{29}Si -NMR** (400 MHz, DMSO- d_6 , 25 °C, ppm): δ = -58.75 (-O-Si(Me)-O_{2/2}). **IR** (ATR, 32 scans, cm⁻¹): 3340.7, 3064.1, 2958.6, 2871.2, 1562.3, 1460.9, 1378.4, 1266.8, 1160.6, 1020.3, 774.2,

633.6, 439.1. **EA** (% , measured (calculated)), repeating unit $C_{12}H_{23}BrN_2O_2Si$: C 36.095 (42.98), H 7.011 (6.91), Br 17.800 (23.83), N 7.289 (8.35), Si 8.499 (8.38).

Synthesis of (4-(polymethylsiloxane)butoxy) pyridinium bromide (**4.22**):

Product **4.22** was synthesized (101 % yield, 0.81 mmol) according to the representative procedure E, using 5 mL EtOH, 5 mL dried Toluene, 5.0 g of **4.1b** (0.80 mmol) and 1.87 mL pyridine (23.20 mmol). The obtained product was a green, milky, sticky, high viscous liquid.

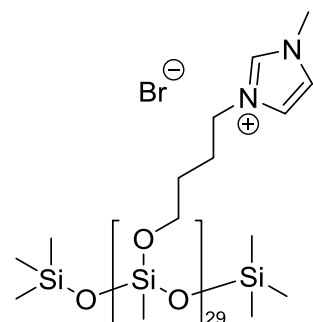
¹H-NMR (400 MHz, CD_3OD , 25 °C, ppm): δ = 9.02 – 8.99 (d, 2H, arom.), 8.54 – 8.47 (m, 1H, arom.), 8.05 – 8.00 (m, 2H; arom.), 4.64 – 4.60 (t, 2H, $-CH_2-N$), 3.47 – 3.42 (m, 2H, $-O-CH_2-$), 2.01 – 1.93 (p, 2H, $-CH_2-CH_2-N$), 1.52 – 1.42 (p, 2H, $-O-CH_2-CH_2-$), 0.08 – 0.07 (s, 3H; $-CH_3$). **¹³C-NMR** (400 MHz, CD_3OD , 25 °C, ppm): δ = 145.97 (arom.), 145.95 (arom.), 129.44 (arom.), 61.82 ($-CH_2-N$), 58.17 ($-O-CH_2-$), 29.80 ($-O-CH_2-CH_2-$), 29.29 ($-CH_2-CH_2-N$), -4.59 ($-CH_3$). **²⁹Si-NMR** (400 MHz, CD_3OD , 25 °C, ppm): δ = 13.33 ($-Si(CH_3)_3$), -57.44 ($-O-Si(Me)-O_{2/2}$). **IR** (ATR, 32 scans, cm^{-1}): 3381.9, 3048.3, 2967.4, 1632.8, 1485.9, 1391.0, 1268.0, 1021.3, 845.4, 770.1, 681.1, 430.7. **EA** (% , measured (calculated)), repeating unit $C_{10}H_{16}BrNO_2Si$: C 33.625 (41.38), H 5.859 (5.56), Br 25.589 (27.53), N 3.518 (4.83), Si 10.575 (9.68).



Synthesis of (4-(polymethylsiloxane)butoxy) 1-methyl-1H-imidazol-3-ium bromide (**4.23**):

Product **4.23** was synthesized (102 % yield, 1.22 mmol) according to the representative procedure E, using 7.5 mL EtOH, 7.5 mL dried Toluene, 7.5 g of **4.1b** (1.20 mmol) and 2.80 mL 1-methyl-1H-imidazole (34.80 mmol). The obtained product was a red/brown, milky, high viscous liquid.

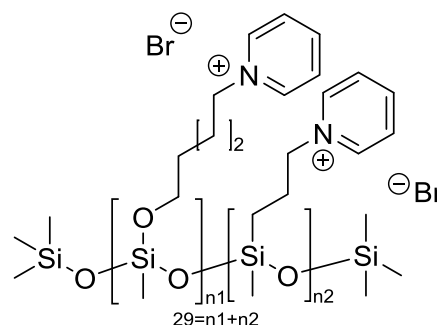
¹H-NMR (300 MHz, CD_3OD , 25 °C, ppm): δ = 9.02 – 8.97 (s, $N=CH-N$), 7.77 – 7.76 (d, $N-CH=CH-N(Me)$), 7.62 – 7.55 (d, $N-CH=CH-N(Me)$), 4.21 – 4.15 (m, 2H, $-CH_2-N$), 3.85 – 3.83 (s, $N-CH_3$), 3.67 – 3.65 (m, 2H, $-O-CH_2-$), 3.45 – 3.43 (m, 2H, $-CH_2-CH_2-CH_2-N$), 1.87 – 1.79 (m, 2H, $-CH_2-CH_2-N$), 1.45 – 1.38 (m, 2H, $-O-CH_2-CH_2-$), 0.07 – -0.05 (s, 3H; $-CH_3$). **¹³C-NMR** (300 MHz, CD_3OD , 25 °C, ppm): δ = 137.49 ($N=CH-N$), 124.97 ($N-CH=CH-N(Me)$), 123.43 ($N-CH=CH-N(Me)$), 61.85 ($-O-CH_2-$), 50.60 ($-CH_2-N$), 36.80 ($N-CH_3$), 29.95 ($-CH_2-CH_2-N$), 27.88 ($-O-CH_2-CH_2-$), -3.76 ($-CH_3$). **²⁹Si-NMR** (300 MHz, CD_3OD , 25 °C, ppm): δ = -59.02 ($-O-Si(Me)-O_{2/2}$). **IR** (ATR, 32 scans, cm^{-1}): 3372.5, 3143.2, 3092.0, 2940.7, 2868.8, 1571.9, 1164.9, 1058.1, 757.2, 621.3. **EA** (% , measured (calculated)), repeating unit $C_9H_{17}BrN_2O_2Si$: C 36.97 (36.86), H 5.812 (5.84), Br 23.84 (27.25), N 9.056 (9.55), Si 4.49 (9.58).



Synthesis of (4-(polymethylsiloxane)pentoxy) pyridinium bromide (4.24):

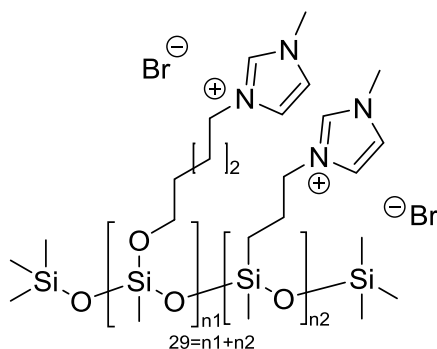
Product **4.24** was synthesized (102 % yield, 0.50 mmol) according to the representative procedure E, using 3 mL EtOH, 3 mL dried Toluene, 3.0 g of **4.12** (0.45 mmol) and 1.04 mL pyridine (12.95 mmol). The obtained product was an orange, milky, sticky, viscous liquid.

¹H-NMR (300 MHz, CD₃OD, 25 °C, ppm): δ = 9.09 – 8.98 (m, 2H, arom.), 8.54 – 8.50 (m, 1H, arom.), 8.07 – 8.08 (m, 2H; arom.), 4.65 – 4.57 (m, 2H, -CH₂-N), 3.69 – 3.57 (m, 2H, -O-CH₂-), 2.01 – 1.97 (p, 2H, -CH₂-CH₂-N), 1.58 – 1.44 (p, 2H, -O-CH₂-CH₂-), 1.39 – 1.28 (p, 2H, -O-CH₂-CH₂-CH₂-), 0.00 (s, 3H; -CH₃). **¹³C-NMR** (300 MHz, CD₃OD, 25 °C, ppm): δ = 145.63 – 145.56 (arom.), 144.77 (arom.), 128.25 (arom.), 60.99 (-O-CH₂-), 58.18 (-CH₂-N), 31.50 (-O-CH₂-CH₂-), 30.92 (-CH₂-CH₂-N), 22.22 (-O-CH₂-CH₂-CH₂-), -4.67 (-CH₃). **²⁹Si-NMR** (300 MHz, CD₃OD, 25 °C, ppm): δ = -58.86 (-O-Si(Me)-O_{2/2}). **IR** (ATR, 32 scans, cm⁻¹): 3346.1, 3019.5, 2933.0, 2864.7, 1632.0, 1484.6, 1266.5, 1027.5, 772.9, 683.4, 435.7. **EA** (% , measured (calculated)), repeating unit C₁₁H₁₈BrNO₂Si: C 38.93 (43.42), H 6.45 (5.956), Br 21.84 (26.26), N 3.803 (4.60), Si 20.14 (9.23).

Synthesis of (4-(polymethylsiloxane)pentoxy) 1-methyl-1H-imidazol-3-ium bromide (4.25):

Product **4.25** was synthesized (105 % yield, 0.80 mmol) according to the representative procedure E, using 3 mL EtOH, 3 mL dried Toluene, 3.0 g of **4.12** (0.45 mmol) and 1.04 mL 1-methyl-1H-imidazole (13.05 mmol). The obtained product was an orange, milky, very sticky, high viscous liquid.

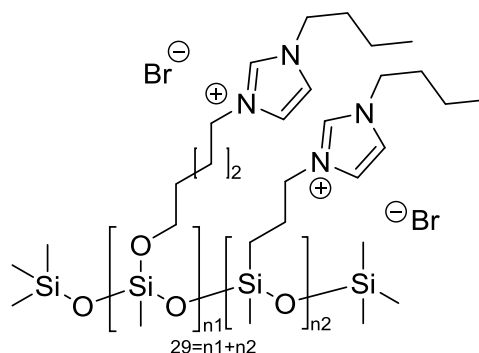
¹H-NMR (300 MHz, CD₃OD, 25 °C, ppm): δ = 9.22 – 9.21 (s, N=CH-N), 7.95 – 7.76 (d, N-CH=CH-N(Me)), 7.71 – 7.68 (d, N-CH=CH-N(Me)), 4.44 – 4.34 (m, 2H, -CH₂-N), 4.10 – 4.09 (s, N-CH₃), 3.92 (m, 2H, -O-CH₂-), 2.14 – 2.00 (p, 2H, -CH₂-CH₂-N), 1.76 – 1.66 (p, 2H, -O-CH₂-CH₂-), 1.59 – 1.50 (p, 2H, -O-CH₂-CH₂-CH₂-), 0.32 – 0.22 (s, 3H; -CH₃). **¹³C-NMR** (300 MHz, CD₃OD, 25 °C, ppm): δ = 137.80 (N=CH-N), 124.87 (N-CH=CH-N(Me)), 123.61 (N-CH=CH-N(Me)), 62.31 (-O-CH₂-), 50.71 (-CH₂-N), 36.72 (N-CH₃), 32.79 (-CH₂-CH₂-N), 30.84 (-O-CH₂-CH₂-), 23.54 (-O-CH₂-CH₂-CH₂-), -3.49 (-CH₃). **²⁹Si-NMR** (300 MHz, CD₃OD, 25 °C, ppm): δ = -58.86 (-O-Si(Me)-O_{2/2}). **IR** (ATR, 32 scans, cm⁻¹): 3334.9, 3064.0, 2934.2, 1570.0, 1518.1, 1457.1, 1267.4, 1166.2, 1021.4, 765.1, 663.6, 618.3. **EA** (% , measured (calculated)), repeating unit C₁₀H₁₉BrN₂O₂Si: C 35.64 (39.09), H 5.91 (6.23), Br 20.64 (26.64), N 9.36 (9.12), Si 14.46 (9.14).



Synthesis of (4-(polymethylsiloxane)pentoxy) 1-butyl-1H-imidazol-3-ium bromide (4.26):

Product **4.26** was synthesized (101 % yield, 0.75 mmol) according to the representative procedure E, using 5 mL EtOH, 5 mL dried Toluene, 5.0 g of **4.12** (0.74 mmol) and 1.04 mL 1-butyl-1*H*-imidazole (21.58 mmol). The obtained product was a slightly yellow to white, milky, sticky, high viscous liquid.

¹H-NMR (300 MHz, DMSO-*d*₆, 25 °C, ppm): δ = 9.69 (s, N=CH-N), 7.94 – 7.84 (d, N-CH=CH-N(Me) and N-CH=CH-N(Me)), 4.26 – 4.15 (m, 2H, -CH₂-N), 4.06 – 4.02 (t, N-CH₂-), 3.62 – 3.58 (m, 2H, -O-CH₂-), 3.55 – 3.47 (m, 2H, -O-CH₂-CH₂-CH₂-), 1.87 – 1.75 (p, 2H, -CH₂-CH₂-N), 1.73 – 1.68 (m, 2H, N-CH₂-), 1.53 – 1.36 (m, 2H, -O-CH₂-CH₂-), 1.29 – 1.21 (m, 2H, -CH₂-CH₃), 0.92 – 0.83 (m (3H, -CH₃), 0.12 – 0.01 (s, 3H; Si-CH₃). **¹³C-NMR** (300 MHz,

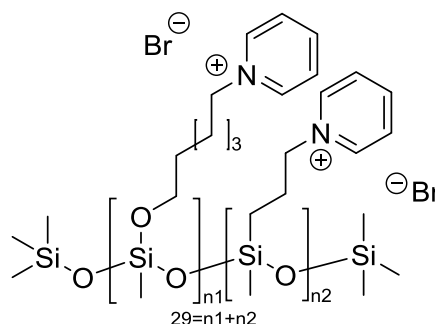


DMSO-*d*₆, 25 °C, ppm): δ = 136.91 (N=CH-N), 122.65 (N-CH=CH-N(Me) and N-CH=CH-N(Me)), 61.88 (-O-CH₂-CH₂-CH₂-), 57.77 (-O-CH₂-), 49.06 (-CH₂-N), 47.21 (N-CH₂-), 32.09 (-CH₂-CH₂-N), 31.67 (-O-CH₂-CH₂-), 29.69 (N-CH₂-CH₂-), 22.29 (CH₃-CH₂-), 13.74 (-CH₃), -3.85 (Si-CH₃). **²⁹Si-NMR** (300 MHz, DMSO-*d*₆, 25 °C, ppm): δ = -58.96 (-O-Si(Me)-O_{2/2}). **IR** (ATR, 32 scans, cm⁻¹): 3358.3, 3064.5, 2933.1, 2867.3, 1561.8, 1459.4, 1377.4, 1265.6, 1160.5, 1022.5, 916.2, 842.8, 773.8, 637.0, 428.3. **EA** (% , measured (calculated)), repeating unit C₁₃H₂₅BrN₂O₂Si: C 44.795 (44.70), H 6.542 (7.21), Br 16.398 (22.87), N 7.648 (8.02), Si 15.84 (8.04).

Synthesis of (4-(polymethylsiloxane)hexyloxy) pyridinium bromide (4.27):

Product **4.27** was synthesized (101 % yield, 0.42 mmol) according to the representative procedure E, using 3 mL EtOH, 3 mL dried Toluene, 3.0 g of **4.13** (0.42 mmol) and 0.98 mL pyridine (12.22 mmol). The obtained product was a yellow to orange, milky, very sticky, high viscous liquid.

¹H-NMR (300 MHz, CD₃OD, 25 °C, ppm): δ = 9.29 (m, 2H, arom.), 8.75 – 8.67 (m, 1H, arom.), 8.31 – 8.20 (m, 2H; arom.), 4.82 – 4.80 (m, 2H, -CH₂-N), 3.85 – 3.80 (t, 2H, -O-CH₂-), 2.19 – 2.11 (p, 2H, -CH₂-CH₂-N), 1.69 – 1.59 (p, 2H, -O-CH₂-CH₂-), 1.55 – 1.48 (m, 4H, -O-CH₂-CH₂-CH₂-CH₂-), 0.21 (s, 3H; -CH₃). **¹³C-NMR** (300 MHz, CD₃OD, 25 °C, ppm): δ = 146.85 (arom.), 146.04 (arom.), 129.48 (arom.), 62.57 (-O-CH₂-), 58.26 (-CH₂-N), 33.40 (-O-CH₂-CH₂-), 32.65



(-CH₂-CH₂-N), 27.11 (-O-CH₂-CH₂-CH₂-), 26.50 (-O-CH₂-CH₂-CH₂-CH₂-), -3.57 (-CH₃). **²⁹Si-NMR** (300 MHz, CD₃OD, 25 °C, ppm): δ = -58.91 (-O-Si(Me)-O_{2/2}). **IR** (ATR, 32 scans, cm⁻¹): 3369.9, 3019.8, 2932.6, 2860.2, 1632.2, 1579.7, 1484.8, 1265.8, 1022.5, 844.3, 722.6, 683.5, 439.4. **EA** (% , measured (calculated)), repeating unit C₁₂H₂₀BrNO₂Si: C 40.88 (45.28), H 6.04 (6.33), Br 21.60 (25.10), N 3.85 (4.40), Si 20.47 (8.82).

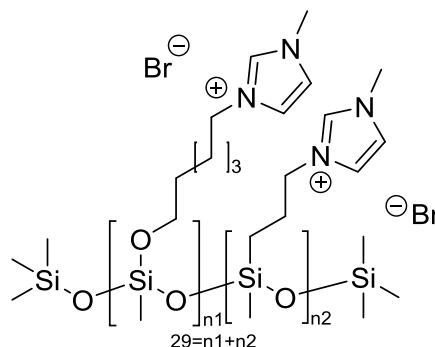
Synthesis of (4-(polymethylsiloxane)hexyloxy) 1-methyl-1H-imidazol-3-ium bromide (4.28):

Product **4.28** was synthesized (112 % yield, 0.47 mmol) according to the representative procedure E, using 3 mL EtOH, 3 mL dried Toluene, 3.0 g of **4.13** (0.42 mmol) and 0.97 mL 1-methyl-1*H*-imidazole (12.22 mmol). The obtained product was an orange, milky, sticky, high viscous liquid.

¹H-NMR (300 MHz, CD₃OD, 25 °C, ppm): δ = 9.25 (s, N=CH-N), 7.84 – 7.80 (d, N-CH=CH-N(Me)), 7.75 – 7.72 (d, N-CH=CH-N(Me)), 4.41 – 4.33 (m, 2H, -CH₂-N), 4.08 – 4.06 (s, N-CH₃), 3.86 – 3.84 (t, 2H, -O-CH₂-), 2.08 – 1.93 (p, 2H, -CH₂-CH₂-N), 1.70 – 1.61 (p, 2H, -O-CH₂-CH₂-), 1.57 – 1.44 (m, 4H, -O-CH₂-CH₂-CH₂-CH₂-), 0.25 – 0.20 (s, 3H; -CH₃).

¹³C-NMR (300 MHz, CD₃OD, 25 °C, ppm): δ = 138.95 (N=CH-N), 128.43 (N-CH=CH-N(Me)), 124.85 (N-CH=CH-N(Me)), 62.57 (-O-CH₂-), 50.68 (-CH₂-N), 36.65 (N-CH₃), 33.26 (-CH₂-CH₂-N), 31.04 (-O-CH₂-CH₂-), 26.92 (-O-CH₂-CH₂-CH₂-), 26.24 (-O-CH₂-CH₂-CH₂-CH₂-), -3.59 (-CH₃).

²⁹Si-NMR (300 MHz, CD₃OD, 25 °C, ppm): δ = -58.99 (-O-Si(Me)-O_{2/2}). **IR** (ATR, 32 scans, cm⁻¹): 3331.6, 3066.0, 2932.8, 2860.2, 1569.9, 1518.1, 1459.4, 1266.5, 1233.1, 1167.0, 1019.2, 908.8, 769.8, 664.0, 618.2, 417.2. **EA** (%), measured (calculated)), repeating unit C₁₁H₂₁BrN₂O₂Si: C 38.85 (41.12), H 6.64 (6.59), Br 17.99 (24.87), N 10.33 (8.72), Si 14.90 (8.74).

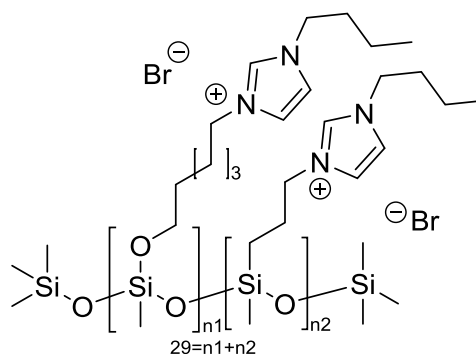
Synthesis of (4-(polymethylsiloxane)hexyloxy) 1-butyl-1H-imidazol-3-ium bromide (4.29):

Product **4.29** was synthesized (100 % yield, 0.70 mmol) according to the representative procedure E, using 5 mL EtOH, 5 mL dried Toluene, 5.0 g of **4.13** (0.70 mmol) and 2.68 mL 1-butyl-1*H*-imidazole (20.37 mmol). The obtained product was a yellow, clear, sticky, viscous liquid.

¹H-NMR (300 MHz, DMSO-d₆, 25 °C, ppm): δ = 9.77 (s, N=CH-N), 7.98 – 7.83 (m, N-CH=CH-N(Me) and N-CH=CH-N(Me)), 4.24 – 4.15 (m, 2H, -CH₂-N), 4.05 – 4.01 (s, N-CH₂-), 3.69 – 3.50 (m, 4H, -O-CH₂-CH₂-CH₂-CH₂-), 1.82 – 1.73 (m, 2H, -CH₂-CH₂-N), 1.73 – 1.66 (p, 2H, N-CH₂-CH₂-), 1.44 – 1.41 (m, 2H, -O-CH₂-CH₂-), 1.32 – 1.17 (m, 4H, -O-CH₂-CH₂-CH₂- and CH₃-CH₂-), 0.91 – 0.84 (m, 3H, -CH₃), 0.09 – 0.00 (s, 3H; Si-CH₃).

¹³C-NMR (300 MHz, DMSO-d₆, 25 °C, ppm): δ = 136.39 (N=CH-N),

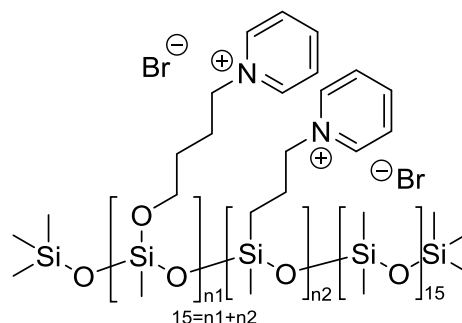
122.26 (N-CH=CH-N(Me) and N-CH=CH-N(Me)), 61.59 (-O-CH₂-), 57.34 (-O-CH₂-CH₂-CH₂-CH₂-), 48.58 (-CH₂-N), 46.51 (N-CH₂-), 31.77 (-O-CH₂-CH₂-), 31.33 (-CH₂-CH₂-N), 24.88 (-O-CH₂-CH₂-CH₂-), 18.82 (-CH₂-CH₃), 13.25 (-CH₃), -4.35 (Si-CH₃). **²⁹Si-NMR** (300 MHz, DMSO-d₆, 25 °C, ppm): δ = -60.20 (-O-Si(Me)-O_{2/2}). **IR** (ATR, 32 scans, cm⁻¹): 3352.0, 3068.7, 2932.4, 2862.9, 1561.8, 1460.2, 1377.3, 1266.2, 1023.9, 917.0, 773.9, 440.0. **EA** (%), measured (calculated)), repeating unit C₁₄H₂₇BrN₂O₂Si: C 44.395 (46.28), H 7.270 (7.49), Br 18.133 (21.99), N 6.826 (7.71), Si 10.405 (7.73).



Synthesis of polydimethylsiloxane-co-(4-(polymethylsiloxane)butoxy) pyridinium bromide (4.30):

Product **4.30** was synthesized (100 % yield, 5.66 mmol) according to the representative procedure E, using 30 mL DMF, 25.0 g of **4.2** (5.56 mmol) and 6.72 mL pyridine (83.44 mmol). The obtained product was a transparent, yellow, sticky, high viscous liquid.

¹H-NMR (400 MHz, DMSO-d₆, 25 °C, ppm): δ = 9.33 – 9.21 (dd, 2H, arom.), 8.66 – 8.60 (tt, 1H, arom.), 8.21 – 8.16 (dd, 2H; arom.), 4.79 – 4.67 (t, 2H, -CH₂-N), 3.65 – 3.55 (m, 2H, -O-CH₂-), 3.43 – 3.28 (m, 2H, -CH₂-CH₂-CH₂-N), 1.98 – 1.89 (p, 2H, -CH₂-CH₂-N), 1.48 – 1.43 (m, 2H, -CH₂-CH₂-CH₂-N), 1.40 – 1.31 (m, 2H, -O-CH₂-CH₂-), 0.82 – 0.77 (t, 2H, -CH₂-CH₂-CH₂-N), 0.09 – -0.09 (s, 3H; -CH₃). **¹³C-NMR** (400 MHz, DMSO-d₆, 25 °C, ppm): δ = 145.47 (arom.), 144.75 (arom.),

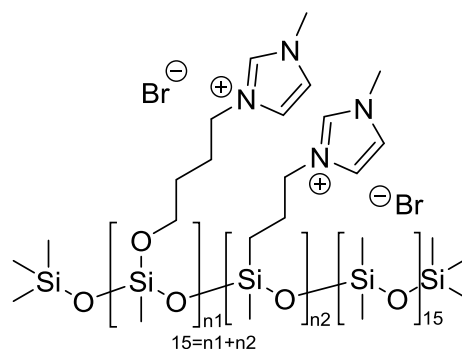


128.02 (arom.), 60.95 (-CH₂-N), 59.74 (-O-CH₂-), 35.80 (-CH₂-CH₂-CH₂-N), 30.74 (-CH₂-CH₂-CH₂-N), 28.01 (-O-CH₂-CH₂-), 27.59 (-CH₂-CH₂-N), 0.62 (-CH₃). **²⁹Si-NMR** (400 MHz, DMSO-d₆, 25 °C, ppm): δ = -20.66 (-O-Si(Me)₂-O-), -58.76 (-O-Si(Me)-O_{2/2}). **IR** (ATR, 32 scans, cm⁻¹): 2960.0, 1667.0, 1632.7, 1485.7, 1388.3, 1259.5, 1013.5, 843.6, 779.9, 682.0. **EA** (%), measured (calculated)), repeating unit C₁₂H₂₂BrNO₃Si₂: C 33.26 (39.55), H 5.522 (6.09), Br 22.966 (21.93), N 3.198 (3.84).

Synthesis of polydimethylsiloxane-co-(4-(polymethylsiloxane)butoxy) 1-methyl-1H-imidazol-3-ium bromide (4.31):

Product **4.31** was synthesized (102 % yield, 1.62 mmol) according to the representative procedure E, using 7.5 mL Toluene and 7.5 mL Ethanol, 7.5 g of **4.2** (1.67 mmol) and 2.00 mL 1-methyl-1H-imidazole (25.03 mmol). The obtained product was a transparent, yellow, sticky, viscous liquid.

¹H-NMR (300 MHz, DMSO-d₆, 25 °C, ppm): δ = 9.44 – 9.35 (s, N=CH-N), 7.91 – 7.76 (m, N-CH=CH-N(Me) and N-CH=CH-N(Me)), 4.26 – 4.15 (m, 2H, -CH₂-N), 3.80 – 3.78 (s, N-CH₃), 3.65 – 3.57 (m, 2H, -O-CH₂-), 3.40 – 3.34 (t, 2H, -CH₂-CH₂-CH₂-N), 1.83 – 1.73 (p, 2H, -CH₂-CH₂-N), 1.45 – 1.40 (m, 2H, -O-CH₂-CH₂-), 0.81 – 0.76 (m, 2H, -CH₂-CH₂-CH₂-N), 0.02 – -0.03 (s, 3H; -CH₃). **¹³C-NMR** (300 MHz, DMSO-d₆, 25 °C, ppm): δ = 135.35 (N=CH-N),

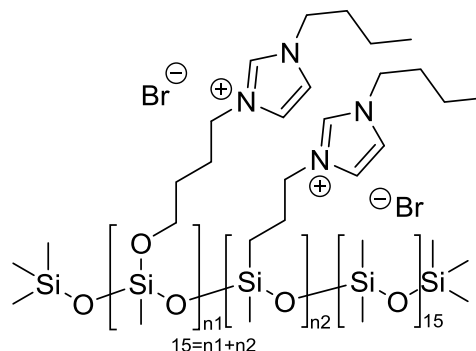


122.28 (N-CH=CH-N(Me)), 120.93 (N-CH=CH-N(Me)), 59.19 (-O-CH₂-), 47.40 (-CH₂-N), 34.59 (N-CH₃), 33.53 (-CH₂-CH₂-CH₂-N), 27.54 (-CH₂-CH₂-N), 24.97 (-O-CH₂-CH₂-), 16.76 (-CH₂-CH₂-CH₂-N), 0.53, -5.46 (-CH₃). **²⁹Si-NMR** (300 MHz, DMSO-d₆, 25 °C, ppm): δ = -20.76 (-O-Si(Me)₂-O-), -58.81 (-O-Si(Me)-O_{2/2}). **IR** (ATR, 32 scans, cm⁻¹): 3397.3, 3080.2, 2960.6, 1571.6, 1451.5, 1260.2, 1166.0, 1015.2, 842.6, 793.9, 650.1, 620.4. **EA** (%), measured (calculated)), repeating unit C₁₁H₂₃BrN₂O₃Si₂: C 33.255 (35.96), H 6.726 (6.31), Br 13.036 (21.75), N 7.693 (7.63).

Synthesis of polydimethylsiloxane-co- (4-(polymethylsiloxane)butoxy) 1-butyl-1H-imidazol-3-ium bromide (4.32):

Product **4.32** was synthesized (101 % yield, 1.62 mmol) according to the representative procedure E, using 7.5 mL Toluene and 7.5 mL Ethanol, 7.5 g of **4.2** (1.67 mmol) and 3.29 mL 1-butyl-1H-imidazole (25.03 mmol). The obtained product was a transparent, slightly yellow, sticky, viscous liquid.

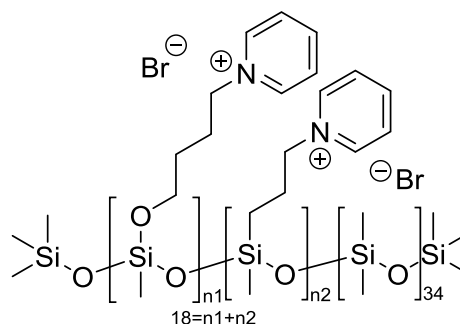
¹H-NMR (400 MHz, DMSO-d₆, 25 °C, ppm): δ = 9.62 – 9.53 (s, N=CH-N), 7.99 – 7.88 (m, 2H, N-CH=CH-N(Bu)), 4.28 – 4.19 (t, 2H, -CH₂-N), 4.08 – 4.05 (t, -CH₂-CH₂-CH₂-CH₃), 3.69 – 3.59 (m, 2H, -O-CH₂-), 3.48 – 3.38 (m, 2H, -CH₂-CH₂-CH₂-N), 1.87 – 1.71 (p, 2H, -CH₂-CH₂-N), 1.70 – 1.66 (m, 2H, CH₂-CH₂-CH₃), 1.45 – 1.42 (m, 2H, -O-CH₂-CH₂-), 1.28 – 1.17 (m, 2H, CH₂-CH₃), 1.04 – 1.00 (t, 3H, -CH₂-CH₃), 0.89 – 0.83 (m, 2H, -CH₂-CH₂-CH₂-N), 0.06 – 0.03 (s, 3H; Si-CH₃). **¹³C-NMR** (400 MHz, DMSO-d₆, 25 °C, ppm): δ = 136.01 (N=CH-N), 122.37 (N-CH=CH-N(Me)), 60.91 (-O-CH₂-), 48.51 (-CH₂-N), 46.61 (-CH₂-CH₂-CH₂-CH₃), 32.11 (CH₂-CH₂-CH₃), 31.34 (-CH₂-CH₂-N), 28.38 (-O-CH₂-CH₂-), 26.15 (-CH₂-CH₂-CH₂-N), 18.70 (CH₂-CH₃), 17.96 (-CH₂-CH₂-CH₂-N), 13.27 (CH₂-CH₃), 0.65, -4.30 (Si-CH₃). **²⁹Si-NMR** (400 MHz, DMSO-d₆, 25 °C, ppm): δ = 8.93 (-Si(Me)₃), -21.07 (-O-Si(Me)₂-O-), -58.78 (-O-Si(Me)-O_{2/2}). **IR** (ATR, 32 scans, cm⁻¹): 2962.5, 2163.4, 1411.2, 1257.9, 1012.3, 906.1, 840.4, 791.4, 701.9. **EA** (% , measured (calculated)), repeating unit C₂₀H₄₇BrN₂O₄Si₄: C 41.245 (42.01), H 7.618 (8.28), Br 14.58 (13.97), N 6.393 (4.90), Si 5.221 (19.65).



Synthesis of polydimethylsiloxane-co-(4-(polymethylsiloxane)butoxy) pyridinium bromide (4.33):

Product **4.33** was synthesized (93 % yield, 0.99 mmol) according to the representative procedure E, using 5 mL Toluene and 5 mL Ethanol, 7.0 g of **4.3** (1.09 mmol) and 1.50 mL pyridine (18.58 mmol). The obtained product was a transparent, yellow, sticky, high viscous liquid.

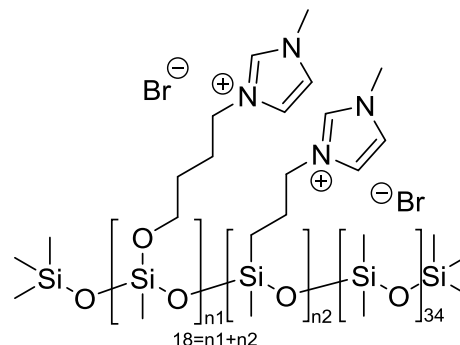
¹H-NMR (400 MHz, DMSO-d₆, 25 °C, ppm): δ = 9.22 – 9.19 (dd, 2H, arom.), 8.66 – 8.60 (tt, 1H, arom.), 8.20 – 8.12 (dd, 2H; arom.), 4.70 – 4.66 (t, 2H, -CH₂-N), 3.59 – 3.56 (t, 2H, -CH₂-CH₂-CH₂-N), 3.41 – 3.30 (t, 2H, -O-CH₂-), 1.99 – 1.91 (p, 2H, -CH₂-CH₂-N), 1.75 – 1.72 (m, 2H, -CH₂-CH₂-CH₂-N), 1.44 – 1.37 (m, 2H, -O-CH₂-CH₂-), 1.05 – 1.01 (t, 2H, -CH₂-CH₂-CH₂-N), 0.10 – -0.03 (s, 3H; -CH₃). **¹³C-NMR** (400 MHz, DMSO-d₆, 25 °C, ppm): δ = 145.49 (arom.), 144.77 (arom.), 128.05 (arom.), 60.54 (-CH₂-N), 59.80 (-O-CH₂-), 35.34 (-CH₂-CH₂-CH₂-N), 30.95 (-CH₂-CH₂-CH₂-N), 28.67 (-O-CH₂-CH₂-), 27.82 (-CH₂-CH₂-N), 0.98 – 0.07 (-CH₃). **²⁹Si-NMR** (400 MHz, DMSO-d₆, 25 °C, ppm): δ = -58.08 (-O-Si(Me)-O_{2/2}). **IR** (ATR, 32 scans, cm⁻¹): 3357.8, 2962.1, 1633.4, 1486.9, 1258.3, 1009.6, 842.5, 789.3, 682.6. **EA** (% , measured (calculated)), C₂₅₂H₅₁₈Br₁₇N₁₇O₇₃Si₅₇: C 28.635 (38.24), H 6.623 (6.60), Br 13.711 (17.16), N 1.736 (3.01).



Synthesis of polydimethylsiloxane-co- (4-(polymethylsiloxane)butoxy) 1-methyl-1H-imidazol-3-ium bromide (4.34):

Product **4.34** was synthesized (98 % yield, 1.05 mmol) according to the representative procedure E, using 5 mL Toluene and 5 mL Ethanol, 7 g of **4.3** (1.09 mmol) and 1.48 mL 1-methyl-1H-imidazole (18.59 mmol). The obtained product was a transparent, yellow, sticky, viscous liquid.

¹H-NMR (400 MHz, DMSO-d₆, 25 °C, ppm): δ = 9.45 – 9.30 (s, N=CH-N), 7.89 – 7.77 (m, N-CH=CH-N(Me) and N-CH=CH-N(Me)), 4.25 – 4.19 (m, 2H, -CH₂-N), 3.89 – 3.87 (s, N-CH₃), 3.65 – 3.60 (m, 2H, -O-CH₂-), 3.44 – 3.34 (t, 2H, -CH₂-CH₂-CH₂-N), 1.85 – 1.77 (p, 2H, -CH₂-CH₂-N), 1.48 – 1.44 (m, 2H, -O-CH₂-CH₂-), 1.08 – 1.01 (m, 2H, -CH₂-CH₂-CH₂-N), 0.05 – -0.10 (s, 3H; -CH₃). **¹³C-NMR**

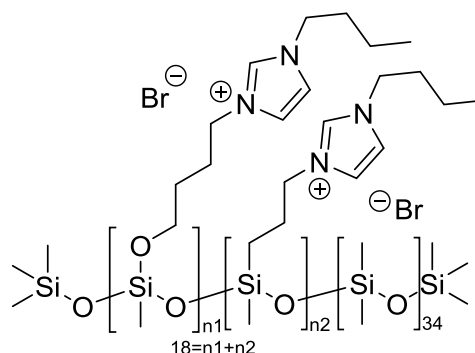


(400 MHz, DMSO-d₆, 25 °C, ppm): δ = 136.50 (N=CH-N), 123.55 (N-CH=CH-N(Me)), 122.21 (N-CH=CH-N(Me)), 60.87 (-O-CH₂-), 48.63 (-CH₂-N), 35.78 (N-CH₃), 33.98 (-CH₂-CH₂-CH₂-N), 28.77 (-CH₂-CH₂-N), 26.41 (-O-CH₂-CH₂-), 17.86 (-CH₂-CH₂-CH₂-N), 0.55, -4.32 (-CH₃). **²⁹Si-NMR** (400 MHz, DMSO-d₆, 25 °C, ppm): δ = -21.73 (-O-Si(Me)₂-O-), -58.91 (-O-Si(Me)-O_{2/2}). **IR** (ATR, 32 scans, cm⁻¹): 3378.6, 2961.5, 1571.9, 1412.1, 1258.8, 1166.2, 1012.2, 792.1, 698.1, 620.3. **EA** (% , measured (calculated)), C₂₃₅H₅₃₅Br₁₇N₃₄O₇₃Si₅₇: C 31.45 (35.44), H 7.277 (6.77), Br 10.318 (17.05), N 3.968 (5.98).

Synthesis of polydimethylsiloxane-co- (4-(polymethylsiloxane)butoxy) 1-butyl-1H-imidazol-3-ium bromide (4.35):

Product **4.35** was synthesized (98 % yield, 1.06 mmol) according to the representative procedure E, using 5 mL Toluene and 5 mL Ethanol, 7 g of **4.3** (1.09 mmol) and 2.44 mL 1-butyl-1H-imidazole (18.59 mmol). The obtained product was a transparent, slightly yellow, sticky, viscous liquid.

¹H-NMR (400 MHz, DMSO-d₆, 25 °C, ppm): δ = 9.75 – 9.59 (s, N=CH-N), 7.97 – 7.89 (m, 2H, N-CH=CH-N(Bu)), 4.26 – 4.19 (m, 2H, -CH₂-N), 4.04 – 4.00 (t, -CH₂-CH₂-CH₂-CH₃), 3.67 – 3.59 (m, 2H, -O-CH₂-), 3.43 – 3.38 (t, 2H, -CH₂-CH₂-CH₂-N), 1.87 – 1.73 (m, 2H, -CH₂-CH₂-N), 1.71 – 1.64 (m, 2H, CH₂-CH₂-CH₃), 1.48 – 1.37 (m, 2H, -O-CH₂-CH₂-), 1.28 – 1.15 (m, 2H, CH₂-CH₃), 1.08 – 1.00 (t, 3H, -CH₂-CH₃), 0.89 – 0.83 (m, 2H, -CH₂-CH₂-CH₂-N),



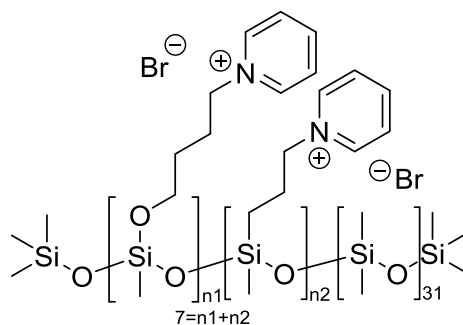
0.05 – -0.09 (s, 3H; Si-CH₃). **¹³C-NMR** (400 MHz, DMSO-d₆, 25 °C, ppm): δ = 136.04 (N=CH-N), 122.36 (N-CH=CH-N(Me)), 60.86 (-O-CH₂-), 48.48 (-CH₂-N), 46.21 (-CH₂-CH₂-CH₂-CH₃), 32.28 (CH₂-CH₂-CH₃), 31.28 (-CH₂-CH₂-N), 28.38 (-O-CH₂-CH₂-), 26.15 (-CH₂-CH₂-CH₂-N), 18.71 (CH₂-CH₃), 17.90 (-CH₂-CH₂-CH₂-N), 13.21 (CH₂-CH₃), 0.56, -4.34 (Si-CH₃). **²⁹Si-NMR** (400 MHz, DMSO-d₆, 25 °C, ppm): δ = -21.60 (-O-Si(Me)₂-O-), -58.80 (-O-Si(Me)-O_{2/2}). **IR** (ATR, 32 scans, cm⁻¹): 2939.7, 2873.2, 1437.6, 1266.3, 1019.1, 845.1, 771.1, 645.2, 560.1. **EA** (% , measured (calculated)),

$C_{286}H_{637}Br_{17}N_{34}O_{73}Si_{57}$: C 39.045 (39.57), H 7.741 (7.40), Br 12.723 (15.65), N 5.116 (5.49), Si 5.235 (18.44).

Synthesis of polydimethylsiloxane-co-(4-(polymethylsiloxane)butoxy) pyridinium bromide (4.36):

Product **4.36** was synthesized (92 % yield, 1.81 mmol) according to the representative procedure E, using 10 mL DMF, 7.5g of **4.4** (1.97 mmol) and 0.95 mL pyridine (11.80 mmol). The obtained product was a transparent, yellow, sticky, high viscous liquid.

¹H-NMR (300 MHz, DMSO-d₆, 25 °C, ppm): δ = 9.28 – 9.26 (dd, 2H, arom.), 8.77 – 8.67 (m, 1H, arom.), 8.32 – 8.23 (m, 2H; arom.), 4.78 – 4.73 (t, 2H, -CH₂-N), 3.72 – 3.61 (m, 2H, -O-CH₂-), 3.50 – 3.46 (t, 2H, -CH₂-CH₂-CH₂-N), 2.08 – 1.98 (p, 2H, -CH₂-CH₂-N), 1.88 – 1.81 (m, 2H, -CH₂-CH₂-CH₂-N), 1.65 – 1.39 (m, 2H, -O-CH₂-CH₂-), 0.84 (t, 2H, -CH₂-CH₂-CH₂-N), 0.11 – 0.00 (s, 3H; -CH₃). **¹³C-NMR** (300 MHz,

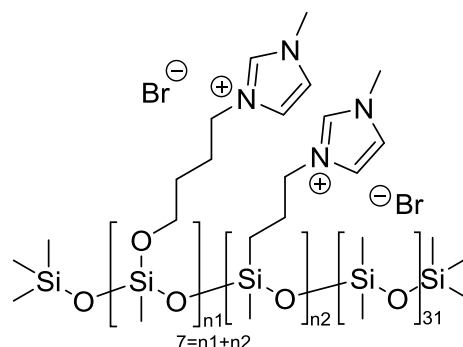


DMSO-d₆, 25 °C, ppm): δ = 145.61 (arom.), 144.77 (arom.), 128.04 (arom.), 60.53 (-CH₂-N), 59.79 (-O-CH₂-), 35.77 (-CH₂-CH₂-CH₂-N), 30.12 (-CH₂-CH₂-CH₂-N), 28.65 (-O-CH₂-CH₂-), 27.81 (-CH₂-CH₂-N). **²⁹Si-NMR** (300 MHz, DMSO-d₆, 25 °C, ppm): δ = 6.53 (-Si(CH₃)₃), -22.66 (-O-Si(Me)₂-O-), -59.25 (-O-Si(Me)-O_{2/2}). **IR** (ATR, 32 scans, cm⁻¹): 2961.6, 1632.9, 1486.3, 1411.7, 1257.9, 1010.4, 788.1, 682.9. **EA** (% , measured (calculated)), C₁₃₀H₃₀₆Br₆N₆O₄₅Si₄₀: C 28.605 (36.51), H 7.095 (7.21), Br 10.519 (11.21), N 0.733 (1.97).

Synthesis of polydimethylsiloxane-co- (4-(polymethylsiloxane)butoxy) 1-methyl-1H-imidazol-3-ium bromide (4.37):

Product **4.37** was synthesized (98 % yield, 1.88 mmol) according to the representative procedure E, using 10 mL DMF, 7.5 g of **4.4** (1.97 mmol) and 0.94 mL 1-methyl-1H-imidazole (11.80 mmol). The obtained product was a milky, yellow, sticky, viscous liquid.

¹H-NMR (300 MHz, DMSO-d₆, 25 °C, ppm): δ = 9.47 (s, N=CH-N), 7.91 – 7.80 (m, N-CH=CH-N(Me) and N-CH=CH-N(Me)), 4.25 – 4.21 (m, 2H, -CH₂-N), 3.89 – 3.88 (s, N-CH₃), 3.69 – 3.61 (m, 2H, -O-CH₂-), 3.30 (m, 2H, -CH₂-CH₂-CH₂-N), 1.85 – 1.76 (p, 2H, -CH₂-CH₂-N), 1.49 – 1.39 (m, 2H, -O-CH₂-CH₂-), 0.82 – 0.79 (m, 2H, -CH₂-CH₂-CH₂-N), 0.06 – 0.10 (s, 3H; -CH₃). **¹³C-NMR** (300 MHz, DMSO-d₆,

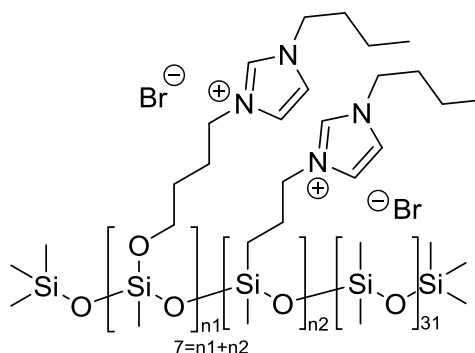


25 °C, ppm): δ = 136.57 (N=CH-N), 123.53 (N-CH=CH-N(Me)), 122.13 (N-CH=CH-N(Me)), 60.84 (-O-CH₂-), 48.41 (-CH₂-N), 35.77 (N-CH₃), 28.40 (-CH₂-CH₂-N), 26.15 (-O-CH₂-CH₂-), 17.75 (-CH₂-CH₂-CH₂-N), 1.05 – 0.25, -4.30 (-CH₃). **²⁹Si-NMR** (300 MHz, DMSO-d₆, 25 °C, ppm): δ = -21.73 (-O-Si(Me)₂-O-), -58.76 (-O-Si(Me)-O_{2/2}). **IR** (ATR, 32 scans, cm⁻¹): 2961.1, 1571.1, 1411.8, 1257.8, 10209.9, 787.8, 687.9, 620.1. **EA** (% , measured (calculated)), C₁₂₄H₃₁₂Br₆N₁₂O₄₅Si₄₀: C 31.165 (34.68), H 6.68 (7.32), Br 6.340 (11.16), N 2.64 (3.91).

Synthesis of polydimethylsiloxane-co- (4-(polymethylsiloxane)butoxy) 1-butyl-1H-imidazol-3-ium bromide (4.38):

Product **4.38** was synthesized (95 % yield, 1.83 mmol) according to the representative procedure E, using 5 mL Toluene and 5 mL Ethanol, 7.5 g of **4.4** (1.97 mmol) and 1.55 mL 1-butyl-1H-imidazole (11.81 mmol). The obtained product was a transparent, colorless, viscous liquid.

¹H-NMR (400 MHz, DMSO-d₆, 25 °C, ppm): δ = 9.64 (s, N=CH-N), 7.95 – 7.84 (m, 2H, N-CH=CH-N(Bu)), 4.24 – 4.17 (m, 2H, -CH₂-N), 4.00 – 3.97 (t, -CH₂-CH₂-CH₂-CH₃), 3.68 – 3.57 (m, 2H, -O-CH₂-), 3.44 – 3.40 (t, 2H, -CH₂-CH₂-CH₂-N), 1.85 – 1.76 (m, 2H, -CH₂-CH₂-N), 1.71 – 1.64 (m, 2H, CH₂-CH₂-CH₃), 1.47 – 1.36 (m, 2H, -O-CH₂-CH₂-), 1.28 – 1.16 (m, 2H, CH₂-CH₃), 1.08 – 1.01 (t, 3H, -CH₂-CH₃), 0.91 – 0.80 (m, 2H, -CH₂-CH₂-CH₂-N), 0.05 – -0.10 (s, 3H; Si-CH₃). **¹³C-NMR** (400 MHz, DMSO-

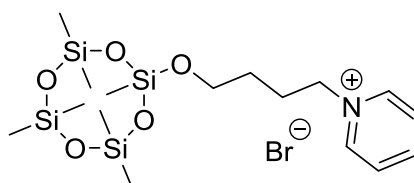


d₆, 25 °C, ppm): δ = 136.80 (N=CH-N), 122.43 (N-CH=CH-N(Me)), 60.87 (-O-CH₂-), 48.52 (-CH₂-N), 46.07 (-CH₂-CH₂-CH₂-CH₃), 32.41 (CH₂-CH₂-CH₃), 31.40 (-CH₂-CH₂-N), 28.45 (-O-CH₂-CH₂-), 26.19 (-CH₂-CH₂-CH₂-N), 19.06 (CH₂-CH₃), 18.74 (-CH₂-CH₂-CH₂-N), 13.34 (CH₂-CH₃), 0.24, -4.35 (Si-CH₃). **²⁹Si-NMR** (400 MHz, DMSO-d₆, 25 °C, ppm): δ = -22.66 (-O-Si(Me)₂-O-), -58.85 (-O-Si(Me)-O_{2/2}). **IR** (ATR, 32 scans, cm⁻¹): 3301.2, 3017.6, 2935.6, 2870.1, 1666.0, 1632.2, 1580.3, 1484.6, 1388.5, 1266.8, 1015.9, 917.4, 847.1, 769.1, 680.6. **EA** (% , measured (calculated)), C₁₄₂H₃₄₈Br₆N₁₂O₄₅Si₄₀: C 37.605 (37.51), H 7.139 (7.71), Br 8.826 (10.54), N 3.641 (3.70), Si 13.30 (24.71).

Synthesis of 1-(4-((1,3,3',5,5',7,7'-heptamethylcyclotetrasiloxyl)oxy)butyl)pyridinium bromide (4.39):

Product **4.39** was synthesized (82 % yield, 8.74 mmol) according to the representative procedure E, using 5 mL Toluene and 5 mL Ethanol, 7.5g of **4.5a** (17.32 mmol) and 1.40 mL pyridine (17.32 mmol). The obtained product was a white/slightly yellow, milky, wet powder.

¹H-NMR (300 MHz, DMSO-d₆, 25 °C, ppm): δ = 9.18 – 9.16 (d, 2H, arom.), 8.65 – 8.59 (t, 1H, arom.), 8.20 – 8.15 (t, 2H; arom.), 4.69 – 4.64 (t, 2H, -CH₂-N), 3.43 – 3.39 (t, 2H, -O-CH₂-), 2.00 – 1.90 (p, 2H, -CH₂-CH₂-N), 1.45 – 1.31 (p, 2H, -O-CH₂-CH₂-), 0.12 – -0.11 (s, 3H; -CH₃). **¹³C-NMR** (400 MHz,

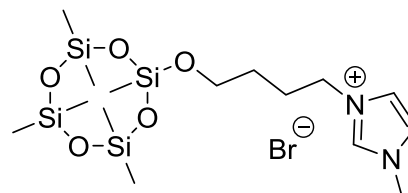


DMSO-d₆, 25 °C, ppm): δ = 145.67 (arom.), 144.88 (arom.), 127.99 (arom.), 60.65 (-CH₂-N), 58.89 (-O-CH₂-), 28.74 (-O-CH₂-CH₂-), 27.91(-CH₂-CH₂-N), 0.74 (-CH₃). **²⁹Si-NMR** (400 MHz, DMSO-d₆, 25 °C, ppm): δ = -18.62 - -19.11 (Si(Me)₂-O_{2/2}), -56.06 (-O-Si(Me)-O_{2/2}). **IR** (ATR, 32 scans, cm⁻¹): 3376.4, 2962.7, 1630.9, 1485.6, 1259.2, 1056.7, 800.8, 686.7, 555.1, 518.9. **EA** (% , measured (calculated)), C₁₁H₂₉BrO₅Si₄: C 33.71 (30.47), H 5.69 (6.74), Br 32.26 (18.43), N 1.259 (2.73).

Synthesis of 1-(4-((1,3,3',5,5',7,7'-heptamethylcyclotetrasiloxyl)oxy)butyl) 1-methyl-1H-imidazol-3-ium bromide (4.40):

Product **4.40** was synthesized (62 % yield, 4.51 mmol) according to the representative procedure E, using 3 mL Toluene and 3 mL Ethanol, 3.0 g of **4.5a** (6.91 mmol) and 0.55 mL 1-methyl-1H-imidazole (6.91 mmol). The obtained product was a milky, colorless, low viscous liquid.

¹H-NMR (300 MHz, DMSO-d₆, 25 °C, ppm): δ = 9.27 – 9.25 (s, N=CH-N), 7.83 – 7.82 (d, N-CH=CH-N(Me)), 7.75 – 7.73 (d, N-CH=CH-N(Me)), 4.22 – 4.17 (t, 2H, -CH₂-N), 3.86 (s, N-CH₃) 3.42 – 3.38 (t, 2H, -O-CH₂-), 1.86 – 1.77 (p, 2H, -CH₂-CH₂-N), 1.42 – 1.33 (p, 2H, -O-CH₂-CH₂-), 0.092 – -0.09 (s, 3H; -CH₃).

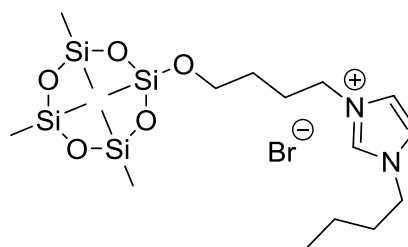


¹³C-NMR (400 MHz, DMSO-d₆, 25 °C, ppm): δ = 132.66 (N=CH-N), 123.48 (N-CH=CH-N(Me)), 122.25 (N-CH=CH-N(Me)), 59.80 (-O-CH₂-), 48.69 (-CH₂-N), 35.52 (N-CH₃), 28.81 (-CH₂-CH₂-N), 26.48 (-O-CH₂-CH₂-), 0.75 (-CH₃). **²⁹Si-NMR** (400 MHz, DMSO-d₆, 25 °C, ppm): δ = -18.63 – -19.12 (Si(Me)₂-O_{2/2}), -56.05 (-O-Si(Me)-O_{2/2}). **IR** (ATR, 32 scans, cm⁻¹): 3347.3, 2959.9, 1568.2, 1446.6, 1259.9, 1053.3, 796.5, 699.2, 617.9, 559.8 **EA** (% , measured (calculated)), repeating unit C₁₁H₂₉BrO₅Si₄: C 35.93 (30.47), H 6.14 (6.74), Br 22.64 (18.43), N 8.54 (9.55), Si 10.24 (25.91).

Synthesis of 1-(4-((1,3,3',5,5',7,7'-heptamethylcyclotetrasiloxyl)oxy)butyl) 1-butyl-1H-imidazol-3-ium bromide (4.41):

Product **4.41** was synthesized (94 % yield, 21.65 mmol) according to the representative procedure E, using 5 mL Toluene and 5 mL Ethanol, 10.0 g of **4.5a** (23.09 mmol) and 3.04 mL 1-butyl-1H-imidazole (23.09 mmol). The obtained product was a milky, white, high viscous liquid.

¹H-NMR (400 MHz, DMSO-d₆, 25 °C, ppm): δ = 9.31 – 9.30 (s, N=CH-N), 7.81 – 7.77 (m, 2H, N-CH=CH-N(Bu)), 4.17 – 4.12 (m, 2H, -CH₂-N), 4.04 (t, -CH₂-CH₂-CH₂-CH₃), 3.66 – 3.55 (m, 2H, -O-CH₂-), 3.36 – 3.25 (m, 2H, -CH₂-CH₂-N), 1.78 – 1.64 (m, 2H, CH₂-CH₂-CH₃), 1.38 – 1.25 (m, 2H, -O-CH₂-CH₂-), 1.23 – 1.14 (m, 2H, CH₂-CH₃), 1.07 – 1.02 (t, 3H, -CH₂-CH₃), 0.02 – -

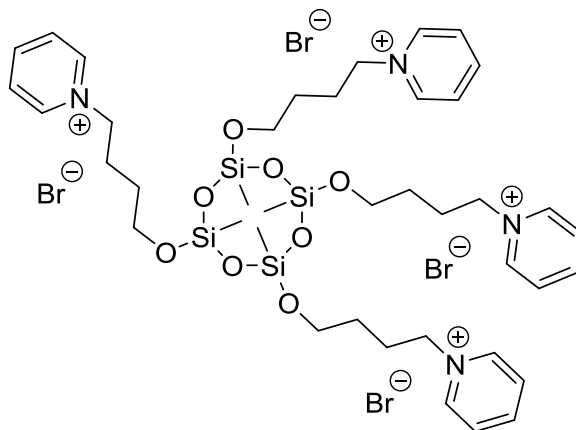


0.09 (s, 3H; Si-CH₃). **¹³C-NMR** (400 MHz, DMSO-d₆, 25 °C, ppm): δ = 135.98 (N=CH-N), 122.42 (N-CH=CH-N(Me)), 59.84 (-O-CH₂-), 48.53 (-CH₂-N), 47.48 (-CH₂-CH₂-CH₂-CH₃), 31.75 (CH₂-CH₂-CH₃), 31.31 (-CH₂-CH₂-N), 28.95 (-O-CH₂-CH₂-), 18.78 (CH₂-CH₃), 13.28 (CH₂-CH₃), 0.65, -4.17 (Si-CH₃). **²⁹Si-NMR** (400 MHz, DMSO-d₆, 25 °C, ppm): δ = -18.20 – -18.51 (-O-Si(Me)₂-O-), -57.03 (-O-Si(Me)-O_{2/2}). **IR** (ATR, 32 scans, cm⁻¹): 2964.3, 1392.8, 1259.6, 1052.2, 957.3, 798.3, 765.9, 698.8, 664.7, 558.1. **EA** (% , measured (calculated)), C₁₄₂H₃₄₈Br₆N₁₂O₄₅Si₄₀: C 39.32 (38.76), H 6.985 (7.41), Br 19.601 (14.33), N 8.037 (5.02), Si 4.003 (20.14).

Synthesis of 1,3,5,7-(4-(1',3',5',7'-etramethylcyclotetrasiloxyl)oxy)butyl) pyridinium bromide (4.42):

Product **4.42** was synthesized (89 % yield, 8.78 mmol) according to the representative procedure E, using 5 mL Toluene and 5 mL Ethanol, 7.5g of **4.6** (8.84 mmol) and 2.85 mL pyridine (35.36 mmol). The obtained product was a yellow, slightly milky, sticky, viscous liquid.

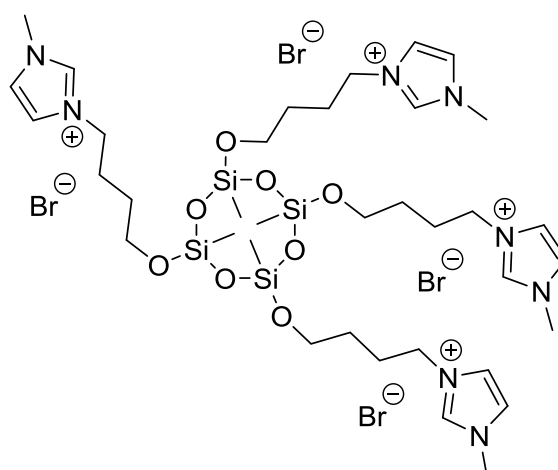
¹H-NMR (400 MHz, CD₃OD, 25 °C, ppm): δ = 9.44 – 9.33 (m, 2H, arom.), 8.91 – 8.84 (m, 1H, arom.), 8.45 – 8.36 (m, 2H; arom.), 5.06 – 4.94 (t, 2H, -CH₂-N), 4.05 – 3.96 (t, 2H, -O-CH₂-), 3.66 – 3.61 (m, 2H, -CH₂-CH₂-CH₂-N), 2.38 – 2.51 (p, 2H, -CH₂-CH₂-N), 1.89 – 1.75 (p, 2H, -O-CH₂-CH₂-), 0.90 – 0.78 (m, 2H, -CH₂-CH₂-CH₂-N), 0.43 – 0.37 (s, 3H; -CH₃). **¹³C-NMR** (400 MHz, CD₃OD, 25 °C, ppm): δ = 146.92 (arom.), 145.95 (arom.), 129.43 (arom.), 62.68 (-O-CH₂-), 61.76 (-CH₂-N), 35.70 (-CH₂-CH₂-CH₂-N), 29.80 (-O-CH₂-CH₂-), 29.28 (-CH₂-CH₂-N), -3.74 (-CH₃). **²⁹Si-NMR** (400 MHz, CD₃OD, 25 °C, ppm): δ = -58.47 (-O-Si(Me)-O_{2/2}). **IR** (ATR, 32 scans, cm⁻¹): 3393.9, 3030.9, 2937.6, 2871.6, 1632.6, 1486.3, 1389.4, 1267.6, 1026.7, 769.6, 681.8. **EA** (%), measured (calculated), C₄₀H₆₄Br₄N₄O₈Si₄: C 39.73 (41.38), 5.46 (5.56), Br 22.87 (27.53), N 3.634 (4.83), Si 9.69 (9.68).



Synthesis of 1,3,5,7-(4-(1',3',5',7'-etramethylcyclotetrasiloxyl)oxy)butyl) 1-methyl-1H-imidazol-3-ium bromide (4.43):

Product **4.43** was synthesized (100 % yield, 8.90 mmol) according to the representative procedure E, using 5 mL Toluene and 5 mL Ethanol, 7.5g of **4.6** (8.84 mmol) and 2.82 mL 1-methyl-1H-imidazole (35.36 mmol). The obtained product was a yellow, transparent, sticky, viscous liquid.

¹H-NMR (400 MHz, CD₃OD, 25 °C, ppm): δ = 9.22 – 9.21 (s, N=CH-N), 7.86 – 7.83 (d, N-CH=CH-N(Me)), 7.79 – 7.76 (d, N-CH=CH-N(Me)), 4.46 – 4.39 (t, 2H, -CH₂-N), 3.97 – 3.86 (s, N-CH₃), 3.74 – 3.70 (t, 2H, -O-CH₂-), 3.69 – 3.66 (t, 2H, -CH₂-CH₂-CH₂-N), 2.16 – 2.07 (p, 2H, -CH₂-CH₂-N), 1.77 – 1.65 (p, 2H, -O-CH₂-CH₂-), 0.75 – 0.72 (m, 2H, -CH₂-CH₂-CH₂-N), 0.32 – 0.20 (s, 3H; -CH₃). **¹³C-NMR** (400 MHz, CD₃OD, 25 °C, ppm): δ = 137.82 (N=CH-N), 124.95 (N-CH=CH-N(Me)), 123.61 (N-CH=CH-N(Me)), 61.88 (-O-CH₂-), 50.56 (-CH₂-N), 36.73 (N-CH₃), 35.07 (-CH₂-CH₂-CH₂-N), 30.36 (-CH₂-CH₂-N), 25.21 (-CH₂-CH₂-CH₂-N), 27.90 (-O-CH₂-CH₂-), 18.63 (-CH₂-CH₂-CH₂-N), -5.39 (-CH₃). **²⁹Si-NMR** (400 MHz, CD₃OD, 25 °C, ppm): δ = -58.78 (-O-Si(Me)-O_{2/2}). **IR** (ATR, 32 scans, cm⁻¹): 3385.2, 3686.8, 2940.3, 1631.3, 1571.4, 1452.0,



1267.8, 1165.4, 1027.6, 918.0, 763.9, 650.2, 619.8. **EA** (% , measured (calculated)), repeating unit $C_{36}H_{68}Br_4N_4O_8Si_4$: C 35.93 (36.86), 6.14 (5.84), Br 22.64 (27.25), N 8.54 (9.55), Si 10.24 (9.58).

Synthesis of 1,3,5,7-(4-(1',3',5',7'-etramethylcyclotetrasiloxyl)oxy)butyl) 1-butyl-1H-imidazol-3-ium bromide (4.44):

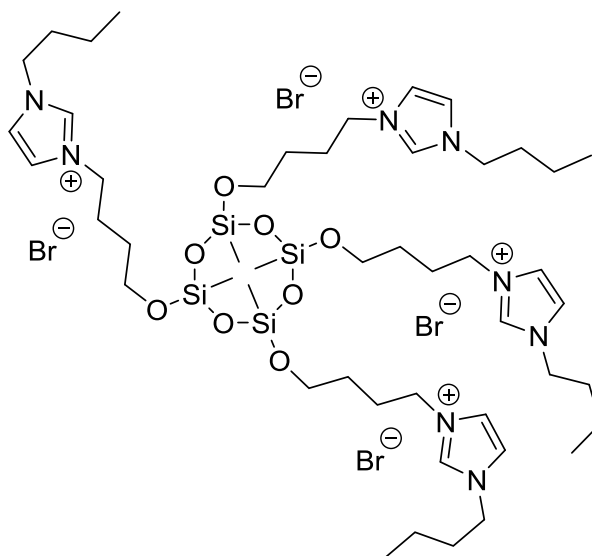
Product **4.44** was synthesized (93 % yield, 8.90 mmol) according to the representative procedure E, using 5 mL Toluene and 5 mL Ethanol, 7.5g of **4.6** (8.84 mmol) and 4.65 mL 1-butyl-1H-imidazole (35.36 mmol). The obtained product was a slightly yellow, milky, sticky, viscous liquid.

¹H-NMR (300 MHz, DMSO-d₆, 25 °C, ppm): δ

= 9.66 (s, N=CH-N), 8.08 – 7.90 (m, 2H, N-CH=CH-N(Bu)), 4.29 – 4.17 (t, 2H, -CH₂-N), 4.08 – 4.03 (t, -CH₂-CH₂-CH₂-CH₃), 3.68 – 3.54 (m, 2H, -O-CH₂-), 3.28 – 3.23 (m, 2H, -CH₂-CH₂-CH₂-N), 1.83 – 1.70 (p, 2H, -CH₂-CH₂-N), 1.67 – 1.60 (p, 2H, CH₂-CH₂-CH₃), 1.44 – 1.37 (m, 2H, -O-CH₂-CH₂-), 1.20 – 1.10 (p, 2H, CH₂-CH₃), 1.08 – 1.00 (3H, CH₂-CH₃), 0.44 – 0.37 (m, 2H, -CH₂-CH₂-CH₂-N), 0.06 – 0.04 (s, 3H; Si-CH₃). **¹³C-NMR** (300 MHz,

DMSO-d₆, 25 °C, ppm): δ = 136.03 (N=CH-N), 122.33 (N-CH=CH-N(Me)), 59.66 (-O-CH₂-),

48.49 (-CH₂-N), 46.67(-CH₂-CH₂-CH₂-CH₃), 32.07 (CH₂-CH₂-CH₃), 31.30 (-CH₂-CH₂-N), 28.71 (-O-CH₂-CH₂-), 23.48 (-CH₂-CH₂-CH₂-N), 18.67 (CH₂-CH₃), 17.94 (-CH₂-CH₂-CH₂-N), 13.18 (CH₂-CH₃), -4.55 (Si-CH₃). **²⁹Si-NMR** (300 MHz, DMSO-d₆, 25 °C, ppm): δ = -58.80 (-O-Si(Me)-O_{2/2}). **IR** (ATR, 32 scans, cm⁻¹): 3347.4, 3057.4, 2957.8, 2871.5, 1562.0, 1458.8, 1379.3, 1266.9, 1162.8, 1059.7, 765.6, 632.4. **EA** (% , measured (calculated)), repeating unit $C_{12}H_{23}BrN_2O_2Si$: C 41.645 (42.98), H 7.538 (6.91), Br 17.531 (23.83), N 7.807 (8.35), Si 8.75 (8.38).



Solvent-Screening of QAS-functionalized Samples 4.19, 4.20 and 4.21:

For the solvent-screening, the experiments of sample **4.19**, **4.20** and **4.21** were performed according to the representative procedure E. The behavior during the synthesis and the purification process, as well as any other observations were determined. The conversions are calculated via integration of ^1H -NMR. The results are listed in Table A-18.

Table A-18: Solvent-Screening of Samples **4.19**, **4.20** and **4.21**; conversions and comments are added.

Sample	Solvent	Conversion QAS [%]	Comments
4.19	Benzene	70.8	no solubility; no complete purification
	Chloroform	82.2	no solubility; no complete purification; foaming
	THF	75.4	no solubility; no complete purification
	DMSO	79.0	no complete purification; coloring
	Acetonitrile	84.0	foaming
	Ethanol	80.2	no complete purification
	DMF	84.2	no complete purification; toxic solvent
	Toluene/EtOH	75.0	no complete purification
4.20	Benzene	82.0	no solubility; no complete purification
	Chloroform	66.0	no solubility; no complete purification
	THF	85.0	no solubility; no complete purification
	DMSO	82.3	no complete purification
	Acetonitrile	79.0	no complete purification
	Ethanol	65.0	no complete purification
	DMF	88.3	no complete purification; toxic solvent
	Toluene/EtOH	80.3	no complete purification
4.21	Benzene	87.7	no solubility; no complete purification; foaming
	Chloroform	80.0	no complete purification
	THF	79.3	no solubility; no complete purification
	DMSO	82.3	no complete purification
	Acetonitrile	84.3	no complete purification
	Ethanol	79.3	no complete purification
	DMF	95.0	no complete purification; toxic solvent
	Toluene/EtOH	78.0	no complete purification

Solubility Test Results of Siloxanes functionalized with Quaternary Ammonium Salt Groups:

Solubility tests were done for all quaternized products, as well as the siloxane starting materials and the halosilated products **4.1a** to **4.5a**, **4.6**, **4.12** and **4.13**. One drop of the product was filled into a GC vial and 0.5 mL of the appropriate solvent was added. The samples were shaken. The solubility was checked after one hour and controlled after 24 hours. The results are listed in Figure A-15 to Figure A-20, with the figures sorted by the starting materials. The green fields symbolize solubility, the red fields show insolubility, and the yellow fields represent the change from solubility to precipitation during time.

	SM-100	4.1a	4.12	4.13	4.19	4.20	4.21	4.24	4.25	4.26	4.27	4.28	4.29
n-Hexane	Green	Red	Red	Red	Red	Red	Red	Red	Red	Red	Red	Red	Red
n-Heptane	Green	Red	Red	Red	Red	Red	Red	Red	Red	Red	Red	Red	Red
Toluene	Green	Green	Green	Green	Red	Red	Red	Red	Red	Red	Red	Red	Red
Benzene	Green	Green	Green	Green	Red	Red	Red	n/s	n/s	n/s	n/s	n/s	n/s
Chloroform	Green	Green	Green	Green	Red	Red	Red	Red	Red	Red	Red	Red	Red
THF	Green	Green	Green	Green	Red	Red	Red	Red	Red	Red	Red	Red	Red
Ethylacetate	Green	Green	Green	Green	Red	Red	Red	Red	Red	Red	Red	Red	Red
Acetone	Green	Green	Green	Green	Red	Red	Red	Red	Red	Red	Red	Red	Red
DMSO	Red	Red	Red	Red	Green	Green	Green	Green	Green	Green	Green	Green	Green
Acetonitrile	Red	Red	Red	Red	Red	Green	Green	n/s	n/s	n/s	n/s	n/s	n/s
EtOH	Green	Red	Red	Red	Green	Green	Green	Green	Green	Green	Green	Green	Green
MeOH	Red	Red	Red	Red	Green	Green	Green	Green	Green	Green	Green	Green	Green
DMF	Red	Green	Green	Green	Green	Green	Green	n/s	n/s	n/s	n/s	n/s	n/s
Water	Red	Red	Red	Red	Yellow	Yellow	Yellow	Yellow	Yellow	Yellow	Yellow	Yellow	Yellow

Figure A-15: Solubility tests of SM-100 and SM-100 based samples **4.1a**, **4.12**, **4.14**, **4.19** to **4.21** and **4.24** to **4.29**; the green fields show solubility, the red fields show insolubility, and the yellow fields represents the change from solubility to precipitation over time or increasing in concentration.

	SM-50	4.2	4.30	4.31	4.32
n-Hexane	Green	Green	Red	Red	Red
n-Heptane	Green	Green	Red	Red	Red
Toluene	Green	Green	Red	Red	Red
Benzene	Green	Green	Red	Red	Red
Chloroform	Green	Green	Red	Red	Red
THF	Green	Green	Red	Red	Red
Ethylacetate	Green	Green	Red	Red	Red
Acetone	Green	Green	Red	Red	Red
DMSO	Red	Red	Green	Green	Green
Acetonitrile	Red	Red	Green	Green	Green
EtOH	Green	Red	Green	Green	Green
MeOH	Red	Red	Green	Green	Green
DMF	Red	Green	Green	Green	Green
Water	Red	Red	Yellow	Yellow	Yellow

Figure A-16: Solubility tests of SM-50 and SM-50 based samples **4.2** and **4.30** to **4.32**; the green fields show solubility, the red fields show insolubility, and the yellow fields represents the change from solubility to precipitation over time or increasing in concentration.

	SM-25	4.3	4.33	4.34	4.35
n-Hexane					
n-Heptane					
Toluene					
Benzene					
Chloroform					
THF					
Ethylacetate					
Acetone					
DMSO					
Acetonitrile					
EtOH					
MeOH					
DMF					
Water					

Figure A-17: Solubility tests of SM-25 and SM-25 based samples 4.3 and 4.33 to 4.35; the green fields show solubility, the red fields show insolubility, and the yellow fields represents the change from solubility to precipitation over time or increasing in concentration.

	SM-15	4.4	4.36	4.37	4.38
n-Hexane					
n-Heptane					
Toluene					
Benzene					
Chloroform					
THF					
Ethylacetate					
Acetone					
DMSO					
Acetonitrile					
EtOH					
MeOH					
DMF					
Water					

Figure A-18: Solubility tests of SM-15 and SM-15 based samples 4.4 and 4.36 to 4.38; the green fields show solubility, the red fields show insolubility, and the yellow fields represents the change from solubility to precipitation over time or increasing in concentration.

	D_3D^H	4.5a	4.39	4.40	4.41
n-Hexane					
n-Heptane					
Toluene					
Benzene					
Chloroform					
THF					
Ethylacetate					
Acetone					
DMSO					
Acetonitrile					
EtOH					
MeOH					
DMF					
Water					

Figure A-19: Solubility tests of D_3D^H and D_3D^H based samples 4.5a and 4.39 to 4.41; the green fields show solubility, the red fields show insolubility, and the yellow fields represents the change from solubility to precipitation over time or increasing in concentration.

	D_H^4	4.6	4.42	4.43	4.44
n-Hexane					
n-Heptane					
Toluene					
Benzene					
Chloroform					
THF					
Ethylacetate					
Acetone					
DMSO					
Acetonitrile					
EtOH					
MeOH					
DMF					
Water					

Figure A-20: Solubility tests of D_H^4 and D_H^4 based samples 4.6 and 4.42 to 4.44; the green fields show solubility, the red fields show insolubility, and the yellow fields represents the change from solubility to precipitation over time or increasing in concentration.

Kinetic Studies of Siloxanes functionalized with Quaternary Ammonium Salt Groups:

Experiments were done based on SM-100 starting material to get optimized ratios of the different integrals. The experiments were done with **4.19** (based on SM-100 and pyridine), since the partially strong overlap of the signals in the ^1H -NMR of **4.20** and **4.21** makes an evaluation of the kinetic data hardly possible without obtaining a very large error. In addition, only the formation of the quaternary compound can be monitored, since the signal **e** (C-Br, s. Figure 4-2) cannot be integrated separately. Samples withdrawn from the reaction medium with a syringe (0.1 mL) were cooled by adding cooled deuterated DMSO (0.5mL). The calibration of the chemical shifts in ^1H spectra was carried out by using the shifts of the deuterated DMSO (δH 2.50 ppm). The following data are the integrals compared to the integral of the Si-CH₃ signal at 0ppm and they are directly transferable to the percentage of unreacted SiH groups *resp.* the formed Si-O-R signals. For the determination of the reaction order, the signals **e**, **i** and **l** (Figure 4-8) were averaged and their squared values were plotted against time reaction time.

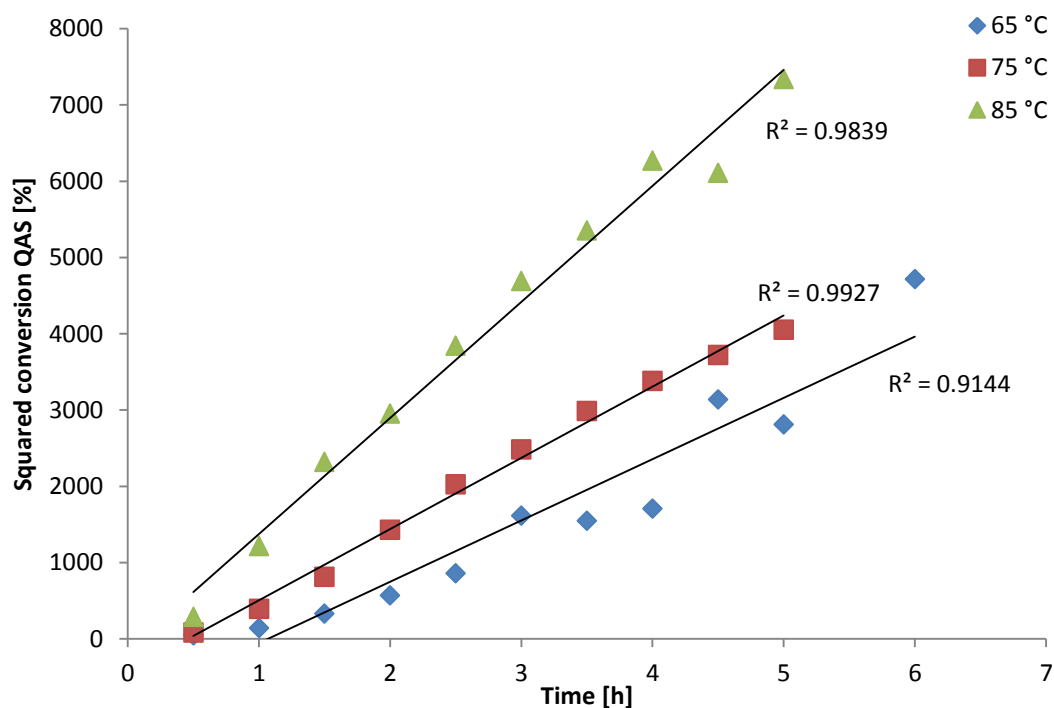


Figure A-21: Kinetic studies of sample **4.19** at different temperatures; the overall reaction follows second order; the y-axis contains the squared data.

Table A-19: Data of the kinetic studies based on integrals of the ^1H -NMR analytics; the equations are based on the slope of the trend line (s. Figure A-21); the standard deviations were calculated from two to three repetitions.

Time [h]	Conversion QAS [%] (T=65°C)	Conversion QAS [%] (T=75°C)	Conversion QAS [%] (T=85°C)
0.5	6.5 ± 0.87	9.0 ± 1.73	17.0 ± 0.87
1	11.8 ± 1.15	19.8 ± 2.02	34.8 ± 2.02
1.5	18.2 ± 0.58	28.5 ± 2.60	48.2 ± 0.58
2	23.8 ± 0.29	37.8 ± 2.02	54.3 ± 2.02
2.5	29.3 ± 2.02	45.0 ± 1.73	62.0 ± 1.73
3	40.2 ± 1.15	49.8 ± 2.02	68.5 ± 1.73
3.5	39.3 ± 1.15	54.7 ± 2.31	73.2 ± 1.15
4	41.3 ± 2.02	58.2 ± 2.31	79.2 ± 0.58
4.5	56.0 ± 4.33	61.0 ± 2.60	78.2 ± 0.58
5	53.0 ± 0.00	63.7 ± 2.31	85.7 ± 4.62
6	68.7 ± 9.78	68.3 ± 3.06	85.8 ± 5.80
7	62.7 ± 3.79	71.8 ± 3.06	89.5 ± 6.54
8	66.0 ± 4.27	75.5 ± 3.28	89.7 ± 6.37
9	70.7 ± 5.58	77.5 ± 3.28	92.8 ± 5.77
10	71.2 ± 5.20	78.5 ± 3.77	86.5 ± 6.56
24	89.7 ± 8.55	85.7 ± 3.01	88.3 ± 6.11
Equation	$y = 803.13x - 857.72$	$y = 933.7x - 430.43$	$y = 1521.4x - 145.75$

DSC Measurements of Siloxanes functionalized with Quaternary Ammonium Salt Groups:

The glass transition temperatures were measured via differential scanning calorimetry (s. Appendix A1). The measurements were performed at atmospheric pressure under inert conditions. Due to the device, no values can be measured below -75 °C. Samples with glass transitions below this temperature are marked with "below -75 °C".

Table A-20: DSC measurements of quaternized products and starting materials and halosilated intermediates for comparison reasons; results which T_G is outside of the measuring range are marked with "below -75 °C"; the standard deviations were calculated from two to three repetitions.

Sample	T_G [°C]	Sample	T_G [°C]
SM-100	below -75 °C	4.26	-61.0 ± 1.00
SM-50	below -75 °C	4.27	-28.4 ± 0.11
SM-25	below -75 °C	4.28	-60.3 ± 0.44
SM-15	below -75 °C	4.29	-57.4 ± 1.07
D ₃ D ^H	below -75 °C	4.30	-48.3 ± 0.94
D ^H ₄	below -75 °C	4.31	-65.7 ± 1.00
4.1a	below -75 °C	4.32	-64.2 ± 1.07
4.2	below -75 °C	4.33	-44.4 ± 1.04
4.3	below -75 °C	4.34	-66.7 ± 0.24
4.4	below -75 °C	4.35	below -75 °C
4.5a	below -75 °C	4.36	-45.7 ± 0.43
4.6	below -75 °C	4.37	below -75 °C
4.12	below -75 °C	4.38	below -75 °C
4.13	below -75 °C	4.39	below -75 °C
4.19	-32.2 ± 9.04	4.40	below -75 °C
4.20	-53.8 ± 8.02	4.41	-61.2 ± 0.45
4.21	-52.9 ± 0.29	4.42	-33.2 ± 0.59
4.24	-37.6 ± 0.04	4.43	below -75 °C
4.25	-56.6 ± 0.23	4.44	-63.5 ± 0.15

Contact Angle measurements of Siloxanes functionalized with Quaternary Ammonium Salt Groups:

The CA samples have to be solid to determine the solid-liquid-CA between the sample and the water droplet. Due to the fact that these products do not contain any groups to form urethane groups, the products were only embedded with an amount of 10% into the PDMS standard formulation without any networking. Further details are shown in Scheme A-2 (Appendix A2).

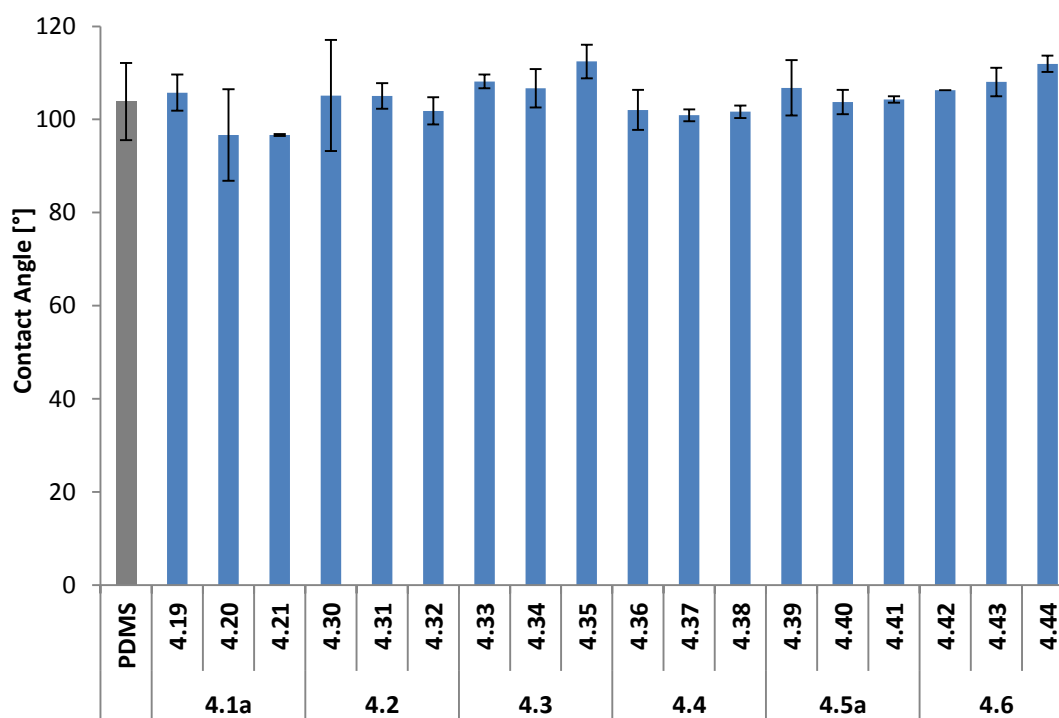


Figure A-22: Static contact angles of quaternized products 4.19 to 4.21, 4.30 to 4.44 and reference material (standard PDMS formulation); the standard deviations were calculated from two to three repetitions.

Table A-21: Summary of the contact angles of the products **4.19** to **4.21** and **4.30** to **4.44**; standard PDMS is added for comparison reasons; samples were cured into a standard PDMS formulation with an amount of 10% (s. Appendix A2).

Sample	CA t(0sec) [deg]
PDMS	103.9 ± 8.27
4.19	105.8 ± 3.89
4.20	96.7 ± 9.83
4.21	96.7 ± 0.21
4.30	105.2 ± 11.95
4.31	105.1 ± 2.76
4.32	101.9 ± 2.90
4.33	108.2 ± 1.48
4.34	106.7 ± 4.10
4.35	112.5 ± 3.61
4.36	102.1 ± 4.31
4.37	100.9 ± 1.27
4.38	101.7 ± 1.34
4.39	106.8 ± 5.94
4.40	103.8 ± 2.62
4.41	104.3 ± 0.71
4.42	106.3
4.43	108.1 ± 3.04
4.44	112.0 ± 1.77

Kirby-Bauer Test of Siloxanes functionalized with Bromoalkyl and Quaternary Ammonium Salt Groups:

The Kirby-Bauer Test can be used for determination of antimicrobial activity in combination with diffusion properties.^[128] The antimicrobial test substrate was diluted in DMSO (ratio 1:3 and 1:5) and was applied to the center of an agar plate (prepared with the respective strain) onto a small filter paper. After incubation time the zone of inhibition is evaluated.

































Zone of Inhibition [mm]			
(maximum 45 mm)			
Samples	<i>Aspergillus brasiliensis</i>	<i>Exophiala dermatitidis</i>	<i>Staphylococcus aureus</i>
4-Bromo-1-butanol	 9.0	 34.0	 21.0
Bromobutane	0.0	0.0	0.0
DMSO	0.0	0.0	n.d
PdCl ₂	 4.0	 4.0	 2.0
Bardac®	 4.5	 11.4	 12.1
Bardac® 1:10	 2.0	 5.3	 8.0
Bardac® 1:100	 1.5	 4.3	 4.5
Pyridine	0.0	 1.0	 1.0
Pyridine 1:10	0.0	0.0	0.0
Pyridine 1:100	0.0	0.0	0.0
1-Methyl-1 <i>H</i> -imidazole	 3.5	 12.3	 6.5
1-Methyl-1 <i>H</i> -imidazole 1:10	0.0	0.0	0.0
1-Methyl-1 <i>H</i> -imidazole 1:100	0.0	0.0	0.0
1-Butyl-1 <i>H</i> -imidazole	 5.0	 15.0	 11.0
4.1a	0.0	 29.0	 17.0
4.1b	 2.0	 2.0	 6.5
4.2	0.0	 10.0	0.0
4.3	0.0	0.0	0.0
4.4	0.0	0.0	0.0
4.5b	0.0	0.0	0.0
4.6	0.0	0.0	0.0
4.12	0.0	0.0	 2.0
4.13	0.0	 1.0	 2.0

Figure A-23: Kirby-Bauer Test of brominated samples (**4.1a** to **4.13**); the red bars symbolize the zone of inhibition in which the maximum number can be 45 mm due to the diameter of the petri dishes; the slightly red highlighted substrates are references; Bardac is a disinfectant containing Didecyl dimethyl ammonium chloride (DDAC).





































































Zone of Inhibition [mm]				
(maximum 45 mm)				
Samples	<i>Aspergillus brasiliensis</i>	<i>Exophiala dermatitidis</i>	<i>Staphylococcus aureus</i>	
4.19	 1.0	 4.4	 2.0	
4.20	 4.4	 8.8	 10.5	
4.21	 3.5	 7.8	 9.0	
4.22	0.0	 0.5	 4.8	
4.23	 2.0	 1.5	 8.0	
4.24	0.0	 6.0	 6.0	
4.25	0.0	 6.0	 7.0	
4.26	 2.8	 8.3	 8.3	
4.27	0.0	 7.0	 6.0	
4.28	0.0	 9.0	 7.0	
4.29	 1.8	 8.3	 8.0	
4.30	0.0	 4.7	 8.5	
4.31	 1.3	 8.0	 8.7	
4.32	 3.0	 7.5	 7.0	
4.33	0.0	 4.3	 7.0	
4.34	 1.0	 5.7	 7.0	
4.35	 1.3	 5.3	 6.0	
4.36	0.0	 1.5	 4.0	
4.37	0.0	 1.5	 4.0	
4.38	0.0	 2.5	 4.0	
4.39	 1.3	 5.8	 7.0	
4.40	 0.4	 2.8	 4.7	
4.41	 2.0	 3.0	 6.0	
4.42	 2.0	 3.3	 7.3	
4.43	 2.5	 5.0	 9.0	
4.44	 3.5	 5.0	 6.5	

Figure A-24: Kirby-Bauer Test of quaternized products (4.19 to 4.38); the red bars symbolize the zone of inhibition in which the maximum number can be 45 mm due to the diameter of the petri dishes.

Minimum Inhibitory Concentration (MIC) of Siloxanes functionalized Quaternary Ammonium Salt Groups:

Minimum inhibitory concentration (MIC) is the lowest concentration of an antimicrobial agent that will inhibit the visible growth of a microorganism after overnight incubation. The utilized strains are *Candida albicans* (pathogenic yeast), *Staphylococcus aureus* (gram-positive bacterium) and *Pseudomonas aeruginosa* (gram-negative bacterium). The evaluation is done optically. The antimicrobial activity is given when the solution is still clear after incubation time.

															no growth 1 to 5 germs begin of growth growth			- (-) (+) +
Staphylococcus aureus	ppm	4.19			4.20			4.21			4.26			4.29				
	5000	-	-	-	-	-	-	-	-	-	-	-	-	-	-	-		
	2500	-	-	-	-	(+)	(+)	-	-	-	-	-	-	-	-	-		
	1250	-	-	-	-	(+)	(+)	-	-	-	-	-	-	(+)	-	-		
	625	-	-	-	-	(+)	(+)	(+)	-	-	-	-	-	-	-	-		
	313	(+)	(+)	(+)	-	(+)	(+)	-	-	(+)	-	-	-	-	-	-		
	156	-	-	-	-	(+)	(+)	(+)	(+)	(+)	-	-	-	-	-	-		
	100	-	-	-	-	(+)	(+)	(+)	(+)	(+)	-	-	-	-	-	-		
	78	-	(+)	(-)	(-)	(+)	(+)	(-)	-	(-)	-	-	(+)	-	-	-		
	50	-	-	-	+	+	+	+	(+)	(+)	-	-	-	-	(-)	(+)		
	39	+	-	(+)	+	+	+	+	(+)	(+)	-	-	(+)	(+)	(-)	-		
	25	-	-	-	+	+	+	+	+	+	-	-	-	-	-	-		
	13	+	+	+	+	+	+	+	+	+	-	-	(+)	-	-	-		
	6	+	+	+	+	+	+	+	+	+	+	+	+	+	+	+		
	3	+	+	+	+	+	+	+	+	+	+	+	+	+	+	+		
Pseudomonas aeruginosa	5000	+	+	+	+	+	+	-	(+)	-	+	-	+	+	-	(+)		
	2500	+	+	+	+	+	+	+	+	+	+	+	+	+	+	(+)		
	1250	+	+	+	+	+	+	+	+	+	+	+	+	+	+	+		
	625	+	+	+	+	+	+	+	+	+	+	+	+	+	+	+		
Candida albicans	5000	-	-	(-)	-	-	(-)	-	-	-	-	-	(-)	-	-	-		
	2500	-	-	(-)	-	(+)	(+)	-	-	-	-	-	(+)	-	-	-		
	1250	-	-	(+)	+	+	+	-	-	(+)	-	-	(+)	-	-	-		
	625	-	(+)	(+)	+	+	+	+	+	+	-	(+)	-	-	(+)	-		
	313	+	+	+	+	+	+	+	+	+	+	+	+	+	+	+		
	156	+	+	+	+	+	+	+	+	+	+	+	+	+	+	+		

Figure A-25: Minimum Inhibition Concentration of SM-100 based samples **4.19**, **4.20**, **4.21**, **4.26** and **4.29**; the green fields are clear solutions, so here the test substance is antimicrobially active, the yellow fields illustrate the beginning of growth and the red fields indicate growth of the molds and thus inactivity of the antimicrobial substance.

	ppm	4.30			4.31			4.32		
<i>Staphylococcus aureus</i>	5000	(+)	(+)	-	(+)	(+)	(+)	-	(+)	(-)
	2500	-	(+)	(-)	-	-	-	(-)	+	(+)
	1250	-	-	-	-	-	-	-	-	-
	625	-	-	-	-	-	(+)	-	-	-
	313	-	-	(-)	-	-	-	-	-	-
	156	+	+	+	-	-	(-)	(+)	-	-
	100	+	+	+	+	+	+	(+)	(+)	(+)
	78	+	+	+	+	+	+	-	-	-
	50	+	+	+	+	+	+	(+)	+	(+)
	39	+	+	+	+	+	+	-	-	-
	25	+	+	+	+	+	+	+	+	+
	13	+	+	+	+	+	+	+	+	+
<i>Pseudomonas aeruginosa</i>	5000	+	+	+	+	+	+	(-)	(+)	(+)
	2500	+	+	+	+	+	+	(-)	(+)	-
	1250	+	+	+	+	+	+	+	+	+
	625	+	+	+	+	+	+	+	+	+
<i>Candida albicans</i>	5000	+	+	+	+	(+)	(+)	-	-	(+)
	2500	+	+	+	+	+	+	-	(+)	(-)
	1250	+	+	+	+	+	+	-	-	-
	625	+	+	+	+	+	+	-	-	-
	313	+	+	+	+	+	+	(-)	(-)	-
	156	+	+	+	+	+	+	+	+	+
	78	+	+	+	+	+	+	+	+	+

Figure A-26: Minimum Inhibition Concentration of SM-50 based samples 4.30, 4.31 and 4.32; the green fields are clear solutions, so here the test substance is antimicrobially active, the yellow fields illustrate the beginning of growth and the red fields indicate growth of the molds and thus inactivity of the antimicrobial substance.

	ppm	4.33			4.34			4.35		
<i>Staphylococcus aureus</i>	5000	-	(-)	-	(+)	(+)	(+)	-	(+)	(+)
	2500	-	-	(-)	(+)	-	(+)	(+)	-	(+)
	1250	+	(+)	-	-	(+)	(+)	-	-	-
	625	+	+	+	-	-	-	-	-	-
	313	+	+	+	-	-	-	-	-	-
	156	+	+	+	-	-	-	-	-	-
	100	+	+	+	-	-	-	(+)	(-)	(-)
	78	+	+	+	(+)	-	-	-	-	-
	50	+	+	+	+	+	+	(-)	(+)	+
	39	+	+	+	+	+	+	-	-	-
	25	+	+	+	+	+	+	+	+	+
	13	+	+	+	+	+	+	+	+	+
<i>Pseudomonas aeruginosa</i>	5000	+	+	+	+	+	+	(+)	(+)	+
	2500	+	+	+	+	+	+	+	+	+
	1250	+	+	+	+	+	+	+	+	+
<i>Candida albicans</i>	5000	+	+	+	(-)	(-)	(-)	-	(+)	-
	2500	+	+	+	-	-	(-)	-	(-)	-
	1250	+	+	+	(+)	(+)	(-)	-	-	-
	625	+	+	+	+	+	+	-	-	-
	313	+	+	+	+	+	+	+	+	+
	156	+	+	+	+	+	+	+	+	+

Figure A-27: Minimum Inhibition Concentration of SM-25 based 4.33, 4.34 and 4.35; the green fields are clear solutions, so here the test substance is antimicrobially active, the yellow fields illustrate the beginning of growth and the red fields indicate growth of the molds and thus inactivity of the antimicrobial substance.

	ppm	4.36			4.37			4.38		
<i>Staphylococcus aureus</i>	5000	+	+	+	+	+	+	(+)	-	(+)
	2500	+	+	+	+	+	+	-	(+)	(+)
	1250	+	+	+	+	+	+	(+)	-	-
	625	+	+	+	+	+	+	-	-	-
	313	+	+	+	+	+	+	(+)	-	(+)
	156	+	+	+	+	+	+	+	(+)	(+)
	78	+	+	+	+	+	+	+	+	+
	39	+	+	+	+	+	+	+	+	+
<i>Pseudomonas aeruginosa</i>	5000	+	+	+	+	+	+	+	+	+
	2500	+	+	+	+	+	+	+	+	+
<i>Candida albicans</i>	5000	+	+	+	+	+	+	-	-	-
	2500	+	+	+	+	+	+	-	(+)	-
	1250	+	+	+	+	+	+	-	-	(-)
	625	+	+	+	+	+	+	+	+	+
	313	+	+	+	+	+	+	+	+	+

Figure A- 28: Minimum Inhibition Concentration of SM-15 based samples **4.36**, **4.37** and **4.38**; the green fields are clear solutions, so here the test substance is antimicrobially active, the yellow fields illustrate the beginning of growth and the red fields indicate growth of the molds and thus inactivity of the antimicrobial substance.

	ppm	4.41			4.42			4.43			4.44			DMSO		
<i>Staphylococcus aureus</i>	5000	(-)	-	-	-	-	-	-	-	-	-	-	-	+	+	+
	2500	-	-	-	-	(+)	-	-	-	-	-	-	-	+	+	+
	1250	-	-	-	-	-	-	-	-	(+)	-	-	-	+	+	+
	625	(+)	-	-	-	(+)	-	(+)	-	(+)	-	-	-	+	+	+
	313	-	-	-	-	-	-	-	-	-	-	-	-	+	+	+
	156	(+)	(-)	(-)	-	-	-	-	-	-	-	-	-	+	+	+
	100	(+)	(-)	(-)	(+)	(+)	(+)	-	(+)	-	-	-	(+)	+	+	+
	78	+	+	(+)	-	-	-	-	-	(+)	-	-	-	+	+	+
	50	+	+	+	-	-	-	(+)	(+)	(+)	-	-	-	+	+	+
	39	+	+	+	-	-	-	(+)	-	-	(+)	-	-	+	+	+
	25	+	+	+	+	+	+	+	+	+	-	-	-	+	+	+
	13	+	+	+	+	+	+	+	+	+	+	+	+	+	+	+
	6	+	+	+	+	+	+	+	+	+	+	+	+	+	+	+
<i>Pseudomonas aeruginosa</i>	5000	+	+	+	+	+	+	+	+	+	+	+	+	+	+	+
	2500	+	+	+	+	+	+	+	+	+	+	+	+	+	+	+
<i>Candida albicans</i>	5000	-	(-)	-	-	-	(-)	-	(-)	-	-	-	-	+	+	+
	2500	+	+	+	-	-	-	(+)	(-)	-	-	-	(-)	+	+	+
	1250	+	+	+	-	-	-	+	+	+	-	-	-	+	+	+
	625	+	+	+	+	+	+	+	+	+	+	+	+	+	+	+
	313	+	+	+	+	+	+	+	+	+	+	+	+	+	+	+

Figure A-29: Minimum Inhibition Concentration of cyclosiloxane based samples **4.41**, **4.42**, **4.43** and **4.44**; DMSO is tested as blank; the green fields are clear solutions, so here the test substance is antimicrobially active, the yellow fields illustrate the beginning of growth and the red fields indicate growth of the molds and thus inactivity of the antimicrobial substance.

ISO 22196:2011 of Siloxanes functionalized Quaternary Ammonium Salt Groups:

The ISO 22196:2011, also called film contact test, is an international standard test method. The utilized strain is *Exophiala dermatitidis* (isolate). The test piece is measured in solid form, so the different samples were cured into a PDMS standard formulation with an amount of 10 %. The strain suspension is placed between the test substrate and a cover glass, incubated and subsequently evaluated via counting by means of plating on culture medium.

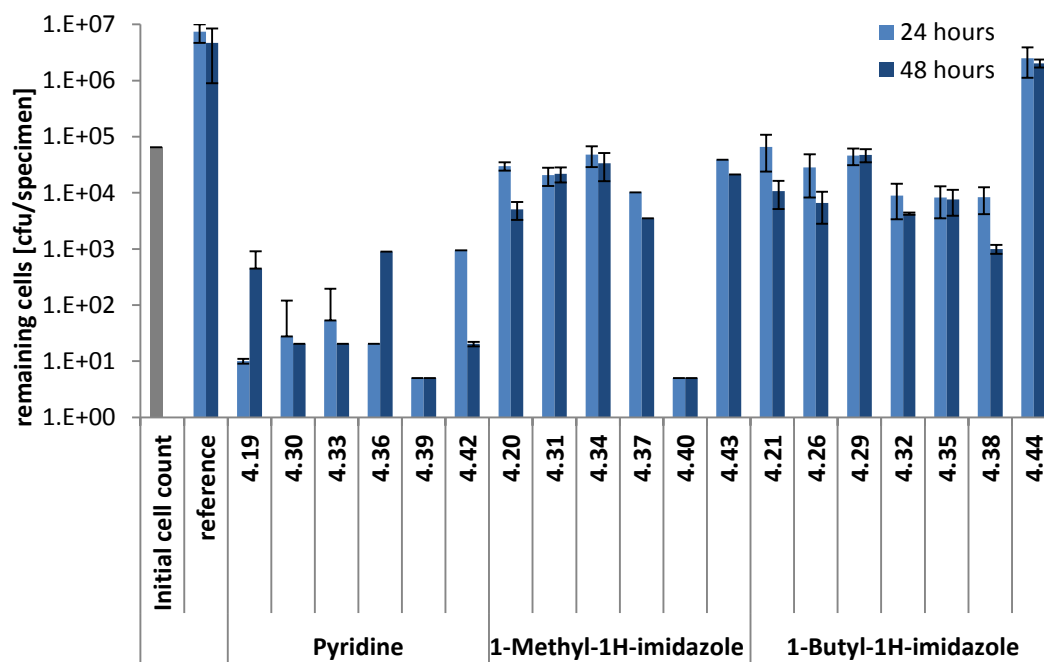


Figure A-30: ISO 22196:2011 test for the measurement of antibacterial activity on plastics and other nonporous surfaces; the test is evaluated after 24 hours (light blue bars) and 48 hours (dark blue bars); the samples are sorted by amines and descending number of side-groups; the reference and the blank are a standard PDMS formulations; the standard deviations were calculated from three repetitions.

Table A-22: Data of the ISO 22196:2011 test for the measurement of antibacterial activity on plastics and other nonporous surfaces; the samples are sorted by amines and descending number of side-groups; the reference and the blank are a standard PDMS formulations; the standard deviations were calculated from three repetitions.

	Amine	Remaining Cells [cfu/specimen]			
		24 Hours	Standard	48 Hours	Standard
			Deviation (24 h)		Deviation (48 h)
Initial cell count		6.50E+04	0.00E+00	-	-
reference		7.37E+06	4.67E+06	2.68E+06	3.77E+06
4.19	pyridine	1.00E+01	4.50E+02	1.00E+00	4.56E+02
4.30		2.78E+01	9.31E+01	2.03E+01	0.00E+00
4.33		5.35E+01	1.41E+02	2.03E+01	0.00E+00
4.36		2.03E+01	0.00E+00	8.94E+02	1.77E+00
4.39		5.00E+00	0.00E+00	5.00E+00	0.00E+00
4.42		9.40E+02	0.00E+00	2.03E+01	1.80E+00
4.20	1-methyl- 1H-imidazole	2.98E+04	5.00E+03	5.08E+03	1.78E+03
4.31		2.06E+04	7.36E+03	2.17E+04	6.50E+03
4.34		4.81E+04	1.93E+04	3.35E+04	1.75E+04
4.37		1.02E+04	0.00E+00	3.50E+03	1.78E+00
4.40		5.00E+00	0.00E+00	5.00E+00	0.00E+00
4.43		3.91E+04	0.00E+00	2.13E+04	1.80E+00
4.21	1-butyl- 1H-imidazole	6.60E+04	4.20E+04	1.07E+04	5.57E+03
4.26		2.85E+04	2.02E+04	6.63E+03	3.81E+03
4.29		4.60E+04	1.51E+04	4.73E+04	1.25E+04
4.32		8.95E+03	5.56E+03	4.25E+03	1.87E+02
4.35		8.25E+03	4.76E+03	7.62E+03	3.73E+03
4.38		8.38E+03	4.23E+03	1.00E+03	1.78E+02
4.41		n/s	-	n/s	-
4.44		2.50E+06	2.03E+06	1.39E+06	3.21E+05

A6. Appendix to Part III

Synthesis of Halogenalkyl and Propyleneglycol functionalized Polysiloxane Copolymers:

Table A-23: Summary of the products **5.1** to **5.7**; unless otherwise indicated, the ratio SiCH₂:SiOR is 1:1; the conversions and formed amounts were calculated by integration of ¹H-NMR.

Sample	Starting Material	Catalyst	1 st Synthesis		2 nd Synthesis		Isolated Yield [%]
			Converted Amount SiH [%]	Formed Amount SiCH ₂ [%]	Converted Amount SiH [%]	Formed Amount Si-OR [%]	
5.1	3.35	Karstedt	56	38.5	> 99	n/d	n/d
5.2	3.35	Pt@C	56	38.5	98	n/d	n/d
5.3	3.35	PdCl ₂	56	38.5	99	9	56.3
5.4^a	3.35f	PdCl ₂	43	19	93	83.5	47.9
5.5^b	3.35g	PdCl ₂	82	60	> 99	7	50.2
5.6	3.35e	PdCl ₂	10	6	80	13.5	40.1
5.7	SM-50	PdCl ₂	-	n/d	> 99	83.5	75.4

^a ratio 1:3

^b ratio 3:1

Synthesis of poly(3-(2-hydroxypropoxy)propyl)methylsiloxane)-co-poly(4-bromobutoxy)methylsiloxane-co-polydimethylsiloxane (5.1):

Representative procedure F:

10 µL of Karstedt (2 % of Pt in the catalyst, 0.1 % mol in the mixture, 0.02 mmol) and 10 mL dried THF were added into the flask under argon atmosphere and stirred at room temperature (20 °C) for a couple of minutes. Then allyl bromide (0.53 mL, 6.07 mmol) was added into the system. **3.35** (2.5 g, 0.81 mmol, Mn 3070 g/mol) were added dropwise. The mixture was stirred (oil bath temperature: 70 °C) under inert atmosphere (Ar) for 24 hours (the reaction was followed by ¹H-NMR). The reaction was stopped after curing and the obtained product was a colorless, transparent cured gel.

No desired product was obtained.

Synthesis of poly(3-(2-hydroxypropoxy)propyl)methylsiloxane)-co-poly(4-bromobutoxy)methylsiloxane-co-polydimethylsiloxane (5.2):

Product **5.2** was synthesized according to the representative procedure F, using 40 mL dried toluene, 0.5 mol% Pt supported on charcoal compared to siloxane (10 % of Pt in the catalyst, 22 mg, 0.11 mmol), **3.35** (6.98 g, 2,26 mmol, Mn 3070 g/mol), 1.38 mL dried THF (17.06 mmol), and 1.47 mL allyl bromide (17.03 mmol). The reaction was stopped after curing and the obtained product was a colorless, transparent cured gel.

No desired product was obtained.

Synthesis of poly(3-(2-hydroxypropoxy)propyl)methylsiloxane)-co-poly(4-bromobutoxy)methylsiloxane-co-polydimethylsiloxane (5.3):

Representative procedure G.^[111d]

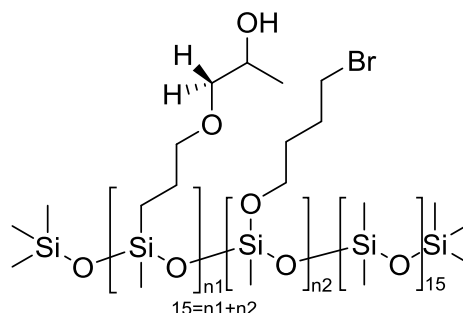
PdCl₂ (48 mg, 1.6 mol-% in the mixture, 0.27 mmol), 40 mL dried toluene and dried THF (1.38 mL, 17.06 mmol) were added into the flask under argon atmosphere and stirred at room temperature (20 °C) for a couple of minutes. Then allyl bromide (1.5 mL, 17.03 mmol) was added into the system. **3.35** (6.98 g, 2,26 mmol, Mn 3070 g/mol) were added dropwise. The mixture was stirred (oil bath temperature: 50°C) under inert atmosphere (Ar) for 24 hours. The mixture (when necessary) was decolorized by adding activated carbon and an excess of pentane and stirred for 16 h at room temperature. The crude was filtrated trough celite, and the solvents and volatiles were evaporated under vacuum. The obtained product (yield 56 %; 1.28 mmol) was a yellow, transparent, viscous liquid.

¹H-NMR (300 MHz, CDCl₃, 25 °C, ppm) δ = 3.93 – 3.90

(m, 1H, O-CH₂-CH(CH₃)-OH), 3.71 – 3.64 (m, 2H, -O-CH₂-), 3.47 – 3.36 (m, 5H, CH₂-O-CH₂-CH(CH₃)-OH and -CH₂-Br), 3.21 – 3.15 (t, 1H, -O-CH₂-CH-), 2.66 (s, 1H, -OH), 1.94 – 1.90 (p, 2H, -CH₂-CH₂-Br), 1.70 – 1.55 (m, 4H, -Si-CH₂-CH₂- and -O-CH₂-CH₂-), 1.12 – 1.10 (d, 3H, CH₃-CH-), 0.54 – 0.46 (m, 2H, -Si-CH₂-), 0.16 – 0.02 (s, 3H, -Si-CH₃).

¹³C-NMR (300 MHz, CDCl₃, 25 °C, ppm) δ = 76.33 (-

O-CH₂-CH-), 73.99 (-Si-CH₂-CH₂-CH₂-), 66.46 (-O-CH₂-CH-), 61.78 (-O-CH₂-), 33.70 (-CH₂-Br), 30.95 (-O-CH₂-CH₂-), 29.48 (-CH₂-CH₂-Br), 23.24 (-Si-CH₂-CH₂-), 18.72 (CH₃-CH-), 13.51 (-Si-CH₂-), 1.90 – 0.68 (-Si-CH₃). ²⁹Si-NMR (300 MHz, CDCl₃, 25 °C, ppm): δ = 7.24 (-Si(CH₃)₃), -21.85 (O-Si-O) -58.84 (-O-Si(Me)-O_{2/2}). IR (ATR, 32 scans, cm⁻¹): 2962.7, 1410.7, 1258.2, 1010.4, 842.2, 790.2 697.9. EA (% , measured (calculated)), repeating unit C₁₈H₄₅BrO₇Si₄: C 34.15 (35.87), H 8.017 (7.34), Br 3.546 (14.92), Si 20.91 (20.97). GPC (THF, 40 °C, g/mol): M_n=2783, M_w=32271, PDI=11.595.



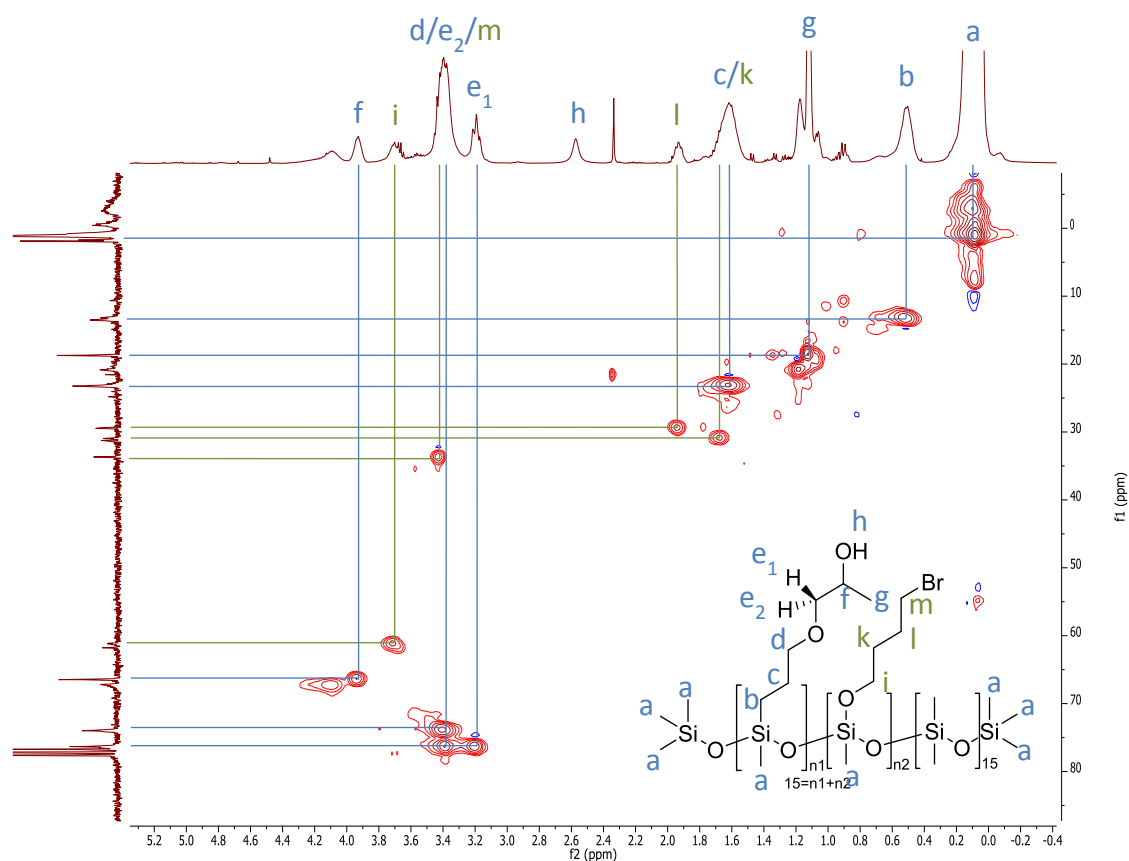


Figure A-31: ^1H - ^{13}C -HSQC-NMR of **5.3** in deuterated chloroform (400 MHz, 25 °C); the overlapping of the signals of the halosilated and hydrosilylated products are shown; for reasons of simplification the methyl groups on the silicon have been grouped together as **a**; signals **b** to **h** belong to the hydrosilylated group and signals **i** to **m** belong to the halosilated one.

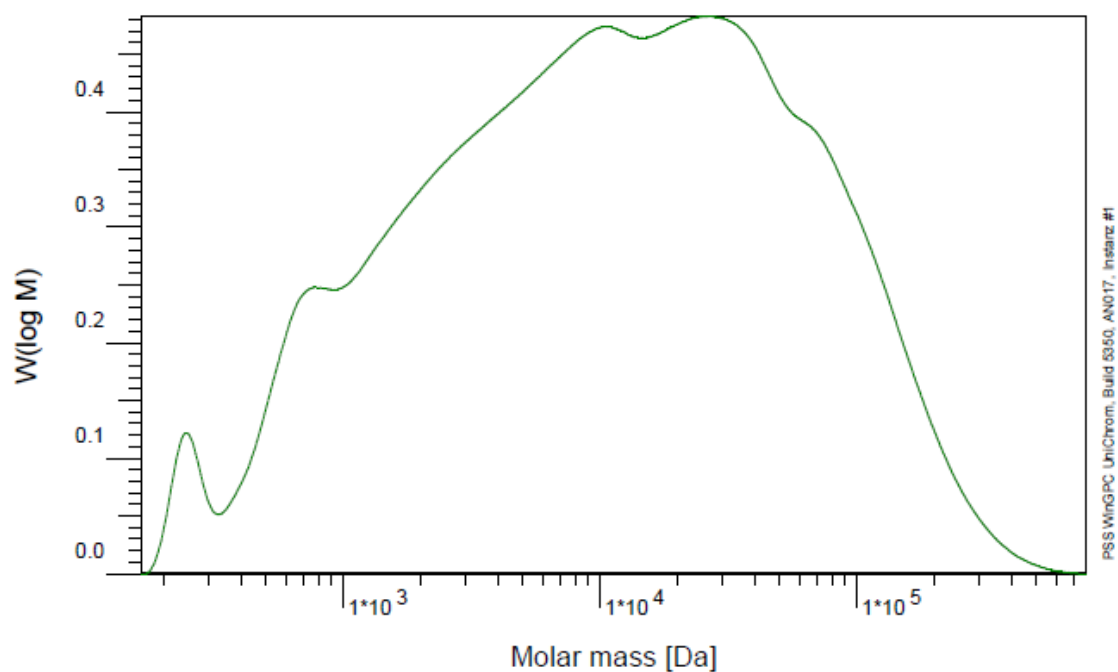


Figure A-32: GPC result of **5.3** in THF.

Synthesis of poly(3-(2-hydroxypropoxy)propyl)methylsiloxane-co-poly(4-bromobutoxy)methylsiloxane-co-polydimethylsiloxane (5.4):

Product **5.4** (48 % yield, 1.10 mmol) was synthesized according to the representative procedure G, using 40 mL dried toluene, 6.0 g of **3.35f** (11.78 mmol, M_n 2780 g/mol), 2.07 mL dried THF (25.59 mmol), and 2.21 mL allyl bromide (25.54 mmol).

¹H-NMR (300 MHz, CDCl₃, 25 °C, ppm) δ = 6.13 – 5.99 (m, 1H, CH₂=CH-), 5.37 – 5.15 (m, 2H, CH₂=CH-), 4.74 (s, 1H, SiH), 3.97 – 3.93 (m, 1H, O-CH₂-CH(CH₃)-OH), 3.79 – 3.67 (m, 2H, -O-CH₂-), 3.49 – 3.44 (m, 5H, CH₂-O-CH₂-CH(CH₃)-OH and -CH₂-Br), 3.25 – 3.20 (t, 1H, -O-CH₂-CH-), 1.89 – 1.85 (m, 2H, -CH₂-CH₂-Br), 1.78 – 1.68 (m, 4H, -Si-CH₂-CH₂- and -O-CH₂-CH₂-), 1.18 – 1.16 (d, 3H, CH₃-CH-), 0.60 – 0.54 (m, 2H, -Si-CH₂-), 0.22 – 0.11 (s, 3H, -Si-CH₃). **¹³C-NMR** (300 MHz, CDCl₃, 25 °C, ppm) δ = 138.00 (CH₂=CH-), 76.74 (-O-CH₂-CH-), 68.12 (-Si-CH₂-CH₂-CH₂-), 66.54 (-O-CH₂-CH-), 62.09 (-O-CH₂-), 25.76 (-CH₂-CH₂-Br), 21.60 (-Si-CH₂-CH₂-), 1.21 – 0.27 (-Si-CH₃). **²⁹Si-NMR** (300 MHz, CDCl₃, 25 °C, ppm): δ = -56.02 (-O-Si(Me)-O_{2/2}). **IR** (ATR, 32 scans, cm⁻¹): 2962.7, 1410.5, 1258.5, 1011.1, 842.6, 789.0, 694.7, 562.9. **EA** (% , measured (calculated)), C₈₀H₁₉₆Br₆O₃₃Si₂₀: C 28.57 (35.23), H 7.52 (7.24), Br 5.15 (17.58), Si 26.18 (20.59). **GPC** (THF, 40 °C, g/mol): M_n =3637, M_w =47690, PDI=13.112.

Synthesis of poly(3-(2-hydroxypropoxy)propyl)methylsiloxane-co-poly(4-bromobutoxy)methylsiloxane-co-polydimethylsiloxane (5.5):

Product **5.5** (50 % yield, 1.18 mmol) was synthesized according to the representative procedure G, using 40 mL dried toluene, 7.97 g of **3.35g** (2.37 mmol, M_n 3360 g/mol), 0.69 mL dried THF (8.53 mmol) and 0.74 mL allyl bromide (8.51 mmol).

¹H-NMR (300 MHz, CDCl₃, 25 °C, ppm) δ = 3.95 – 3.89 (m, 1H, O-CH₂-CH(CH₃)-OH), 3.66 – 3.62 (t, 2H, -O-CH₂-), 3.54 – 3.34 (m, 5H, CH₂-O-CH₂-CH(CH₃)-OH and -CH₂-Br), 3.22 – 3.16 (t, 1H, -O-CH₂-CH-), 2.72 (s, 1H, -OH), 1.96 – 1.92 (p, 2H, -CH₂-CH₂-Br), 1.71 – 1.56 (m, 4H, -Si-CH₂-CH₂- and -O-CH₂-CH₂-), 1.12 – 1.09 (d, 3H, CH₃-CH-), 0.54 – 0.45 (m, 2H, -Si-CH₂-), 0.15 – 0.02 (s, 3H, -Si-CH₃). **¹³C-NMR** (300 MHz, CDCl₃, 25 °C, ppm) δ = 76.35 (-O-CH₂-CH-), 73.99 (-Si-CH₂-CH₂-CH₂-), 66.44 (-O-CH₂-CH-), 61.77 (-O-CH₂-), 33.73 (-CH₂-Br), 31.23 (-O-CH₂-CH₂-), 29.34 (-CH₂-CH₂-Br), 23.12 (-Si-CH₂-CH₂-), 18.71 (CH₃-CH-), 13.16 (-Si-CH₂-), 1.94 – 0.68 (-Si-CH₃). **²⁹Si-NMR** (300 MHz, CDCl₃, 25 °C, ppm): δ = 7.47 (-Si(CH₃)₃), -19.05 – -21.95 (O-Si-O) -56.67 (-O-Si(Me)-O_{2/2}). **IR** (ATR, 32 scans, cm⁻¹): 3421.6, 2962.4, 1411.5, 1258.4, 1017.0, 842.2, 792.6, 695.5. **EA** (% , measured (calculated)), C₈₄H₂₀₆Br₄O₃₅Si₂₀: C 40.56 (37.96), H 6.94 (7.81), Br 2.28 (12.03), Si 12.81 (21.13). **GPC** (THF, 40 °C, g/mol): M_n =1456, M_w =2632, PDI=1.808.

Synthesis of poly(3-(2-hydroxypropoxy)propyl)methylsiloxane-co-poly(4-bromobutoxy)methylsiloxane-co-polydimethylsiloxane (5.6):

Product **5.6** (40 % yield, 0.85 mmol) was synthesized according to the representative procedure G, using 40 mL dried toluene, 5.98 g of **3.35f** (2.55 mmol, M_n 2347 g/mol), 1.38 mL dried THF (17.06 mmol) and 1.47 mL allyl bromide (17.03 mmol).

¹H-NMR (400 MHz, CDCl₃, 25 °C, ppm) δ = 5.92 – 5.85 (m, 1H, CH₂=CH-), 5.30 – 5.13 (m, 2H, CH₂=CH-), 4.72 – 4.68 (s, 1H, SiH), 4.05 – 3.96 (m, 1H, O-CH₂-CH(CH₃)-OH), 3.75 – 3.67 (m, 2H, -O-CH₂-), 3.45 – 3.37 (m, 5H, CH₂-O-CH₂-CH(CH₃)-OH and -CH₂-Br), 3.31 – 3.21 (t, 1H, -O-CH₂-CH-), 1.96 – 1.92 (p, 2H, -CH₂-CH₂-Br), 1.71 – 1.66 (m, 4H, -Si-CH₂-CH₂- and -O-CH₂-CH₂-), 1.21 – 1.19 (d, 3H, CH₃-CH-), 0.51 (m, 2H, -Si-CH₂-), 0.20 – 0.04 (s, 3H, -Si-CH₃). **¹³C-NMR** (400 MHz, CDCl₃, 25 °C, ppm) δ = 137.94 (CH₂=CH-), 117.32 (CH₂=CH-), 75.75 (-O-CH₂-CH-), 72.30 (-Si-CH₂-CH₂-CH₂-), 67.44 (-O-CH₂-CH-), 61.18 (-O-CH₂-), 33.75 (-CH₂-Br), 30.98 (-O-CH₂-CH₂-), 29.49 (-CH₂-CH₂-Br), 20.77 (-Si-CH₂-CH₂-), 18.76 (CH₃-CH-), 13.99 (-Si-CH₂-), 1.91 – 0.86 (-Si-CH₃). **²⁹Si-NMR** (400 MHz, CDCl₃, 25 °C, ppm): δ = 7.30 (-Si(CH₃)₃), -21.47 (O-Si-O) -59.80 (-O-Si(Me)-O_{2/2}). **EA** (% , measured (calculated)), C₇₄H₁₈₁Br₉O₃₀Si₂₀: C 31.19 (35.87), H 7.81 (7.34), Br 4.92 (14.92), Si 24.27 (20.97). **GPC** (THF, 40 °C, g/mol): M_n=1479, M_w=3791, PDI=2.563.

Synthesis of poly(3-(2-hydroxypropoxy)propyl)methylsiloxane-co-poly(4-bromobutoxy)methylsiloxane-co-polydimethylsiloxane (5.7):

Representative procedure H:

PdCl₂ (97 mg, 1.6 mol-% in the mixture, 0.54 mmol) and 40 mL dried Toluene were added into the flask under argon atmosphere and stirred at room temperature (20 °C) for a couple of minutes. Then dried THF (1.38 mL, 17.06 mmol), allyl bromide (1.47 mL, 17.03 mmol) and 1-(allyloxy)propan-2-ol (2.16 mL, 17.05 mmol) were added into the system. SM-50 (4.97 mL, 2.27 mmol, M_n 2200 g/mol) was added dropwise. The mixture was stirred (oil bath temperature: 70 °C) under inert atmosphere (Ar) for 24 hours. The mixture (when necessary) was decolorized by adding activated carbon and an excess of pentane and stirred for 16 h at room temperature. The crude was filtrated through celite, and the solvents and volatiles were evaporated under vacuum. The obtained product (yield 75 %; 1.72 mmol) was a yellow, transparent, viscous liquid.

¹H-NMR (300 MHz, CDCl₃, 25 °C, ppm) δ = 5.95 – 5.82 (m, 1H, CH₂=CH-), 5.28 – 5.12 (m, 2H, CH₂=CH-), 4.19 – 3.97 (m, 1H, O-CH₂-CH(CH₃)-OH), 3.78 – 3.65 (m, 2H, -O-CH₂-), 3.47 – 3.36 (m, 5H, CH₂-O-CH₂-CH(CH₃)-OH and -CH₂-Br), 3.26 – 3.20 (t, 1H, -O-CH₂-CH-), 1.99 – 1.89 (p, 2H, -CH₂-CH₂-Br), 1.71 – 1.64 (m, 4H, -Si-CH₂-CH₂- and -O-CH₂-CH₂-), 1.12 – 1.07 (d, 3H, CH₃-CH-), 0.19 – 0.04 (s, 3H, -Si-CH₃). **¹³C-NMR** (300 MHz, CDCl₃, 25 °C, ppm) δ = 135.11 (CH₂=CH-), 116.75 (CH₂=CH-), 75.73 (-O-CH₂-CH-), 73.18 (-Si-CH₂-CH₂-CH₂-), 67.47 (-O-CH₂-CH-), 61.29 (-O-CH₂-), 33.79 (-CH₂-Br), 30.98 (-O-CH₂-CH₂-), 29.48 (-CH₂-CH₂-Br), 23.04 (-Si-CH₂-CH₂-), 12.24 (CH₃-CH-), 1.92 – 1.05 (-Si-CH₃). **²⁹Si-NMR** (300 MHz, CDCl₃, 25 °C, ppm): δ = -21.59 (O-Si-O) -59.13 (-O-Si(Me)-O_{2/2}). **IR** (ATR, 32 scans, cm⁻¹): 2963.4, 1377.2, 1259.9, 1012.3, 843.2, 793.2, 562.6. **EA** (% , measured (calculated)), repeating unit C₁₈H₄₅BrO₇Si₄: C 30.21 (35.87), H 6.97 (7.34), Br 10.44 (14.92), Si 26.31 (20.97). **GPC** (THF, 40 °C, g/mol): M_n=1647, M_w=3546, PDI=2.152.

Rheological measurements of Halogenalkyl and Propyleneglycol functionalized Polysiloxane Copolymers:

Table A-24: Viscosity results of the samples 5.1 to 5.7; the sample 5.6 and 5.7 follow the behavior of Newtonian liquids.

Sample	Viscosity [mPas]
5.1	n/d
5.2	n/d
5.3	non-Newtonian liquid
5.4	n/d
5.5	non-Newtonian liquid
5.6	0.0639
5.7	0.0766

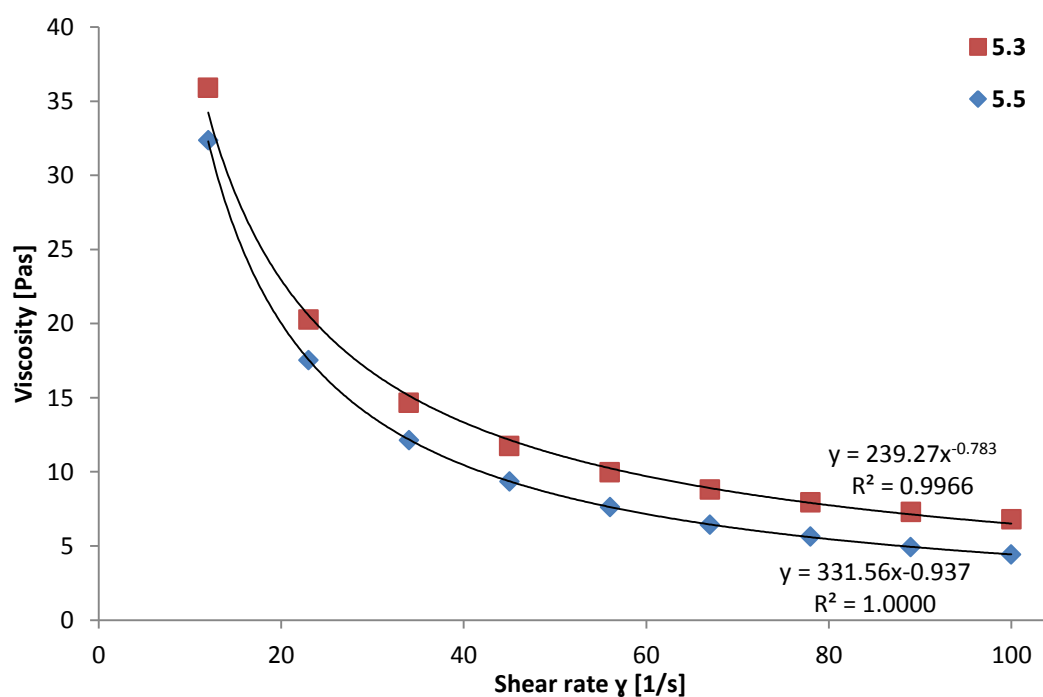


Figure A-33: Viscosity results of sample 5.3 and 5.5; both samples have a non-Newtonian behavior at 25 °C; the trend line is calculated by a power function; the first data point at 1.0 is not shown in the graph.

Table A-25: Rheological data of the samples 5.3 and 5.5 at 25 °C; both samples have a non-Newtonian behavior.

	Shear rate $\dot{\gamma}$ [1/s]	Shear stress τ [Pa]	Viscosity η [Pas]
5.3	1.0	369.9	363.717
	12.0	430.5	35.909
	23.0	466.0	20.270
	34.0	498.1	14.659
	45.0	528.9	11.753
	56.0	558.5	9.974
	67.0	589.5	8.802
	78.0	619.7	7.946
	89.0	649.2	7.295
	100.0	680.9	6.809
5.5	1.0	355.7	365.568
	12.0	388.8	32.378
	23.0	403.3	17.545
	34.0	412.7	12.141
	45.0	421.1	9.354
	56.0	427.4	7.628
	67.0	431.9	6.447
	78.0	439.5	5.635
	89.0	437.5	4.917
	100.0	443.8	4.439

A7. Scientific Contributions

Patents

A. Dietrich, N. Mohebbati, E. Mejia, T. Hémerly, A. Gutacker, J. Klein, *Preparation of polysiloxane polyalkyleneglycol brush copolymers*. European patent application EP 18210646.8, (Priority: 6th of December 2018)

A. Dietrich, E. Mejia, T. Hémerly, A. Gutacker, J. Klein, *Curable composition comprising polysiloxane polyalkyleneglycol brush copolymers*. European patent application EP 18210647.6, (Priority: 6th of December 2018)

A. Dietrich, E. Mejia, T. Hémerly, A. Gutacker, J. Klein, *Process for the Preparation of Functionalized Polysiloxanes*. European patent application EP 18209736.0, (Priority: 3rd of December 2018)

M. Winterberg, H. Lund, M. Wosnicka, A. Dietrich, E. Mejia, U. Kragl, *Process for the preparation of hydroxyl-functionalized polysiloxanes*. EP 3336129, WO 2018108863, (Priority: 16th of December 2016)

Publications

A. Kottmann, E. Mejía, T. Hémerly, J. Klein, U. Kragl, Recent Developments on the Preparation of Silicones with Antimicrobial Properties, *Chemistry – An Asian Journal* **2017**, 12, 1168 (DOI: 10.1002/asia.201700244)

Participations in Conferences and Symposia

A. Dietrich, E. Mejía, U. Kragl (2019), *Hydrosilylation of Siloxanes with Allyl Cyanide*, Poster contribution, 21. Frühjahrssymposium, Bremen

A. Dietrich, E. Mejía, U. Kragl (2018), *(Pseudo-)Halogenation of Silicone side-groups via Hydrosilylation*, Oral Presentation, Silicon-Containing Polymers and Composites 2018, San Diego

A. Dietrich, E. Mejía, U. Kragl (2018), *(Pseudo-)Halogenation of Silicone side-groups via Hydrosilylation*, Poster contribution, Forschungscamp 2018, Rostock

A. Kottmann, E. Mejía, U. Kragl (2018), *Synthesis of Brominated Silicones via Hydrosilylation*, Poster contribution, 20. Frühjahrssymposium, Konstanz

A8. Curriculum Vitae

Persönliche Daten

Name: Annika Dietrich geb. Kottmann

Anschrift: Patriotischer Weg 86

D-18057 Rostock

+49 151 55508820

Annika@drdiedrich.de

Geburtsdatum u. -ort: 18.01.1991 in Recklinghausen

Staatsangehörigkeit: deutsch

Familienstand: verheiratet

Berufliche Praxis

[2016 – 2019] **Promotion** zum Dr. rer. nat. Chemie

(Assoziierte AG Prof. Kragl (Universität Rostock) am Leibniz-Institut für Katalyse e. V. in Kooperation mit Henkel AG & Co. KGaA)

Ausbildung

[2014 – 2016] **Masterstudium** Chemie (Master of Science, Note 1,3)

Universität Rostock

Die Masterarbeit wurde am Leibniz-Institut für Katalyse e. V. in Kooperation mit Henkel AG & Co. KGaA angefertigt (Assoziierte AG Prof. Kragl (Universität Rostock) am Leibniz-Institut für Katalyse e. V.)

[2010 – 2014] **Duales Bachelorstudium** Chemie und Biotechnologie (Bachelor of Science, Note 1,5)

inkl. Ausbildung zur Chemielaborantin (Henkel AG & Co. KGaA in Düsseldorf, Note gut 85%)

Hochschule Niederrhein, Krefeld

Schwerpunkt: Organische Chemie

Die Bachelorarbeit wurde im Rahmen eines 6 monatigen Praktikums bei Henkel AG & Co. KGaA angefertigt (Abteilung AR – Surface Treatment – Metal Pretreatment)

[2000 – 2010] Gymnasium Petrinum zu Recklinghausen (Abitur, Note 1,3)

GDCh-Abiturienten Preis 2010 (Gesellschaft Deutscher Chemiker)

Tätigkeiten

[Januar 2005] zweiwöchiges Schülerpraktikum als Chemielaborantin (AQura GmbH am Chemiepark Marl)

[September 2009] zweiwöchiges freiwilliges Praktikum als Chemielaborantin (Fresenius SE & Co. KGaA in Herten)

[SS2013]	studentische Hilfskraft (Mathematik-Tutor für Mathematik II)
[WS2013/2014]	studentische Hilfskraft (Mathematik-Tutor für Mathematik I)
[Nov2013 – Juni2014]	freie Autorentätigkeit produktbezogener Fachinformationen für Vichy (L'Oréal Deutschland GmbH)
[WS14/15 – SS2016]	wissenschaftliche Hilfskraft (AK Kragl Leibniz-Institut für Katalyse e. V.)
[WS2015/2016]	viermonatiges Forschungspraktikum im Rahmen des Master-Studiengangs (AK Kragl Leibniz-Institut für Katalyse e. V.)

Kenntnisse und Fähigkeiten

Sprachkenntnisse	Deutsch – Muttersprache
	Englisch – fließend (Sprachniveau C1)
	Schwedisch – Grundkenntnisse (Sprachniveau A1)
	Latein – Latinum
	Griechisch – Graecum
EDV-Kenntnisse	Zwei Semester „Datenverarbeitung“
	(Microsoft Office (Word, PowerPoint, Excel, Outlook); LaTeX; Lotus Notes; NMR-MestReNova; EndNote; ChemBioDraw)
[SS2013 – WS13/14]	„ Betriebswirtschaftslehre “ der Hochschule Niederrhein Krefeld
[WS2013/2014]	„ Qualitätsmanagement, Führungslehre und Umweltrecht “ im Rahmen des Moduls Management und Recht der Hochschule Niederrhein Krefeld
[Februar 2017]	„ Projektmanagement “ der Graduiertenakademie der Universität Rostock
[März 2017]	„ Patentrecherche im Internet “ der Graduiertenakademie der Universität Rostock
[März 2017]	„ Zeit- & Selbstmanagement für Promovierende “ der Graduiertenakademie der Universität Rostock
[Juni 2017]	„ Improved Reading “ der Improved Reading GmbH & Co. KG
[April 2018]	„ Führungskompetenzen für Akademiker*innen “ der Graduiertenakademie der Universität Rostock
[Juni 2018]	„ Einführung in LATEX “ der Graduiertenakademie der Universität Rostock
[März 2019]	„ Introduction to Statistical Data Analysis using R “ der Graduiertenakademie der Universität Rostock

Sonstige Aktivitäten

[seit 2014]	Mitglied in Gesellschaft Deutscher Chemiker (GDCh)
	(Fachgruppe: Vereinigung Chemie & Wirtschaft)
[seit März 2017]	Aktives Mitglied im JungChemikerForum Rostock
[seit Nov 2017]	Stellvertretende Sprecherin des JungChemikerForums Rostock
	(u.a. Pflege der Internetpräsenz, Organisation und Moderation diverser Veranstaltungen, Kassenwart)